University of Nevada, Reno

CHARACTERIZATION OF UNBOUND MATERIALS FOR MECHANISTIC-EMPIRICAL PAVEMENT DESIGN FOR NDOT DISTRICTS 2 AND 3

A thesis submitted in partial fulfillment of the

requirements for the degree of Master of Science in

Civil and Environmental Engineering

by

Omar Othman

Dr. Peter E. Sebaaly/Thesis Advisor

December, 2021

THE GRADUATE SCHOOL

We recommend that the thesis
prepared under our supervision by

OMAR OTHMAN

entitled

Characterization of Unbound Materials for Mechanistic-Empirical Pavement Design for NDOT Districts 2 and 3

be accepted in partial fulfillment of the
requirements for the degree of

MASTER OF SCIENCE

Peter E. Sebaaly, Ph.D., P.E.
Advisor

Elie Y. Hajj, Ph.D.
Committee Member

Adam J.T. Hand, Ph.D.
Committee Member

Anna K. Panorska., Ph.D.
Graduate School Representative

David W. Zeh, Ph. D., Dean
Graduate School

December, 2021

Abstract

The American Association of State Highway and Transportation Officials (AASHTO) adopted the Mechanistic-Empirical Pavement Design Guide (MEPDG) as an interim pavement design standard in 2008. The Nevada Department of Transportation (NDOT) started the implementation of the MEPDG for the structural design of flexible and rigid pavements. The resilient modulus (Mr) for unbound materials is an important parameter in pavement design and is used to characterize unbound materials in the MEPDG. The MEPDG follows a hierarchical approach in defining the required engineering properties of the pavement structure, where three levels of input are specified in the AASHTOWare® Pavement ME design software. The levels include using direct measurements from laboratory testing offering the highest level of accuracy (i.e., Level 1), estimating input values through correlations with other soil properties (i.e., Level 2), and using typical values offering the lowest level of accuracy (i.e., Level 3). NDOT has been using the resistance value (R-value) to estimate the Mr of unbound materials through an equation which was not originally developed for Nevada materials. In 2017, NDOT took a major step towards updating the process for determining the unbound materials' design Mr in District 1 by developing models correlating it to other physical properties. The major objective of this study is to conduct similar research to develop resilient modulus prediction equations for NDOT Districts 2 and 3, and ultimately combine all collected materials in the aim to develop statewide design Mr prediction models for Nevada materials.

The unbound materials were collected from Districts 2 and 3 and tested for particle size distribution, Atterberg limits, specific gravity, moisture-density relationship, unconfined compressive strength, R-value, and Mr. The Mr test was conducted according to AASHTO T307, and the stress dependent constitutive models for the unbound materials were obtained. In summary, the stress-dependent behavior of the Mr in Districts 2 and 3 was found to fit well with the Theta model for base materials, and with the Uzan and Universal models for the subgrade materials. The developed Mr constitutive models were used along with the MEPDG procedure to obtain the design Mr for new projects. The design Mr for rehabilitation projects was obtained differently through a stepwise mechanistic approach. The design Mr values were used with the measured empirical and physical properties to develop prediction models for Districts 2 and 3 unbound materials for new and rehabilitation projects. The results from this study and the one conducted for District 1 materials were compiled and analysis was done to develop Mr prediction models for Nevada materials.

Keywords: Resilient modulus, Prediction models, MEPDG, Unbound materials, R-value, Stress dependent, Theta model, Uzan model, and Universal model.

Dedication

I dedicate this effort to my family.

Acknowledgements

I would like to thank Dr. Peter Sebaaly, my thesis advisor, for giving me this opportunity and for all his help, motivation, and support throughout my thesis.

I would also like to thank Dr. Elie Hajj for his help and advice towards completing this work and for serving as a committee member.

In addition, thanks to Dr. Anna Panorska for her help in the statistical analysis and for serving as part of my committee.

Thanks to Dr. Adam Hand for serving as a committee member and for all the knowledge he shared with me.

Additionally, thanks to Murugaiyah Piratheepan and my colleagues for all their help in the laboratory.

Finally, thanks to my family and my girlfriend for their constant support and for always believing in me.

And most importantly, thank God for blessing me with all what I am thankful for.

Table of Contents

List of Tables

Table of Figures

Chapter 1. Introduction

The American Association of State Highway and Transportation Officials (AASHTO) adopted the Mechanistic-Empirical Pavement Design Guide (MEPDG) as an interim pavement design standard in 2008 (1). The AASHTOWare®Pavement ME design software is currently being used to implement the MEPDG, where it incorporates the combined effects of traffic, climate, and material properties to conduct advanced mechanistic analysis of the pavement structure. The Nevada Department of Transportation (NDOT) already started the implementation of the MEPDG for the structural design of flexible pavements (2). Currently, NDOT has a MEPDG draft manual that covers the various parts of the design process including an extensive database on the properties and performance of asphalt concrete (AC) mixtures. The next step followed by NDOT in the MEPDG implementation process was to develop a database on the properties of unbound materials (base, subbase/borrow, and subgrade). In 2017, NDOT took a major step in achieving this goal by updating the process for determining design resilient modulus (Mr) of unbound materials in District 1 through the development of prediction models relating Mr to some physical properties of unbound materials (3). The research study documented in this thesis extended the development of the unbound materials database through conducting a similar study on unbound materials from NDOT Districts 2 and 3.

The MEPDG follows a hierarchical approach in defining the required engineering properties of the pavement structure. Three levels of input are specified: 1, 2, and 3, with level 1 offering the highest level of accuracy and level 3 offering the lowest one. In the case of unbound materials, the design Mr value for each of the base, subbase (borrow), and

subgrade layers is the main required engineering property. Additional unbound materials properties include Poisson's ratio (μ), Atterberg limits, gradation, conductivity, and coefficient of lateral pressure.

The Mr has a highly significant impact on the response of the pavement structure to the combined actions of traffic load and climate; hence, each pavement layer should have an accurately specified Mr value. Level 1 requires the Mr property to be measured in the laboratory under repeated load triaxial (RLT) conditions. Level 2 allows the determination of the Mr through correlations with other empirical properties such as the Resistance value (R-value) or the California Bearing Ratio (CBR). Level 3 permits the use of default Mr values or the estimation of Mr from other basic unbound materials properties such as Atterberg limits, gradation, etc.

Even though the RLT test provides a fundamental approach to characterize the non-linear stress-dependent behavior of unbound materials, the test is time consuming and costly; thus, it has not been commonly conducted in the design phase of pavement projects. As a result, most state highway agencies have chosen to employ level 2 input for unbound materials. Therefore, a well-defined fundamental approach must be followed to establish a highly reliable relationship for determining the design Mr value of unbound materials encountered throughout Nevada from other properties that can be practically and reliably measured.

Since the Mr input parameter for unbound materials plays a major role in pavement designs and has a significant influence on the projected pavement performance, a proper estimation of the design Mr value for locally available unbound materials becomes crucial for

designing long-lasting flexible and rigid pavements in Nevada. Currently, the Mr properties of unbound materials from NDOT District 1 are being estimated from the relationships developed in the 2017 study (3), while Districts 2 and 3 Mr properties are still being determined using the old relationship based on the R-value (Equation 1). This old relationship was established for specific group of soil types obtained from specific geographic areas that do not represent the type of unbound materials typically used in NDOT Districts 2 and 3.

$$Mr = 145 \times 10^{(0.0147 \times R + 1.23)} \quad \text{(Eq. 1)}$$

1.1. Objectives

The main objective of this research study is to conduct evaluations similar to the ones undertaken in the 2017 study to develop resilient modulus prediction models relating Mr to R-value and other physical properties for unbound materials to be used in new and rehabilitation projects in NDOT Districts 2 and 3. This objective was achieved through conducting the following tasks:

- Collecting commonly used base, borrow, and subgrade materials from NDOT Districts 2 and 3.
- Performing laboratory testing to evaluate material properties, including: sieve analysis, specific gravity, moisture-density relationship, Atterberg limits, unconfined compressive strength (UCS), R-value, and Mr.
- Developing Mr stress-dependent models for all tested unbound materials.
- Identifying the design Mr values for new and rehabilitation projects.

- Developing design Mr prediction models for unbound materials for new and rehabilitation projects for NDOT Districts 2 and 3.
- Examine the development of state-wide design Mr prediction models for unbound materials for new and rehabilitation projects.

Chapter 2. Literature Review

The MEPDG was adopted by AASHTO as an interim pavement design standard in 2008 (1). Many agencies have either transitioned to this method (Arizona, Colorado, Georgia, Indiana, Missouri, Utah, Virginia, etc.) or are in the process of doing so through evaluating the procedure and creating input libraries to calibrate the MEPDG procedure to their local conditions and materials (Georgia, Maine, Michigan, Mississippi, Nevada, etc.) (4). Since 2007, the Nevada Department of Transportation, in collaboration with the University of Nevada, has been working on the implementation of the MEPDG procedure for the design of flexible pavements by developing the necessary materials databases for Nevada (2).

The MEPDG implementation plan for NDOT follows a phased approach that consists of building material libraries with some of the inputs tied to their daily practice in order to make most use of the historical data and minimize deviations from present practices. One of the MEPDG input categories is the characterization of unbound materials and subgrade layers. The parameters used for unbound material characterization include gradation, optimum moisture content, dry density, Atterberg limits, Poisson's ratio, resilient modulus, etc. The resilient modulus is a key parameter that significantly affects the pavement's structural responses, thus affecting pavement design and performance.

Many sensitivity analyses have been conducted to investigate input parameters that significantly impact pavement responses. The Mr of unbound materials has been found to affect many flexible and rigid pavements performance indicators as shown below (4):

- Flexible Pavements
    - Longitudinal Cracking – Moderate to High Impact
    - Alligator Cracking – Low to Moderate Impact
    - Transverse Cracking – None to Low Impact
    - Rutting – Low to Moderate Impact
    - IRI – Variable
- Rigid Pavements
    - Faulting – Low Impact
    - Transverse Cracking – Moderate to High Impact
    - IRI – None to Low Impact

As the important role of the Mr of unbound materials on pavement design and performance was recognized, state Departments of Transportation need to resolve some issues before the full implementation of the MEPDG. These issues include choosing the test method used to identify the Mr, and the correlations used to relate the Mr to other unbound materials properties.

2.1. Purpose and Scope

The purpose of this section is to assemble information regarding the MEPDG procedure implementation and development, and to review correlation equations currently used by transportation agencies to estimate the design Mr value from other unbound materials properties.

This literature review is composed of the following sections: 1) the hierarchical input structure of the MEPDG as related to unbound layers; 2) an overview of laboratory Mr test methods; 3) correlations for estimating Mr; 4) Implementation of Mr correlations by state DOTs; and (5) NDOT District 1 correlations.

2.2. The MEPDG Hierarchical Input Levels

The hierarchical input levels option offered by the MEPDG equips its users with different ways of characterizing their pavement materials in the design process with various levels of accuracy. This provides a flexible way of inputting required material parameters, which allows the use of this method even with the lack of sufficient resources to accurately define these parameters. There are three levels, as discussed previously, with level 1 having the highest accuracy, and level 3 having the lowest one (1).

In the case of unbound materials, the guide provides the recommended level 1 testing methods for measuring the required properties. Table 1, derived from the MEPDG, shows the recommended testing protocols presented in the MEPDG. The majority of the methods are used by agencies on a regular basis and hence the corresponding properties can be accurately measured or estimated. In the case of the Mr, the recommended method is the repeated load triaxial (RLT) test, which is time consuming and calls for equipment not always available for agencies (1).

Recognizing the impact of the Mr on the pavement responses and performance, characterizing it for all unbound layers including base, borrow, and subgrade becomes

critical. The structural response computation models in the MEPDG require the Mr as an input. The MEPDG allows for three levels of input to define the Mr as listed below (5):

Table 1. Unbound Aggregate Base, Subbase, Embankment, and Subgrade Soil Input Parameters and Test Protocols for New and Existing Materials (1).

Design Type	Measured Property	Source of Data		Recommended Test Protocol and/or Data Source
		Test	Estimate	
New (lab samples) and existing (extracted materials)	Determine the average design resilient modulus for the expected in-place stress state from laboratory resilient modulus tests	X		AASHTO T307 or NCHRP 1-28A The generalized model used in MEPDG design procedures is presented in Equation 2
	Poisson's ratio		X	No national test standard, use default values included in the MEPDG
	Maximum dry density	X		AASHTO T180
	Optimum moisture content	X		AASHTO T180
	Specific gravity	X		AASHTO T100
	Saturated hydraulic conductivity	X		AASHTO T215
	Soil water characteristic curve parameters	X		Pressure plate (AASHTO T99) OR Filter Paper (AASHTO T180) OR Tempe cell (AASHTO T100)
Existing material to be left in place	FWD backcalculated modulus	X		AASHTO T256 and ASTM D5858
	Poisson's ratio		X	No national test standard, use default values included in the MEPDG

- Mr Input Level 1 – Laboratory Testing:

  This input level requires Mr to be determined trhough RLT testing done in the laboratory following NCHRP 1-28A, “Harmonized Test Methods for Laboratory Determination of Resilient Modulus for Flexible Pavement Design”, or AASHTO T307 test method, “Determining the Resilient Modulus of Soil and Aggregate Materials”. These methods describe sample preparation, testing sequence including different levels of confining and deviator stresses, and computation of test results. The measured data are analyzed to develop the generalized Mr model presented in Equation 2:

$$M_r = k_1 P_a \left(\frac{\theta}{P_a}\right)^{k_2} \left(\frac{\tau_{oct}}{P_a} + 1\right)^{k_3} \quad \text{(Eq. 2)}$$

  Where;
  - M_r= Resilient Modulus (psi)
  - θ= bulk stress (psi)= sum of major, intermediate, and minor principal stresses
  - τ_{oct}= octahedral shear stress (psi)
  - P_a= normalizing stress (atmospheric pressure= 14.7 psi)
  - k_1, k_2, k_3= regression constants (obtained by fitting Mr test data to equation)

  The use of the generalized model addresses the stress dependency of the unbound materials. Therefore, the design Mr value can be estimated depending on the stress state encountered by each unbound layer.

- Mr Input Level 2 – Correlations with Other Material Properties:

  This is the mostly used input level due to the complexity and time constraints of the RLT test. This level determines the Mr using general correlations relating it to other properties like the R-value or the CBR. Direct or indirect methods have been used, where direct correlations relate the Mr to the property itself (i.e., Mr to CBR), whereas indirect correlations estimate the property of interest from other properties, then uses this estimation to obtain the Mr (i.e., CBR from plasticity index and gradation, then Mr from CBR). Table 2 presents some of the models relating material index and strength properties to Mr.

Table 2. Models Relating Material Index and Strength Properties to Mr (5).

Strength/Index Property	Model	Comments	Test Standard
CBR	$Mr = 2555(CBR)^{0.64}$ Mr, psi	CBR= California Bearing Ratio, percent	AASHTO T 193, "The California Bearing Ratio"
R-value	$Mr = 1155 + 555R$ Mr, psi	R= R-value	AASHTO T 190, "Resistance R-value and Expansion Pressure of Compacted Soils"
AASHTO layer coefficient	$Mr = 30000\left(\frac{a_i}{0.14}\right)$ Mr, psi	a_i = AASHTO layer coefficient	AASHTO Guide for the Design of Pavement Structures
PI and gradation*	$CBR = \frac{75}{1 + 0.728(wPI)}$	wPI = P200*PI P200= percent passing No. 200 sieve size PI = plasticity index, percent	AASHTO T27, "Sieve Analysis of Coarse and Fine Aggregates" AASHTO T90, "Determining the Plastic Limit and Plasticity Index of Soils"
DCP*	$CBR = \frac{292}{DCP^{1.12}}$	CBR= California Bearing Ratio, percent DCP = DCP index, mm/blow	ASTM D 6951, "Standard Test Method for Use of Dynamic Cone Penetrometer in Shallow Pavement Applications"

- Mr Input Level 3 - Typical Values (Based on local soil classification or experience): This input level approximates the Mr value from default global values that depend on the material's soil classification. The Mr value can also be approximated from history and local experience. Global default values are built in the software and are meant to represent the Mr value at optimum moisture content and maximum dry density. Caution must be used for this level as the values may be very inaccurate.

2.3. Overview of the Resilient Modulus Test

The Mr of a material is defined as the ratio of the deviatoric stress to the resilient (elastic) strain it experiences under repeated loading. Figure 1 shows a graphical representation of the parameters used for Mr definition. Even though most unbound materials are not elastic and may experience permanent deformations under high loads, the deformations measured during Mr testing cycles are considered recoverable, and hence the elastic strain can be used to measure the Mr. This is because the loads applied in the laboratory are very small compared to the material's failure load and since these loads are being applied over many cycles, the plastic deformation is reduced. The main reason for using Mr as the parameter for characterizing unbound materials is that it denotes a basic material property that can be used in mechanistic analyses for the prediction of several distresses such as rutting and roughness (6).

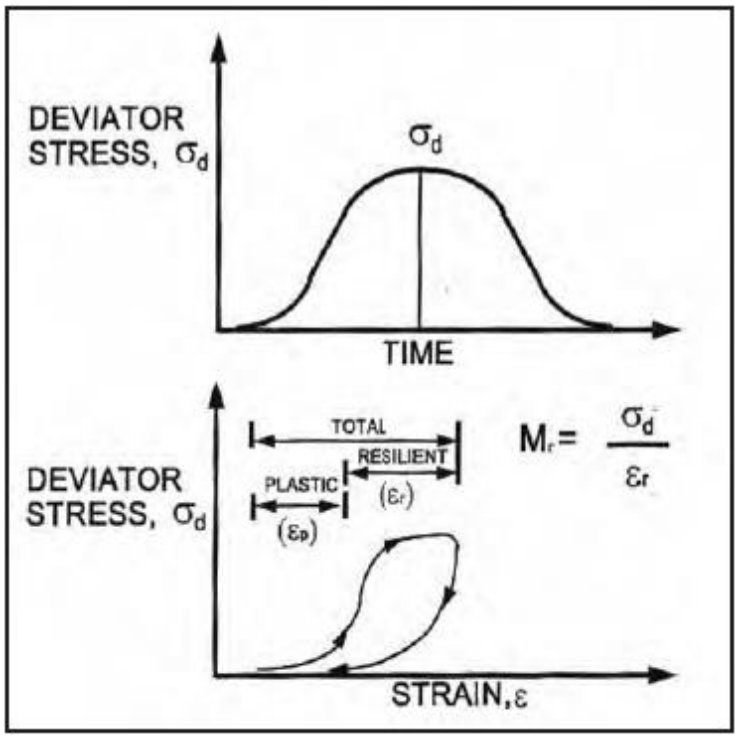

Figure 1. Definition of Resilient Modulus (6).

In NCHRP Synthesis 382 (6), literature describing Mr testing procedures and how their results were applied to the pavement mechanistic design, were compiled and presented into three categories as: 1) before 1986, 2) from 1986 to 1996, and 3) after 1996.

The literature conducted before 1986 mainly addressed the development of test procedures and equipment modifications to test cohesive subgrades and granular base materials, the development of suitable models to demonstrate the resilient behavior, and the introduction of a few correlations to predict resilient properties based on soil properties.

Literature conducted between 1986 and 1996 aimed for the utilization of various laboratory and field equipment to determine the resilient properties of both subgrades and bases. During this phase, test procedures including AASHTO T292, T294 and P46 were

established and assessed. Also, displacement measuring systems were researched where the deformation was measured at different locations along the specimen in hope of providing more realistic Mr values. In addition, some studies examined various local unbound bases and subgrades in aim of building databases of resilient properties, which were later used to develop predictive models.

After 1996, modifications of AASHTO testing procedures T294 to T307 occurred, leading multiple DOTs to perform additional research to validate previous work, and new research to determine Mr values for local materials. This resulted in the establishment of large Mr databases leading to better interpretations of resilient properties for mechanistic pavement design.

Recent research shows that the RLT test is the most prominent method for laboratory testing, primarily because AASHTO standardized this test as it better simulates pavement responses under traffic loading. The RLT test is designed to simulate traffic wheel loading on unbound pavement layers through the application of sequences of repeated or cyclic loads on compacted unbound samples. The stress levels applied in this method are based on the location of the unbound layer within the pavement structure and are comprised of a confining pressure and a deviatoric stress. The confining pressure typically represents the overburden pressure experienced by the layer within the structure and is applied all around the specimen. The deviatoric stress is an axial stress and is composed of two components, the contact stress (seating load on the specimen), and the cyclic stress (actual applied stress). The contact stress is usually equivalent to 10% of the total deviatoric stress (6).

The test method covers compaction methods to prepare the specimen, transferring it to the triaxial chamber, applying the confining pressure, and then starting the test by applying the deviatoric stresses. The test consists of multiple loading sequences composed of different combinations of confining and deviatoric stresses, which differ between granular base and subbase materials, and fine-grained subgrade soils. The testing sequences are presented in the AASHTO standard. In general, the repeated load is a haversine wave pulse load with a 0.1 sec loading period and a 0.9 sec relaxation period. The different stress states applied result in multiple Mr values for the tested material, which can then be used to develop prediction models through regression analyses (6).

Several AASHTO test methods (T274, T292, T294, and T307) have been used by state agencies and industry for measuring the resilient modulus of unbound materials. These methods differ from each other in one or more aspects including sample preparation, conditioning methodology prior to actual loading, seating stress application, test sequences of applying confining and cyclic deviatoric stresses, and deformation measurements inside/outside of triaxial chamber (4). Table 3 describes the chronology of the development of these test methods.

Table 3. Chronology of AASHTO Test Procedures for Mr Measurements (6).

Test Procedure	Details
AASHTO T274-1982	Earliest AASHTO test procedure; No details on the sensitivities of displacement measurement devices were given; Criticisms on test procedure, test duration (5 hours long test) and probable failures of soil sample during conditioning phase; testing stresses are too severe.
AASHTO T292-1991	AASHTO procedure introduced in 1991; Internal measurement systems are recommended; Testing sequence is criticized owing to the possibility of stiffening effects of cohesive soils.
AASHTO T294-1992	AASHTO modified the T292 procedure with different sets of confining and deviatoric stresses and their sequence; Internal measurement system is followed; 2-parameter regression models (bulk stress for granular and deviatoric stress model for cohesive soils) to analyze test results; Criticism on the analyses models.
Strategic Highway Research Program P 46-1996	Procedural steps of P46 are similar to T294 procedure of 1992; External measurement system was allowed for displacement measurement; Soil specimen preparation methods are different from those used in T292.
AASHTO T307-1999	T307-1999 was evolved from P46 procedure; recommends the use of external displacement measurement system. Different procedures are followed for both cohesive and granular soil specimen preparation.
NCHRP 1-28 A: Harmonized Method-2004 (RRD 285)	This recent method recommends a different set of stresses for testing. Also, a new 3-parameter model is recommended for analyzing the resilient properties. The use of internal measurement system is recommended in this method.

Survey results presented in NCHRP Synthesis 382 on the test protocols that state DOTs use in characterizing the Mr of unbound materials showed that 22 out of 30 states use AASHTO T307. Table 4 lists the Mr test procedures being used by different agencies (4 and 6).

Table 4. State DOT/Other Laboratories Conducting Resilient Modulus Testing (4).

State DOT/Other Laboratories	Test Protocol Followed
Alaska DOT	AASHTO T307-99
Alabama DOT	AASHTO T307-99
Arizona DOT/ASU Geotechnical Laboratory	NCHRP 1-28A
Cold Regions Research & Engineering Laboratory (CRREL)	AASHTO T307-99
Colorado DOT	AASHTO T307-99
Florida DOT	AASHTO T307-99
Georgia DOT	AASHTO T307-99
Iowa DOT	NCHRP 128A/ AASHTO T307-99
Idaho Transportation Department Laboratory	AASHTO T307-99
Indiana DOT	AASHTO T307-99
Kansas DOT	AASHTO T307-99
Kentucky DOT/University of Kentucky Transportation Center	AASHTO T307-99
Louisiana DOT/Louisiana Transportation Research Center (LTRC) Laboratory	AASHTO T307-99
Manitoba Provence, Canada	NCHRP 1-28A
Michigan DOT	AASHTO T307-99
Minnesota DOT	NCHRP 1-28A
Missouri DOT	AASHTO T307-99
Mississippi DOT	AASHTO T307-99
Montana DOT	AASHTO T307-99
Nebraska DOT/University of Nebraska-Lincoln (UNL) Geomaterials Laboratory	AASHTO T307-99
North Dakota DOT	NCHRP 1-28A
New Hampshire DOT	AASHTO TP46-94
New Jersey DOT/Rutgers University Asphalt/Pavement Laboratory (RAPL)	AASHTO TP46-94
OH DOT/ORITE Pavement Material Test Laboratory	AASHTO T274
Oklahoma DOT	AASHTO T307-99
Rhode Island DOT	AASHTO T307-99
Tennessee DOT	AASHTO T307-99
Texas DOT	AASHTO T307-99
Virginia DOT	AASHTO T307-99
Wisconsin DOT	AASHTO T307-99

Even with the standardization of the Mr test in many test protocols, DOTs had low satisfaction with the use of Mr in M-E design due to constant modifications. Also, previous studies have shown that Mr test results can vary significantly by sampling techniques, testing procedure, and some errors that can be encountered during testing. These errors may happen due to incorrect conditioning or stress sequence, membrane leakage making the load distribution nonuniform, wrong stress levels, specimen disruption at higher stress levels, unstable Linear Variable Differential Transducer (LVDT) clamps attached to specimen, and exceeding LVDT linear range limits (4 and 7).

The research reported by FHWA on the precision and bias of the Mr test (4) outlined some studies focusing on practices that could cause variability in the test. The following conclusions were drawn from the reviewed studies:

- Several test systems are in the market, as some so-called high-end equipment (MTS, Interlaken and Instron) and lower-end equipment (GCTS, GeoComp and IBC) are available. The high-end equipment are about double the price of lower-end ones, but do not necessarily result in double the accuracy. Some studies have focused on determining the existence of bias between these systems, as well as defining their precision.
- Different LVDTs placement (on/off specimen) have shown different results. Off-specimen LVDTs showed a significant increase in test variability compared to on-specimen LVDTs. However, different studies reported opposite results; hence, both methods should be evaluated in a ruggedness test program before measuring their precision and bias.

- Variation from optimum moisture content in the tested specimen resulted in huge impact on the resulting Mr value. Almost none of the reviewed studies allowed deviations in water content or degree of saturation, and it was found that the Mr of all soils decreased with increasing moisture content. Furthermore, it was observed that an increase of 3 to 5 percent in the optimum moisture content resulted in a 50 to 70 percent decrease in the Mr value. It was also reported that the drying of the specimen results in a significant increase in the Mr value, sometimes by tenfold. Hence, moisture content and dry density are important in measuring the Mr, and the deviations allowed in AASHTO T307 and NCHRP 128a procedures should be checked in a ruggedness test program to confirm that differences between laboratories and test specimens are not caused by large difference in the specimens' volumetric properties.
- In addition, the studies reviewed reported that the Mr values were affected by soil suction, Atterberg limits, moisture content and degree of saturation, gradation, source lithology, stress-strain levels, aggregate singularity and texture, and seasonal variation.

2.4. Correlations for Estimating Resilient Modulus

Many Mr correlation equations have been developed over the years (8). These equations are mostly regression-based, as they were developed by comparing Mr values from RLT test results to less expensive tests that are routinely done such as the R-value, CBR, Unconfined compressive strength (UCS) test, Dynamic Cone Penetrometer (DCP), and other physical properties (9). An extensive literature review showed that most Mr

correlations were developed for specific material types and relatively small sample sets (10). Therefore, it was recommended to further evaluate the suitability and reliability of developed equations before implementing them. Currently, two approaches are used when analyzing Mr data to come up with Mr correlation equations for use in pavement design: direct and indirect (6), as explained in the following sections.

2.4.1. Indirect Correlations

In the indirect approach, the Mr data are analyzed with some formulations that account for confining pressure, deviatoric stress, or both which usually contain several model parameters. Once determined, these parameters are correlated with different soil properties, then these correlation equations are substituted in the corresponding formulation to come up with the indirect Mr correlation (6). Yau and Von Quintus used the extensive Long-Term Pavement Performance (LTPP) database to develop some indirect correlations for different soil types (7).

The parameters obtained correspond to the formulation presented in Equation 2, including the bulk stress, the octahedral shear stress, and three model parameters (k_1, k_2, and k_3). The correlations for different materials are presented in the remainder of this section.

Crushed Stone Materials – LTPP Code 303

$$M_r = \left[0.7632 + 0.0084\left(P_{3/8}\right) + 0.0088LL - 0.0371W_{opt} - 0.0001\gamma_{opt}\right]P_a \times$$

$$\left[\frac{\theta}{P_a}\right]^{\left(2.2159-0.0016\left(P_{3/8}\right)+0.0008LL-0.038W_{opt}-0.0006\gamma_{opt}+2.4\times10^{-7}\left[\frac{\gamma_{opt}^2}{P_{40}}\right]\right)} \times$$

$$\left[\frac{\tau_{oct}}{P_a} + 1\right]^{-1.1720-0.0082LL-0.0014W_{opt}+0.0005\gamma_{opt}} \quad \text{(Eq. 3)}$$

Number of Points= 853; Mean squared error= 1699.6; Se= 41.23; Sy= 87.42; Se/Sy= 0.4716

Crushed Gravel – LTPP Code 304

$$M_r = \left[-0.8282 + 0.0065\left(P_{3/8}\right) + 0.0114LL + 0.0004PI - 0.0187W_{opt} + 0.0013\gamma_s - 2.6 \times 10^{-6}\left(\frac{\gamma_{opt}^2}{P_{40}}\right)\right]P_a \times$$

$$\left[\frac{\theta}{P_a}\right]^{\left(4.9555-0.0057LL-0.0075PI-0.0470W_s-0.0022\gamma_{opt}+2.8\times10^{-6}\left[\frac{\gamma_{opt}^2}{P_{40}}\right]\right)} \times$$

$$\left[\frac{\tau_{oct}}{P_a} + 1\right]^{-3.514+0.0016\gamma_s} \quad \text{(Eq. 4)}$$

Number of Points= 404; Mean squared error= 854.4; Se= 29.23; Sy= 66.74; Se/Sy= 0.4380

Uncrushed Gravel – LTPP Code 302

$$M_r = \left[-1.8961 + 0.0014\gamma_s - 0.1184\left(\frac{W_s}{W_{opt}}\right)\right] P_a \times$$

$$\left[\frac{\theta}{P_a}\right]^{\left(0.4960 - 0.0074P_{200} - 0.0007\gamma_s + 1.6972\left[\frac{\gamma_s}{\gamma_{opt}}\right]\right)} \times$$

$$\left[\frac{\tau_{oct}}{P_a} + 1\right]^{\left(-0.5979 + 0.0349W_{opt} + 0.0004\gamma_{opt} - 0.5166\left[\frac{W_s}{W_{opt}}\right]\right)} \quad \text{(Eq. 5)}$$

Number of Points= 461; Mean squared error= 475.9; Se= 21.81; Sy= 63.05; Se/Sy= 0.3460

Sand – LTPP Code 306

$$M_r = \left[-0.2786 + 0.0097P_{3/8} + 0.0219LL - 0.0737PI + 1.8 \times 10^{-7}\left(\frac{\gamma_{opt}^2}{P_{40}}\right)\right] P_a \times$$

$$\left[\frac{\theta}{P_a}\right]^{\left(1.1148 - 0.0053P_{3/8} - 0.0095LL + 0.0325PI + 7.2 \times 10^{-7}\left(\frac{\gamma_{opt}^2}{P_{40}}\right)\right)} \times$$

$$\left[\frac{\tau_{oct}}{P_a} + 1\right]^{\left(-0.4508 + 0.0029P_{3/8} - 0.0185LL + 0.0798PI\right)} \quad \text{(Eq. 6)}$$

Number of Points= 519; Mean squared error= 512.7; Se= 22.64; Sy= 51.61; Se/Sy= 0.4388

Coarse-Grained Soil-Aggregate Mixture – LTPP Code 308

$$M_r = \left[-0.5856 + 0.0130P_{3/8} - 0.0174P_4 + 0.0027P_{200} + 0.0149PI + 1.6 \times 10^{-6}(\gamma_{opt}) - 0.0426W_s + 1.6456\left(\frac{\gamma_s}{\gamma_{opt}}\right) + 0.3932\left(\frac{W_s}{W_{opt}}\right) - 8.2 \times 10^{-7}\left(\frac{\gamma_{opt}^2}{P_{40}}\right)\right] P_a \times \left[\frac{\theta}{P_a}\right]^{\left(0.7833 - 0.0060P_{200} - 0.0081PI + 0.0001\gamma_{opt} - 0.1483\left(\frac{W_s}{W_{opt}}\right) - 2.7\times10^{-7}\left(\frac{\gamma_{opt}^2}{P_{40}}\right)\right)} \times \left[\frac{\tau_{oct}}{P_a} + 1\right]^{\left(-0.1906 - 0.0026P_{200} + 8.1\times10^{-7}\left(\frac{\gamma_{opt}^2}{P_{40}}\right)\right)} \quad \text{(Eq. 7)}$$

Number of Points= 2323; Mean squared error= 1883.9; Se= 43.4; Sy= 80.19; Se/Sy= 0.541

Fine-Grained Soil-Aggregate Mixture – LTPP Code 307

$$M_r = \left[-0.7668 + 0.0051P_4 + 0.0128P_{200} + 0.0030LL - 0.0510W_{opt} + 1.1729\left(\frac{\gamma_s}{\gamma_{opt}}\right)\right] P_a \times \left[\frac{\theta}{P_a}\right]^{\left(0.4951 - 0.0141P_4 - 0.0061P_{200} + 1.3941\left(\frac{\gamma_s}{\gamma_{opt}}\right)\right)} \times \left[\frac{\tau_{oct}}{P_a} + 1\right]^{\left(0.9303 + 0.0293P_{3/8} + 0.0036LL - 3.8903\left(\frac{\gamma_s}{\gamma_{opt}}\right)\right)} \quad \text{(Eq. 8)}$$

Number of Points= 390; Mean squared error= 588.2; Se=24.25; Sy= 49.37; Se/Sy= 0.4912

Fine-Grained Soil – LTPP Code 309

$$M_r = [0.8409 + 0.0004P_{40} + 0.0161PI]P_a \times \left[\frac{\theta}{P_a}\right]^{(0.6668-0.0007P_{40}-0.0139PI)} \times$$

$$\left[\frac{\tau_{oct}}{P_a} + 1\right]^{(-0.1667-0.0207PI)} \quad \text{(Eq. 9)}$$

Number of Points= 1079; Mean squared error= 1167; Se= 34.16; Sy= 62.80; Se/Sy= 0.5440

Coarse-Grained Gravel Soils

$$M_r = \left[1.3429 - 0.0051P_{3/8} + 0.0124(\%Clay) + 0.0053LL - 0.0231W_s\right]P_a \times$$

$$\left[\frac{\theta}{P_a}\right]^{(0.3311+0.0010P_{3/8}-0.0019(\%Clay)-0.0050LL-0.0072PI+0.0093W_s)} \times$$

$$\left[\frac{\tau_{oct}}{P_a} + 1\right]^{(1.5167-0.0302P_{3/8}+0.0435(\%Clay)+0.0626LL+0.0377PI-0.2353W_s)} \quad \text{(Eq. 10)}$$

Number of Points= 957; Mean squared error= 301.3; Se= 17.36; Sy= 26.81; Se/Sy= 0.6474

Coarse-Grained Sand Soils

$$M_r = \left[3.2868 - 0.0412P_{3/8} + 0.0267P_4 + 0.0137(\%Clay) + 0.0083LL - 0.0379W_{opt} - 0.0004\gamma_s\right]P_a \times \left[\frac{\theta}{P_a}\right]^{\begin{pmatrix} 0.5670+0.0045P_{3/8}-2.98\times10^{-5}(P_4)-0.0043(\%Silt)-0.0102(\%Clay)-0.0041LL+0.0014W_{opt} \\ -3.41\times10^{-5}\gamma_s-0.4582\left(\frac{\gamma_s}{\gamma_{opt}}\right)+0.1779\left(\frac{W_s}{W_{opt}}\right) \end{pmatrix}} \times \left[\frac{\tau_{oct}}{P_a} + 1\right]^{\begin{pmatrix} -3.5677+0.1142P_{3/8}-0.0839P_4-0.1249P_{200}+0.1030(\%Silt) \\ +0.1191(\%Clay)-0.0069LL-0.0103W_{opt} \\ -0017\gamma_s+4.3177\left(\frac{\gamma_s}{\lambda_{opt}}\right)-1.1095\left(\frac{W_s}{W_{opt}}\right) \end{pmatrix}} \quad \text{(Eq. 11)}$$

Number of Points= 3117; Mean squared error= 357.7; Se= 18.91; Sy= 24.79; Se/Sy= 0.7630

Fine-Grained Silt Soils

$$M_r = [1.0480 + 0.0177(\%Clay) + 0.0279PI - 0.370W_s]P_a \times \left[\frac{\theta}{P_a}\right]^{(0.5097-0.0286PI)} \times \left[\frac{\tau_{oct}}{P_a} + 1\right]^{(-0.2218+0.0047(\%Silt)+0.0849PI-0.1399W_s)} \quad \text{(Eq. 12)}$$

Number of Points= 464; Mean squared error= 193.0; Se= 13.89; Sy= 24.71; Se/Sy= 0.5622

Fine-Grained Clay Soils

$$M_r = [1.3577 + 0.0106(\%Clay) - 0.0437W_s]P_a \times$$

$$\left[\frac{\theta}{P_a}\right]^{(0.5193-0.0073P_4+0.0095P_{40}-0.0027P_{200}-0.0030LL-0.0049W_{opt})} \times$$

$$\left[\frac{\tau_{oct}}{P_a}+1\right]^{\left(\begin{array}{c}1.4258-0.0288P_4+0.0303P_{40}-0.0521P_{200}+0.0251(\%Silt)\\+0.0535LL-0.0672W_{opt}-0.0026\gamma_{opt}+0.0025\gamma_s-0.6055\left(\frac{W_s}{W_{opt}}\right)\end{array}\right)} \quad \text{(Eq. 13)}$$

Number of Points= 1484; Mean squared error= 557.9; Se= 23.62; Sy= 29.22; Se/Sy= 0.808

Where;

- $P_{3/8}$= Percentage passing 3/8" sieve (%)
- P_4= Percentage passing No. 4 sieve (%)
- P_{40}= Percentage passing No. 40 sieve (%)
- P_{200}= Percentage passing No. 200 sieve (%)
- %Silt= Percentage of silt (%)
- %Clay= Percentage of clay (%)
- LL= Liquid limit of soil (%)
- PI= Plasticity index of soil (%)
- W_{opt}= Optimum water content (%)
- γ_{opt}= Maximum dry unit weight of soil (kg/m^3)
- W_s= Water content of test specimen (%)
- γ_s= Dry density of test specimen (kg/m^3)

2.4.2. Direct Correlations

In the direct approach, correlations are developed between the Mr and other soil properties or in situ test results (6). This literature review will focus on direct correlations with soil properties such as CBR, UCS, and PI, etc. Correlations with R-value are the most common for direct correlations with soil properties, however, they will not be presented in this

section and instead will be featured more in the next section when previewing correlations used by state DOTs.

Presented below are some selected direct correlations, noting that similar coefficients discussed previously are not explained again.

Heukelom and Klomp, 1962 (11):

$$Mr = 1500 \times CBR \quad \text{(Eq. 14)}$$

Powell et al., 1984 (12):

$$Mr = 2555 \times CBR^{0.64} \quad \text{(Eq. 15)}$$

Where (for both CBR equations):

Mr= Resilient Modulus (psi)

CBR= California Bearing Ratio

Drumm, et al., 1990 (13):

$$Mr = 45.8 + 0.00052\left(\frac{1}{a}\right) + 0.188(UC) + 0.45(PI) + 0.216(\gamma_s) - 0.25(S) - 0.15(P_{200}) \quad \text{(Eq. 16)}$$

Where:

a= Initial tangent modulus, psi

UC= Unconfined compressive strength, psi

S= Degree of saturation, percent

Coefficient of Determination, $R^2 = 0.83$.

Lee, et al., 1997 (14):

$$Mr = 695.4 \times S_{u1\%} - 5.93 \times (S_{u1\%})^2 \quad \text{(Eq. 17)}$$

Where:

$S_{u1\%}$ = Stress at 1.0 percent strain in the UCS test.

Coefficient of Determination, $R^2 = 0.97$.

Hossain and Kim, 2014 (15), Static Compaction:

$$Mr = 6082 + 142(UC) \quad \text{(Eq. 18)}$$

Coefficient of Determination, $R^2 = 0.64$.

$$Mr = 7884.2 + 99.7(UC) + 193.1(PI) - 47.9(P_{200}) \quad \text{(Eq. 19)}$$

Coefficient of Determination, $R^2 = 0.86$.

Hossain and Kim, 2014 (15), Impact Compaction (Proctor Hammer):

$$Mr = 4283 + 143(UC) \quad \text{(Eq. 20)}$$

Coefficient of Determination, $R^2 = 0.73$.

$$Mr = 6113 + 95.1(UC) + 173.7(PI) - 27.8(P_{200}) \quad \text{(Eq. 21)}$$

Coefficient of Determination, $R^2 = 0.91$.

$$Mr = 657 \times S_{u1\%} - 6.75 \times (S_{u1\%})^2 \quad \text{(Eq. 22)}$$

Coefficient of Determination, $R^2 = 0.97$.

2.5. Implementation of Mr Correlations by State DOTs

When implementing the MEPDG, it is recommended to use input Level 1 or 2 for the unbound materials Mr characterization. However, due to Mr test's complexity, cost, and time constraints, most state DOTs use input Level 2 or 3, with Level 2 being the preferred one due to its higher accuracy as discussed previously. This section will focus on reviewing the Mr correlations used by state DOTs for MEPDG input Level 2. Table 5 presents the Mr test procedures adopted by some state DOTs, as well as the method used to obtain the correlated Mr values (3).

Since the objective of this research is to correlate the Mr value with R-value and other physical properties, this section will focus more on these types of correlations rather than correlations with the CBR. In short, most agencies east of the Mississippi river use the CBR to estimate the Mr (3). For these agencies, the two most common CBR correlations used are Equations 14 and 15 (11 and 12) reported in section 2.4.2. Other state DOTs correlations including ones with the R-value are presented in the remainder of this section.

Table 5. State DOTs Mr Determination Practices (3).

State DOT	Test Procedure	Mr Correlated with and/or determined by
Arizona	NCHRP 1-28A	R-value and a library of Mr values.
Colorado	AASHTO T307-99	R-value and a library of Mr values.
Florida	AASHTO T307-99	LBR-value, backcalculated from deflection basins, and a library of Mr Values.
Georgia	AASHTO T307-99	Soil Support, Physical properties, and a library of Mr values.
Idaho	AASHTO T307-99	R-value and a library of Mr values.
Michigan	AASHTO T307-99	Library of Mr values and backcalculated from deflection basins.
Missouri	AASHTO T307-99	Regression equations to calculate k_1, k_2, and k_3 from soil physical properties; similar to FHWA regression equations.
Mississippi	AASHTO T307-99	CBR and a library of Mr values.
Montana	AASHTO T307-99	Library of Mr values and backcalculated from deflection basins.
Pennsylvania	AASHTO T307-99	Unconfined compressive strength and a library of values
Tennessee	AASHTO T307-99	Index of soil properties.
Texas	AASHTO T307-99	Texas Triaxial Classification Value
Virginia	AASHTO T307-99	Unconfined compressive strength
Wisconsin	AASHTO T307-99	Regression equations to calculate k_1, k_2, and k_3 from soil physical properties; similar to FHWA regression equations.
Wyoming	AASHTO T307-99	R-value and a library of Mr values.

Arizona DOT

The MEPDG has been implemented by ADOT in 2019, with material characterization completed around 2000. Darter et al. (16) stated that default level 3 inputs for subgrade resilient modulus at optimum moisture content were developed from DARWin-ME, LTPP, and ADOT projects. These resilient modulus values were obtained through backcalculation from nearly all Arizona sections using FWD tests, then adjusted to optimum moisture content.

The ADOT pavement design manual (17) provides an equation to estimate the R-value (Equation 23) and a correlation to convert the design R-value (referred to as R_{mean}) to a resilient modulus value (Equation 24).

$$R_{\ at\ 300\ psi} = 10^{[2.0-0.006P_{200}-0.017(PI)]} \quad \text{(Eq. 23)}$$

$$Mr = \frac{1815+225(R_{mean})+2.40(R_{mean})^2}{0.6(SVF)^{0.6}} \quad \text{(Eq. 24)}$$

Where; SVF= Seasonal Variation Factor

Colorado DOT

CDOT fully implemented MEPDG in July 2014. Yeh and Su (18) indicated that attempts were made to relate the Mr to the R-value for Colorado soils for over 30 years. They conducted an extensive laboratory testing program, and the resulting correlation was established (Equation 25):

$$Mr = 3500 + 125(R - value) \quad \text{(Eq. 25)}$$

Chang et al. (19) conducted a study to correlate Mr to R-value by analyzing 39 Mr test results for granular soils with varying fine contents. The materials classification ranged from A-1-a to A-7-6. The correlation obtained is shown below (Equation 26).

$$Mr = 1.312(R)^{0.517} \quad \text{(Eq. 26)}$$

This correlation had a coefficient of determination of 42.79% and did not offer a significant improvement from the previous one developed by Yeh and Su (Equation 25). This

correlation was recommended to be used with caution and for materials with less than 30% fines.

Another Mr-R correlation by CDOT was included in the 2012 pavement design guide (20) for coarse- and fine-grained materials as shown below (Equation 27):

$$Mr = 10^{[((R-5)/11.29)+21.72]/6.24} \quad \text{(Eq. 27)}$$

During the phase of implementation of the MEPDG by CDOT, Mallela et al. (21) recommended the use of Level 2 Mr values for subgrade materials with FWD backcalculation, and Level 3 for other unbound materials from MEPDG default values.

CDOT included another Mr-R correlation equation in their 2021 M-E Pavement Design Manual (22). This correlation (Equation 28) should be used only for materials with R-value of 50 or less.

$$Mr = 3438.6 \times R^{0.2753} \quad \text{(Eq. 28)}$$

Idaho TD

Idaho Transportation Department (ITD) completed the unbound material database in 2017-2018 and implemented the MEPDG in 2020. In the IDT 2011 materials manual (23), the Mr was calculated based on the R-value using the following relationship (Equation 29):

$$Log(Mr) = (222 + R)/67 \quad \text{(Eq. 29)}$$

Bayomy et al. (24) worked on the implementation of flexible pavements in Idaho where an equation to estimate R-value developed by El-Badawy et al. (25) was presented following

the ADOT model but optimized for ITD's historical R-value database (Equation 30), with a coefficient of determination of 0.637.

$$R = 10^{[1.893-0.00159P_{200}-0.022(PI)]} \quad \text{(Eq. 30)}$$

This study also presented an Mr-R relation developed for Idaho (Equation 31) with a coefficient of determination of 0.579, based on limited literature data and regression analysis.

$$Mr = 1004.4(R)^{0.6412} \quad \text{(Eq. 31)}$$

It was recommended that the ITD uses the R-value correlation equation (if direct laboratory measurements are not available) along with the Mr correlation for MEPDG Level 2 subgrade strength characterization. This is because the materials used to develop these relationships were mostly fine-graded, and hence, using these equations with similar materials would yield more reliable results (24).

Indiana DOT

IDOT fully implemented MEPDG in 2009-2010, and materials database were developed in 2000. Kim and Siddiki (26) evaluated 14 cohesive subgrade soils from Indiana by conducting Mr, UCS, standard Proctor, DCP, and other routine tests. These researchers proposed three Mr estimation models based on the UCS tests. They also developed a predictive model to estimate k_1, k_2, and k_3 using twelve soil parameters.

Michigan DOT

The MEPDG was fully implemented by MDOT in 2014. The current procedures for determining Mr values for Michigan unbound materials are mostly applicable for Level 3 input. Baladi et al. (27) conducted a study on Michigan subgrade Mr design values and developed Mr correlation equations based on the soil classification. For this to be accomplished, the state of Michigan was divided into fifteen clusters where the soils in these divisions had similar physical and engineering characteristics. These clusters were further divided into ninety-nine areas and soil samples were collected and tested from each area. Tests included moisture content determination, grain-size distribution, Atterberg limits, and Mr measurement using RLT tests. Finally, Mr correlation equations were developed for different USCS soil classifications, as shown in table 6.

Table 6. Mr Correlations Summary for Different Soil Types (27).

USCS	Number of		Predictive equation	Variable equation
	Clusters	Areas		
SP1	6	8	$MR = 89.825(SVSP1)^{2.9437}$	$SVSP1 = \frac{\gamma_d^{1.15}}{\left(P_4^{1.5} - P_{40}^{0.25}\right)^{0.5}}$
SP2	6	12	$MR = 0.8295(SVSP2)^{3.6006}$	$SVSP2 = \frac{\gamma_d^{1.35} * P_{200}^{-0.1}}{\left(P_4^{1.5} - P_{40}^{0.25}\right)^{0.5}}$
SM	11	16	$MR = 0.0303(SVSM)^{4.1325}$	$SVSM = \frac{\gamma_d^{0.8}}{S^{0.15}}$
			$MR = 45722\exp[(-0.0258)(MI)]$	$MI = LL^{1.1} + MC^{1.25}$
SC,CL, ML	10	28	$MR = 650486\exp -0.0501(S)$	$S = \left[\frac{G_s * (MC/100) * \gamma_d}{G_s * \gamma_w - \gamma_d}\right] * 100$
SP-SM	7	8	$MR = 1749.6\exp 0.0054(SVSP-SM)$	$SVSP-SM = \frac{\gamma_d^{1.75}}{MC^{0.5} + LL^{0.6} + (P_{40} - P_{200})^{0.01}}$
SC-SM	5	7	$MR = 39638\exp - 0.0037(SVSC-SM)$	$SVSC-SM = C_u^{0.2} * \left(LL^{1.15} + MC^{1.3}\right)$

γ_d = dry unit weight (pcf), P_4, P_{40}, P_{200} = percent passing sieves number 4, 40, and 200, S = saturation (%), LL = liquid limit, MC = moisture content, G_s = specific gravity of the solid ≈ 2.7, γ_w = unit weight of water = 62.4 pcf, C_u = coefficient of uniformity

Missouri DOT

MODOT implemented the MEPDG in 2004 with national models, made the initial local calibration in 2009, and made a second local calibration in 2019. In the recent local calibration study, it was stated that the unbound base and subgrade materials Mr was either measured by input Level 1 through FWD backcalculation or by input Level 3 from the LTPP database (28).

Richardson et al. (29) assessed the Mr values for common Missouri typical unbound granular base and subgrade soils. The study included 27 common subgrade soils and 5 unbound base materials. Following AASHTO T307, Mr values for the tested soils were obtained at optimum moisture content and at an elevated moisture content to account for the worst-case scenario. The regression model resulted in a coefficient of determination greater than 0.9 for all tested materials as recommended by the standard. The study concluded that the amount of fines and the material source had a significant impact on the resilient modulus, and that the regression coefficients (k1, k2, and k3) obtained for the tested soils be used for MEPDG input Level 1.

Montana DT

The MDT is another state DOT planning to implement the MEPDG. A study conducted by Akin et al. (30) compared over 30 Mr correlation equations to laboratory results for soils from two Montana soil survey reports. The researchers concluded that the results obtained from the reviewed correlation equations were inconsistent and recommended to refrain

from using existing correlations without evaluating their applicability and reliability to the tested material.

Oklahoma DOT

A study conducted by Hossain et al. (31) investigated the unbound materials Mr regression models and recommended Mr inputs for ODOT, which is planning to implement the MEPDG. The study looked into Mr data from 105 samples comprised of limestone and sandstone materials. Four different models were checked, and the study concluded that the octahedral model is recommended to be used for MEPDG input Level 1 and provided coefficients that can be readily used by ODOT. The study also recommended that the obtained Mr values be used in MEPDG input Level 3. In addition, the universal model (containing bulk stress and deviatoric stress) was found to have the best developed model coefficient correlations with other soil properties and was recommended to be used for input Level 2 (Equations 32, 33, and 34). The coefficients of determination for the equations are 0.38, 0.78, and 0.42, respectively.

$$k_1 = 259.440(P_{200}) - 1.951(UCS) \quad \text{(Eq. 32)}$$

$$k_2 = 0.530 - 0.902(k_3) \quad \text{(Eq. 33)}$$

$$k_3 = -0.044(OMC) + 0.087(PI) \quad \text{(Eq. 34)}$$

Utah DOT

The MEPDG has been fully implemented by UDOT since 2011. Darter et al. (32) published the UDOT M-E pavement design guide draft, where the recommended Level 2 and 3 Mr

inputs for unbound materials were explained with the Level 2 input being backcalculation from FWD testing.

The UDOT Pavement Design Manual of Instruction (33) also recommends using backcalculation from FWD testing, with adjustment for moisture content and laboratory conditions, as the most practical and accurate way of defining the Mr in input Level 2. In addition, the CBR relation presented in section 2.4.2 (Equation 15) is stated to be used for subgrade materials with CBR less than 30% as an input Level 2. The manual also offers some default Mr values to be used for input Level 3.

A study by Jackson (34) evaluated two aggregate base materials from each of the four UDOT regions. Some important properties including particle-size distribution, soil classification, moisture-density relationship, CBR, and Mr were evaluated. The study concluded that the CBR did not have good correlation with the Mr, and instead, a correlation equation to estimate the Mr was developed based on other properties (Equation 35). This prediction equation had a coefficient of determination of 0.968.

$$Mr = (-200 - 1.51 * P_{200} - 418 * D_{30} - 3.09 * OMC + 1.94 * MDD) * \gamma_{dr} \quad \text{(Eq. 35)}$$

Where;

- D_{30}= particle diameter corresponding to 30 percent finer (inch)
- OMC= optimum moisture content (%)
- MDD= maximum dry density (pcf)
- γ_{dr}= ratio of dry density to MDD, expressed as a fraction

Virginia DOT

VDOT implemented the MEPDG in 2018. A study by Virginia Transportation Research Council (VTRC) assessed over 100 different soils from all over Virginia for Mr, soil index properties, standard Proctor, and CBR. It was concluded that the CBR, which was used by VDOT to obtain the Mr, had no correlation with the Mr. The quick shear test was the only test that correlated well with the Mr results, and hence was recommended to be used through correlation equations for MEPDG Level 2. Three Mr prediction equations were developed from the quick shear test results, and the one shown in Equation 36 is the one developed for the Mr model used in the MEPDG (35).

$$Mr = 1622.8 * S_{u1\%} - 2707.1 \quad \text{(Eq. 36)}$$

Where; $S_{u1\%}$= stress at 1% strain

Another VTRC study was published as a supplement to the previous one, where it was found that the simpler UCS test can be used instead of the quick shear test to evaluate the Mr of fine cohesive soils. Hence, a model was developed relating Mr to the initial tangent modulus (both in psi) produced on the stress-strain curve obtained from the UCS test for samples prepared with Static Compactor or a Proctor Hammer (Equations 37 and 38). Using this relation for MEPDG Level 2 was recommended, in addition to conducting further investigations and building a more extensive Mr (or k-values) database (36).

$$Mr\ (Static) = 2558.13 + 154.15(Initial\ Tangent\ Modulus) \quad \text{(Eq. 37)}$$

$$Mr\ (Proctor) = 361.18(Initial\ Tangent\ Modulus) \quad \text{(Eq. 38)}$$

In 2015, VTRC conducted yet another research aiming to provide VDOT with a resilient modulus catalog for aggregate base. This study evaluated 16 aggregate bases from different geophysical regions in Virginia and reported their Mr values, as well as checking the effect of fines, plasticity, and moisture content on the Mr. It was recommended that VDOT implement this catalog of Mr values for use with the MEPDG (37).

Washington DOT

WSDOT is in the process of implementing the MEPDG, with their design catalog updated in 2009 being used as a baseline (38). In this catalog, WSDOT presents a correlation equation used for estimating the Mr from the R-value (Equation 39).

$$Mr = 720.5\left[e^{(0.0521*R)} - 1\right] \quad \text{(Eq. 39)}$$

Wisconsin DOT

WisDOT first implemented the MEPDG in 2014. For unbound material characterization, a study was conducted by Wisconsin Highway Research Program (WHRP) in 2004 that looked into correlations between Mr and other properties. Testing was done on 37 aggregate sources; however, correlations were found to be weak and not suited for predicting Mr accurately. The data from this study was ultimately considered as a base of information for WisDOT when implementing a M-E design process (39).

Another WHRP study in 2006 conducted testing on soils selected by the WisDOT to represent common soil distributions in Wisconsin, in order to develop constitutive models' coefficients estimation equations. The analysis did not yield good results when the whole

database was used; however, results were better when the coarse- and fine-grained materials were separated. The equations developed relating the coefficients to other soil properties showed reasonable accuracy in estimating the subgrade Mr. In addition, a comparison with LTPP models showed that the developed models performed better, and hence were recommended for use with MEPDG Level 2 (40).

Wyoming DOT

WYDOT has implemented the MEPDG in 2012. In 2016, a comprehensive field and laboratory testing program was conducted in Wyoming, where a total of 36 pavement sites with different subgrade AASHTO soil types and pavement structures were examined (41). Tests in field and laboratory included FWD, DCP, R-value, standard Proctor, and Mr test in accordance with AASHTO T307. Correlations between Mr and other parameters were established. Two correlation equations with R-value were developed (Equations 40 and 41), with very similar residual standard error (3347 and 3335).

$$Mr = 9713.91 + 61.56R \quad \text{(Eq. 40)}$$

$$Mr = 6644R^{0.1748} \quad \text{(Eq. 41)}$$

In addition, using the FWD data to backcalculate in-place Mr and adjusting it to laboratory conditions was recommended for MEPDG Level 2 input (Equation 42). Furthermore, tables of unbound materials characteristics were reported for MEPDG Level 3 input.

$$Mr(lab) = 0.49Mr(field) \quad \text{(Eq. 42)}$$

2.6. Nevada DOT District 1 Mr Correlations

NDOT typically predicts Mr of unbound materials from the R-value using Equation 1 presented previously, which was developed for a specific type of materials from specific geographic regions that were found to be different from the materials encountered in Nevada. Thus, in 2017, NDOT took a major step towards updating the process of estimating the design Mr of unbound materials for flexible and rigid pavement design for NDOT District 1. This research study developed design Mr prediction models for unbound materials including base, subbase (borrow), and subgrade for District 1. The findings and recommendations from this study have been published in NDOT Report No. P361-16-803; "*Characterization of Unbound Materials (Soils/Aggregates) for Mechanistic-Empirical Pavement Design Guide (MEPDG)*", January 2018 (3), and are summarized in this section as follows:

- The stress dependent behavior of the Mr was well defined by the Theta model for base and borrow materials, while the subgrade soils fit very well both the Universal and Uzan models.
- The design Mr for base and borrow materials is significantly influenced by the pavement structure while the design Mr for subgrade is not influenced by the pavement structure.
- In combination with other physical properties, the R-value was a more reliable predictor of the design Mr property for base, borrow, and subgrade materials compared to the UCS.

- The design Mr for new and rehabilitation designs for subgrade materials can be obtained from the R-value or the UCS along with other physical properties using the following prediction models (Equations 43, 44, 45, and 46):

$$ln(Mr_{SG-New}) = 7.4081 + 0.0037 * P\#200 - 0.0129 * P\#3/8 + 0.0160 * \gamma_d + 0.0972 * UCS + 0.0307 * PI \quad \text{(Eq. 43)}$$

$$ln(Mr_{SG-New}) = 3.1211 + 0.018 * R - value + 0.0037 * P \nparallel 40 + 0.0317 * \gamma_d + 0.0429 * PI \quad \text{(Eq. 44)}$$

$$ln\,(Mr_{SG-Reh}) = 9.2335 + 0.0028 * P\#200 - 0.0045 * P\#3/8 - 0.0401 * OMC + 0.0318 * UCS + 0.0158 * PI \quad \text{(Eq.45)}$$

$$ln\,(Mr_{SG-Reh}) = 5.3982 + 0.0134 * R - value + 0.0125 * P\#40 - 0.0032 * P\#3/8 + 0.0168 * \gamma_d + 0.0177 * PI \quad \text{(Eq. 46)}$$

- The design Mr for new and rehabilitation designs for base materials can be obtained from the R-value along with other physical properties using the following prediction models (Equations 47 and 48):

$$ln(Mr_{CAB-New}) = 7.5134 + 0.0357 * R - value - 0.0650 * P \nparallel 40 + 0.0249 * P\#3/8 - 0.0853 * OMC - 0.0313 * H_{eq} \quad \text{(Eq. 47)}$$

$$ln(Mr_{CAB-Reh}) = 8.0140 + 0.0261 * R - value \ - 0.0485 * P \# 40 \quad \text{(Eq. 48)}$$

$$+ 0.0161 * P\#3/8 - 0.0659 * OMC - 0.0089 * H_{eq}$$

- The design Mr for new and rehabilitation designs for borrow materials can be obtained from the R-value along with other physical properties using the following prediction models (Equations 49 and 50):

$$ln(Mr_{BOR-New}) = 9.0267 + 0.0099 * R - value + 0.0124 * P \# 3/8 \quad \text{(Eq. 49)}$$

$$-0.0688 * OMC - 0.0207 * H_{eq}$$

$$ln(Mr_{BOR-Reh}) = 9.2304 + 0.0136 * R - value - 0.0229 * P \# 40 \quad \text{(Eq. 50)}$$

$$+ 0.0079 * P\#3/8 - 0.0661 * OMC - 0.00127 * H_{eq}$$

- The equivalent thickness (Heq) is calculated for the layer being analyzed based on the depth (D) to the location for state of stress calculation (base and borrow) using the following equations (Equations 51, 52, 53, and 54):

$$H_{eqNew-CAB} = 2.3027 * D - 2.3859 \quad \text{(Eq. 51)}$$

$$H_{eqNew-Bor} = 1.4552 * D + 7.3821 \quad \text{(Eq. 52)}$$

$$H_{eqReh-CAB} = 2.399 * D - 1.7468 \quad \text{(Eq. 53)}$$

$$H_{eqReh-BOR} = 1.543 * D + 8.044 \quad \text{(Eq. 54)}$$

The definitions of the parameters used in the above equations along with the units used and the test procedures are shown in table 7. Table 8 shows the range of the data used in the statistical analysis to develop the prediction models.

Table 7. Definitions of the Parameters Used in the NDOT District 1 Mr Prediction Equations (3).

Parameter	Definition	Units	Test Procedure
R-value	Resistance R-Value	–	Nev. T115D
P40	Percent passing No. 40 sieve	Percent	Nev. T206; ASTM D421; ASTM D422
P3/8	Percent passing 3/8 inch	Percent	Nev. T206; ASTM D421; ASTM D422
γd-max	Maximum dry density	pcf	Nev. T108B
OMC	Optimum moisture content	Percent	Nev. T108B
PI	Plasticity index	–	Nev. T212I
Heq	Equivalent thickness	inch	–

–Not applicable

Table 8. Range of Data Used in the Statistical Analysis for NDOT District 1 Mr Prediction Equations (3).

Parameter	Range of Data					
	Subgrade		Base		Borrow	
	Min	Max	Min	Max	Min	Max
R-value	44	82	71	85	78	83
P#200(%)	5.4	66.9	5.3	10	7.3	16.4
P#40(%)	15.2	84.2	12.6	19.3	15.4	28.7
P# 3/8(%)	52.2	99.3	54.1	76.3	69.8	99.9
Maximum dry density (pcf)	119.4	139.2	135.8	147.5	133.8	143.2
Optimum moisture content (%)	6.1	10.7	3.5	6.7	5.4	7.2
UCS (psi)	2.7	8.9	2.8	9.7	1.3	6.6
PI	1	4.7	0	0	0	3.3
H_{eq} (inch)	48.5	71.3	17.1	31.8	38.3	47.3
Mr (new design)	7,700	12,750	11,600	27,250	11,700	20,400
Mr (rehabilitation)	5,400	8,400	14,000	22,900	10,600	15,500

Figure 2 shows a comparison between Mr values predicted using the previously used NDOT Mr-R correlation (Equation 1), and the correlations developed in the research for District 1. The graph shows that the previous NDOT correlation consistently overestimates the Mr for all materials for both new and rehabilitation designs. This reinforces the importance of developing Mr prediction equations specifically for Nevada's materials.

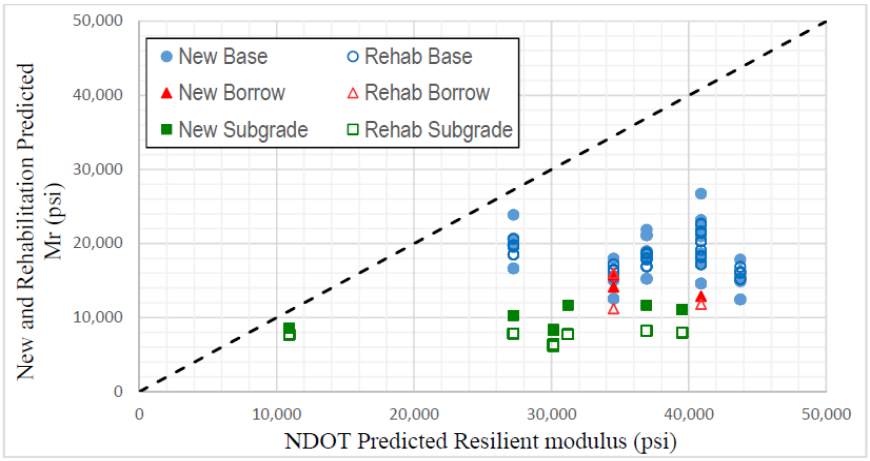

Figure 2. Comparison between current NDOT Mr prediction model and the newly developed District 1 New and Rehabilitation Mr prediction models using R-value (3).

The impact of the accuracy of the estimated Mr for unbound materials was investigated using the AASHTOWare® Pavement ME design software, where a design for 10 million ESALs was done for a pavement structure to have no more than 10% fatigue cracking in 20 years life. The designs were done as follows:

1. A control pavement structure was designed with a base Mr of 26000 psi, which is the value used in the current NDOT manual regardless of the R-value, with a subgrade Mr of 12000 psi.

2. A new design with Mr estimated from the developed models with R-value, resulting in a base Mr of 18963 psi and a subgrade Mr of 8618 psi.

While keeping the same base layer thickness of 16 inches, the required AC layer thickness increased by 0.5 inches (from 6.5 to 7 inches) when using the newly developed Mr models.

Chapter 3: Material Collection

Nevada Department of Transportation (NDOT) divides Nevada into three districts as shown in figure 3. This research study targeted unbound materials commonly used in NDOT District 2 and District 3. A total of 28 unbound materials were collected including base, borrow, and subgrade. Table 9 lists the source, district, and type of sampled materials.

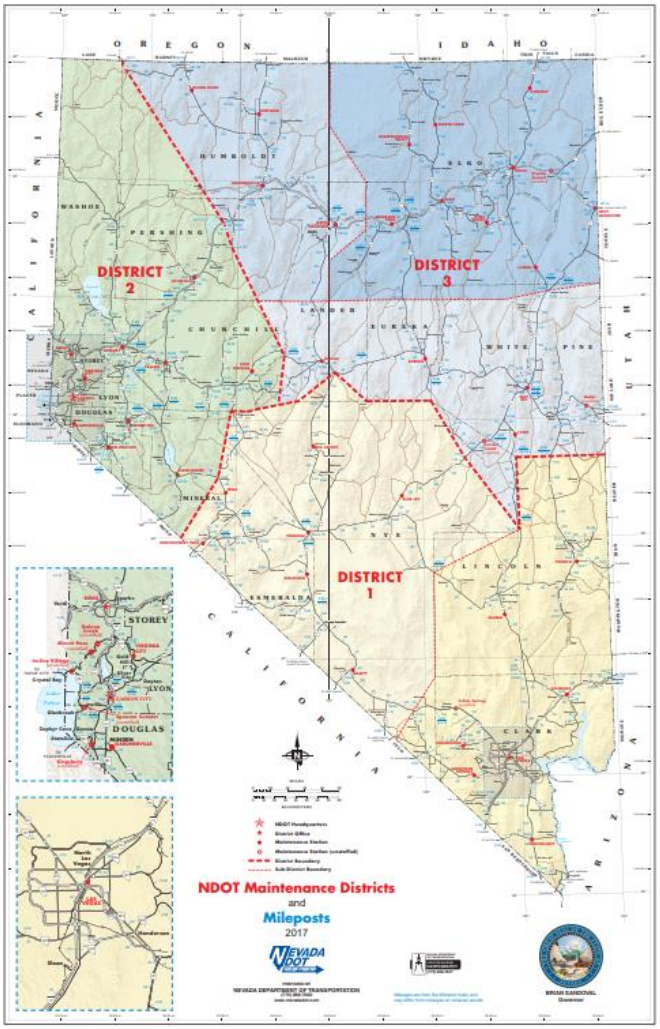

Figure 3. NDOT Districts (dot.nv.gov).

Table 9. Collected Materials.

Source	District	Material	Source	District	Material
Lockwood	2	Base	Lemmon Dr.	2	Subgrade 1
		Borrow	Lemmon Dr.	2	Subgrade 2
Goni Pit	2	Base	Spaghetti Bowl	2	Subgrade
		Borrow	Sonoma Pit	3	Base
Spanish Springs	2	Base			Borrow
		Borrow	Carlin Pit	3	Base
Imlay Pit	2	Base	Vega Construction Shop	3	Base
		Borrow			Borrow
Trico Pit	2	Base A	Silver State Rock products	3	Base
		Base B			Borrow
		Borrow	Elko	3	Borrow 1
Fallon Big Dig	2	Subgrade 1	Elko	3	Borrow 2
Fallon Big Dig	2	Subgrade 2	Contract #3817	3	Subgrade
Kings Row	2	Subgrade	Contract #3824	3	Subgrade

Materials were collected from various locations in order to cover wide geographical areas within Districts 2 and 3. The locations of the collected materials are shown in figure 4.

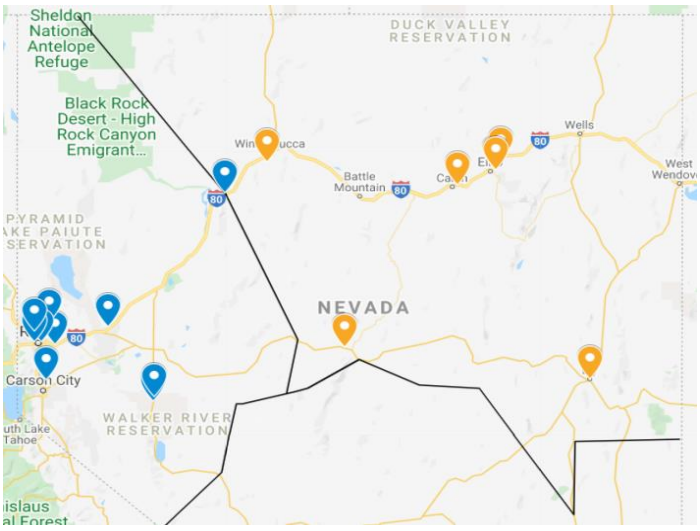

Figure 4. Map Showing Locations of Collected Materials from Districts 2 and 3.

Chapter 4. Laboratory Testing

This chapter presents the testing conducted on the collected materials from NDOT Districts 2 and 3. In summary, the tests performed were: soil classification through sieve analysis and Atterberg limits, specific gravity, modified proctor test for moisture-density relationship, unconfined compressive strength (UCS), Resistance value (R-value), and repeated load triaxial (RLT) for Mr. The following sections describe the tests standards and summarizes the measured results.

4.1. Soil Classification Testing

All collected materials were tested for particle size distribution through sieve analysis testing, and for Atterberg limits. Materials were then classified using the AASHTO classification and Unified Soil Classification System (USCS).

4.1.1. Sieve Analysis

This test was done following NDOT test method Nev. T206H (42), AASHTO T11, and AASHTO T27 (43). Samples were split to the appropriate size according to the NMAS and dried to a constant weight at temperature of 110^{o}C. The dry samples were t

hen weighed and washed over #16 and #200 sieves until the water became almost clear. Afterward, the samples were dried again at 110^{o}C until dry mass, left to cool to room temperature, and pulverized with a rubber head hammer if clumps formed. Finally, the samples were carefully transferred to a set of sieves and placed in a mechanical sieve shaker. The results for the sieve analysis for base, borrow, and subgrade materials for

Districts 2 and 3 are shown in tables 10 to 14, and the 0.45 power charts are presented in figures 4 to 8.

The results indicated that all base and borrow materials met NDOT specifications, except for the Trico Pit's Base A which exceeded the maximum limit for the #200 sieve.

Table 10. District 2 Base Sieve Analysis Results.

Seive Size	NDOT District 2 Base %Passing						NDOT Type 1 Base Specs	
	Lockwood	Goni Pit	Spanish Springs	Imlay Pit	Trico Pit A	Trico Pit B	Min	Max
1.5"	100.0	100.0	100.0	100.0	100.0	100.0	100	
1"	88.7	94.0	98.7	98.3	100.0	100.0	80	100
3/4 "	76.6	88.1	92.2	91.5	99.7	98.2		
1/2 "	72.4	78.3	75.0	78.6	90.8	73.6		
3/8 "	71.4	70.6	63.1	69.9	84.3	62.2		
#4	49.5	42.9	41.5	48.2	61.0	39.7	30	65
#8	37.6	26.6	29.3	33.0	45.5	26.9		
#10	35.4	23.9	26.9	29.9	42.2	25.1		
#16	28.9	17.6	21.9	23.8	35.5	19.7	15	40
#30	21.7	12.8	17.0	18.1	29.0	15.3		
#40	17.1	11.0	15.3	16.3	26.7	13.4		
#50	12.1	9.3	13.6	14.6	24.3	12.0		
#100	5.1	6.4	11.0	12.0	20.2	9.6		
#200	2.9	3.9	8.6	9.8	15.9	7.5	2	12

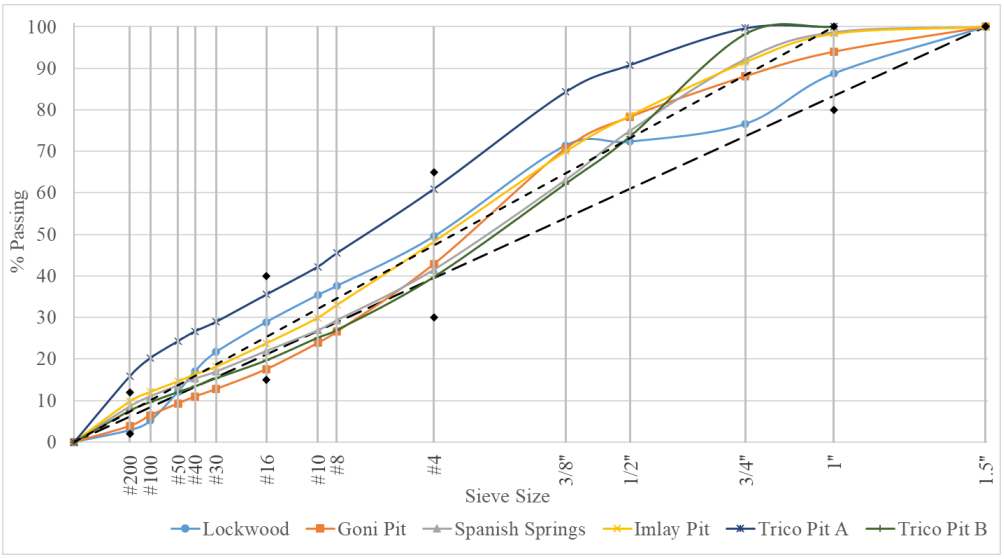

Figure 5. District 2 Base Gradation Curves.

Table 11. District 3 Base Sieve Analysis Results.

Seive Size	NDOT District 3 Base %Passing				NDOT Type 1 Base Specs	
	Sonoma Pit	Carlin Pit	Vega	Silver State	Min	Max
1.5"	100.0	100.0	100.0	100.0	100	
1"	99.1	100.0	100.0	100.0	80	100
3/4 "	92.0	93.3	96.3	100.0		
1/2 "	77.4	78.4	79.9	97.3		
3/8 "	67.8	70.7	69.7	89.8		
#4	48.0	50.8	50.4	63.4	30	65
#8	36.7	38.2	37.5	44.5		
#10	34.1	35.7	34.5	40.4		
#16	28.3	29.9	27.3	31.5	15	40
#30	21.5	23.8	18.6	23.8		
#40	18.8	21.1	14.3	20.8		
#50	16.4	18.6	11.1	18.5		
#100	12.7	14.9	7.7	14.6		
#200	9.4	11.1	5.8	10.8	2	12

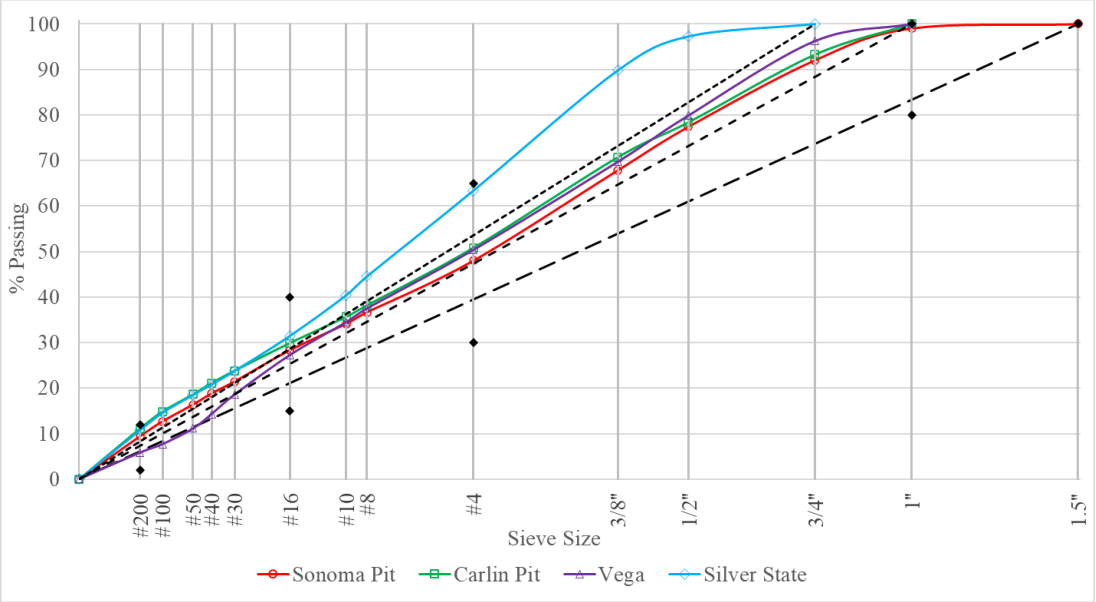

Figure 6. District 3 Base Gradation Curves.

Table 12. District 2 Borrow Sieve Analysis Results.

Seive Size	District 2 Borrow % Passing					NDOT Specs
	Lockwood	Goni Pit	Spanish Springs	Imlay Pit	Trico Pit	
3"	100.0	100.0	100.0	100.0	100.0	100
2"	100.0	100.0	100.0	100.0	100.0	
1.5"	100.0	100.0	98.1	100.0	98.4	
1"	100.0	100.0	86.7	100.0	97.0	
3/4 "	97.4	98.4	80.3	100.0	96.1	
1/2 "	70.8	97.6	70.6	98.8	93.3	
3/8 "	53.2	96.6	64.1	93.4	92.4	
#4	32.4	92.4	50.0	55.9	87.7	
#8	23.4	78.6	39.7	40.2	71.3	
#10	22.1	74.5	37.4	37.8	65.6	
#16	18.5	61.6	32.3	32.2	52.4	
#30	15.0	49.2	26.7	26.9	41.7	
#40	13.0	44.0	24.7	24.6	36.8	
#50	10.9	39.0	22.7	22.3	32.0	
#100	7.7	29.2	18.7	16.4	25.8	
#200	6.0	17.2	13.2	11.7	19.5	

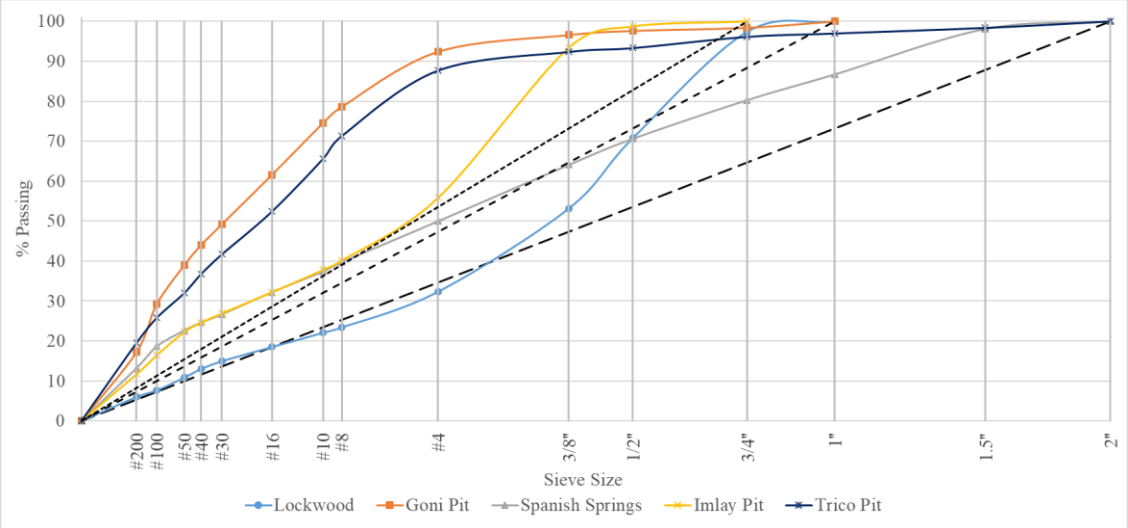

Figure 7. District 2 Borrow Gradation Curves.

Table 13. District 3 Borrow Sieve Analysis Results.

Seive Size	District 3 Borrow % Passing					NDOT Specs
	Sonoma Pit	Vega	Silver State	Elko 1	Elko 2	
3"	100.0	100.0	100.0	100.0	100.0	100
2"	100.0	100.0	100.0	100.0	100.0	
1.5"	100.0	93.9	97.0	100.0	93.9	
1"	100.0	85.4	87.2	100.0	84.7	
3/4 "	100.0	79.7	81.7	100.0	78.0	
1/2 "	87.6	71.6	73.6	99.3	70.6	
3/8 "	78.7	65.8	68.7	93.2	65.9	
#4	53.1	50.2	53.6	71.1	56.0	
#8	35.0	37.6	39.9	54.4	47.5	
#10	32.0	34.3	36.2	50.7	45.5	
#16	22.9	27.2	26.7	41.3	39.5	
#30	16.2	18.8	15.4	31.6	32.7	
#40	14.0	14.6	10.6	27.7	29.5	
#50	12.6	11.5	7.1	24.3	26.6	
#100	11.0	8.4	4.4	19.1	21.4	
#200	9.4	6.3	3.5	14.1	15.6	

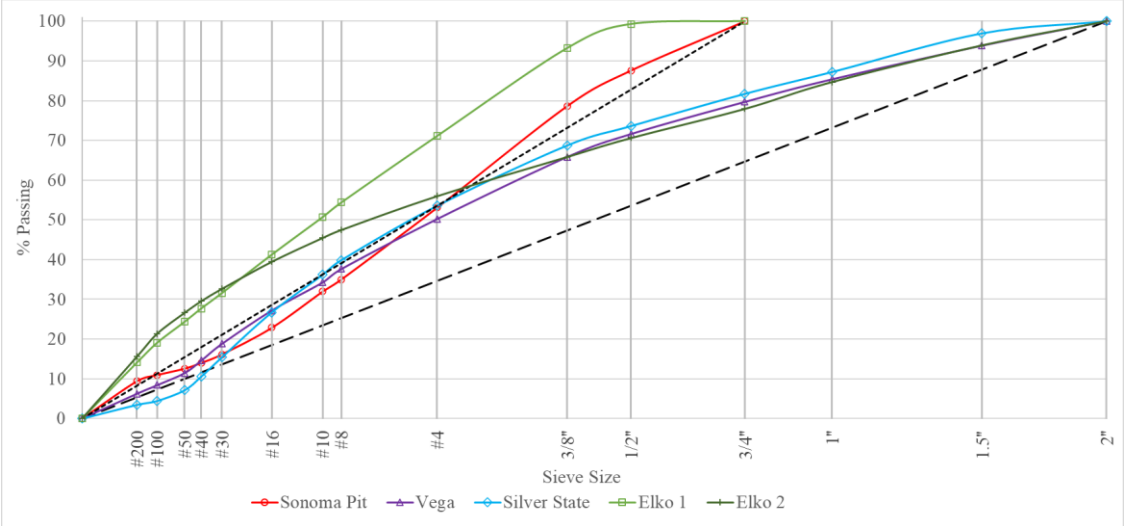

Figure 8. District 3 Borrow Gradation Curves.

Table 14. Districts 2 and 3 Subgrade Sieve Analysis Results.

Districts 2 and 3 Subgrade % Passing								
Sieve Size	3817	3824	Spag. Bowl	Fallon Big Dig1	Fallon Big Dig2	Kings Row	Lemmon Dr.1	Lemmon Dr.2
2.5"	100.0	100.0	100.0	100.0	100.0	100.0	100.0	100.0
2"	100.0	100.0	100.0	100.0	100.0	97.2	100.0	100.0
1.5"	100.0	99.0	97.2	100.0	100.0	97.2	100.0	100.0
1"	100.0	95.3	95.3	98.8	100.0	90.0	100.0	98.7
3/4 "	99.0	93.0	92.9	96.1	100.0	85.4	100.0	98.0
1/2 "	98.1	87.9	86.1	92.9	100.0	78.1	99.3	96.8
3/8 "	97.1	84.0	82.2	90.3	100.0	72.9	99.0	96.5
#4	92.2	71.8	73.0	80.5	100.0	62.1	95.3	95.8
#8	74.3	58.2	63.5	66.9	100.0	53.3	92.0	95.0
#10	68.2	55.6	61.2	63.3	100.0	50.9	91.3	94.6
#16	52.5	48.7	54.1	52.5	99.8	44.7	89.6	91.2
#30	35.4	41.8	43.1	40.4	96.4	36.6	84.7	84.4
#40	29.2	38.8	37.2	33.9	94.1	32.2	81.1	79.5
#50	23.4	36.1	32.0	27.2	91.8	27.7	77.0	73.6
#100	15.3	31.6	24.6	16.6	86.4	20.1	56.8	59.7
#200	11.0	22.3	17.0	9.4	78.1	14.0	36.0	42.2

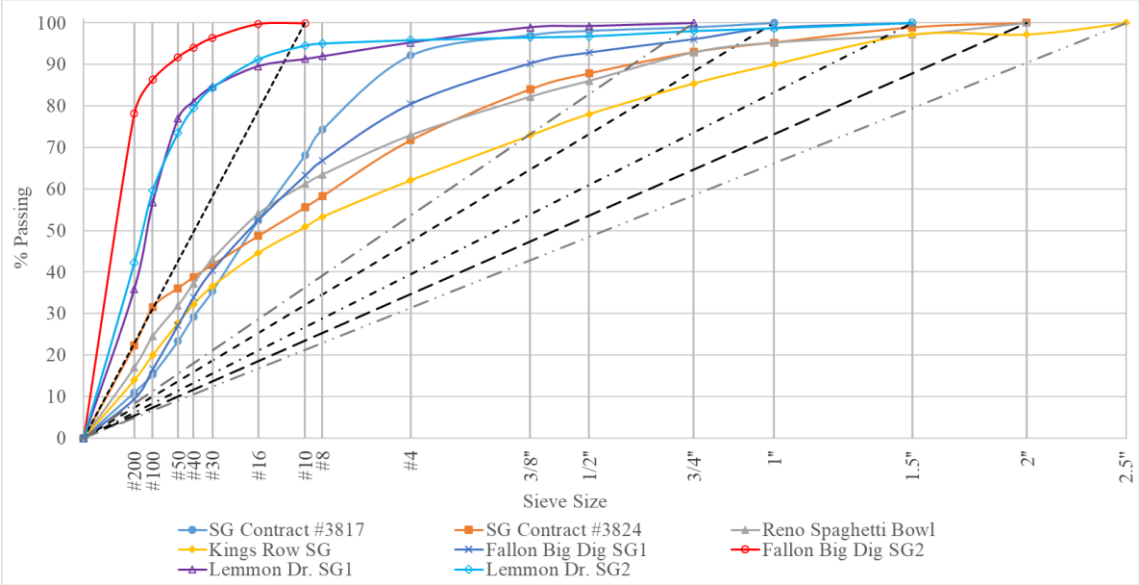

Figure 9. Districts 2 and 3 Subgrade Gradation Curves.

4.1.2. Atterberg Limits

Atterberg limits typically refer to the liquid limit and the plastic limit, which are moisture content values that distinguish the boundaries of the consistency states of plastic soils. The liquid limit (LL) defines the boundary between the plastic state and the semi-liquid state, whereas the plastic limit (PL) defines the boundary between the semi-solid state and the plastic state. The plasticity index (PI) is the range at which the soil behaves as plastic, and is numerically defined as the difference between the LL and the PL. The LL, PL, and PI were obtained according to NDOT standards Nev. T210J and T211J/T212J, respectively (42).

The LL is the moisture content required to close the 13 mm groove on the Casagrande cup apparatus with 25 blows. To get this number of blows, three blow ranges are used to close the 13 mm groove: 25-35 blows, 20-30 blows, and 15-25 blows. A 100 g ± 15 g sample of

materials passing the #40 sieve are obtained and mixed with 25 mL of water until uniform. If the desired consistency is not reached for the first range of blows, more water is added at increments of 1, 2, or 3 mL until testing can commence. The moisture contents from the three ranges are obtained and plotted against the number of blows, then the LL at 25 blows is obtained.

An 8 g sample was taken from the material used for the first blows range for PL testing. This sample is split to 1.5 to 2 g portions and hand-rolled on a glass plate until it forms a 3 mm diameter thread. This procedure is repeated until the thread crumbles at this diameter, and the PL is identified. Finally, the PI is obtained as the difference between the LL and the PL reported to the nearest 1%.

The testing apparatus (Casagrande cup and glass plate) used for LL and PL testing, and an example of the LL plot for the Spaghetti Bowl subgrade material are shown in figures 10 and 11, respectively.

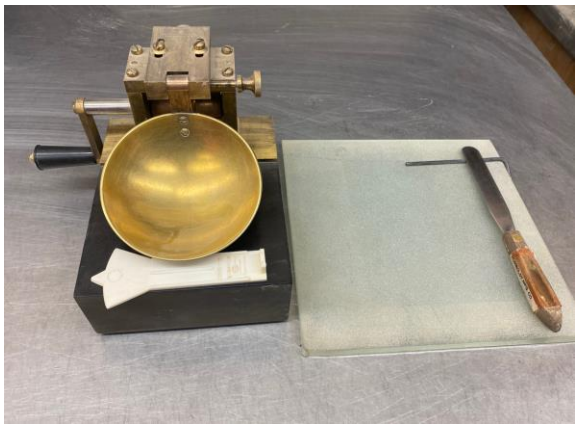

Figure 10. Atterberg Limits Testing Apparatus.

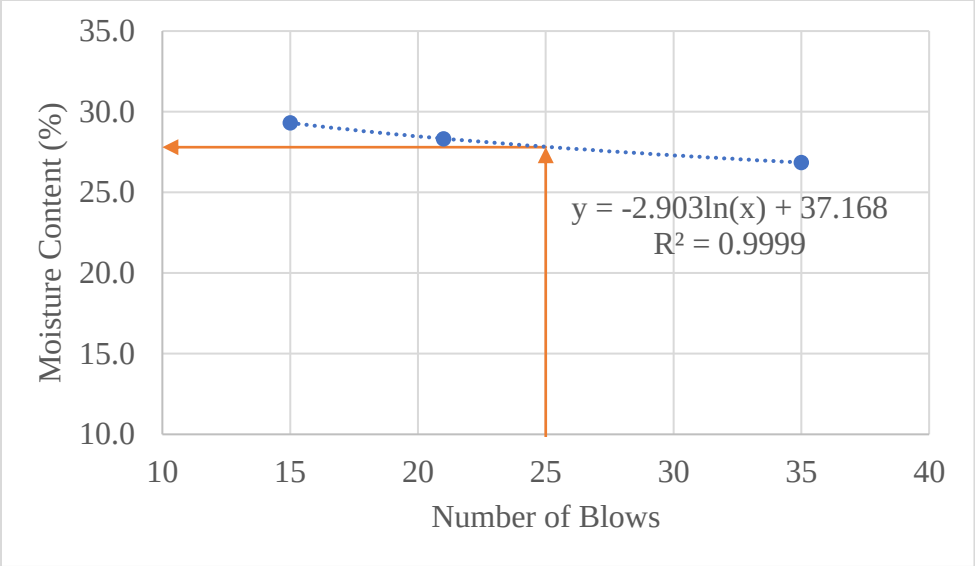

Figure 11. Spaghetti Bowl Subgrade Liquid Limit Plot.

Table 15 presents the Atterberg limits test results. Materials not shown in the table did not exhibit a LL or a PL.

Table 15. Atterberg Limits Test Results.

District	Source	Material	Liquid Limit (%)	Plastic Limit (%)	Plasticity Index (%)
2	Spanish Spring	Base	36.6	27.6	9
2	Spanish Spring	Borrow	34.8	23.4	11
2	Goni Pit	Borrow	24	22.6	2
2	Spaghetti Bowl	Subgrade	27.8	20.5	7
2	Fallon Big Dig 2	Subgrade	75.4	31.3	44
2	Kings Row	Subgrade	32.8	15.4	17
2	Lemmon Dr. 1	Subgrade	67.9	34.8	33
2	Lemmon Dr. 2	Subgrade	47.2	22.8	24
3	Silver State	Base	30.3	25.9	4
3	Sonoma Pit	Borrow	28.8	14.2	15
3	Elko 1	Borrow	29.3	24.3	5
3	Elko 2	Borrow	35.6	27.6	8

NDOT requires base materials to have a maximum LL of 35% and assigns PI limits based on the percent passing #200 sieve as shown in table 16.

Table 16. NDOT PI Specifications for Base Materials.

P#200	Max PI
4	12
5	9
6-8	6
9-11	4
12-15	3

The results show that all base materials pass the NDOT specifications except for the Spanish Springs source, which has 9% passing sieve #200 with a LL of 36.6% (greater than 35%) and a PI of 9% (greater than the 4% limit for 9% P#200).

4.1.3. Soil Classification

All materials were classified according to AASHTO and USCS classification systems. The procedure for AASHTO classification (from AASHTO M145) (43) and USCS (from ASTM D2487) (44) are shown in tables 17 and 18, respectively.

Table 17. AASHTO Soil Classification.

General Classification	*Granular materials (35% or less passing No. 200 Sieve (0.075 mm)*							*Silt-clay Materials More than 35% passing No. 200 Sieve (0.075 mm)*			
Group Classification	*A—1*		*A—3*	*A—2*				*A—4*	*A—5*	*A—6*	*A—7*
	A—1—a	*A—1—b*		*A—2—4*	*A—2—5*	*A—2—6*	*A—2—7*				*A—7—5 A—7—6*
(*a*) Sieve Analysis: Percent Passing											
(*i*) 2.00 mm (No. 10)	50 max										
(*ii*) 0.425 mm (No. 40)	30 max	50 max	51 min								
(*iii*) 0.075 mm (No. 200)	15 max	25 max	10 max	35 max	35 max	35 max	35 max	36 min	36 min	36 min	36 min
(*b*) Characteristics of fraction passing 0.425 mm (No. 40)											
(*i*) Liquid limit				40 max	41 min	40 max	41 min	40 max	41 min	40 max	41 min
(*ii*) Plasticity index	6 max		N.P.	10 max	10 max	11 min	11 min	10 max	10 max	11 min	11 min*
(*c*) Usual types of significant Constituent materials	Stone Fragments Gravel and sand		Fine Sand	Silty or Clayey Gravel Sand				Silty Soils		Clayey Soils	
(*d*) General rating as subgrade.	Excellent to Good							Fair to Poor			

* If plasticity index is equal to or less than (liquid Limit—30), the soil is A—7—5 (*i.e.* PL > 30%)
If plasticity index is greater than (Liquid Limit—30), the soil is A—7—6 (*i.e.* PL < 30%)

Table 18. USCS Classification Chart.

Criteria for Assigning Group Symbols and Group Names Using Laboratory Tests[A]				Soil Classification	
				Group Symbol	Group Name[B]
COARSE-GRAINED SOILS	Gravels (More than 50 % of coarse fraction retained on No. 4 sieve)	Clean Gravels (Less than 5 % fines[C])	$Cu \geq 4.0$ and $1 \leq Cc \leq 3.0$[D]	GW	Well-graded gravel[E]
			$Cu < 4.0$ and/or [$Cc < 1$ or $Cc > 3.0$][D]	GP	Poorly graded gravel[E]
		Gravels with Fines (More than 12 % fines[C])	Fines classify as ML or MH	GM	Silty gravel[E,F,G]
			Fines classify as CL or CH	GC	Clayey gravel[E,F,G]
More than 50 % retained on No. 200 sieve	Sands (50 % or more of coarse fraction passes No. 4 sieve)	Clean Sands (Less than 5 % fines[H])	$Cu \geq 6.0$ and $1.0 \leq Cc \leq 3.0$[D]	SW	Well-graded sand[I]
			$Cu < 6.0$ and/or [$Cc < 1.0$ or $Cc > 3.0$][D]	SP	Poorly graded sand[I]
		Sands with Fines (More than 12 % fines[H])	Fines classify as ML or MH	SM	Silty sand[F,G,I]
			Fines classify as CL or CH	SC	Clayey sand[F,G,I]
FINE-GRAINED SOILS	Silts and Clays Liquid limit less than 50	inorganic	PI > 7 and plots on or above "A" line[J]	CL	Lean clay[K,L,M]
			PI < 4 or plots below "A" line[J]	ML	Silt[K,L,M]
		organic	$\frac{\text{Liquid limit – oven dried}}{\text{Liquid limit – not dried}} < 0.75$	OL	Organic clay[K,L,M,N] / Organic silt[K,L,M,O]
50 % or more passes the No. 200 sieve	Silts and Clays Liquid limit 50 or more	inorganic	PI plots on or above "A" line	CH	Fat clay[K,L,M]
			PI plots below "A" line	MH	Elastic silt[K,L,M]
		organic	$\frac{\text{Liquid limit – oven dried}}{\text{Liquid limit – not dried}} < 0.75$	OH	Organic clay[K,L,M,P] / Organic silt[K,L,M,O]
HIGHLY ORGANIC SOILS	Primarily organic matter, dark in color, and organic odor			PT	Peat

Tables 19, 20, and 21present the AASHTO and USCS classifications for the base, borrow, and subgrade soils, respectively.

Table 19. Base Materials Classifications.

Base	District	AASHTO	USCS
Lockwood	2	A-1-a	GW
Goni	2	A-1-a	GW
Imlay	2	A-1-a	GP-GM
Spanish Springs	2	A-2-4	GP-GM
TricoA	2	A-1-b	SM
TricoB	2	A-1-a	GP-GM
Sonoma	3	A-1-a	GW-GM
Carlin	3	A-1-a	GP-GM
Vega	3	A-1-a	GW-GM
Silver State	3	A-2-4	SP-SM

Table 20. Borrow Materials Classifications.

Borrow	District	AASHTO	USCS
Lockwood	2	A-1-a	GP-GM
Goni	2	A-1-b	SM
Imlay	2	A-1-a	GW-GM
Spanish Springs	2	A-2-6	GC
Trico	2	A-1-b	SM
Sonoma	3	A-2-6	GP-GC
Vega	3	A-1-a	GW-GM
Silver State	3	A-1-a	SP
Elko 1	3	A-2-4	SM
Elko 2	3	A-2-4	GM

Table 21. Subgrade Materials Classifications.

Subgrade	District	AASHTO	USCS
Spaghetti Bowl	2	A-2-4	SC
Kings Row	2	A-2-6	SC
Fallon Big Dig 1	2	A-2-4	SP-SM
Fallon Big Dig 2	2	A-7-5	CH
Lemmon Dr 1	2	A-7-5	SM
Lemmon Dr 2	2	A-7-6	SC
# 3817	3	A-2-4	SW-SM
# 3824	3	A-2-4	SM

4.2. Specific Gravity and Absorption

The specific gravity (G_s) is the ratio of the mass of a unit volume of a material to the mass of the same volume of water. The bulk dry, bulk saturated surface-dry (SSD), and apparent specific gravity values were calculated for each material. The test was done for both the coarse and fine portions of the materials, following AASHTO T85 and T84, respectively (43).

For the coarse aggregates, a sample mass depending on the NMAS was obtained and submerged in water for 16 to 19 hours, then dried to SSD condition using a damp towel and weighed. The SSD aggregates were then weighed underwater at 23 ± 1.7^{o}C, and oven-dried to a constant mass at 110 ± 5^{o}C to obtain the dry weight.

For the fine aggregates, a sample of minimum 1000 g mass was obtained and mixed with at least of 6% water by dry mass of the sample until uniform, then covered for 15-19 hours. The sample was then dried to SSD condition determined visually using the cone test, where after 25 light hammer drops, the cone is removed, and the fines should slump slightly. A 500 ± 5 g of the SSD sample was then added to a pycnometer with added water, and constant agitation was maintained for 15-20 minutes to let air voids out. The pycnometer was then filled to line mark and weighed. Finally, the sample was oven-dried to a constant mass at 110 ± 5^{o}C and weighed.

The recorded masses from the procedures described above were used to calculate the specific gravities and absorption of the materials. The results are shown in tables 22 to 26.

Table 22. District 2 Base Materials Specific Gravity and Absorption Results.

Base Source	Lockwood	Goni	Imlay	Spanish Springs	Trico A	Trico B
Coarse Gsb, Dry	2.642	2.605	2.594	2.639	2.161	2.526
Coarse Gsb, SSD	2.686	2.642	2.631	2.671	2.348	2.599
Coarse Gsa	2.763	2.705	2.694	2.726	2.657	2.726
Coarse Abs. (%)	1.7	1.4	1.4	1.2	8.6	2.9
Fine Gsb, Dry	2.578	2.632	2.473	2.471	2.222	2.558
Fine Gsb, SSD	2.644	2.663	2.560	2.550	2.395	2.621
Fine Gsa	2.760	2.717	2.709	2.684	2.686	2.731
Fine Abs. (%)	2.6	1.2	3.5	3.2	7.8	2.5

Table 23. District 2 Borrow Materials Specific Gravity and Absorption Results.

Borrow Source	Lockwood	Goni	Imlay	Spanish Springs	Trico
Coarse Gsb, Dry	2.630	-	2.571	2.595	-
Coarse Gsb, SSD	2.682	-	2.617	2.645	-
Coarse Gsa	2.775	-	2.695	2.732	-
Coarse Abs. (%)	2.0	-	1.8	1.9	-
Fine Gsb, Dry	2.456	2.509	2.487	2.340	1.765
Fine Gsb, SSD	2.577	2.576	2.568	2.450	2.058
Fine Gsa	2.793	2.689	2.708	2.629	2.498
Fine Abs. (%)	4.9	2.7	3.3	4.7	16.6

Table 24. District 3 Base Materials Specific Gravity and Absorption Results.

Base Source	Sonoma	Carlin	Vega	Silver State
Coarse Gsb, Dry	2.587	2.461	2.542	2.308
Coarse Gsb, SSD	2.621	2.508	2.569	2.417
Coarse Gsa	2.678	2.582	2.614	2.590
Coarse Abs. (%)	1.3	1.9	1.1	4.7
Fine Gsb, Dry	2.458	2.339	2.402	2.300
Fine Gsb, SSD	2.547	2.409	2.483	2.424
Fine Gsa	2.697	2.515	2.614	2.625
Fine Abs. (%)	3.6	3.0	3.4	5.4

Table 25. District 3 Borrow Materials Specific Gravity and Absorption Results.

Borrow Source	Sonoma	Vega	Silver State	Elko 1	Elko 2
Coarse Gsb, Dry	2.547	2.544	2.494	2.396	2.347
Coarse Gsb, SSD	2.599	2.569	2.535	2.505	2.454
Coarse Gsa	2.687	2.610	2.599	2.688	2.629
Coarse Abs. (%)	2.0	1.0	1.6	4.5	4.6
Fine Gsb, Dry	2.494	2.396	2.486	2.292	2.179
Fine Gsb, SSD	2.569	2.474	2.537	2.424	2.350
Fine Gsa	2.698	2.599	2.621	2.642	2.626
Fine Abs. (%)	3.0	3.3	2.1	5.8	7.8

Table 26. Subgrade Materials Specific Gravity and Absorption Results.

Subgrade Source	Sp. Bowl	Kings Row	Fallon Big Dig 1	Fallon Big Dig 2	Lemmon Dr. 1	Lemmon Dr. 2	#3817	#3824
District	2	2	2	2	2	2	3	3
Coarse Gsb, Dry	2.413	2.444	2.280	-	-	-	-	2.161
Coarse Gsb, SSD	2.516	2.538	2.397	-	-	-	-	2.337
Coarse Gsa	2.690	2.698	2.583	-	-	-	-	2.621
Coarse Abs. (%)	4.3	3.9	5.1	-	-	-	-	8.1
Fine Gsb, Dry	2.324	2.315	2.146	1.788	1.732	2.084	2.510	2.360
Fine Gsb, SSD	2.454	2.458	2.301	2.079	2.049	2.278	2.568	2.445
Fine Gsa	2.672	2.701	2.540	2.523	2.533	2.586	2.664	2.580
Fine Abs. (%)	5.6	6.2	7.2	16.3	18.3	9.3	2.3	3.6

4.3. Moisture-Density Relationship

Compaction is the densification of the material by rearranging the particles to fill voids through mechanical energy. Initially, adding water to the material will increase the density since it will make it easier for the particles to slip and fill the voids. However, maximum density is reached at the optimum moisture content (OMC), after which any addition of water will lead to a decrease in the density due to the displacement of particles. The objective of this test is to obtain the OMC and the corresponding maximum dry density (MDD).

The modified proctor test was conducted following Nev. T108D (42) test method, where the material is screened over a 3/4” sieve, then compacted in a 6 inch mold using a 10 lb rammer at an 18 inch drop height. Figure 12 shows the mold and rammer used for this test.

Figure 12. Modified Proctor Equipment.

Compaction is done in 5 lifts with 56 blows per lift, with the final lift leaving the soil surface at about 0.25 inches above the top of the mold. A straightedge is used to level the surface, the weight after compaction is obtained, and the specimen is extruded for moisture content sampling vertically along the center of the specimen. The procedure is repeated at different moisture content levels, until a minimum of 4 points are obtained for plotting the Moisture-Density curve: one or two below the OMC, one close to the OMC, and one or two above the OMC.

Figures 13, 14, and 15 show typical moisture-density relationship curves for a base, a borrow, and a subgrade material, respectively.

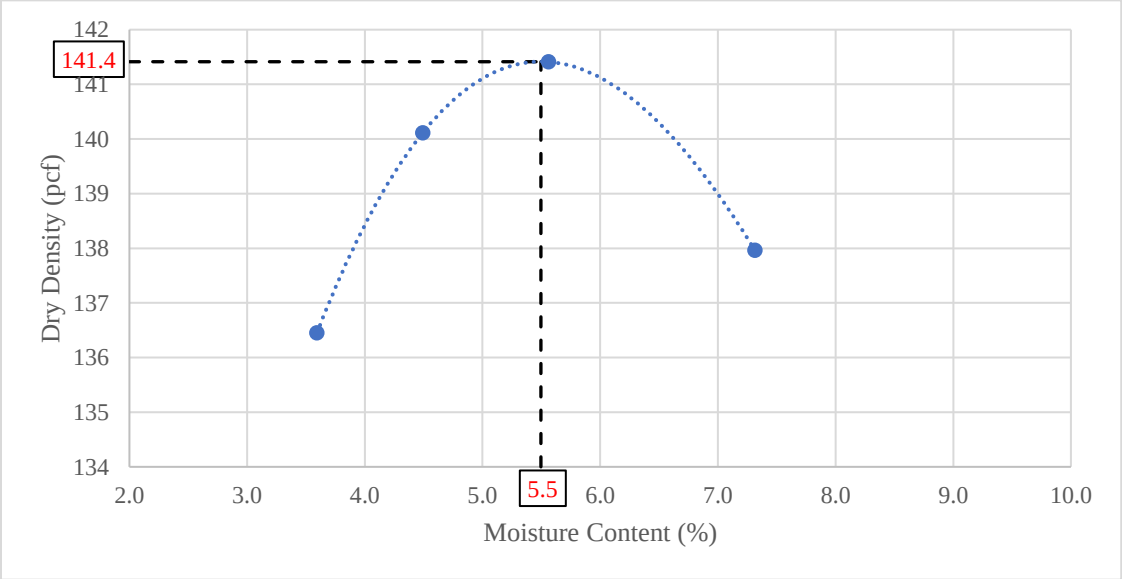

Figure 13. Imlay Base Moisture-Density Curve.

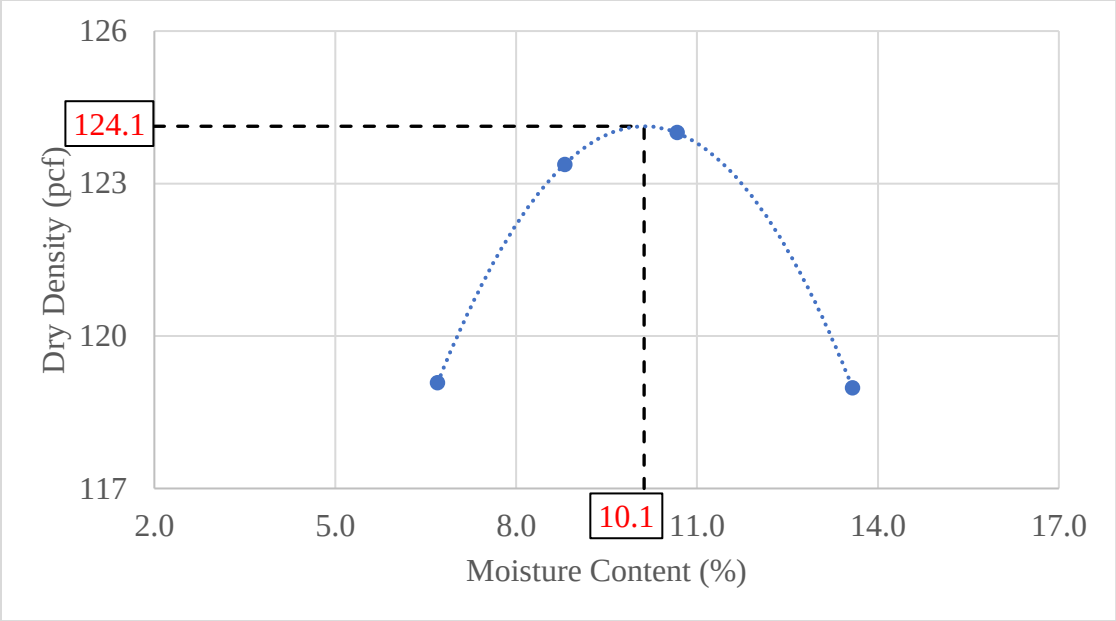

Figure 14. Elko Borrow 1 Moisture-Density Curve.

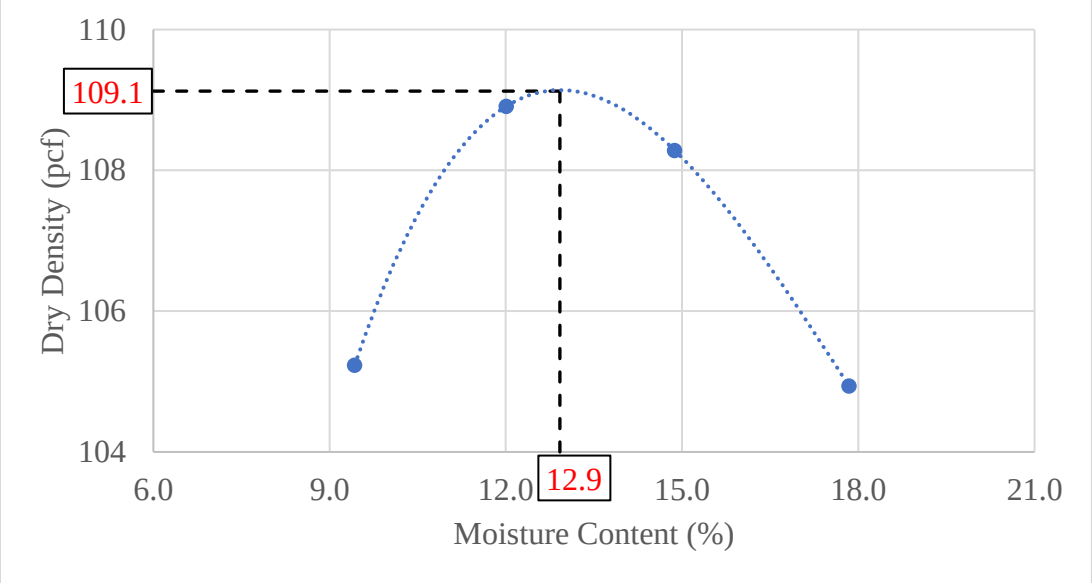

Figure 15. Fallon Big Dig Subgrade 1 Moisture-Density Curve.

After obtaining the OMC and MDD from the moisture-density curve, corrections are done to account for material screened over the 3/4" sieve if they were greater than 5%. The corrections are explained by the test method Nev. T108D for MDD (Equation 55), and for OMC (Equation 56).

$$MDD_{corrected} = \frac{MDD \times G}{MDD \times (1 - P) + (G)(P)} \quad \text{(Eq. 55)}$$

$$OMC_{corrected} = [(1 - P) \times 2] + P \times OMC \quad \text{(Eq. 56)}$$

Where;

- G= Mass per volume of coarse aggregates= Coarse aggregate G_{sa}*62.4 (pcf)
- P= percent passing 3/4" sieve (%)

Summary of the test results for the base, borrow, and subgrade materials are shown in tables 27, 28, and 29, respectively.

Table 27. Base Materials Moisture-Density Relationship Results.

Source	District	OMC (%)	Corrected OMC (%)	MDD (pcf)	Corrected MDD (pcf)
Lockwood	2	8.7	7.2	135.3	142.5
Goni	2	7.1	6.5	131.2	134.7
Spanish Spring	2	6.3	5.9	139.6	141.6
Imlay	2	5.5	5.2	141.4	143.3
Trico A	2	10.6	10.6	123.4	123.4
Trico B	2	8.6	8.6	137.2	137.2
Sonoma	3	6.1	5.8	142.2	143.9
Carlin	3	5.7	5.5	134.5	136.0
Vega	3	5.2	5.2	135.3	135.3
Silver State	3	8.4	8.4	126.6	126.6

Table 28. Borrow Materials Moisture-Density Relationship Results.

Source	District	OMC (%)	Corrected OMC (%)	MDD (pcf)	Corrected MDD (pcf)
Lockwood	2	8.6	8.6	137.7	137.7
Goni	2	7.2	7.2	134.5	134.5
Spanish Spring	2	7.3	6.3	134.6	140.4
Imlay	2	6.8	6.8	141.0	141.0
Trico	2	22.2	22.2	96.7	96.7
Sonoma	3	5.6	5.6	139.9	139.9
Vega	3	5.6	4.9	135.6	140.4
Silver State	3	5.8	5.1	129.1	134.1
Elko 1	3	10.1	10.1	124.1	124.1
Elko 2	3	11.4	9.3	121.5	128.8

Table 29. Subgrade Materials Moisture-Density Relationship Results.

Source	District	OMC (%)	Corrected OMC (%)	MDD (pcf)	Corrected MDD (pcf)
Spaghetti Bowl	2	8.3	7.8	129.2	131.3
Kings Row	2	10.8	9.5	126.4	131.2
Fallon Big Dig 1	2	12.9	12.9	109.1	109.1
Fallon Big Dig 2	2	22.8	22.8	95.0	95.0
Lemmon Dr. 1	2	24.8	24.8	92.7	92.7
Lemmon Dr. 2	2	19.0	19.0	109.1	109.1
#3817	3	7.2	7.2	133.9	133.9
#3824	3	12.2	11.5	119.1	121.4

4.4. Unconfined Compressive Strength

This test was done according to ASTM D2166 (44). The mold used for sample preparation has a 6 inch diameter and a 12 inch height. Samples were screened over a 3/4” sieve, water was added to reach the OMC and MDD, compacted in 10 lifts using a vibratory compactor, then extruded and transferred to the testing machine.

The test is strain-controlled where the samples are unconfined laterally and loaded axially at an axial strain rate of 0.5-2%/min. The UCS is defined as the highest load per unit area before failure.

Figures16 and 17 show a prepared UCS sample after extrusion, and after testing, respectively.

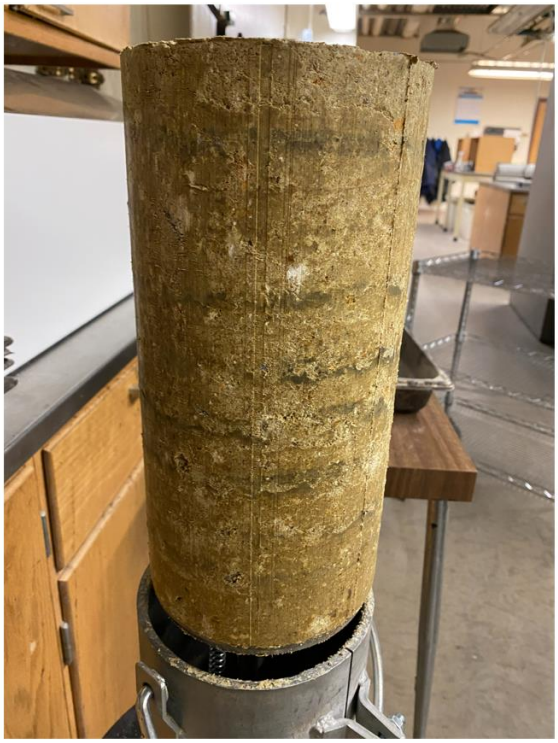

Figure 16. Extruded UCS Sample.

Figure 17. UCS Sample After Testing.

Figures 18 to 20 show the stress-strain curves for Imlay base, Goni borrow, and subgrade #3817, respectively, as examples of the test results. Table 30 summarizes the UCS test results for all the materials tested.

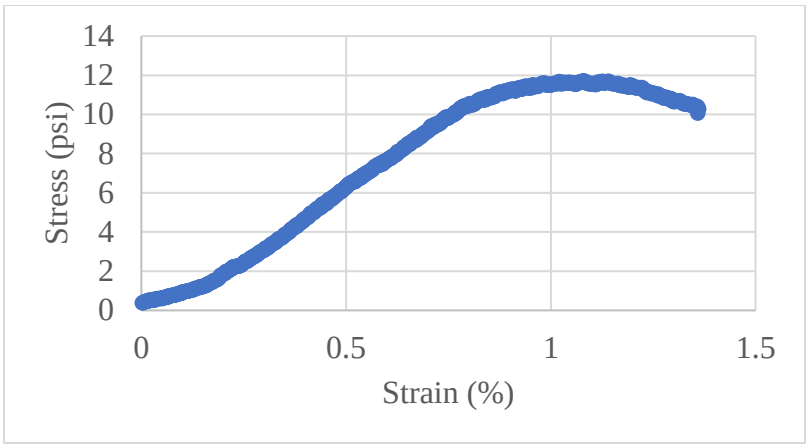

Figure 18. Imlay Base UCS Stress-Strain Curve.

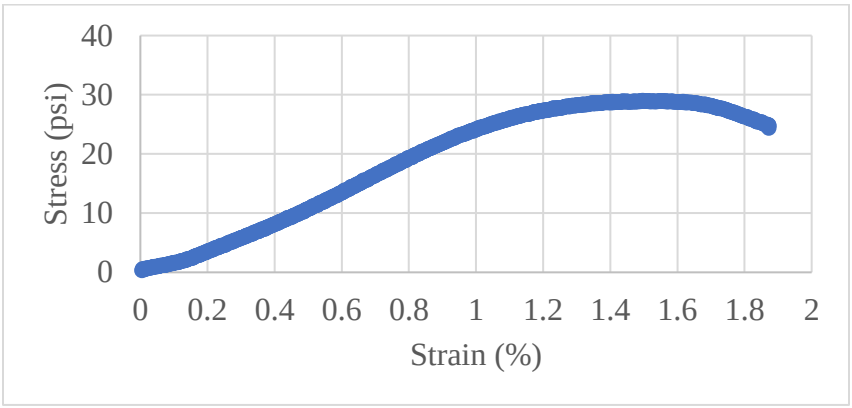

Figure 19. Goni Borrow UCS Stress-Strain Curve.

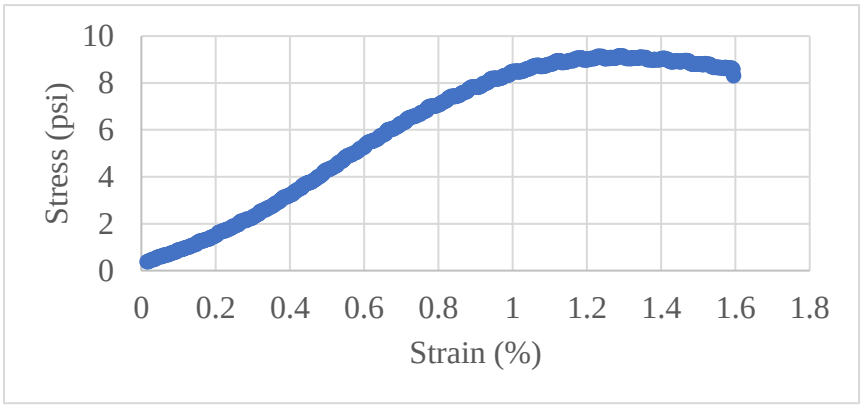

Figure 20. Subgrade #3817 UCS Stress-Strain Curve.

Table 30. UCS Test Results.

Material	District	Source	UCS (psi)
Base	2	Lockwood	2.3
	2	Goni	4.9
	2	Spanish Spring	12.6
	2	Imlay	11.2
	2	Trico A	33.3
	2	Trico B	N.A.[1]
	3	Sonoma	13.1
	3	Carlin	10.2
	3	Vega	5.4
	3	Silver State	32.0
Borrow	2	Lockwood	N.A.[1]
	2	Goni	26.2
	2	Spanish Spring	25.9
	2	Imlay	13.4
	2	Trico	25.2
	3	Sonoma	13.9
	3	Vega	15.7
	3	Silver State	1.8
	3	Elko 1	N.E.M.[2]
	3	Elko 2	N.E.M.[2]
Subgrade	2	Spaghetti Bowl	56.4
	2	Kings Row	35.3
	2	Fallon Big Dig 1	14.4
	2	Fallon Big Dig 2	47.9
	2	Lemmon Dr. 1	54.4
	2	Lemmon Dr. 2	21.6
	3	#3817	8.1
	3	#3824	25.6

[1]Not applicable, sample crumbles when extruded

[2]Not enough material to conduct UCS test

4.5. Resistance Value (R-value) Test

The Resistance value (R-value) is an empirical measure of the strength of unbound materials. It represents the resistance of soils to deformation, defined as a function of the ratio of the applied vertical pressure to the generated horizontal pressure. This material property is used by NDOT for pavement design to characterize the strength of the unbound materials. The R-value for the tested materials was measured in accordance with NDOT test method Nev. T115D (42). Materials were split according to their gradation, and four 1200 g samples were batched for the test, with one sample used as a guide for the three other Stabilometer samples. Different moisture contents were added to the samples and compaction was achieved in a 4 inch diameter by 5 inch height steel mold with a mechanical kneading compactor as shown in figure 21. Specimens were compacted by applying 100 tamps at 200 psi foot pressure.

Figure 21. Kneading Compactor.

The compacted mold was then placed on an exudation device as shown in figure 22, and load was applied at a rate of 2000 lb/min until exudation is achieved. The exudation pressure is then calculated by dividing the exudation load by the specimen's cross-sectional area. The specimens are covered and left in the mold for at least half an hour, then 200 mL of water was added to the specimen in the mold and left undisturbed for 16 to 20 hours to measure the expansion pressure. Following the expansion pressure testing, the specimens were forced into the Hveem Stabilometer, shown in figure 23, where a vertical pressure of 160 psi was applied, and the horizontal pressure and displacement were recorded.

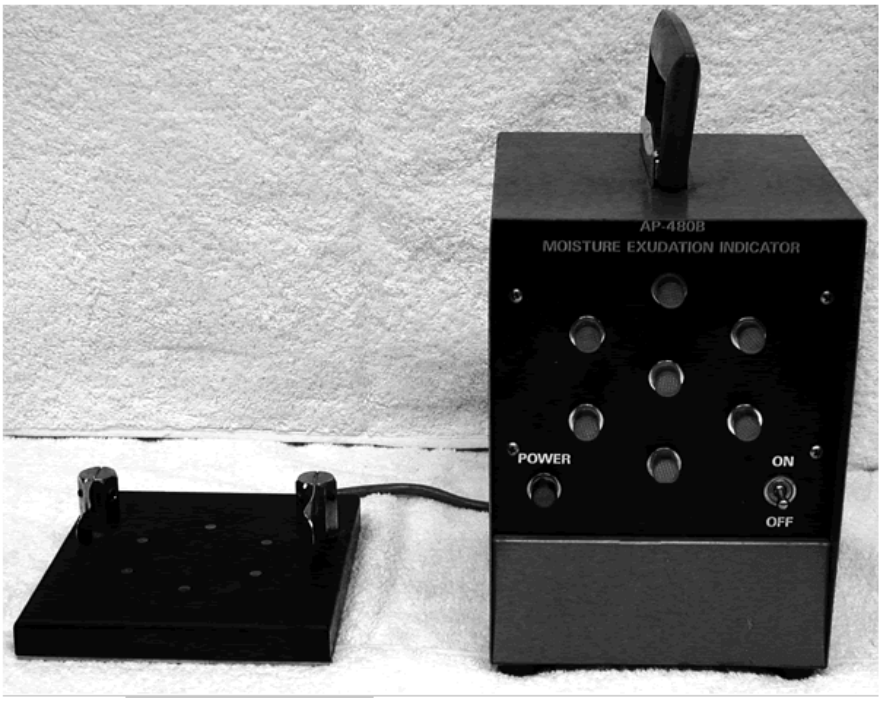

Figure 22. Exudation Indicator Device (3).

Figure 23. Hveem Stabilometer.

The Stabilometer R-value was calculated using the following formula (Equation 57).

$$R - value = 100 - \frac{100}{\frac{2.5}{D} \times \left(\frac{P_v}{P_h} - 1\right) + 1} \quad \text{(Eq. 57)}$$

Where;

- P_v= Vertical pressure (160 psi)
- P_h= Horizontal pressure (psi) at vertical pressure of 160 psi
- D= Turns displacement reading

The R-value was plotted against the exudation pressure for the three specimens and the resultant R-value was obtained from the graph at a 300-psi exudation pressure.

The testing was done by Wood Rogers Inc. and an example for the R-value versus exudation pressure graph is shown in figure 24 for Silver State base material.

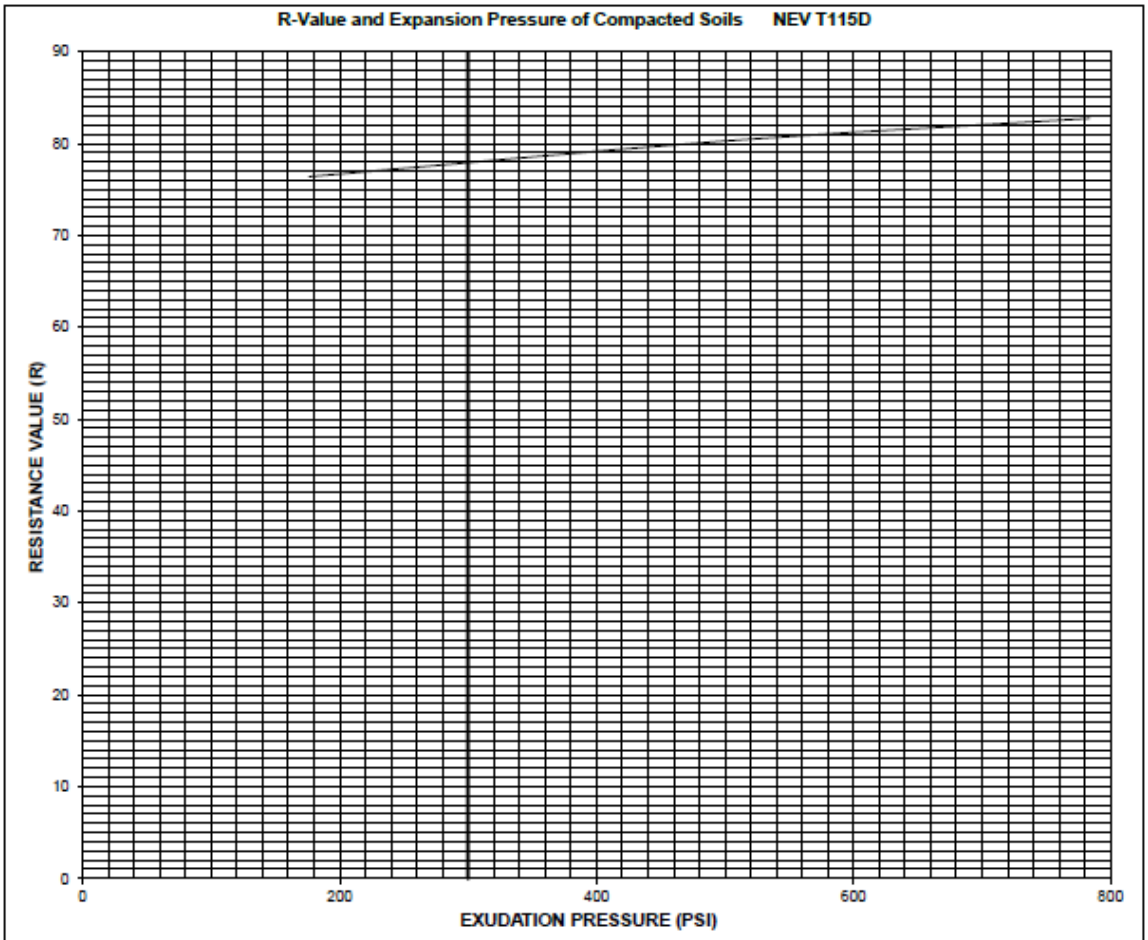

Lab Log #	Sample Source	Material	Expansion Pressure (psf) @ 300 (psi)	R-Value @ 300 (psi)
6062	Silver State Rock Products	Base	0	78

POINT #	WATER CONTENT (%)	DRY DENSITY (PCF)	EXUDATION PRESS. (PSI)	EXPANSION PRESS. (PSF)	RESISTANCE VALUE (R)
1	14.2	113.4	176	0	76
2	12.9	114.3	496	0	80
3	11.9	115.4	784	0	83
4					
5					

WOOD RODGERS
BUILDING RELATIONSHIPS ONE PROJECT AT A TIME
1361 Corporate Boulevard
Reno, NV 89502
Tel: 775.823.4068
Fax: 775.823.4066

UNR - SAO
Base

AASHTO ACCREDITED

Figure 24. R-value Results for Silver State Base Material.

Tables 31 to 33 summarize the R-value test results for base, borrow, and subgrade materials, respectively.

Table 31. Base Materials R-value Test Results.

Source	Sample No	Dry Density (pcf)	Moist. (%)	Exud. Pressure (psi)	R Value	R Value Corr.	R-Value @300 psi Exud.Pres
Lockwood Base (District 2)	1	133.8	7.2	780	70.5	70.3	62
	2	132.7	8.6	496	66.8	66.7	
	3	130.9	10.4	281	61.4	61.1	
Goni Base (District 2)	1	125.7	8.6	751	58.8	59.2	51
	2	123.9	9.1	432	54.5	54.4	
	3	125.5	9.5	271	50.3	50.0	
Imlay Base (District 2)	1	122.1	7.1	602	76.4	75.4	74
	2	123.4	8.2	319	74.4	74.2	
	3	123.9	9.5	118	72.3	72.7	
Spanish Springs Base (District 2)	1	134.2	7.2	795	68.6	67.6	65
	2	132.0	7.4	312	65.5	65.3	
	3	125.8	8.4	151	63.9	63.6	
Trico A Base (District 2)	1	113.6	16.9	154	78.1	78.8	83
	2	114.9	16.5	229	80.9	80.5	
	3	116.0	16.1	317	83.5	83.2	
Trico B Base (District 2)	1	128.8	12.3	265	84.7	84.6	87
	2	128.0	11.6	286	86.2	86.2	
	3	127.4	10.8	315	87.6	87.4	
Sonoma Base (District 3)	1	126.0	8.1	450	77.3	76.8	79
	2	126.9	8.5	308	79.1	78.7	
	3	127.3	9.2	127	82.1	81.8	
Carlin Base (District 3)	1	126.4	7.8	113	67.5	66.9	70
	2	122.8	8.6	312	70.2	70.1	
	3	123.5	9.4	556	75.4	75.6	
Vega Base (District 3)	1	122.2	9.8	782	68.7	69.0	57
	2	121.4	10.7	477	62.4	62.3	
	3	120.1	11.8	261	56.4	55.8	
Silver State Base (District 3)	1	113.4	14.2	176	76.2	76.4	78
	2	114.3	12.9	496	80.4	80.2	
	3	115.4	11.9	784	83.3	82.7	

Table 32. Borrow Materials R-value Test Results.

Material	Sample No	Dry Density (pcf)	Moist. (%)	Exud. Pressure (psi)	R Value	R Value Corr.	R-Value @300 psi Exud.Pres
Goni Borrow (District 2)	1	128.4	11.2	240	70.4	69.6	77
	2	127.5	10.8	276	74.3	74.2	
	3	126.9	9.8	319	79.8	79.3	
Spanish Springs Borrow (District 2)	1	127.6	12.5	145	13.4	13.4	46
	2	130.4	9.7	308	48.3	48.2	
	3	132.9	8.1	409	69.3	69.0	
Sonoma Borrow (District 3)	1	127.4	9.5	487	80.7	80.2	64
	2	127.9	10.3	316	66.0	65.3	
	3	128.4	11.4	192	54.3	54.2	
Elko 1 Borrow (District 3)	1	113.6	15.6	111	41.4	42.2	63
	2	114.5	14.3	251	57.5	57.9	
	3	119.5	12.1	481	79.9	79.8	
Elko 2 Borrow (District 3)	1	113.5	16.6	180	27.8	27.7	38
	2	115.0	16.1	319	39.5	39.7	
	3	118.0	15.5	493	53.1	52.7	

According to NDOT specifications, Type 1 base materials must have a minimum R-value of 70 and borrow materials require a minimum R-value of 45.

The tables above show that base materials from Lockwood, Goni, Spanish Springs, and Vega had an R-value less than 70, and hence failed the NDOT criterion. Also, Elko 2 borrow had an R-value of 38, which does not meet NDOT's minimum required R-value of 45.

Table 33. Subgrade Materials R-value Test Results.

Material	Sample No	Dry Density (pcf)	Moist. (%)	Exud. Pressure (psi)	R Value	R Value Corr.	R-Value @300 psi Exud.Pres
Spaghetti Bowl Subgrade (District 2)	1	120.7	12.6	227	52.8	52.8	59
	2	124.2	11.9	370	64.9	64.5	
	3	126.1	11.1	510	72.7	71.8	
Kings Row Subgrade (District 2)	1	116.5	16.6	234	17.2	16.6	20
	2	117.0	17.8	398	24.6	24.2	
	3	115.1	14.2	573	32.3	31.1	
Fallon BD 1 Subgrade (District 2)	1	116.8	12.1	473	83.2	83.9	74
	2	116.7	14.3	317	74.8	74.9	
	3	116.4	13.8	221	67.8	67.3	
Fallon BD 2 Subgrade (District 2)	1	83.0	34.5	751	32.4	31.8	13
	2	79.0	37.2	457	19.1	18.3	
	3	75.1	39.3	158	8.8	8.4	
Lemmon Dr. 1 Subgrade (District 2)	1	81.6	40.1	126	19.6	19.9	20
	2	86.0	39.1	299	20.8	20.7	
	3	81.9	37.8	463	22.2	21.6	
Lemmon Dr. 2 Subgrade (District 2)	1	97.8	23.9	774	16.5	15.7	9
	2	97.2	26.3	455	10.7	10.3	
	3	95.1	28.4	240	8.5	8.3	
#3817 Subgrade (District 3)	1	126.0	9.1	569	75.0	75.0	75
	2	126.3	9.4	344	75.0	74.9	
	3	127.2	9.9	159	74.6	74.6	
#3824 Subgrade (District 3)	1	109.7	16.2	142	59.4	60.5	67
	2	112.7	14.6	467	73.5	73.7	
	3	114.4	12.8	753	83.7	83.6	

4.6. Resilient Modulus Repeated Load Triaxial Test

The Mr is an important property that represents the stress-dependent stiffness of unbound materials and is widely used in pavement analysis and design. The testing was done in accordance with AASHTO T307 (43), which was identified as the most commonly used

method in the literature review. The specimens are placed in a triaxial chamber and subjected to a dynamic cyclic loading sequence with a 0.1 sec loading time and a 0.9 sec resting period. Resilient (recoverable) strains of the specimens are measured while being subjected to different combinations of contact stresses, cyclic stresses, and confining pressures. The resilient strains are used along with the deviatoric stresses to calculate the Mr values at the different stress states. Base and subbase (borrow) materials are subjected to higher stress states than subgrade soils in the loading sequence due to their location in the pavement structure. Tables 34 and 35 show the loading sequence presented in the AASHTO T307 standard for base/subbase and subgrade materials, respectively.

Table 34. Testing Sequence for Base/Subbase Materials.

Sequence No.	Confining Pressure (psi)	Max. Axial Stress (psi)	Cyclic Stress (psi)	Contact Stress (psi)	No. of Load Applications
0	15	15	13.5	1.5	500-1000
1	3	3	2.7	0.3	100
2	3	6	5.4	0.6	100
3	3	9	8.1	0.9	100
4	5	5	4.5	0.5	100
5	5	10	9	1	100
6	5	15	13.5	1.5	100
7	10	10	9	1	100
8	10	20	18	2	100
9	10	30	27	3	100
10	15	10	9	1	100
11	15	15	13.5	1.5	100
12	15	30	27	3	100
13	20	15	13.5	1.5	100
14	20	20	18	2	100
15	20	40	36	4	100

Table 35. Testing Sequence for Subgrade Soils.

Sequence No.	Confining Pressure (psi)	Max. Axial Stress (psi)	Cyclic Stress (psi)	Contact Stress (psi)	No. of Load Applications
0	6	4	3.6	0.4	500-1000
1	6	2	1.8	0.2	100
2	6	4	3.6	0.4	100
3	6	6	5.4	0.6	100
4	6	8	7.2	0.8	100
5	6	10	9	1	100
6	4	2	1.8	0.2	100
7	4	4	3.6	0.4	100
8	4	6	5.4	0.6	100
9	4	8	7.2	0.8	100
10	4	10	9	1	100
11	2	2	1.8	0.2	100
12	2	4	3.6	0.4	100
13	2	6	5.4	0.6	100
14	2	8	7.2	0.8	100
15	2	10	9	1	100

4.6.1. Sample Preparation and Testing

A 4 inch diameter by 8 inch height mold was used for sample preparation. Materials were sieved over the 3/4” sieve to satisfy the maximum particle size requirement of AASHTO T307, where the minimum mold diameter has to be five times the maximum aggregate size. The optimum moisture content was added to the samples, mixed until uniform, then the samples were sealed for 16-48 hours. Specimens were compacted to 90% of the maximum dry density in 6 equal-mass lifts using a vibratory compactor as shown in figure 25. Samples were carefully extruded and sealed by installing a membrane, filter papers, sandstones, and ‘O’ rings. Finally, sealed samples were transferred to the triaxial chamber and drainage tubes were connected, as shown in figure 26.

Figure 25. Compaction with Vibratory Compactor.

Figure 26. Sealed Sample in Triaxial Chamber.

Vacuum was applied through the drainage valves to ensure no leakage. The chamber was closed tightly and LVDTs were mounted outside of the chamber and connected to the load cell to measure axial deformation, as shown in figures 27 and 28, respectively. The test was run by the software which controlled the loading patterns, and frequent checks were done to ensure that stresses and confining pressure were correct.

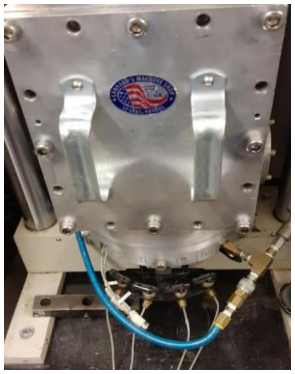

Figure 27. Closed Chamber and Drainage Valves.

Figure 28. LVDTs Connected Outside the Chamber.

4.6.2. Mr Models Development

The RLT test results were used to develop non-linear models relating the Mr of the unbound materials to the stress states. The constitutive models that best fit the tested materials were the Theta model (45) which describes the stress-hardening behavior, the Uzan, and Universal models (46). Although the Universal model (shown in Equation 2 previously) showed good correlations with most subgrade materials and many borrow materials, the Uzan model performed consistently better and hence was used later for the analysis. The Theta model (Equation 58) and Uzan model (Equation 59) are shown below.

Theta Model: $$Mr = K_1\theta^{K_2} \quad \text{(Eq. 58)}$$

Uzan Model: $$Mr = K_1\theta^{K_2}\sigma_d^{K_3} \quad \text{(Eq. 59)}$$

Where;

- θ= Bulk Stress (sum of the three principal stresses, psi)
- σ_d= Deviator Stress (psi)
- K_1, K_2, K_3= Regression Coefficients

For each loading sequence, the resilient strain values of the last five cycles were averaged to obtain the Mr. The least squares method was used in Microsoft Excel to derive the coefficients for the constitutive models. Carlin base Mr test results summary is shown in table 36, along with the necessary parameters for the regression analysis. Figures 29 to 31 show the measured versus predicted Mr values for Carlin base, Goni borrow, and subgrade #3817, using the Theta model, the Uzan model, and the Universal model, respectively.

Table 36. Resilient Modulus Test Results Summary for Carlin Base Materials.

Sequence	Cyclic Axial Stress (psi)	Contact Stress (psi)	Confine Stress (psi)	Axial Resilient Modulus (psi)	Deviator Stress, σd (psi)	Sigma 1 (psi)	Sigma 3 (psi)	Bulk Stress,θ (psi)	Octahedral Shear Stress (psi)
0	13.5	1.5	14.4	32812	13.5	29.5	14.4	58.3	7.1
1	2.7	0.3	2.4	14986	2.7	5.4	2.4	10.3	1.4
2	5.4	0.6	2.4	15693	5.4	8.4	2.4	13.3	2.8
3	8.1	0.9	2.4	16910	8.1	11.4	2.4	16.3	4.2
4	4.5	0.5	4.4	18085	4.5	9.4	4.4	18.3	2.4
5	9.0	1.0	4.4	20297	9.0	14.4	4.4	23.2	4.7
6	13.5	1.5	4.4	21922	13.5	19.4	4.4	28.3	7.1
7	9.0	1.0	9.4	*26459*	9.0	19.4	9.4	38.2	4.7
8	18.0	2.0	9.4	29442	18.0	29.4	9.4	48.2	9.4
9	26.7	3.0	9.4	31135	26.7	39.1	9.4	58.0	14.0
10	9.0	1.0	14.4	30487	9.0	24.4	14.4	53.3	4.7
11	13.5	1.5	14.4	32223	13.5	29.4	14.4	58.3	7.1
12	26.7	3.0	14.4	*36342*	26.7	44.1	14.4	73.0	14.0
13	13.5	1.5	19.4	36119	13.5	34.4	19.4	73.2	7.1
14	18.0	2.0	19.4	38249	18.0	39.5	19.4	78.3	9.4
15	34.7	4.0	19.4	42256	34.7	58.1	19.4	97.0	18.2

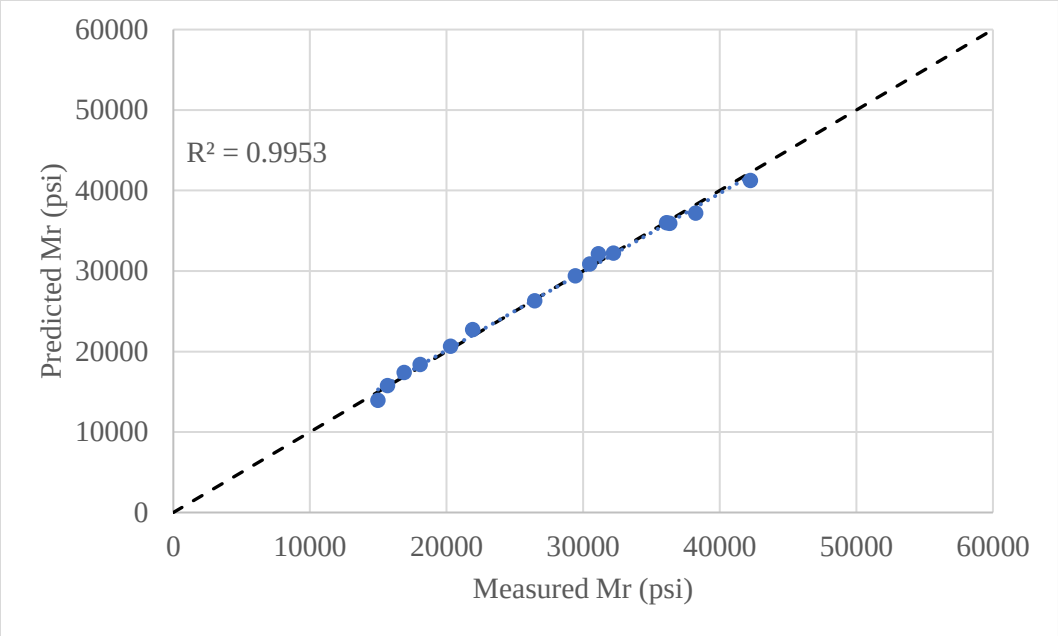

Figure 29. Carlin Base Materials Theta Model.

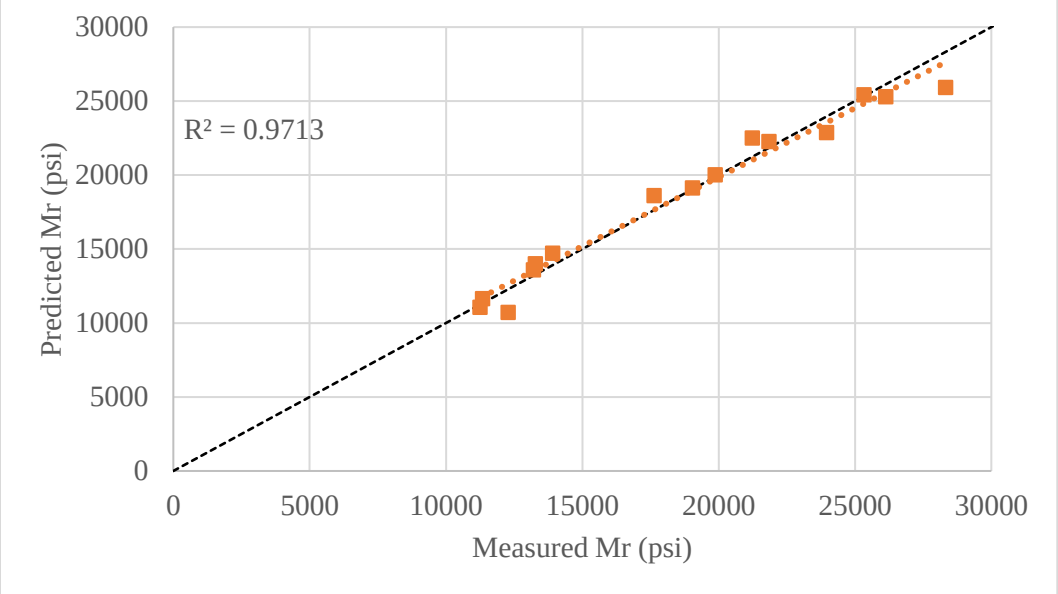

Figure 30. Goni Borrow Materials Uzan Model.

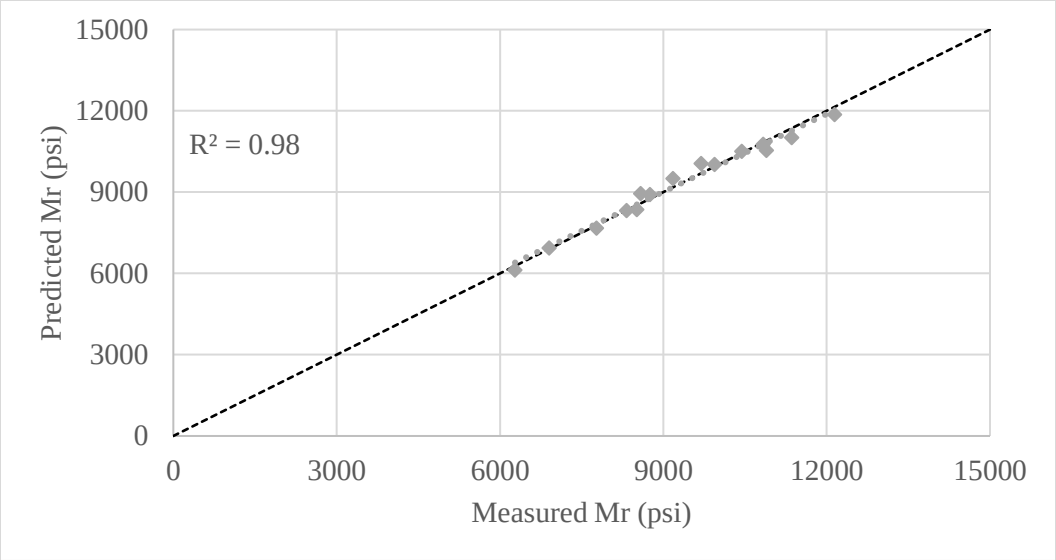

Figure 31. Subgrade #3817 Universal Model

Tables 37, 38, and 39 show the three constitutive models' regression results for base, borrow, and subgrade materials, respectively. The best fit model for each material is also shown. It is worth to note that some materials showed better Uzan or Universal model fit, but the regression coefficient K_3 was positive, which means that the model does not really reflect the material behavior. This is because K_3 is the coefficient of the deviator stress (Uzan model), or the octahedral shear stress (Universal model), which represents stress softening behavior, and hence should be negative. Such cases are highlighted in the tables.

Figures 32, 33, and 34 show the variation of the resilient modulus with the bulk stress for the base, borrow, and subgrade materials, respectively.

Table 37. Base Materials Constitutive Models Regression Results.

Model	Regression Coefficient	Base Source									
		District 2						District 3			
		Lockwood	Goni	Imlay	Spanish Springs	Trico A	Trico B	Carlin	Sonoma	Vega	Silver State
Theta	K_1	2990.0	1682.7	4178.2	4269.6	3330.1	2346.2	4512.8	3656.0	3474.0	3315.4
	K_2	0.531	0.545	0.507	0.325	0.451	0.515	0.484	0.524	0.456	0.455
	R^2	0.983	0.971	0.989	0.588	0.974	0.977	0.995	0.991	0.975	0.960
Uzan	K_1	3113.1	1653.1	4192.0	6307.4	3228.2	2508.7	4412.0	3702.6	3609.3	3625.5
	K_2	0.483	0.567	0.503	-0.135	0.488	0.432	0.512	0.508	0.406	0.342
	K_3	0.055	-0.026	0.004	0.524	-0.042	0.096	-0.033	0.018	0.058	0.130
	R^2	0.986	0.972	0.989	0.939	0.976	0.985	0.995	0.991	0.978	0.978
Universal	K_1	809.4	484.9	1087.8	536.4	754.9	597.8	1129.1	991.3	764.3	707.0
	K_2	0.462	0.516	0.476	-0.064	0.437	0.421	0.487	0.488	0.384	0.340
	K_3	0.282	0.121	0.127	1.608	0.060	0.395	-0.015	0.148	0.305	0.484
	R^2	0.991	0.973	0.990	0.974	0.975	0.993	0.994	0.993	0.986	0.989
Chosen Model		Theta	Uzan	Theta	Theta	Uzan	Theta	Theta	Theta	Theta	Theta

Table 38. Borrow Materials Constitutive Models Regression Results.

Model	Regression Coefficient	Borrow Source									
		District 2					District 3				
		Lockwood	Goni	Imlay	Spanish Springs	Trico	Elko 1	Elko 2	Vega	Silver State	Sonoma
Theta	K_1	2401.8	3413.1	3037.9	5922.7	1825.4	3538.9	6695.8	4427.6	2699.9	4092.4
	K_2	0.603	0.451	0.538	0.354	0.507	0.434	0.307	0.459	0.510	0.488
	R^2	0.988	0.944	0.979	0.854	0.972	0.976	0.896	0.987	0.979	0.984
Uzan	K_1	2462.8	3014.3	3062.5	4951.2	1697.2	3441.8	5876.8	4367.9	2552.5	3999.8
	K_2	0.575	0.587	0.529	0.551	0.589	0.470	0.476	0.476	0.585	0.515
	K_3	0.032	-0.152	0.011	-0.221	-0.093	-0.042	-0.196	-0.020	-0.088	-0.030
	R^2	0.989	0.970	0.979	0.935	0.979	0.978	0.977	0.987	0.985	0.985
Universal	K_1	802.5	805.8	852.5	1105.5	491.0	770.4	1116.8	1023.7	732.1	1025.4
	K_2	0.557	0.502	0.493	0.449	0.527	0.428	0.407	0.445	0.527	0.475
	K_3	0.189	-0.205	0.186	-0.383	-0.085	0.025	-0.421	0.058	-0.075	0.054
	R^2	0.991	0.949	0.982	0.883	0.972	0.976	0.940	0.987	0.980	0.984
Chosen Model		Theta	Uzan	Theta	Uzan	Uzan	Uzan	Uzan	Uzan	Uzan	Uzan

Table 39. Subgrade Materials Constitutive Models Regression Results.

Model	Regression Coefficient	Subgrade Source							
		District 2						District 3	
		Fallon Big Dig1	Fallon Big Dig2	Spaghetti Bowl	Kings Row	Lemmon Dr. 1	Lemmon Dr. 2	#3817	#3824
Theta	K_1	4465.6	7570.1	7226.2	10018.2	8112.5	10170.1	2546.0	6679.6
	K_2	0.242	0.055	0.197	0.212	0.063	0.086	0.470	0.243
	R^2	0.778	0.259	0.749	0.360	0.058	0.150	0.982	0.419
Uzan	K_1	4350.5	7369.0	7004.1	8836.4	7403.3	9371.8	2541.7	6098.5
	K_2	0.286	0.086	0.250	0.370	0.203	0.199	0.473	0.399
	K_3	-0.059	-0.038	-0.072	-0.201	-0.188	-0.148	-0.003	-0.215
	R^2	0.855	0.505	0.916	0.963	0.965	0.946	0.982	0.949
Universal	K_1	615.3	626.9	902.2	1532.5	822.3	1048.3	615.5	1123.3
	K_2	0.274	0.088	0.242	0.367	0.201	0.199	0.473	0.388
	K_3	-0.315	-0.296	-0.460	-1.455	-1.362	-1.104	-0.024	-1.475
	R^2	0.817	0.525	0.870	0.927	0.914	0.940	0.982	0.870
Chosen Model		Uzan	Uzan	Uzan	Uzan	Uzan	Uzan	Uzan	Uzan

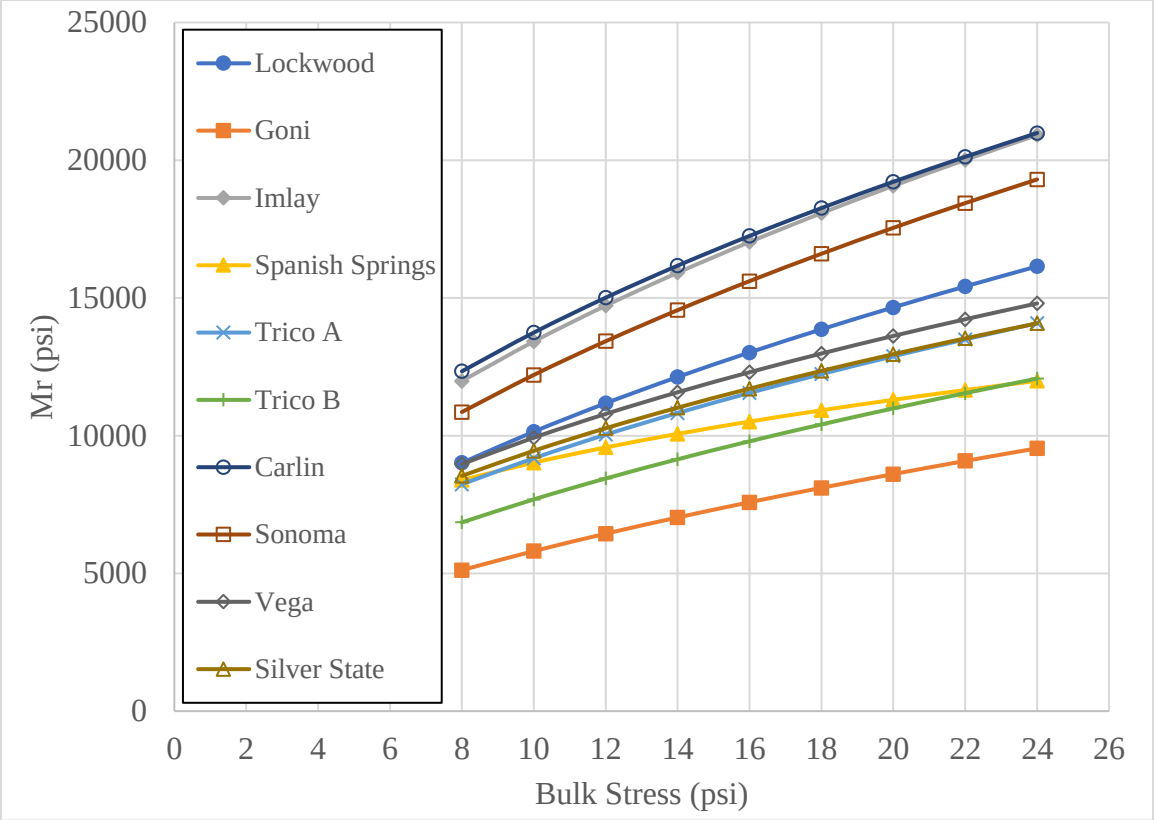

Figure 32. Variation of Mr with Bulk Stress for Base Materials.

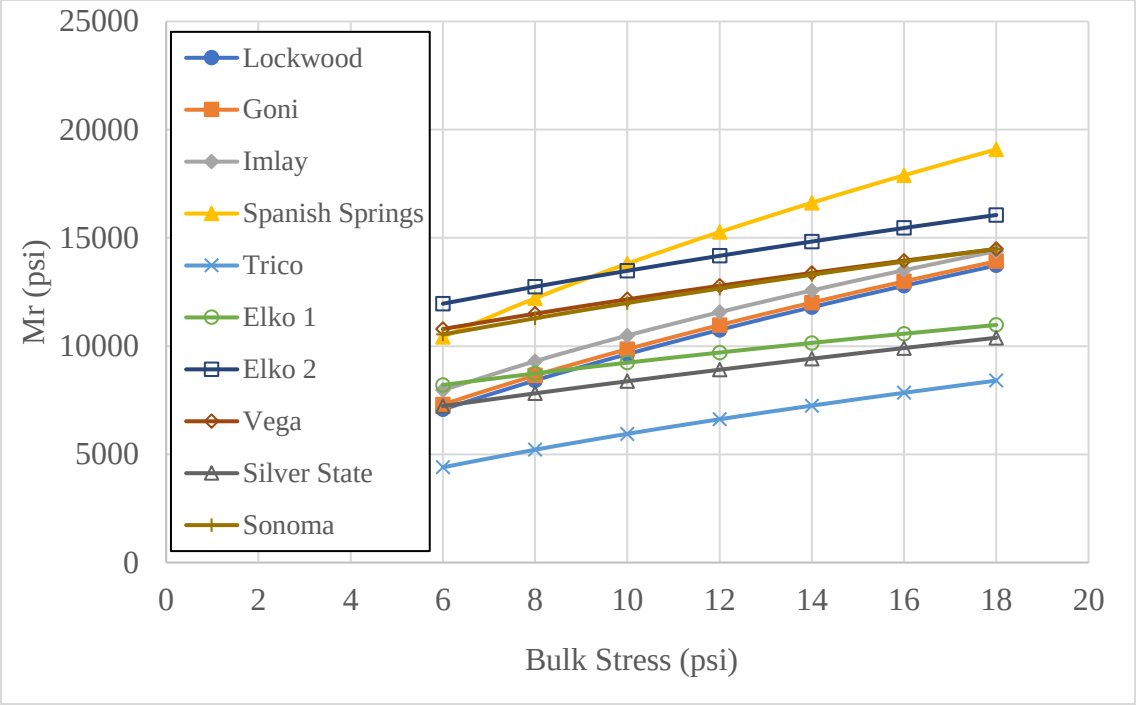

Figure 33. Variation of Mr with Bulk Stress for Borrow Materials.

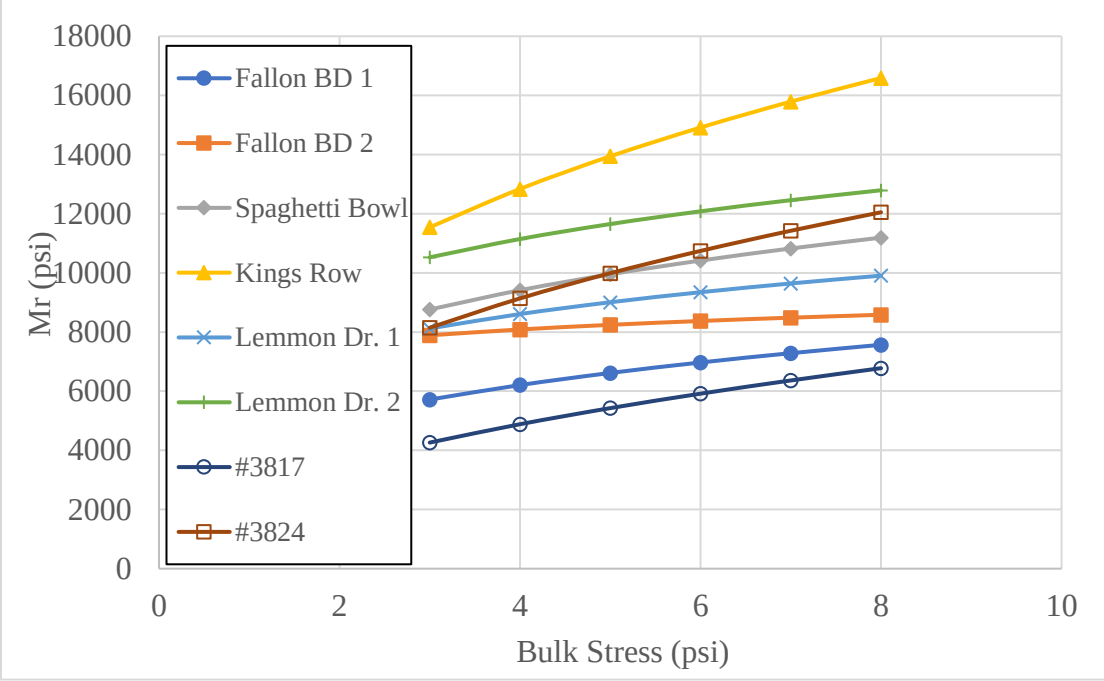

Figure 34. Variation of Mr with Bulk Stress for Subgrade Materials.

4.7. Test Results Comparison with NDOT Specifications

Before starting the analysis for determining the design Mr values, test results were checked against NDOT specifications. Tables 40 and 41 show this comparison for District 2 and District 3 base materials, respectively. As stated previously, borrow material from Elko 2 failed the R-value specification, and hence was excluded from further analysis. Similarly, all base materials failing any of the specifications (as highlighted in tables 40 and 41) were excluded from base materials and treated as borrow materials during analysis, except for Spanish Springs base. This material was excluded from the analysis since it showed an unexpected stress hardening behavior with the deviator stress, where its Mr increased with increasing deviator stress as shown in figure 35. It is worth noting that the Mr results for the base materials that pass NDOT specifications fit the Theta model.

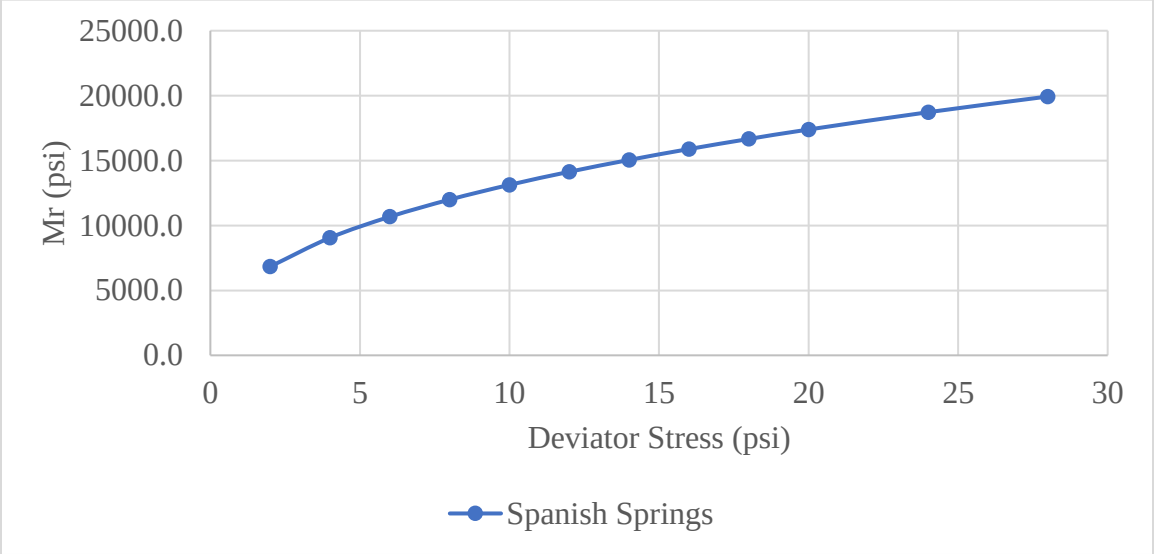

Figure 35. Variation of Mr with Deviator Stress for Spanish Springs Base Material.

Table 40. District 2 Base Test Results Comparison with NDOT Specifications

Source	Lockwood	Goni	Imlay	Spanish Springs	Trico A	Trico B	NDOT Specs	
%Passing:							Min	Max
1.5"	100	100	100	100	100	100	100	-
1"	89	94	98	99	100	100	80	100
#4	50	43	48	42	61	40	30	65
#16	29	18	24	22	36	20	15	40
#200	3	4	10	9	16	8	2	12
R-value	62	51	74	65	83	87	70	-
L.L. (%)	N.A.	N.A.	N.A.	37	N.A.	N.A.	-	35
P.I. (%)	N.P.	N.P.	N.P.	9	N.P.	N.P.	-	4*

*: Limit for material with 9-11% passing sieve #200

Table 41. District 3 Base Test Results Comparison with NDOT Specifications

Source	Sonoma Pit	Carlin Pit	Vega Pit	Silver State	NDOT Specs	
%Passing:					Min	Max
1.5"	100	100	100	100	100	-
1"	99	100	100	100	80	100
#4	48	51	50	63	30	65
#16	28	30	27	31	15	40
#200	9	11	6	11	2	12
R-value	79	70	57	78	70	-
L.L. (%)	N.A.	N.A.	N.A.	30	-	35
P.I. (%)	N.P.	N.P.	N.P.	4	-	4*

*: Limit for material with 9-11% passing sieve #200

Chapter 5. Design Resilient Modulus for New Projects

Proper characterization of the subgrade and unbound layers for structural design (new and rehabilitation) is essential since they significantly affect pavement performance. The Mr is

the primary material property used to characterize these materials for flexible pavement design in the AASHTO 1993 Design Guide (47) and in the MEPDG developed under NCHRP project 1-37A (48), which is currently being implemented as the AASHTOWare® Pavement ME design software (49).

This chapter focuses on the determination of the unbound materials' Mr values for the design of new flexible pavements as recommended by the MEPDG. Establishing these Mr values is needed for the development of correlations between the Mr and other materials properties.

5.1. Procedure for Determination of Mr values for New Design

The steps to determine the Mr values for unbound layers (aggregate base, borrow materials and subgrade soil) using the results of the repeated load resilient modulus tests are listed and defined below. These steps are in accordance with the MEPDG Manual of Practice (1) as well as in the final report for NCHRP project 1-37A (48) for both flexible and rigid pavements.

1. Based on previous experience, a trial flexible pavement structure is assumed that can satisfy the requirements of traffic loads and available materials.

2. Use the trial pavement structure to calculate the at-rest stress state from the overburden pressures for the aggregate base layer, embankment, and/or subgrade. The at-rest stress state for the aggregate base layer and embankment are determined at their quarter depth, while the at-rest stress state for the subgrade is determined 18 inches into the subgrade. These material characterization depths are explained

by Von Quintus et al in comparing laboratory resilient modulus values to backcalculated elastic layer modulus values. These depths are debatable but were selected for estimating the c-factor included in the 1993 AASHTO Design Guide, as well as in the MEPDG Manual of Practice.

3. Start with the subgrade or lowest unbound layer and move upward in the pavement structure to establish the design resilient modulus for all unbound material layers using a linear elastic layer program for calculating layer responses or stresses at the locations defined in step 2. Assume the Mr for the unbound layers above which the design Mr is being estimated.

4. For the design truck axle load and season, calculate the load-related vertical and horizontal stresses using a linear elastic layered program to be consistent with the Pavement ME Design pavement response program. The load-related stresses are calculated at the material/soil characterization depths listed in step 2.

5. Calculate the at-rest horizontal and vertical stresses from overburden at the same critical points or locations in the unbound layers used to calculate the load-related stresses. The at-rest vertical pressure (p_1) is calculated using Equation 60, while the at-rest horizontal stresses (p_2 and p_3) are calculated as using Equation 61.

$$p_1 = p_0 = (D_{HMA}\gamma_{HMA} + D_{Base}\gamma_{Base} + D_{Soil}\gamma_{Soil}) \quad \text{(Eq. 60)}$$

$$p_2 = p_3 = p_0 K_0 \quad \text{(Eq. 61)}$$

Where;

- p_0, p_1= At-rest vertical or overburden pressure from the layers above a specific point
- p_2, p_3= At-rest horizontal stress
- K_0= At-rest earth pressure coefficient
- D_{HMA}= Thickness of the AC layers
- D_{Base}= Thickness of the unbound aggregate base and/or embankment layers. If determining the at-rest stresses in the unbound base layer the point or depth into the base is ¼ of its thickness (see step 1)
- D_{Soil}= Point for computing at rest stress state in subgrade, 18 inches
- γ_{HMA}= Average in place density of the AC layers
- γ_{Base}= Average in place wet density of the unbound aggregate base and/or embankment layers
- γ_{Soil}= Average in place wet density of the subgrade soil

6. Superimpose the at-rest and load-related stresses in the vertical and horizontal directions. In other words, add the at-rest and load-related vertical stresses, and add the at-rest and load related horizontal stresses.
7. Superimpose the total stress state versus Mr calculated with the linear elastic layer theory and the repeated load Mr values versus stress state measured in the laboratory. The stress-state at which the elastic theory and laboratory Mr values are equal is the value to be used in the Pavement ME Design software for quasi-input level 1.
8. Check the design Mr determined for the lower unbound layers to be sure it is the same, as previously determined. This step can be an iterative process to determine a stable design Mr.

5.2. Identification of Mr Values for New Design of Typical NDOT Pavements

In this section, the unbound materials' Mr values for new flexible pavement design were identified using the same procedure followed in the research for District 1 (3). The typical NDOT sections were designed using the AASHTO 1993 design procedure (47) for three traffic level of low, medium, and high. The NDOT Pavement Structural Design Manual (50) was used as a reference for the input parameters as shown in table 42.

As recommended by the NDOT manual, structural coefficients for the AC layer, base layer, and borrow layer were 0.35, 0.1, and 0.07, respectively. Two levels of subgrade strength were used: strong with a Mr of 14000 psi, and weak with a Mr of 8000 psi. The Mr for the base layer was kept constant at 26000 psi.

Pavements on weak subgrade were designed with and without a borrow layer. When incorporating the borrow layer as a subbase in the design, the Mr for the base, borrow, and subgrade was taken to be 26000 psi, 11250 psi, and 6800 psi, respectively. Tables 43 and 44 show the structures without and with borrow layer, respectively.

Table 42. Major Inputs for AASHTO 1993 Design.

Traffic Level	Design Traffic in Million ESALs (MESALs)	Reliability Level (%)	Initial Serviceability Index (pi)	Terminal Serviceability Index (pt)	Standard Deviation (S_o)
Low	5	85	4.2	2	0.45
Medium	15	90	4.2	2.5	0.45
High	30	95	4.2	2.5	0.45

Table 43. Pavement Structures without Borrow Materials.

Traffic Level	Subgrade Mr (psi)	Thickness (inch)	
		AC	Base
Low	14000	5	16
	8000	7	16
Medium	14000	7	18
	8000	9.5	18
High	14000	8	23
	8000	10.5	23

Table 44. Pavement Structures with Borrow Materials.

Traffic Level	Thickness (inch)		
	AC	Base	Borrow
Low	5.5	16	10
Medium	8.5	18	10
High	9.5	23	10

The 3D-Move analysis software (51) was used to calculate the load-induced principal stresses for a single wheel load of 9000 lb and a tire pressure of 100 psi, which is a typical truck tire pressure. Following the MEPDG procedure, the AC layer was subdivided into sublayers, as shown in figure 36, to capture its viscoelastic behavior.

The AC layer was modeled as a viscoelastic material in the 3D-Move analysis software, where the modulus changes with temperature and frequency. A 100^{o}F median temperature and a vehicle speed of 45 mph were used for Districts 2 and 3 to calculate the dynamic modulus (E*) of the AC layer. E* master curves for Districts 2 and 3 were developed by using representative mean E* data for PG64-28NV mixtures. Tables 45 and 46 summarize

the mean E* values for Districts 2 and 3, respectively. Figures 37 and 38 show the E* master curves for District 2 and 3, respectively.

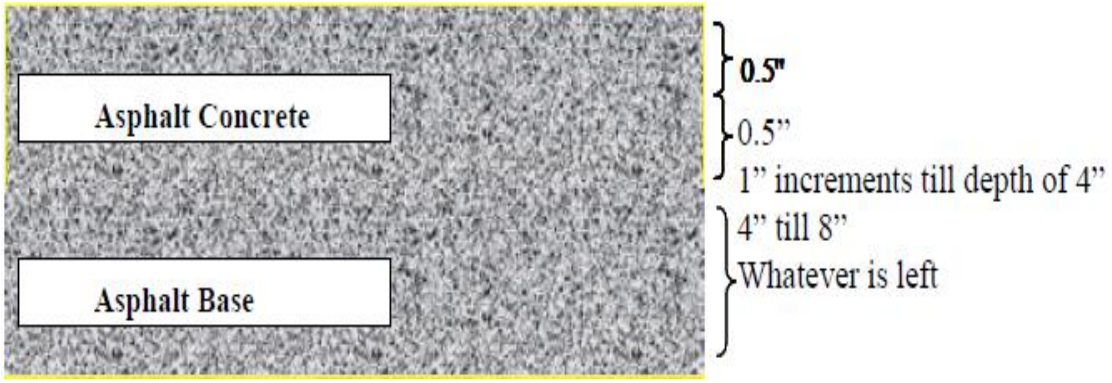

Figure 36. Sublayer Thicknesses for the AC layer.

Table 45. Mean Dynamic Modulus Values for District 2 PG64-28NV Mixture.

Temperature (°F)	Frequency (Hz)					
	0.1	0.5	1	5	10	25
14	1631380	2008344	2164343	2500790	2632250	2792318
40	628946	885602	1008706	1324511	1472121	1685424
70	122675	212544	264370	436082	526218	678018
100	25282	41756	52208	97192	126317	183386
130	12340	17689	23032	34827	44416	71565

Table 46. Mean Dynamic Modulus Values for District 3 PG64-28NV Mixture.

Temperature (°F)	Frequency (Hz)					
	0.1	0.5	1	5	10	25
14	1727052	2107737	2263477	2595567	2723831	2878790
40	661937	934530	1066170	1385400	1528233	1751700
70	124687	213457	266323	442423	538683	706700
100	34902	54718	67373	118600	151013	222847
130	14977	20178	23423	39520	50332	74025

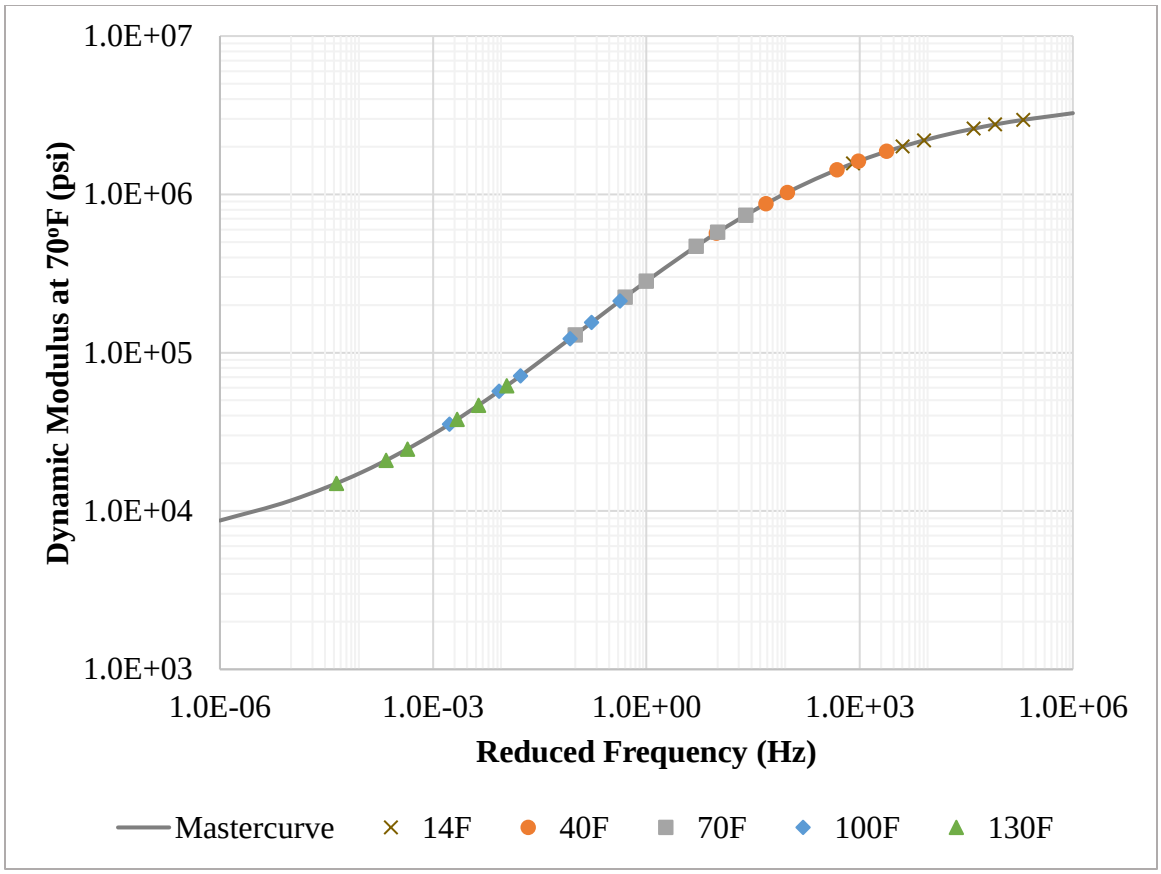

Figure 37. Dynamic Modulus Master Curve for District 2 PG64-28NV Mixture at 70ºF.

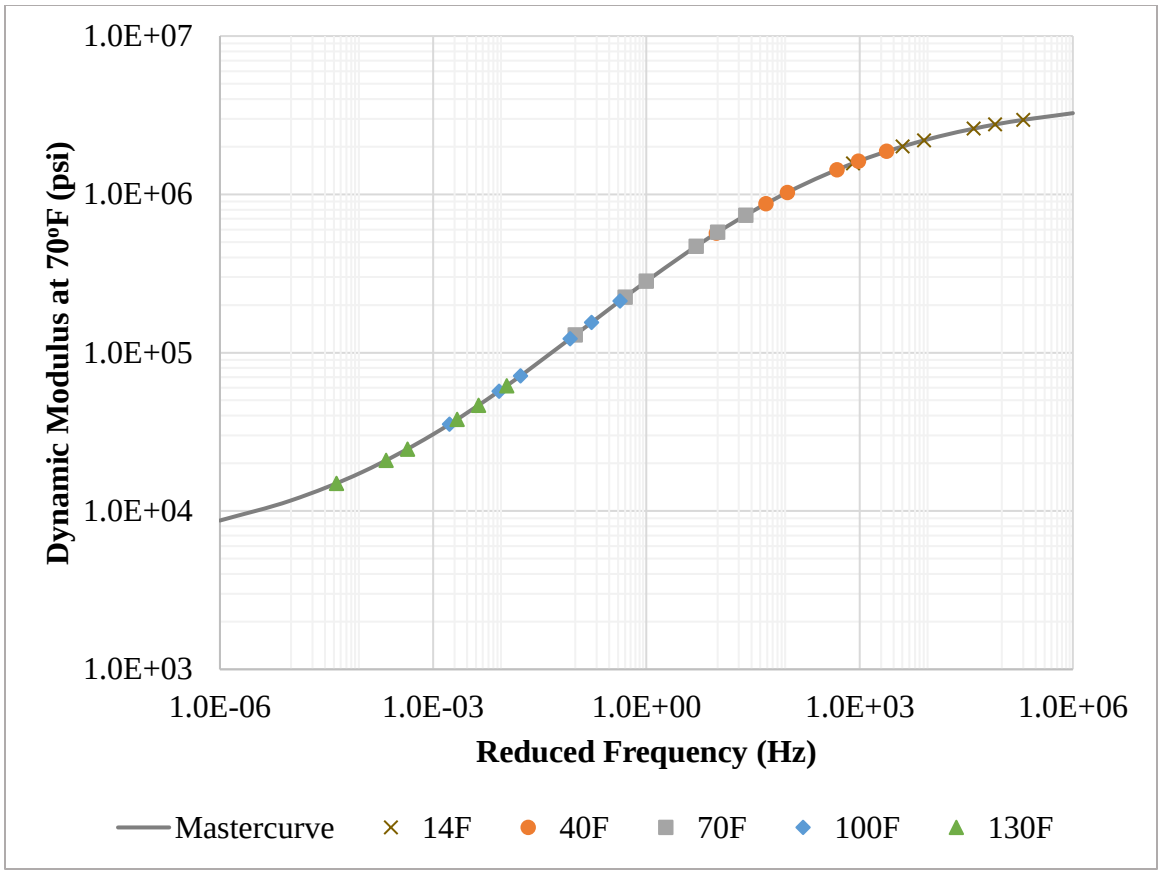

Figure 38. Dynamic Modulus Master Curve for District 3 PG64-28NV Mixture at 70ºF.

The loading frequency imparted by the moving vehicle changes with the depth of the AC layer. To obtain the frequency experienced by each AC sublayer, the method of equivalent thickness (MET) was used to transform the AC sublayers into equivalent thicknesses as shown in figure 39.

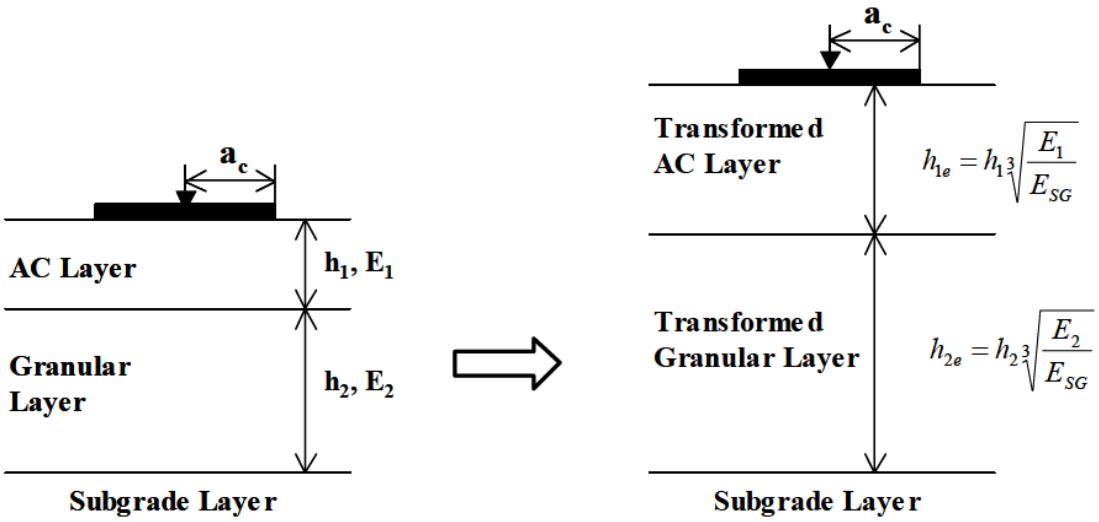

Figure 39. Equivalent Thickness Transformation Using MET.

The pulse time was calculated using Equation 62. The vehicle speed used was 45 mph, and the effective length was calculated using the MEPDG procedure as shown in figure 40. The frequency for each sublayer was calculated as the inverse of the pulse time, and the dynamic modulus master curve was used to obtain the E* values at the corresponding frequencies. Tables 47 and 48 show the procedure to calculate the E* values for the sublayers of a 5 inch AC layer for Districts 2 and 3, respectively.

$$t = \frac{L_{eff}}{17.6 v_s} \quad \text{(Eq. 62)}$$

Where;

- t= loading time (sec)
- L_{eff}= effective length (inch)
- v_s= velocity (mph)

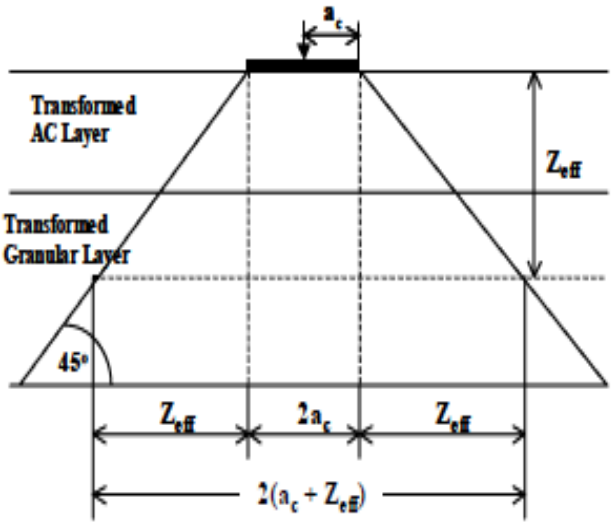

Figure 40. Effective Length Computation for Single Axle Load Configuration.

Table 47. Summary of Sublayers E* Calculation for a 5 inch AC Layer for District 2.

AC Sublayers	Thickness (inch)	Z_{eff} (inch)	L_{eff} (inch)	Pulse time (sec)	Frequency (Hz)	E* (psi)
Sublayer 1	0.5	1.32	13.35	0.01685	59.34	258033
Sublayer 2	0.5	2.61	15.93	0.02012	49.71	242481
Sublayer 3	1	5.12	20.94	0.02644	37.82	220119
Sublayer 4	1	7.56	25.83	0.03261	30.66	204245
Sublayer 5	1	9.96	30.62	0.03866	25.87	192181
Sublayer 6	1	12.31	35.33	0.04460	22.42	182539

Table 48. Summary of Sublayers E* Calculation for a 5 inch AC Layer for District 3.

AC Sublayers	Thickness (inch)	Z_{eff} (inch)	L_{eff} (inch)	Pulse time (sec)	Frequency (Hz)	E* (psi)
Sublayer 1	0.5	1.35	13.41	0.01693	59.05	277934
Sublayer 2	0.5	2.68	16.07	0.02029	49.29	261826
Sublayer 3	1	5.25	21.21	0.02679	37.33	238675
Sublayer 4	1	7.77	26.24	0.03313	30.18	222238
Sublayer 5	1	10.23	31.17	0.03936	25.41	209711
Sublayer 6	1	12.66	36.02	0.04548	21.99	199698

The subdivided AC layer was used in the 3D-Move analysis. The Poisson's ratio for the AC, base, borrow, and subgrade were assumed to be 0.3, 0.35, 0.4, and 0.45, respectively. The responses were obtained at the center and edge of the tire at the depths specified in step 2 previously. The principal stresses obtained from the 3D-Move analysis were used to calculate the octahedral normal and shear stresses (Equations 63 and 64). The octahedral stresses were used in Equations 65 and 66 (52 and 53) to calculate the corresponding triaxial state of stresses (i.e., the deviatoric and confining stresses).

$$\sigma_{oct} = \frac{1}{3}(\sigma_1 + \sigma_2 + \sigma_3) \quad \text{(Eq. 63)}$$

$$|\tau_{oct}| = \frac{1}{3}\sqrt{(\sigma_1 - \sigma_2)^2 + (\sigma_1 - \sigma_3)^2 + (\sigma_2 - \sigma_3)^2} \quad \text{(Eq. 64)}$$

$$\sigma_d = \frac{3}{\sqrt{2}}|\tau_{oct}| \quad \text{(Eq. 65)}$$

$$\sigma_c = \sigma_{oct} - \frac{\sigma_d}{3} \quad \text{(Eq. 66)}$$

Where;

- σ_1= major principal stress
- σ_2= intermediate principal stress
- σ_3= minor principal stress
- σ_{oct}= octahedral normal stress
- τ_{oct}= octahedral shear stress
- σ_d= deviatoric stress
- σ_c= confining stress

Stresses from overburden were also converted into triaxial state of stress and superimposed to the load-induced stresses. The Theta model for base materials, the Uzan model for subgrade materials, and the best fitting model for the borrow materials, were used to

calculate the Mr values. This iterative process continued until the error became less than one percent. The iterative process for a pavement structure with a 5 inch AC layer and a 16 inch base layer is shown in tables 49 and 50. For this scenario, the new design Mr value for the base and subgrade layers were 19100 psi and 11750 psi, respectively.

The subgrade materials were divided into two categories depending on their Mr test results. Kings Row, Lemmon Dr. 2, Spaghetti Bowl, and #3824 subgrade materials were categorized as strong, whereas Lemmon Dr. 1, Fallon Big Dig 1, Fallon Big Dig 2, and #3817 subgrade materials were categorized as weak. Tables 51, 52, and 53 present the Mr values for new design of structures with strong subgrade, weak subgrade, and weak subgrade with a borrow layer, respectively.

Due to limited base and subgrade materials per District, the analysis was done for Districts 2 and 3 combined, while considering the different AC layer's E* values for each of the corresponding District. This means that the analysis with District 2 base materials used the E* values for District 2, whereas analysis with District 3 base materials used the E* values for District 3.

Table 49. Procedure for Obtaining Triaxial State of Stress.

Trial	Location	3-D Move Stress (psi)							Static (psi)	
		σ_1	σ_2	σ_3	τ_{oct}	σ_d	σ_{oct}	σ_c	σ_d	σ_c
Trial 1	CAB ct	18.35	-0.03	-0.04	8.66	18.38	6.09	-0.03	0.38	0.38
	CAB edg	15.48	-0.05	-0.23	7.36	15.62	5.07	-0.14	0.38	0.38
	SG ct	2.10	0.05	0.04	0.97	2.06	0.73	0.05	1.45	1.45
	SG edg	2.06	0.05	0.04	0.95	2.01	0.72	0.04	1.45	1.45
Trial 2	CAB ct	18.71	-0.08	-0.09	8.86	18.80	6.18	-0.09	0.38	0.38
	CAB edg	15.75	-0.10	-0.30	7.52	15.96	5.12	-0.20	0.38	0.38
	SG ct	2.09	0.05	0.04	0.96	2.05	0.73	0.04	1.45	1.45
	SG edg	2.05	0.05	0.04	0.94	2.00	0.71	0.04	1.45	1.45

Table 50. Procedure for Obtaining Mr Values.

Trial	Location	Total (psi)		Bulk Stress θ (psi)	Octahedral Shear Stress (psi)	Assumed Mr (psi)	Predicted Mr (psi)	Error (%)
		σd	σc					
Trial 1	CAB ct	18.76	0.35	19.82	8.84	18000	18980	5.4
	CAB edg	16.00	0.25	16.74	7.54	18000	17420	3.2
	SG ct	3.51	1.49	7.99	1.65	11500	11770	2.4
	SG edg	3.46	1.49	7.94	1.63	11500	11780	2.4
Trial 2	CAB ct	19.18	0.30	20.07	9.04	19100	19100	0.0
	CAB edg	16.34	0.18	16.89	7.70	19100	17500	8.4
	SG ct	3.49	1.49	7.97	1.65	11750	11770	0.2
	SG edg	3.45	1.49	7.93	1.63	11750	11780	0.3

Table 51. Summary of Mr Values (psi) for New Design for Structures on Strong Subgrade.

Material		Low Traffic		Medium Traffic		High Traffic	
Base	Subgrade	Base	Subgrade	Base	Subgrade	Base	Subgrade
Imlay	Kings Row	19500	15000	15600	15400	13900	15950
Imlay	Lemmon Dr. 2	19100	11750	15200	12000	13650	12200
Imlay	Spaghetti Bowl	18950	10850	15050	11000	13550	11250
Imlay	#3824	18950	10800	15100	11100	13550	11500
Trico B	Kings Row	10700	15000	8550	15450	7600	15950
Trico B	Lemmon Dr. 2	10500	11750	8350	12000	7450	12200
Trico B	Spaghetti Bowl	10450	10850	8300	11050	7400	11250
Trico B	#3824	10450	10750	8300	11100	7450	11500
Carlin	Kings Row	19400	14950	15650	15350	14050	15850
Carlin	Lemmon Dr. 2	19000	11750	15250	11950	13750	12200
Carlin	Spaghetti Bowl	18850	10800	15150	11000	13700	11200
Carlin	#3824	18850	10750	15150	11050	13700	11450
Sonoma	Kings Row	17600	15000	13950	15450	12400	15950
Sonoma	Lemmon Dr. 2	17200	11750	13600	12000	12150	12250
Sonoma	Spaghetti Bowl	17050	10850	13450	11050	12100	11250
Sonoma	#3824	17050	10750	13450	11100	12100	11500
Silver State	Kings Row	12700	14900	10400	15350	9350	15800
Silver State	Lemmon Dr. 2	12450	11700	10150	11950	9200	12200
Silver State	Spaghetti Bowl	12350	10800	10100	10950	9150	11150
Silver State	#3824	12350	10650	10100	11000	9150	11400

Table 52. Summary of Mr Values (psi) for New Design for Structures on Weak Subgrade.

Material		Low Traffic		Medium Traffic		High Traffic	
Base	Subgrade	Base	Subgrade	Base	Subgrade	Base	Subgrade
Imlay	Lemmon Dr. 1	14950	9050	12500	9250	11800	9400
Imlay	Fallon Big Dig 1	14950	9050	12100	7500	11550	7650
Imlay	Fallon Big Dig 2	14800	8400	12350	8450	11700	8550
Imlay	#3817	14400	6900	12000	7050	11500	7350
Trico B	Lemmon Dr. 1	8350	9000	7000	9250	6550	9400
Trico B	Fallon Big Dig 1	8350	9000	6850	7500	6450	7650
Trico B	Fallon Big Dig 2	8250	8400	6950	8450	6500	8550
Trico B	#3817	8050	6950	6800	7100	6400	7350
Carlin	Lemmon Dr. 1	15000	9050	12650	9250	12000	9400
Carlin	Fallon Big Dig 1	15000	9050	12250	7450	11750	7600
Carlin	Fallon Big Dig 2	14850	8400	12500	8450	11900	8500
Carlin	#3817	14400	6850	12150	7000	11700	7250
Sonoma	Lemmon Dr. 1	13350	9050	11150	9250	10500	9400
Sonoma	Fallon Big Dig 1	13350	9050	10800	7500	10300	7650
Sonoma	Fallon Big Dig 2	13250	8400	11000	8450	10400	8550
Sonoma	#3817	12850	6900	10700	7100	10250	7350
Silver State	Lemmon Dr. 1	10100	9000	8650	9200	8200	9400
Silver State	Fallon Big Dig 1	10100	9000	8400	7400	8050	7600
Silver State	Fallon Big Dig 2	10000	8400	8550	8450	8100	8500
Silver State	#3817	9750	6850	8350	6950	8000	7200

Table 53. Summary of Mr Values (psi) for New Design for Structures with a Borrow Layer.

Material			Low Traffic			Medium Traffic			High Traffic		
Base	Borrow	Subgrade	Base	Borrow	Subgrade	Base	Borrow	Subgrade	Base	Borrow	Subgrade
Sonoma	Sonoma	Fallon BD1	15850	10350	7550	11850	10400	7750	11000	10750	7900
Sonoma	Sonoma	#3817	15800	10250	7250	11800	10350	7500	11000	10750	7800
Imlay	Spanish Springs	Fallon BD1	17600	9950	7550	13300	10500	7750	12350	11100	7900
Imlay	Spanish Springs	#3817	17550	9900	7250	13250	10450	7500	12350	11100	7800
Sonoma	Vega Base	Fallon BD1	15600	8600	7550	11650	8500	7750	10850	8750	7900
Sonoma	Vega Base	#3817	15600	8500	7250	11650	8500	7500	10850	8750	7800
Imlay	Goni	Fallon BD1	17250	7650	7550	13000	7850	7700	12150	8250	7900
Imlay	Goni	#3817	17200	7600	7250	12950	7800	7450	12150	8200	7750
Imlay	Goni Base	Fallon BD1	16700	5150	7600	12500	5100	7750	11850	5200	7900
Imlay	Goni Base	#3817	16650	5100	7250	12500	5050	7500	11850	5200	7800
Imlay	Lockwood Base	Fallon BD1	17400	8550	7600	13050	8500	7750	12200	8700	7900
Imlay	Lockwood	Fallon BD1	17300	8000	7550	13000	7900	7750	12150	8150	7900
Imlay	Imlay	Fallon BD1	17450	8800	7600	13100	8700	7750	12250	9000	7900
Imlay	Trico Base A	Fallon BD1	17300	7950	7550	13000	7950	7700	12150	8250	7900
Imlay	Trico	Fallon BD1	16650	5000	7500	12500	5000	7650	11850	5150	7850
Sonoma	Elko 1	#3817	15500	8150	7200	11600	8200	7450	10850	8450	7750
Sonoma	Silver State	#3817	15350	7200	7250	11500	7250	7500	10750	7550	7750
Sonoma	Vega	#3817	15850	10500	7250	11850	10600	7500	11000	10950	7800

Chapter 6. Design Resilient Modulus for Rehabilitation Projects

Rehabilitation projects (i.e., overlay) are the most common type of construction for NDOT; hence, a relationship between the backcalculated and design modulus is needed for the implementation of the AASHTOWare® Pavement ME Design software (51). This chapter focuses on the methodology to obtain representative design Mr values for unbound materials for pavement rehabilitation projects. A stepwise mechanistic analysis approach was followed for determining the unbound materials' Mr values for rehabilitation design. The ILLI-PAVE 2005 finite element (FE) program (54) was employed as an advanced structural model for computing stresses and deflection basins in typical Nevada pavements under representative tire loading. In comparison with other pavement analysis software, the main unique features that prompted the use of this program are (3):

- The inclusion of six different constitutive models allowing for the characterization of the non-linear (stress-dependent) Mr behavior of unbound materials under repetitive loading, unlike Linear Elastic Programs (LEP).
- The implementation of Mohr-Coulomb failure criteria (c and ϕ) for unbound materials.
- The significantly lower computational effort resulting from the use of axis-symmetric FE formulation.
- The ability to handle pavement structures with up to ten layers.

It should also be noted that the ILLI-PAVE program is the only model that allows the use of the constitutive models acquired from the AASHTO T307 test.

6.1. Procedure for Determination of Mr Values for Rehabilitation Design

The stepwise mechanistic approach for determining Mr values for rehabilitation design using ILLI-PAVE is summarized as follows (3).

1. Select Representative Pavement Structures: The analysis starts by establishing representative NDOT flexible pavement structures.
2. Pavement Layer Properties:
    i. Asphalt Concrete (AC): The AC layer was subdivided into sublayers in ILLI-PAVE to capture its viscoelastic behavior, and the appropriate E* master curve was used to assign a proper E* value for each sublayer depending on the temperature and frequency.
    ii. Crushed Aggregate Base (CAB), Borrow, and Subgrade (SG): The constitutive Mr models developed from the AASHTO T307 test as well as the Mohr-Coulomb failure criteria (c and ϕ) were used in ILLI-PAVE.
3. Pavement Responses: The unbound layers' Mr values are not constant at different locations within the respective layer. In other words, the stress dependency of the unbound materials results in a different Mr value at each location due to the changing state of stresses. Hence, assigning a Mr for the entire layer based on stresses at a specific location is questionable. In this study, surface deflection basins (i.e., vertical deflections at various radial distances from the applied loads) were generated for different pavement sections by applying the tire load on a circular plate using ILLI-PAVE. The generated surface deflection basins were then employed in a backcalculation analysis to identify the Mr for each pavement layer.

4. Establish the Mr Correlation Equations: Using the backcalculated moduli values for various types of unbound materials and pavement structures, correlations between Mr and other physical properties were developed and examined for their effectiveness.

6.2. Identification of Mr Values for Rehabilitation Design for NDOT Pavements

Flexible pavement structures used for the new design analysis were also used for this analysis. The AC layer was subdivided into sublayers as explained previously. The damaged E* master curve for the AC mix was used to simulate the in-situ condition of the AC layer in need for rehabilitation. Equation 67 was used to obtain the damaged E* values at different temperatures and frequencies, as shown in tables 54 and 55 for Districts 2 and 3, respectively. The damage factor in the equation (d_{AC}) can be determined based on the condition of the AC layer as follows: a) Excellent condition, d_{AC} between 0.00 and 0.20, b) Good condition, d_{AC} between 0.20 and 0.40, c) Fair condition d_{AC} between 0.40 and 0.80, d) Poor condition d_{AC} between 0.80 and 1.20, and e) Very Poor condition d_{AC} greater than 1.20. In this research, a Fair condition was assumed for the existing AC layer and a damage value of 0.60 was selected for use in Equation 67.

Figures 41 and 42 present the master curves for the undamaged and damaged E* of the AC layer for a typical PG64-28NV mix for Districts 2 and 3, respectively. It should be noted that due to the use of the logarithmic scale, small differences between the damaged and

undamaged E* master curves represent large changes in the actual E* value. The developed master curves were used to assign appropriate damaged E* values for each AC sublayer.

$$E^*_{dam} = 10^{\delta} + \frac{E^* - 10^{\delta}}{1 + e^{-0.3+5\times\log(d_{AC})}} \quad \text{(Eq. 67)}$$

Where;

- E^*_{dam}= damaged dynamic modulus
- δ= regression parameter
- d_{AC}= AC layer damage factor

Table 54. Damaged Dynamic Modulus Values for District 2 PG64-28NV Mixture.

Temperature (°F)	Frequency (Hz)					
	0.1	0.5	1	5	10	25
14	1312050	1614996	1740364	2010749	2116396	2245034
40	506447	712708	811640	1065436	1184062	1355482
70	99585	171807	213457	351453	423890	545884
100	21315	34554	42954	79105	102511	148375
130	10914	15213	19507	28986	36692	58510

Table 55. Damaged Dynamic Modulus Values for District 3 PG64-28NV Mixture.

Temperature (°F)	Frequency (Hz)					
	0.1	0.5	1	5	10	25
14	1388915	1694851	1820011	2086894	2189973	2314505
40	532939	752007	857799	1114347	1229135	1408723
70	101180	172519	215005	356527	433886	568912
100	29024	44949	55119	96288	122336	180066
130	13012	17191	19799	32735	41424	60465

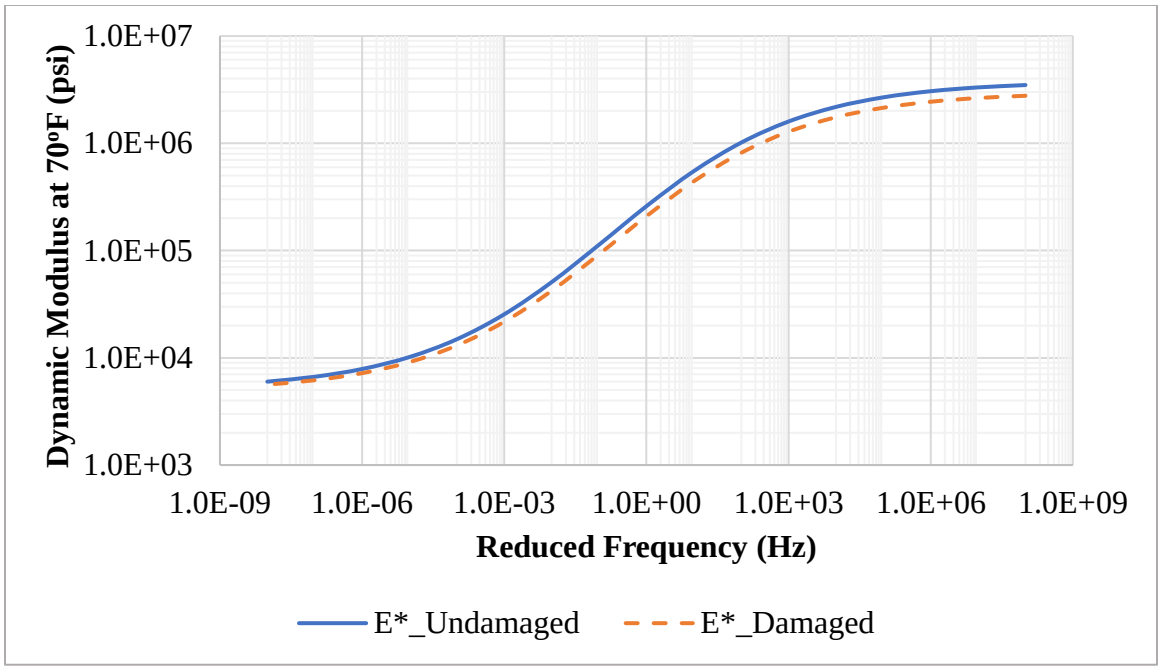

Figure 41. Undamaged and Damaged Dynamic Modulus Master Curves for District 2 PG64-28NV Mixture.

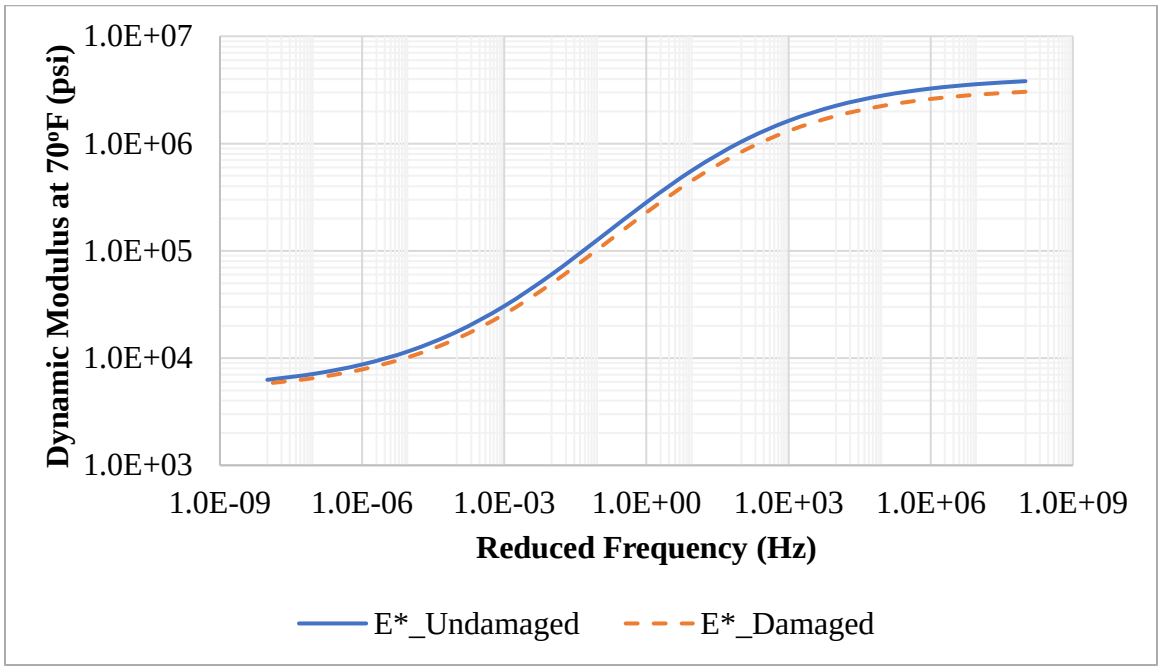

Figure 42. Undamaged and Damaged Dynamic Modulus Master Curves for District 3 PG64-28NV Mixture.

The Theta model was used for the base materials, the Uzan model was used for the subgrade materials, and the better model was used for the borrow materials. The Poisson's ratio values for the various layers and the subgrade strength categorization were the same as used in the new design analysis. The cohesion and friction angle for all unbound materials were estimated based on their corresponding USCS classification. The Falling Weight Deflectometer (FWD) was simulated in the ILLI-PAVE program by applying a circular load of 9000 lbs over a 5.35 inch radius.

Modulus-6.1 computer software (55) was used to backcalculate the moduli for the various layers using the surface deflection basins obtained from ILLI-PAVE. An apparent rigid layer was introduced in the Modulus-6.1 software to capture the non-linearity of the unbound materials and avoid having compensation effects. The backcalculation process was considered complete when the deflection basins calculated by the Modulus-6.1 software closely matched the ILLI-PAVE ones, and the identified modulus values were assigned to the corresponding layers.

A sample calculation for a flexible pavement structure with 5 inch AC and 16 inch base material from Carlin on top of the #3824 subgrade material is presented in this section. Table 56 shows the forward calculated deflections by ILLI-PAVE and the corresponding backcalculated ones by Modulus-6.1. The absolute error was 0.61 and the E4/Stiff Layer ratio was 6. Figure 43 presents the comparison between the deflections obtained from forward calculation and backcalculation. The backcalculated layer moduli are shown in table 57.

The results for this analysis are shown in tables 58 and 59 for structures with strong and weak subgrade, respectively. Results for structures on weak subgrade with a borrow layer are shown in tables 60 and 61 for low, and medium/high traffic, respectively.

Table 56. Forward calculated and Backcalculated Surface Deflections.

Radial Distance (inch)	Vertical Surface Deflections (mils)	
	ILLI-PAVE	Modulus-6.1
0	27.86	27.88
8	19.78	19.79
12	15.49	15.41
24	7.68	7.79
36	4.30	4.24
48	2.33	2.34
60	1.24	1.29

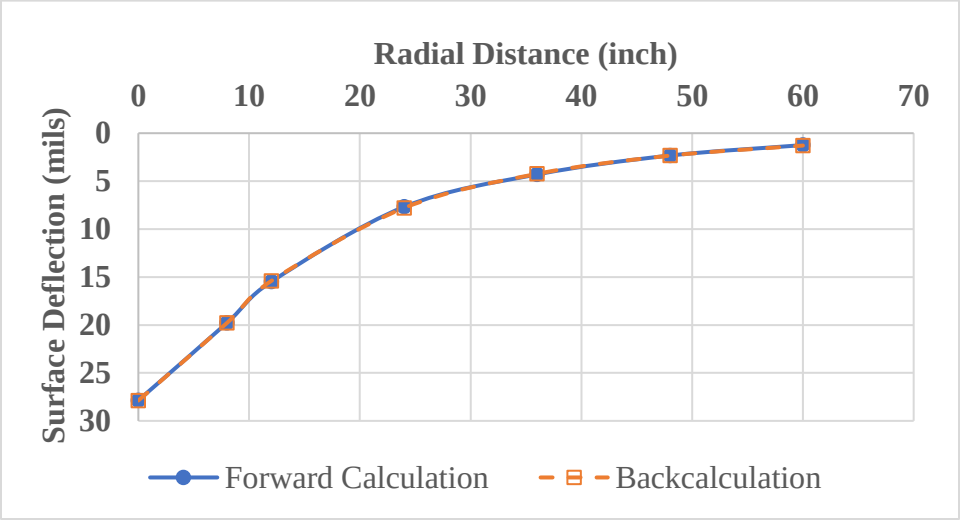

Figure 43. Forward calculated and Backcalculated Surface Deflections.

Table 57. Backcalculated Layer Moduli.

Layer	AC	CAB	SG
Backcalculated Modulus (psi)	171200	18500	6800

Table 58. Summary of Mr Values (psi) for Rehabilitation Design for Structures on Strong Subgrade.

Material		Low Traffic			Medium Traffic			High Traffic		
Base	Subgrade	AC	Base	Subgrade	AC	Base	Subgrade	AC	Base	Subgrade
Imlay	Kings Row	160400	19100	9000	145400	18200	9000	143900	16200	8800
Imlay	Lemmon Dr. 2	161100	18500	7400	143300	18200	6900	142400	16200	6700
Imlay	Spaghetti Bowl	162500	18200	6800	146300	17500	6600	145100	15600	6500
Imlay	#3824	163200	18100	6800	146700	17400	6700	145600	15500	6600
Trico B	Kings Row	142300	13300	7000	140200	12600	7000	138300	10900	6200
Trico B	Lemmon Dr. 2	140400	13200	5900	137200	12800	5500	137200	10800	5000
Trico B	Spaghetti Bowl	142600	12900	5600	139000	12400	5300	138500	10500	4800
Trico B	#3824	143900	12700	5600	139200	12300	5300	139100	10500	4900
Carlin	Kings Row	168800	19400	9000	157200	18700	9000	156600	16500	8800
Carlin	Lemmon Dr. 2	169700	18800	7500	156900	18200	7200	155500	16400	6700
Carlin	Spaghetti Bowl	171900	18500	6800	157200	17900	6600	156500	16000	6500
Carlin	#3824	171200	18500	6800	157900	17800	6700	156900	15900	6600
Sonoma	Kings Row	169100	18100	8800	157300	17200	8700	156500	15100	8300
Sonoma	Lemmon Dr. 2	169000	17600	7000	156000	17100	6700	155500	15000	6300
Sonoma	Spaghetti Bowl	171000	17400	6400	158000	16500	6400	157100	14500	6100
Sonoma	#3824	170700	17300	6500	158200	16400	6500	157100	14500	6300
Silver State	Kings Row	151500	15400	8100	151500	14600	7900	148600	13300	6500
Silver State	Lemmon Dr. 2	150600	15100	6500	148000	14700	6200	147900	13100	5200
Silver State	Spaghetti Bowl	151000	15000	6000	150400	14200	5900	147900	12900	5000
Silver State	#3824	150300	14900	6000	150000	14200	6000	148100	12900	5000

Table 59. Summary of Mr Values (psi) for Rehabilitation Design for Structures on Weak Subgrade.

Material		Low Traffic			Medium Traffic			High Traffic		
Base	Subgrade	AC	Base	Subgrade	AC	Base	Subgrade	AC	Base	Subgrade
Imlay	Lemmon Dr. 1	138800	17700	6100	130500	16800	6100	131300	14900	6100
Imlay	Fallon Big Dig 1	143000	16500	5300	131300	15800	5400	131900	14300	5300
Imlay	Fallon Big Dig 2	139800	17500	5700	130600	16600	5800	131600	14700	5900
Imlay	#3817	146200	15700	5100	133300	14900	5400	133100	13700	5500
Trico B	Lemmon Dr. 1	131300	12600	5200	126000	12000	5200	129000	10100	5100
Trico B	Fallon Big Dig 1	135000	11800	4500	128100	11200	4600	130100	9500	4600
Trico B	Fallon Big Dig 2	131200	12600	4900	127400	11700	5000	130100	9800	4900
Trico B	#3817	136300	11400	4400	129300	10600	4600	131000	9200	4600
Carlin	Lemmon Dr. 1	149400	18100	6100	142400	17200	6200	143700	15200	6200
Carlin	Fallon Big Dig 1	155000	16700	5300	143100	16300	5300	143300	14700	5400
Carlin	Fallon Big Dig 2	151100	17900	5800	142000	17200	5800	144700	15000	5800
Carlin	#3817	158900	15900	5100	145900	15300	5400	144800	14100	5400
Sonoma	Lemmon Dr. 1	150300	16700	5900	141300	15900	6000	144000	13700	6000
Sonoma	Fallon Big Dig 1	155000	15500	5100	143400	14800	5200	144700	13100	5300
Sonoma	Fallon Big Dig 2	150000	16700	5600	142200	15700	5700	143400	13700	5700
Sonoma	#3817	157600	14800	5000	145100	14000	5300	145600	12700	5400
Silver State	Lemmon Dr. 1	141900	14600	5600	137900	14200	5500	139800	11300	5500
Silver State	Fallon Big Dig 1	144500	13600	4800	138700	13300	4900	141700	11000	5000
Silver State	Fallon Big Dig 2	141300	14600	5300	138500	13900	5200	139500	11400	5200
Silver State	#3817	148100	12900	4700	141000	12400	4900	141400	10900	5000

Table 60. Summary of Mr Values (psi) for Rehabilitation Design for Structures with a Borrow layer (Low Traffic).

Material			Low Traffic			
Base	Borrow	Subgrade	AC	Base	Borrow	Subgrade
Sonoma	Sonoma	Fallon BD1	169100	15200	8400	4000
Sonoma	Sonoma	#3817	172100	14900	8000	4100
Imlay	Spanish Springs	Fallon BD1	152400	16900	8000	4100
Imlay	Spanish Springs	#3817	155800	16500	7400	4200
Sonoma	Vega Base	Fallon BD1	164400	15700	7300	3900
Sonoma	Vega Base	#3817	170000	15000	7400	4000
Imlay	Goni	Fallon BD1	153900	16400	6400	4100
Imlay	Goni	#3817	158200	15700	6500	4100
Imlay	Goni Base	Fallon BD1	152200	16600	4100	4000
Imlay	Goni Base	#3817	154800	16000	4000	4000
Imlay	Lockwood Base	Fallon BD1	152300	17100	6500	4000
Imlay	Lockwood	Fallon BD1	153700	16800	6200	4000
Imlay	Imlay	Fallon BD1	153000	16900	7100	4000
Imlay	Trico Base A	Fallon BD1	152400	17000	6500	4000
Imlay	Trico	Fallon BD1	153000	16400	3900	3900
Sonoma	Elko 1	#3817	166500	15300	6800	3900
Sonoma	Silver State	#3817	166500	15300	6200	3900
Sonoma	Vega	#3817	168000	15600	8200	4100

Table 61. Summary of Mr Values (psi) for Rehabilitation Design for Structures with a Borrow layer (Medium and High Traffic).

Material			Medium Traffic				High Traffic			
Base	Borrow	Subgrade	AC	Base	Borrow	Subgrade	AC	Base	Borrow	Subgrade
Sonoma	Sonoma	Fallon BD1	143700	15200	7400	4400	143100	14100	6400	4300
Sonoma	Sonoma	#3817	145500	14800	7400	4500	144900	13600	6700	4600
Imlay	Spanish Springs	Fallon BD1	130700	16800	7000	4400	129900	15800	5500	4300
Imlay	Spanish Springs	#3817	132000	16300	6900	4600	130500	15600	5400	4600
Sonoma	Vega Base	Fallon BD1	143900	15300	6000	4200	142500	14400	4400	4400
Sonoma	Vega Base	#3817	144900	14900	6000	4300	143100	14100	4600	4500
Imlay	Goni	Fallon BD1	132200	16100	6000	4400	129800	15500	4400	4400
Imlay	Goni	#3817	133700	15400	6300	4400	131300	15100	4600	4600
Imlay	Goni Base	Fallon BD1	131400	16100	3900	4300	131400	14600	3900	4100
Imlay	Goni Base	#3817	133400	15500	4000	4400	132200	14300	4100	4300
Imlay	Lockwood Base	Fallon BD1	130700	16600	5900	4400	130200	15600	4300	4700
Imlay	Lockwood	Fallon BD1	131700	16100	6000	4300	131300	15200	4500	4600
Imlay	Imlay	Fallon BD1	132200	16300	6400	4400	129900	15600	4500	4700
Imlay	Trico Base A	Fallon BD1	130600	16700	5700	4400	130100	15600	4300	4700
Imlay	Trico	Fallon BD1	131500	16000	3900	4300	140000	14500	3700	4300
Sonoma	Elko 1	#3817	144300	14800	6000	4300	143000	14300	4000	4500
Sonoma	Silver State	#3817	146100	14300	6000	4200	143200	14000	4300	4300
Sonoma	Vega	#3817	144700	15200	7000	4400	142200	14800	4600	4500

Chapter 7. Development of Mr Prediction Models

In this chapter, all data presented in previous chapters were compiled and used to develop prediction models for unbound materials Mr value, as a function of their empirical and physical properties, to be used in the structural design of new or rehabilitation pavement projects. The properties considered in the development of Mr prediction models included; R-value, UCS, OMC, MDD, LL, PI, and materials passing sieves #200, #40, #4, 3/8", 3/4", 1", and 1.5". In addition, the pavement equivalent thickness in terms of the base, borrow, or subgrade layer were identified as critical parameters in the determination of the design Mr for unbound layers. The structure thickness above the base, borrow, and subgrade used for the state of stress calculations was transformed into equivalent thickness using the MET as presented in Equations 68, 69, and 70.

$$H_{eq,CAB} = h_{AC}\left[\frac{E_{AC}(1-\nu_{SG}{}^2)}{E_{SG}(1-\nu_{AC}{}^2)}\right]^{1/3} + \frac{h_{CAB}}{4}\left[\frac{E_{CAB}(1-\nu_{SG}{}^2)}{E_{SG}(1-\nu_{CAB}{}^2)}\right]^{1/3} \quad \text{(Eq. 68)}$$

$$H_{eq,BOR} = h_{AC}\left[\frac{E_{AC}(1-\nu_{SG}{}^2)}{E_{SG}(1-\nu_{AC}{}^2)}\right]^{1/3} + h_{CAB}\left[\frac{E_{CAB}(1-\nu_{SG}{}^2)}{E_{SG}(1-\nu_{CAB}{}^2)}\right]^{1/3} + \frac{h_{BOR}}{4}\left[\frac{E_{BOR}(1-\nu_{SG}{}^2)}{E_{SG}(1-\nu_{BOR}{}^2)}\right]^{1/3} \quad \text{(Eq. 69)}$$

$$H_{eq,SG} = h_{AC}\left[\frac{E_{AC}(1-\nu_{SG}{}^2)}{E_{SG}(1-\nu_{AC}{}^2)}\right]^{1/3} + h_{CAB}\left[\frac{E_{CAB}(1-\nu_{SG}{}^2)}{E_{SG}(1-\nu_{CAB}{}^2)}\right]^{1/3} + h_{BOR}\left[\frac{E_{BOR}(1-\nu_{SG}{}^2)}{E_{SG}(1-\nu_{BOR}{}^2)}\right]^{1/3} + 18 \quad \text{(Eq. 70)}$$

Where;

- $H_{eq,CAB}$= Equivalent thickness of the base layer
- $H_{eq,BOR}$= Equivalent thickness of the borrow layer
- $H_{eq,SG}$= Equivalent thickness of the subgrade layer
- h_{AC}= Thickness of the AC layer
- h_{CAB}= Thickness of the base layer
- h_{BOR}= Thickness of the subgrade layer
- E_{AC}= Modulus of the AC layer
- E_{CAB}= Resilient modulus of the base layer
- E_{BOR}= Resilient modulus of the borrow layer
- E_{SG}= Resilient modulus of the subgrade layer
- ν_{AC}= Poisson's ratio of the AC layer
- ν_{CAB}= Poisson's ratio of the base layer
- ν_{BOR}= Poisson's ratio of the borrow layer
- ν_{SG}= Poisson's ratio of the subgrade layer

7.1. Statistical Analysis

Multi-linear regression analysis was conducted using the computer software, Minitab (56). The models were checked for normal distribution of errors using the Anderson-Darling normality test (57) and for multi-collinearity using the variance inflation factors (VIFs) (58). It is important to mention that models failing the normality test (i.e., residuals are not normally distributed) would result in inability of conducting statistical tests, such as F-tests and t-tests.

The steps followed in this analysis were as follows:

1. All measured properties were included as prediction variables for preliminary analysis.
2. Variables were tested for correlations, and highly correlated variables were removed in order to avoid high VIFs.

3. The backward elimination method was used to identify the best fit model, where all remaining variables after step 2 were introduced into the Mr prediction model, then the insignificant variables (having a p-value greater than 0.05) were removed. This is an iterative process where the most insignificant variable (with the highest p-value) is removed first, and the model is re-established again until all insignificant variables are identified and removed.

The analysis was done to obtain three different sets of design Mr prediction models:

- General Models: R-value and UCS excluded from prediction variables.
- UCS Models: include UCS as a prediction variable but exclude the R-value.
- R-value Models: include R-value as a prediction variable but exclude the UCS.

The collected materials were not enough to develop different models for Districts 2 and 3 separately. Hence, the models for base, borrow, and subgrade materials were developed from the combined Districts 2 and 3 materials. In addition, the database for District 1 unbound materials (3) was included in a separate analysis to develop statewide models to predict the design Mr values for Nevada materials.

7.1.1. Models Development for Districts 2 and 3 Materials

This section presents the effort for developing design Mr values prediction models for Districts 2 and 3 materials. Table 62 shows the range of data that were used for the development efforts.

Table 62. Range of Variables for Districts 2 and 3 Mr Models.

Parameters	Base		Borrow		Subgrade	
	Min	Max	Min	Max	Min	Max
R-value	70	87	46	83	9	75
UCS (psi)	10.2	32.0	1.8	33.3	8.1	56.4
P#200 (%)	7.5	11.1	2.9	19.5	9.4	78.1
P#40 (%)	13.4	21.1	10.6	44.0	29.2	94.1
P#4 (%)	39.7	63.4	32.4	92.4	62.1	100.0
P3/8" (%)	62.2	89.8	53.2	96.6	72.9	100.0
P3/4" (%)	91.5	100.0	76.6	100.0	85.4	100.0
P1" (%)	98.3	100.0	85.4	100.0	90.0	100.0
P1.5" (%)	-	-	93.9	100.0	97.2	100.0
Maximum dry density (pcf)	126.6	143.9	96.7	142.5	92.7	133.9
Optimum moisture content (%)	5.2	8.6	4.9	22.2	7.2	24.8
LL (%)	0.0	30.3	0.0	34.8	0.0	75.4
PI (%)	0.0	4.4	0.0	14.7	0.0	44.1
H_{eq} (New) (inch)	15.0	36.3	37.9	54.3	43.4	80.6
H_{eq} (Rehab) (inch)	17.5	37.9	44.9	65.4	49.9	91.6
Mr (New) (psi)	6,400	19,500	5,000	11,100	6,850	15,950
Mr (Rehab) (psi)	9,200	19,400	3,700	8,400	3,900	9,000

Typical residual and normality plots from Minitab are shown in figures 43 and 44, respectively. The residual plot must show random distribution, such that no patterns exist, whereas the normality plot must be linear to satisfy the linear regression assumption. The data in figures 44 and 45 indicate that both the random distribution and normality assumptions are satisfied.

Tables 63 and 64 present the summary for the developed General Mr models. Tables 65 and 66 present the summary for the developed UCS Mr models. Tables 67 and 68 present the summary for the developed R-value Mr models. It should be noted that, in the case of Mr values for the CAB layer in new design, multiple models were developed and are presented since they produced the same level of fit (i.e., similar R-square values). The multiple models are presented to allow more flexibility for NDOT to use the model with the more readily available properties.

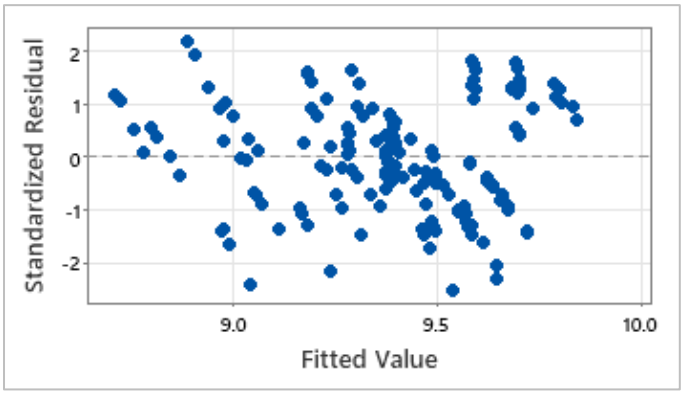

Figure 44. Typical Prediction Model Residual Plot for Districts 2 and 3 Materials.

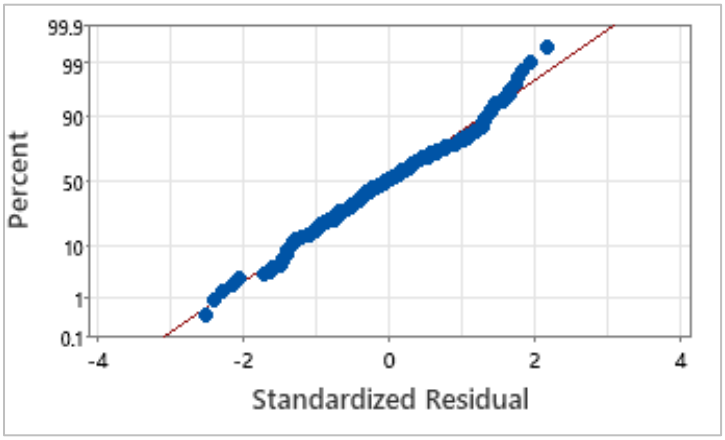

Figure 45. Typical Prediction Model Normality Plot for Districts 2 and 3 Materials.

Table 63. Summary of General Mr Models for Districts 2 and 3.

Ln (Mr)	Intercept	Heq (inch)	P1.5" (%)	P1" (%)	P3/4" (%)	P3/8" (%)	P#40 (%)
$Ln(Mr_{CAB-New})$ (1)	10.6855	-0.027189					
$Ln(Mr_{CAB-New})$ (2)	10.5108	-0.027179				0.00251	
$Ln(Mr_{CAB-New})$ (3)	14.45	-0.027191			-0.05697		-0.00945
$Ln(Mr_{BOR-New})$	12.28		-0.0647		0.00787		
$Ln(Mr_{SG-New})$	7.913					-0.026875	
$Ln(Mr_{CAB-Rehab})$	12.033	-0.012366			-0.02901		-0.0071
$Ln(Mr_{BOR-Rehab})$	13.15	-0.0174	-0.0681	0.01836			
$Ln(Mr_{SG-Rehab})$	13.034	-0.003485		-0.04932			0.005425

Table 64. Summary of General Mr Models for Districts 2 and 3 (Continued).

Ln (Mr)	P#200 (%)	OMC (%)	MDD (pcf)	PI (%)	R-sq (%)	Norm.[1]	Multi-Col.[2]
$Ln(Mr_{CAB-New})$ (1)	0.0406	-0.15704		0.0142	96.99	Pass	Pass
$Ln(Mr_{CAB-New})$ (2)	0.03832	-0.15281			96.98	Pass	Pass
$Ln(Mr_{CAB-New})$ (3)	0.12045				96.99	Pass	Pass
$Ln(Mr_{BOR-New})$	0.01279		0.01669	0.01454	70.87	Fail	Pass
$Ln(Mr_{SG-New})$		0.07316	0.0231		91.55	Fail	Pass
$Ln(Mr_{CAB-Rehab})$	0.08106				91.33	Pass	Pass
$Ln(Mr_{BOR-Rehab})$			0.01024	0.0192	75.28	Fail	Pass
$Ln(Mr_{SG-Rehab})$			0.003188		76.45	Fail	Pass

[1]Normality; [2]Multi Collinearity

Table 65. Summary of UCS Mr Models for Districts 2 and 3.

Ln (Mr)	Intercept	Heq (inch)	P1.5" (%)	P1" (%)	P3/4" (%)	P3/8" (%)	P#40 (%)	P#200 (%)
$Ln(Mr_{CAB-New})$	10.2206	-0.027272					-0.0168	0.05367
$Ln(Mr_{BOR-New})$	12.04		-0.0614		0.00817			
$Ln(Mr_{SG-New})$	10.813					-0.03383	0.01266	
$Ln(Mr_{CAB-Rehab})$	9.8386	-0.011756					-0.01062	0.04896
$Ln(Mr_{BOR-Rehab})$	9.607	-0.01661						
$Ln(Mr_{SG-Rehab})$	13.286	-0.004861		-0.04482				

Table 66. Summary of UCS Mr Models for Districts 2 and 3 (Continued).

Ln (Mr)	OMC (%)	MDD (pcf)	LL (%)	PI (%)	UCS (psi)	R-sq (%)	Norm.[1]	Multi-Col.[2]
$Ln(Mr_{CAB-New})$					-0.01841	95.29	Pass	Pass
$Ln(Mr_{BOR-New})$		0.0161		0.01392	0.00632	72.07	Fail	Pass
$Ln(Mr_{SG-New})$		0.007702			-0.003478	91.51	Fail	Pass
$Ln(Mr_{CAB-Rehab})$					-0.009525	84.56	Pass	Pass
$Ln(Mr_{BOR-Rehab})$	-0.02736			0.01648	0.00539	68.73	Fail	Pass
$Ln(Mr_{SG-Rehab})$			0.003992		-0.002202	74.89	Fail	Pass

[1]Normality; [2]Multi Collinearity

Table 67. Summary of R-value Mr Models for Districts 2 and 3.

Ln (Mr)	Intercept	Heq (inch)	P1" (%)	P3/4" (%)	P3/8" (%)	P#4 (%)	P#40 (%)
$Ln(Mr_{CAB-New})$ (1)	15.989	-0.027211		-0.05463	0.004271		0.0085
$Ln(Mr_{CAB-New})$ (2)	8.028	-0.027211			0.004092		0.01786
$Ln(Mr_{CAB-New})$ (3)	10.983	-0.027211			0.003722		0.00757
$Ln(Mr_{BOR-New})$	9.344				-0.02498		
$Ln(Mr_{SG-New})$	10.3238					-0.012419	
$Ln(Mr_{CAB-Rehab})$	9.163	-0.012367			0.002422		0.0098
$Ln(Mr_{BOR-Rehab})$	8.446	-0.01685	0.01696		-0.01712		0.01042
$Ln(Mr_{SG-Rehab})$	12.479	-0.004428	-0.03483				

Table 68. Summary of R-value Mr Models for Districts 2 and 3 (Continued).

Ln (Mr)	OMC (%)	MDD (pcf)	LL (%)	PI (%)	R-value	R-sq (%)	Norm.[1]	Multi-Col.[2]
$Ln(Mr_{CAB-New})$ (1)					-0.01573	97.00	Pass	Pass
$Ln(Mr_{CAB-New})$ (2)		0.02676			-0.029417	97.00	Pass	Pass
$Ln(Mr_{CAB-New})$ (3)	-0.15258				-0.00418	97.00	Pass	Pass
$Ln(Mr_{BOR-New})$			0.01503		0.02242	72.75	Pass	Pass
$Ln(Mr_{SG-New})$		0.003422	-0.002379		-0.009552	91.65	Fail	Pass
$Ln(Mr_{CAB-Rehab})$		0.01305			-0.017671	91.33	Pass	Pass
$Ln(Mr_{BOR-Rehab})$				0.02744	0.00759	77.90	Pass	Pass
$Ln(Mr_{SG-Rehab})$					-0.003312	76.05	Fail	Pass

[1]Normality; [2]Multi Collinearity

The established models showed that the Mr for the unbound materials can be estimated very well by the General models. The inclusion of the UCS resulted in slightly lower R-square values except in the case of borrow materials in new design, where the UCS made it slightly better (i.e., from 71 to 72%). The R-value models resulted in consistently better R-square values; however, this increase was not very significant either.

After the analysis of the data generated, a possible correlation was found between the equivalent thickness (H_{eq}) and the depth (D) from the pavement surface to the location where the state of stress was calculated as shown in figure 46. The MEPDG procedure requires a trial pavement to be assumed in the design process; therefore, using the assumed trial pavement structure, D can be determined and used to calculate H_{eq} in terms of the layer being analyzed using Equations 71 to 74. Once H_{eq} is computed, the Mr of the layer being analyzed can be estimated from the model developed models and can be used as a Level 2 input for the AASHTOWare® Pavement ME Design software (51).

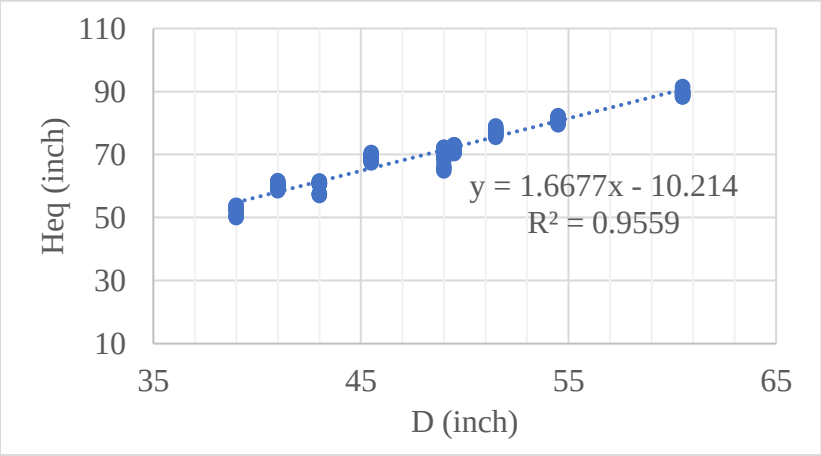

Figure 46. Correlation Between H_{eq} and D for Subgrade Materials for Districts 2 and 3 Materials Rehabilitation Design.

$$H_{eq(CAB-New)} = 2.1806 \times D - 1.6 \quad \text{(Eq. 71)}$$

$$H_{eq(CAB-Rehab)} = 2.3747 \times D - 0.8886 \quad \text{(Eq. 72)}$$

$$H_{eq(BOR-Rehab)} = 1.6915 \times D + 5.2513 \quad \text{(Eq. 73)}$$

$$H_{eq(SG-Rehab)} = 1.6677 \times D - 10.214 \quad \text{(Eq. 74)}$$

Where;

- $H_{eq(CAB-New)}$= H_{eq} of the base layer for new design (inch)
- $H_{eq(CAB-Rehab)}$= H_{eq} of the base layer for rehabilitation design (inch)
- $H_{eq\ (BOR-Rehab)}$= H_{eq} of the borrow layer for rehabilitation design (inch)
- $H_{eq\ (SG-Rehab)}$= H_{eq} of the subgrade layer for rehabilitation design (inch)
- D= Depth to location for state of stress calculation in the corresponding layer (inch)

7.1.2. Development of Statewide Models for Nevada Materials

This section presents the effort for developing statewide models for predicting design Mr values for Nevada materials. Table 69 shows the range of data that were used for the development efforts.

Typical residual and normality plots from Minitab are shown in figures 46 and 47, respectively. The residual plot must show random distribution, such that no patterns exist, whereas the normality plot must be linear to satisfy the linear regression assumption. The data in figures 47 and 48 indicate that both the random distribution and normality assumptions are satisfied.

Tables 70 and 71 present the summary for the developed General Mr models. Tables 72 and 73 present the summary for the developed UCS Mr models. Tables 74 and 75 present the summary for the developed R-value Mr models.

Table 69. Range of Variables for Statewide Mr Models.

Parameters	Base		Borrow		Subgrade	
	Min	Max	Min	Max	Min	Max
R-value	70	87	46	83	9	82
UCS (psi)	10.2	32.0	1.8	33.3	8.1	56.4
P#200 (%)	5.3	11.1	2.9	19.5	5.4	78.1
P#40 (%)	12.6	21.1	10.6	44.0	15.2	94.1
P#4 (%)	35.3	63.4	32.4	92.4	33.5	100.0
P3/8" (%)	54.1	89.8	53.2	99.9	52.5	100.0
P3/4" (%)	88.9	100.0	76.6	100.0	77.0	100.0
P1" (%)	98.3	100.0	85.4	100.0	83.5	100.0
P1.5" (%)	100.0	100.0	93.9	100.0	92.5	100.0
Maximum dry density (pcf)	126.6	147.5	96.7	143.2	92.7	139.2
Optimum moisture content (%)	3.5	8.6	4.9	22.2	6.1	24.8
LL (%)	0.0	30.3	0.0	34.8	0.0	75.4
PI (%)	0.0	4.4	0.0	14.7	0.0	44.1
H_{eq} (New) (inch)	15.0	36.3	37.9	54.3	43.4	80.6
H_{eq} (Rehab) (inch)	17.5	37.9	44.9	65.4	49.9	91.6
Mr (New) (psi)	6,400	27,250	5,000	20,400	6,850	15,950
Mr (Rehab) (psi)	9,200	22,900	3,700	15,500	3,900	9,000

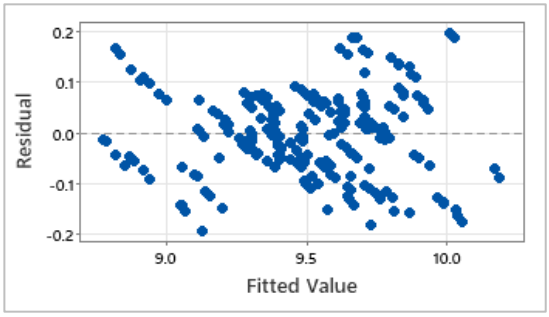

Figure 47. Typical Prediction Model Residual Plot for Nevada Materials.

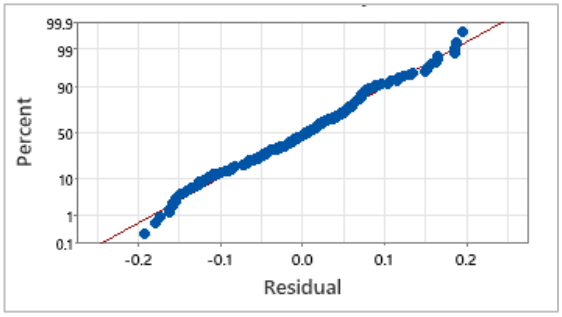

Figure 48. Typical Prediction Model Normality Plot for Nevada Materials.

Table 70. Summary of General Mr Statewide Models.

Ln (Mr)	Intercept	Heq (inch)	P1.5" (%)	P1" (%)	P3/4" (%)	P3/8" (%)	P#4 (%)	P#40 (%)
$Ln(Mr_{CAB-New})$ (1)	12.92	-0.02865		-0.0691	0.05993	-0.01454		0.02669
$Ln(Mr_{CAB-New})$ (2)	6.533	-0.028607			0.0422	-0.00912		0.01466
$Ln(Mr_{BOR-New})$	9.75		-0.0528				0.00866	-0.02357
$Ln(Mr_{SG-New})$	11.976	-0.00581		-0.03079				0.002527
$Ln(Mr_{CAB-Rehab})$ (1)	7.556	-0.01168			0.02689	-0.00995		0.00829
$Ln(Mr_{CAB-Rehab})$ (2)	8.108	-0.011915			0.02287	-0.007292		
$Ln(Mr_{BOR-Rehab})$	6.745	-0.02379				-0.00807	0.01511	-0.03116
$Ln(Mr_{SG-Rehab})$	11.204	-0.007215		-0.02151				0.005381

Table 71. Summary of General Mr Statewide Models (Continued).

Ln (Mr)	P#200 (%)	OMC (%)	MDD (pcf)	LL (%)	PI (%)	R-sq (%)	Norm.[1]	Multi-Col.[2]
$Ln(Mr_{CAB-New})$ (1)	0.04493	-0.22338				92.51	Fail	Pass
$Ln(Mr_{CAB-New})$ (2)	0.05761	-0.20149	0.00543			92.36	Pass	Pass
$Ln(Mr_{BOR-New})$	0.0576		0.02983			52.66	Fail	Pass
$Ln(Mr_{SG-New})$			0.00309		0.00289	68.36	Fail	Pass
$Ln(Mr_{CAB-Rehab})$ (1)	0.04442	-0.12585	0.00546		0.04769	89.09	Fail	Pass
$Ln(Mr_{CAB-Rehab})$ (2)	0.04454	-0.12418	0.00392		0.0406	88.42	Pass	Pass
$Ln(Mr_{BOR-Rehab})$	0.05823		0.02283			77.89	Fail	Pass
$Ln(Mr_{SG-Rehab})$		-0.02116		0.001836		70.08	Pass	Pass

[1]Normality; [2]Multi Collinearity

Table 72. Summary of UCS Mr Statewide Models.

Ln (Mr)	Intercept	Heq (inch)	P1.5" (%)	P1" (%)	P3/4" (%)	P3/8" (%)	P#40 (%)	P#200 (%)
$Ln(Mr_{CAB-New})$	9.224	-0.028228			0.01205	0.00562	-0.00767	
$Ln(Mr_{BOR-New})$	12.16		-0.0783					0.1018
$Ln(Mr_{SG-New})$	11.81	-0.00479		-0.0316			0.003287	
$Ln(Mr_{CAB-Rehab})$	9.8784	-0.010466				0.003483		0.01746
$Ln(Mr_{BOR-Rehab})$	11.12	-0.01907	-0.0463				-0.01848	0.0988
$Ln(Mr_{SG-Rehab})$	10.691	-0.008651		-0.01419				0.0021

Table 73. Summary of UCS Mr Statewide Models (Continued).

Ln (Mr)	OMC (%)	MDD (pcf)	LL (%)	PI (%)	UCS (psi)	R-sq (%)	Norm.[1]	Multi-Col.[2]
$Ln(Mr_{CAB-New})$					-0.027999	95.30	Pass	Pass
$Ln(Mr_{BOR-New})$		0.03092	-0.01526	0.0389	-0.0327	72.27	Fail	Pass
$Ln(Mr_{SG-New})$		0.004016			0.003029	71.29	Fail	Pass
$Ln(Mr_{CAB-Rehab})$				0.06669	-0.02712	85.28	Pass	Pass
$Ln(Mr_{BOR-Rehab})$		0.02189			-0.02386	84.90	Pass	Pass
$Ln(Mr_{SG-Rehab})$	-0.01375		0.003718		-0.001428	65.91	Pass	Pass

[1]Normality; [2]Multi Collinearity

Table 74. Summary of R-value Mr Statewide Models.

Ln (Mr)	Intercept	Heq (inch)	P1.5" (%)	P1" (%)	P3/4" (%)	P3/8" (%)	P#4 (%)	P#40 (%)	P#200 (%)
$Ln(Mr_{CAB-New})$ (1)	5.788	-0.028626			0.03241		-0.002819		0.1149
$Ln(Mr_{CAB-New})$ (2)	5.452	-0.028753			0.03079				0.10738
$Ln(Mr_{BOR-New})$ (1)	27.59		-0.1943					-0.0282	
$Ln(Mr_{BOR-New})$ (2)	11.646			-0.03607				-0.03453	0.0408
$Ln(Mr_{SG-New})$	12.415	-0.004229		-0.02878					-0.000904
$Ln(Mr_{CAB-Rehab})$	7.604	-0.011713			0.02089	-0.003264			0.06318
$Ln(Mr_{BOR-Rehab})$	10.805	-0.01854			-0.02183	0.01114		-0.03433	0.07736
$Ln(Mr_{SG-Rehab})$	10.777	-0.008373		-0.01375					0.001934

Table 75. Summary of R-value Mr Statewide Models (Continued).

Ln (Mr)	OMC (%)	MDD (pcf)	LL (%)	PI (%)	R-value	R-sq (%)	Norm.[1]	Multi-Col.[2]
$Ln(Mr_{CAB-New})$ (1)	-0.26949				0.02638	96.70	Pass	Pass
$Ln(Mr_{CAB-New})$ (2)	-0.26878	0.00264		0.00897	0.02701	96.65	Pass	Pass
$Ln(Mr_{BOR-New})$ (1)	-0.0603		0.02836	-0.0388	0.0258	73.59	Pass	Pass
$Ln(Mr_{BOR-New})$ (2)	-0.1043		0.01973	-0.0291	0.02831	74.01	Fail	Pass
$Ln(Mr_{SG-New})$		0.002055		-0.0052	-0.006889	78.41	Fail	Pass
$Ln(Mr_{CAB-Rehab})$	-0.15673			0.022	0.01265	91.63	Fail	Pass
$Ln(Mr_{BOR-Rehab})$	-0.1261				0.01408	85.65	Pass	Pass
$Ln(Mr_{SG-Rehab})$	-0.01796		0.002423		-0.00164	66.14	Pass	Pass

[1]Normality; [2]Multi Collinearity

Figures 49, 50, and 51 show the R-square values comparison between the statewide models and the models developed for District 1 and Districts 2 and 3, for general models, UCS models, and R-value models, respectively. Figures 52, 53, and 54 show the R-square values comparison for the models developed for base, borrow, and subgrade materials, respectively. Based on the R-square values, the developed statewide models for design Mr values for combined Nevada materials resulted in better models only for base and borrow materials used in rehabilitation design. This is a promising result since rehabilitation projects are the most common for NDOT. It should also be noted that the models for the borrow material developed for District 1 (3) were based on the combined data from base and borrow materials, and hence the models for borrow materials based on the combined Nevada materials probably represent a better estimation of Mr values for borrow materials than the District 1 models, regardless of the R-square values. In addition, including the R-value resulted in better models for all materials except for the case of subgrade materials Mr for rehabilitation design. Similar results were shown when the UCS was used, where models became better for all materials except for the case of base and subgrade materials Mr for rehabilitation design.

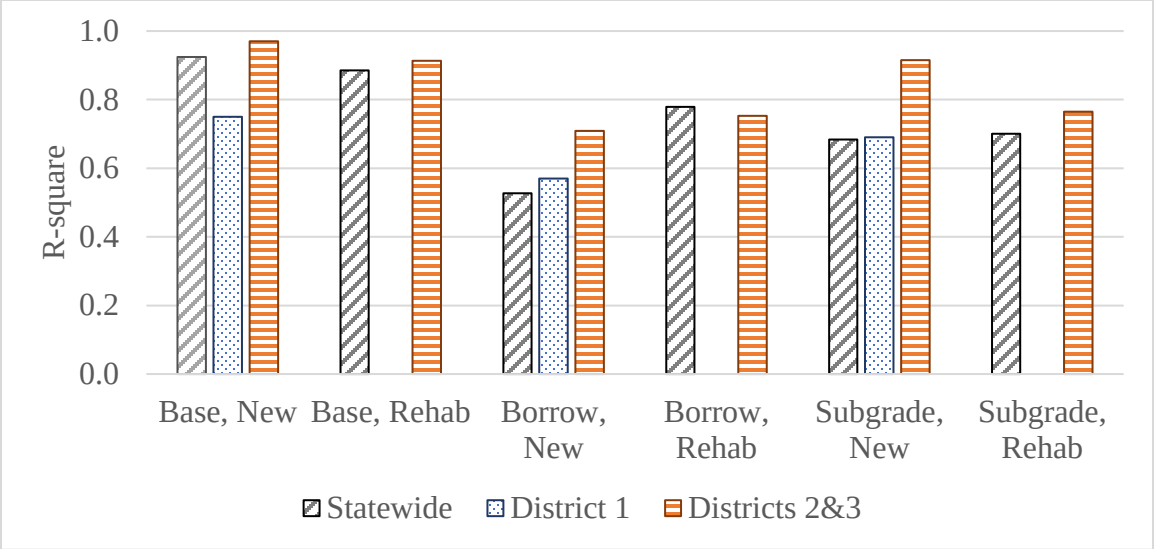

Figure 49. R-square Comparison for General Models.

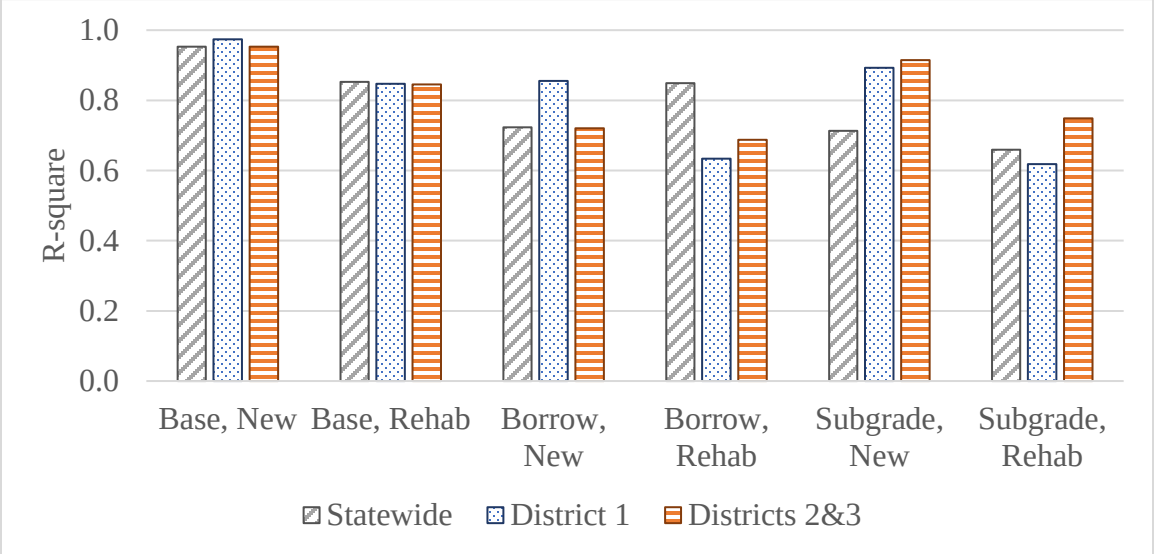

Figure 50. R-square Comparison for UCS Models.

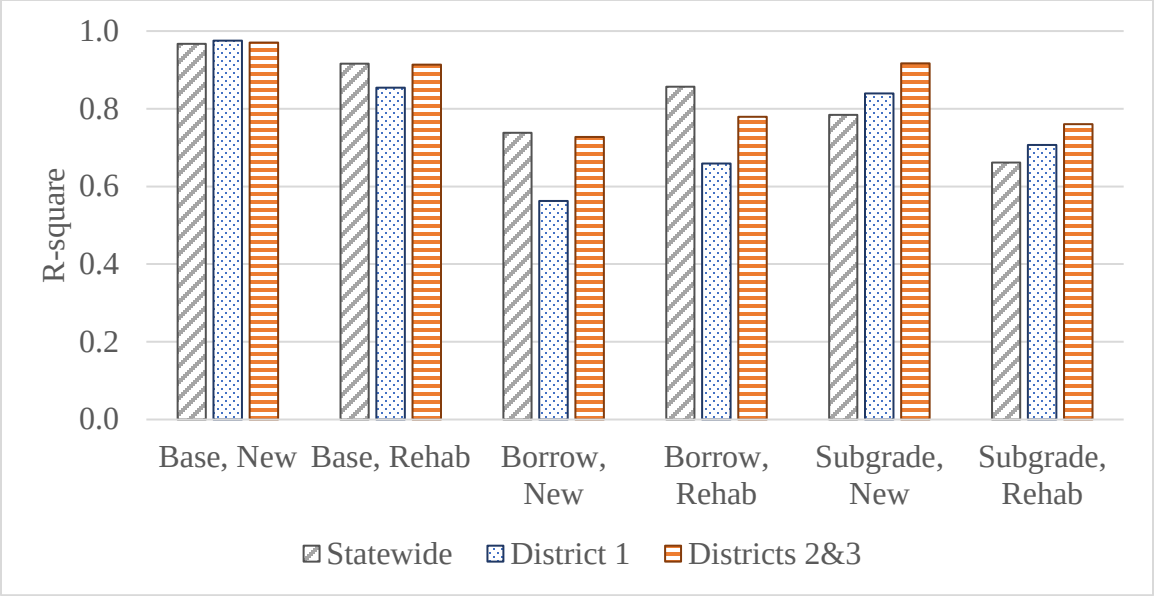

Figure 51. R-square Comparison for R-value Models.

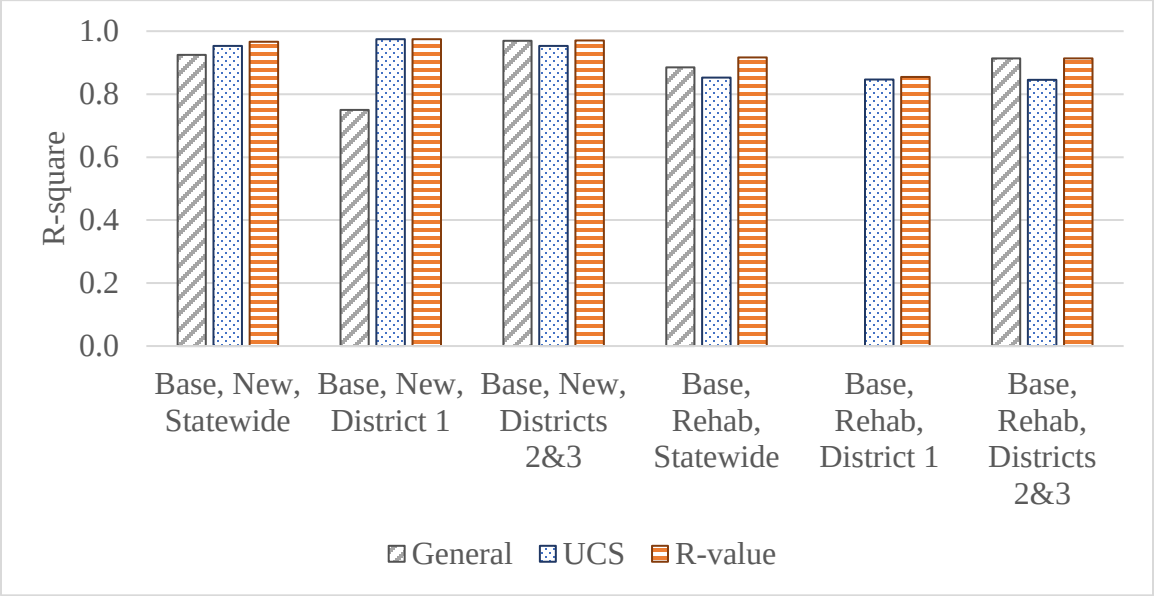

Figure 52. R-square Comparison for Base Materials.

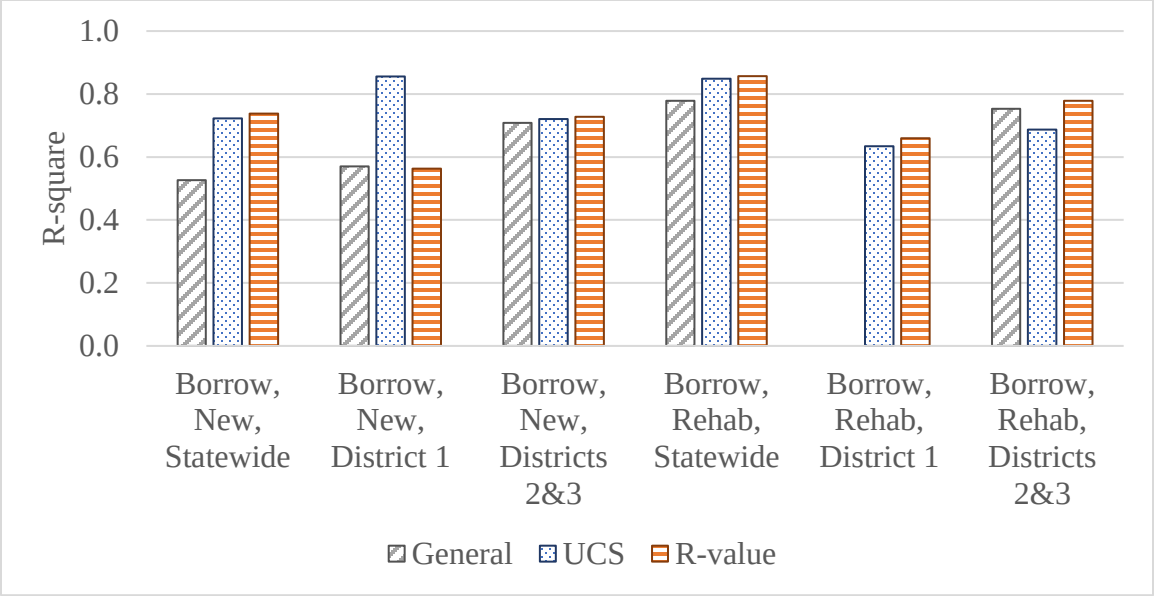

Figure 53. R-square Comparison for Borrow Materials.

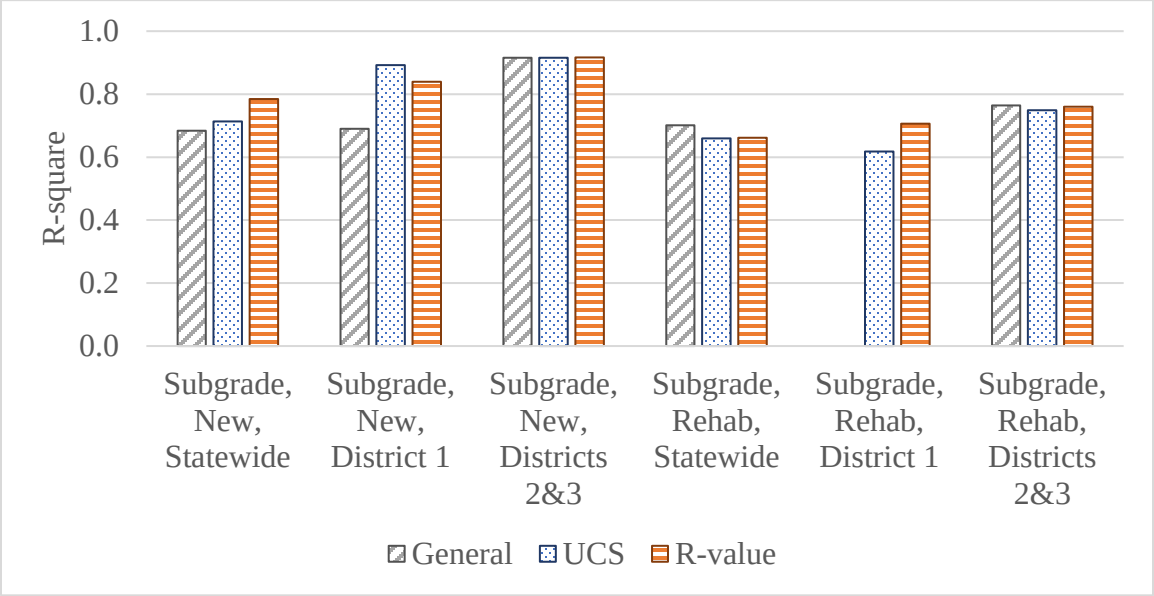

Figure 54. R-square Comparison for Subgrade Materials.

Similar to Districts 2 and 3 statistical analysis, H_{eq} and D correlations were established as shown in figure 55. The trial pavement to be assumed in the MEPDG design process can be used to determine D, which is used to calculate H_{eq} in terms of the layer being analyzed using Equations 75 to 79.

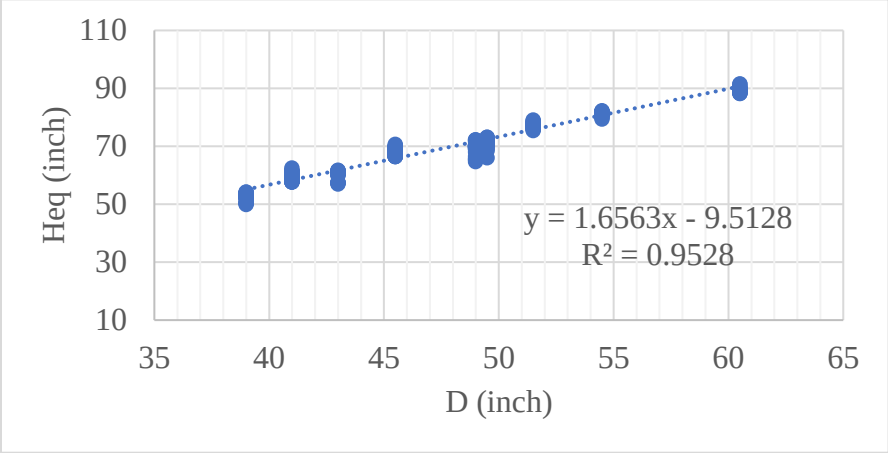

Figure 55. Correlation Between H_{eq} and D for Subgrade Materials for Nevada Materials Rehabilitation Design.

$$H_{eq(CAB-New)} = 2.1846 \times D - 1.4186 \quad \text{(Eq. 75)}$$

$$H_{eq(SG-New)} = 1.2921 \times D + 0.3671 \quad \text{(Eq. 76)}$$

$$H_{eq(CAB-Rehab)} = 2.4033 \times D - 1.4359 \quad \text{(Eq. 77)}$$

$$H_{eq(BOR-Rehab)} = 1.787 \times D + 2.0876 \quad \text{(Eq. 78)}$$

$$H_{eq(SG-Rehab)} = 1.6563 \times D - 9.5128 \quad \text{(Eq. 79)}$$

Where;

- $H_{eq(CAB-New)}$= H_{eq} of the base layer for new design (inch)
- $H_{eq(SG-New)}$= H_{eq} of the subgrade layer for new design (inch)
- $H_{eq(CAB-Rehab)}$= H_{eq} of the base layer for rehabilitation design (inch)
- $H_{eq\ (BOR-Rehab)}$= H_{eq} of the borrow layer for rehabilitation design (inch)
- $H_{eq\ (SG-Rehab)}$= H_{eq} of the subgrade layer for rehabilitation design (inch)
- D= Depth to location for state of stress calculation in the corresponding layer (inch)

7.2. Comparison of Mr Prediction Models

In this section, some plots will be presented for the sake of comparison and to better visualize the goodness of fit for the developed models. This section will be divided such that the comparison is done for 1) Districts 2 and 3 materials models, and 2) statewide models for combined Nevada materials, as follows:

- R-value models predicted Mr for new versus rehabilitation design.
- General models predicted Mr versus measured Mr for new design.
- General models predicted Mr versus measured Mr for rehabilitation design.
- UCS models predicted Mr versus measured Mr for new design.
- UCS models predicted Mr versus measured Mr for rehabilitation design.
- R-value models predicted Mr versus measured Mr for new design.
- R-value models predicted Mr versus measured Mr for rehabilitation design.

Note that in case there was more than one prediction model (i.e., more than one General or R-value model for single case), only one was used for plotting, as the resulting goodness of fit was almost the same.

In addition, a final plot will be presented for predicted Mr using NDOT's R-value equation versus new and rehabilitation design Mr value for Nevada materials. This plot will be used in order to assess the result of using the R-value alone to predict the Mr, from an equation that was not developed specifically for Nevada materials.

7.2.1. Comparison of Districts 2 and 3 Materials Mr Prediction Models

The comparison of the predicted Mr using R-value models for new and rehabilitation designs is shown in figure 56. The comparison of the predicted Mr using General models with the measured Mr for new and rehabilitation designs is shown in figures 57 and 58, respectively. The comparison of the predicted Mr using UCS models with the measured Mr for new and rehabilitation designs is shown in figures 59 and 60, respectively. The comparison of the predicted Mr using R-value models with the measured Mr for new and rehabilitation designs is shown in figures 61 and 62, respectively.

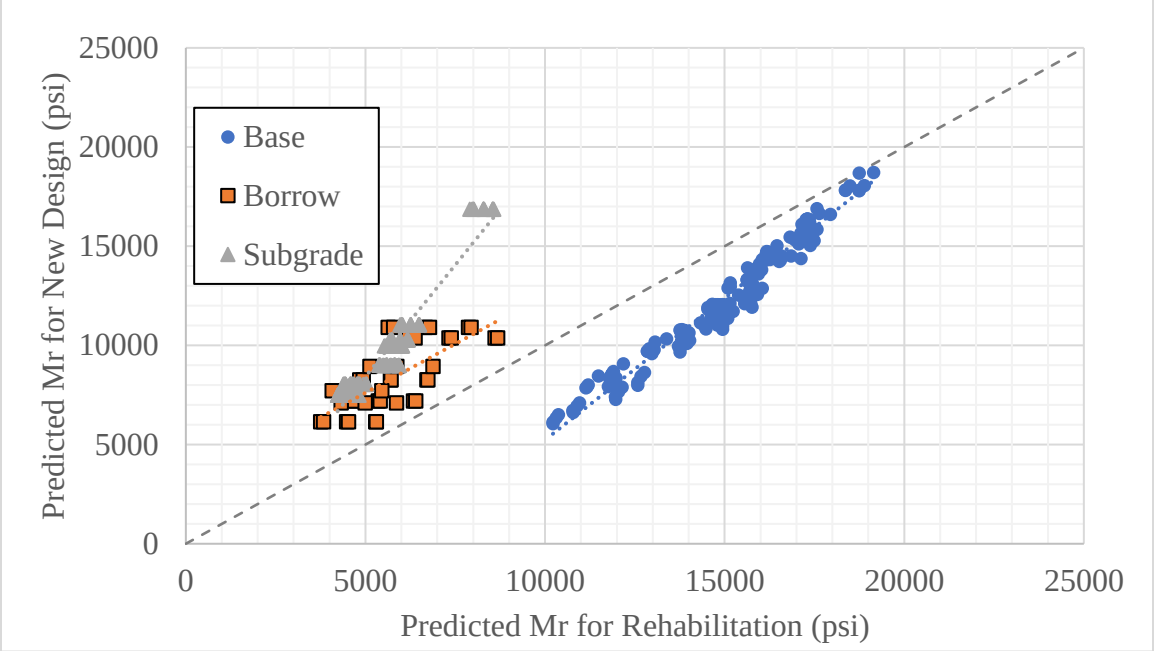

Figure 56. Comparison of New and Rehabilitation Predicted Mr (Districts 2 and 3 R-value Model).

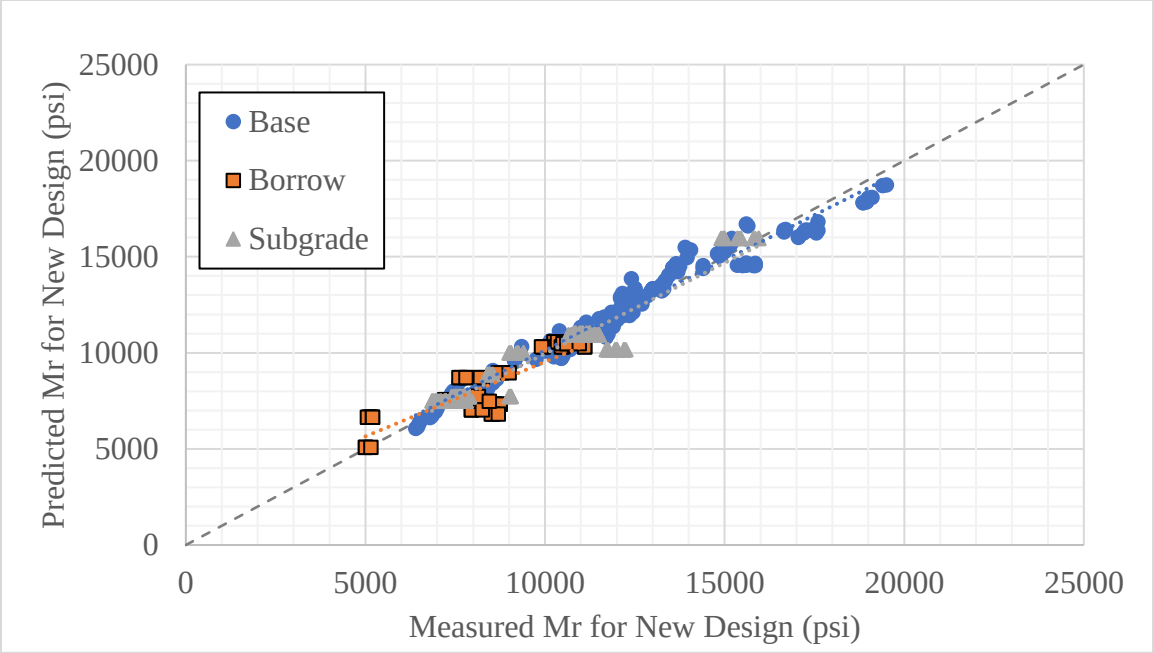

Figure 57. Variation of Measured Mr with Predicted Mr (Districts 2 and 3 General Model) for New Design.

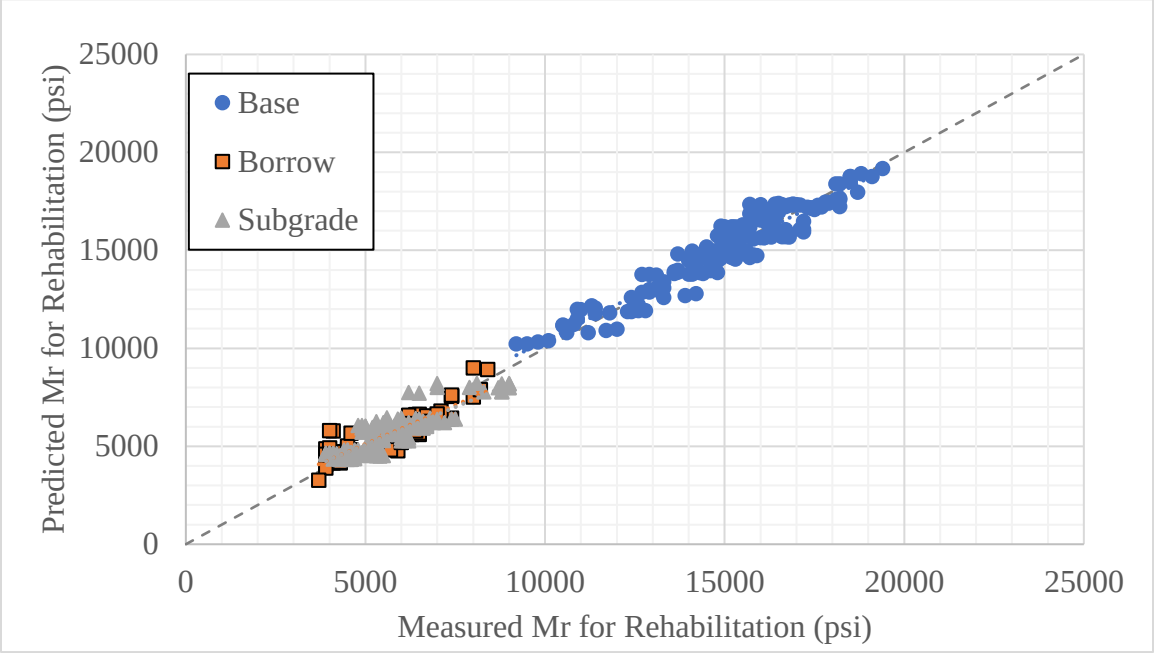

Figure 58. Variation of Measured Mr with Predicted Mr (Districts 2 and 3 General Model) for Rehabilitation Design.

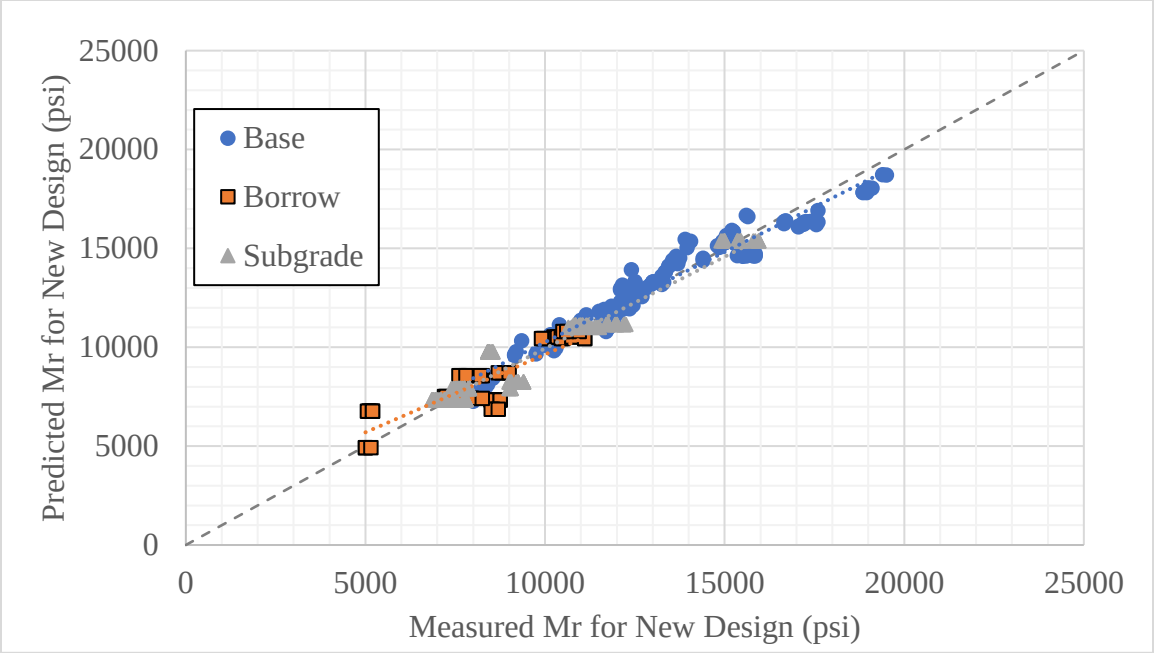

Figure 59. Variation of Measured Mr with Predicted Mr (Districts 2 and 3 UCS Model) for New Design.

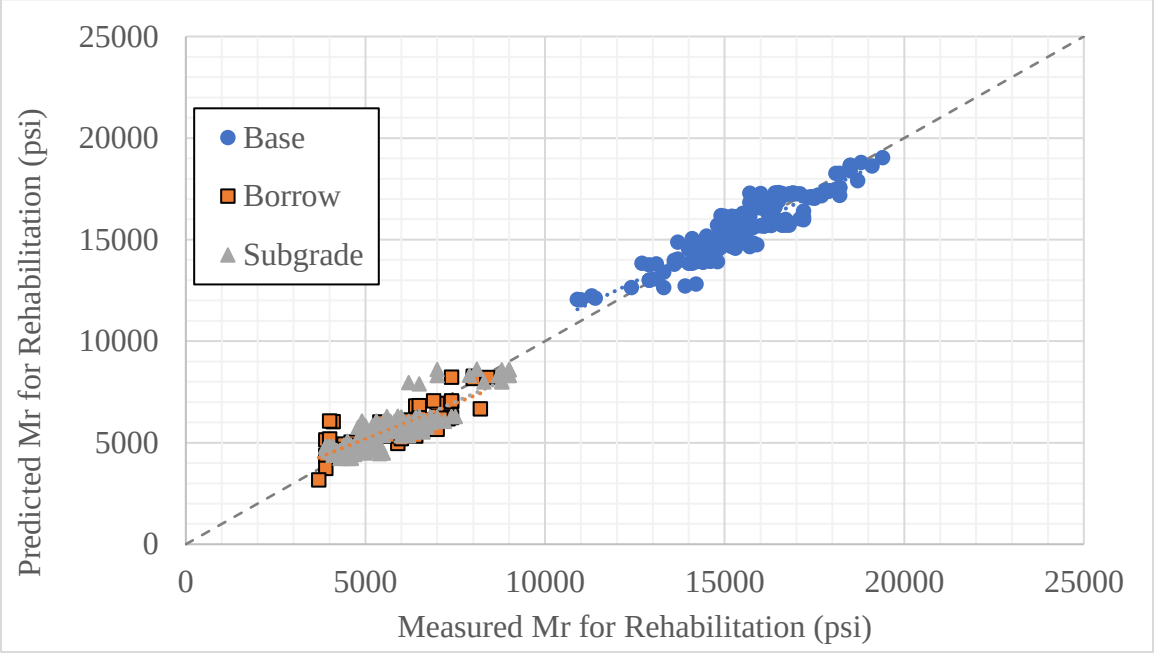

Figure 60. Variation of Measured Mr with Predicted Mr (Districts 2 and 3 UCS Model) for Rehabilitation Design.

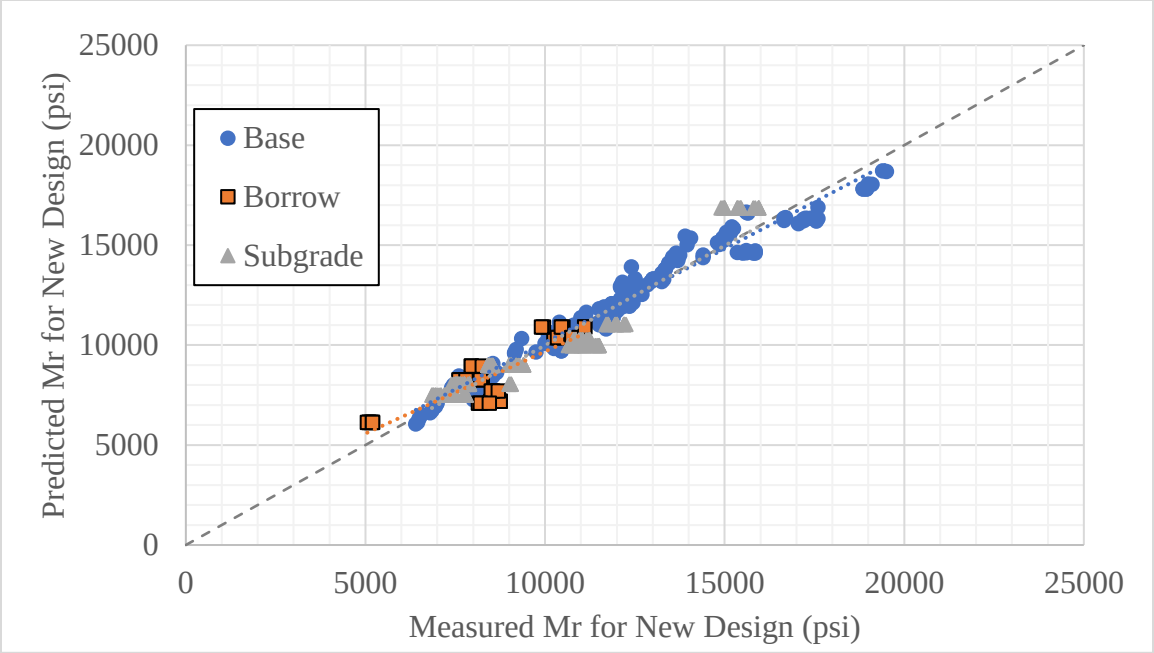

Figure 61. Variation of Measured Mr with Predicted Mr (Districts 2 and 3 R-value Model) for New Design.

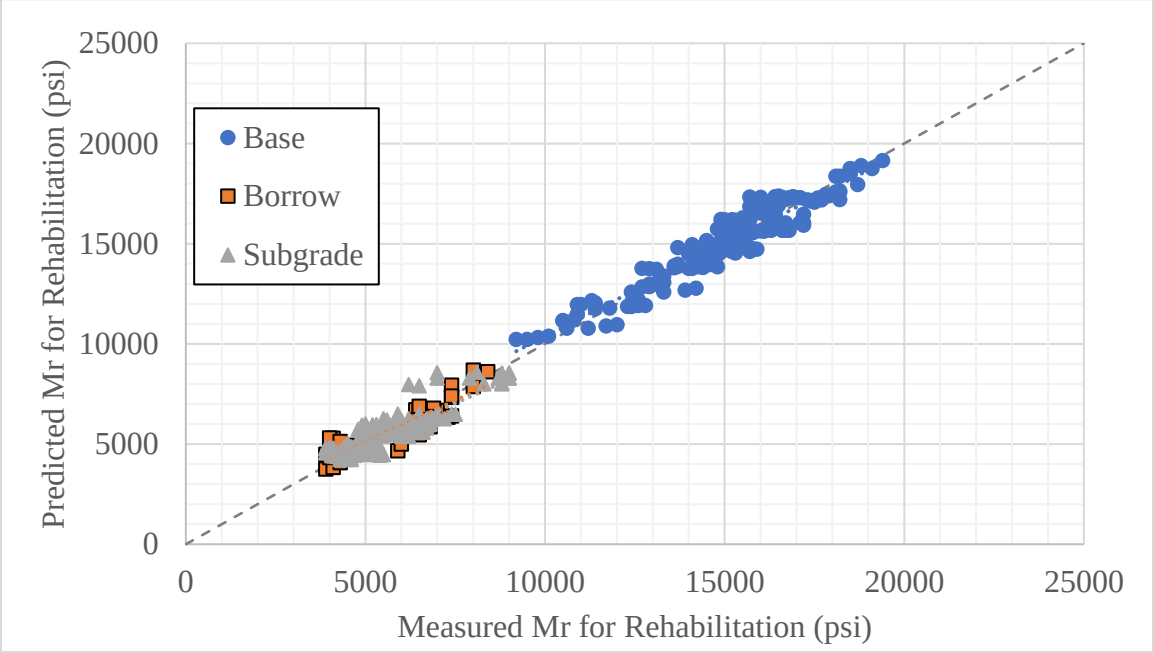

Figure 62. Variation of Measured Mr with Predicted Mr (Districts 2 and 3 R-value Model) for Rehabilitation Design.

7.2.2. Comparison of Statewide Mr Prediction Models for Combined Nevada Materials

The comparison of the predicted Mr using R-value models for new and rehabilitation designs is shown in figure 63. The comparison of the predicted Mr using General models with the measured Mr for new and rehabilitation designs is shown in figures 64 and 65, respectively. The comparison of the predicted Mr using UCS models with the measured Mr for new and rehabilitation designs is shown in figures 66 and 67, respectively. The comparison of the predicted Mr using R-value models with the measured Mr for new and rehabilitation designs is shown in figures 68 and 69, respectively. Figure 70 shows the comparison of the predicted new and rehabilitation design Mr with the predicted Mr from NDOT's R-value equation.

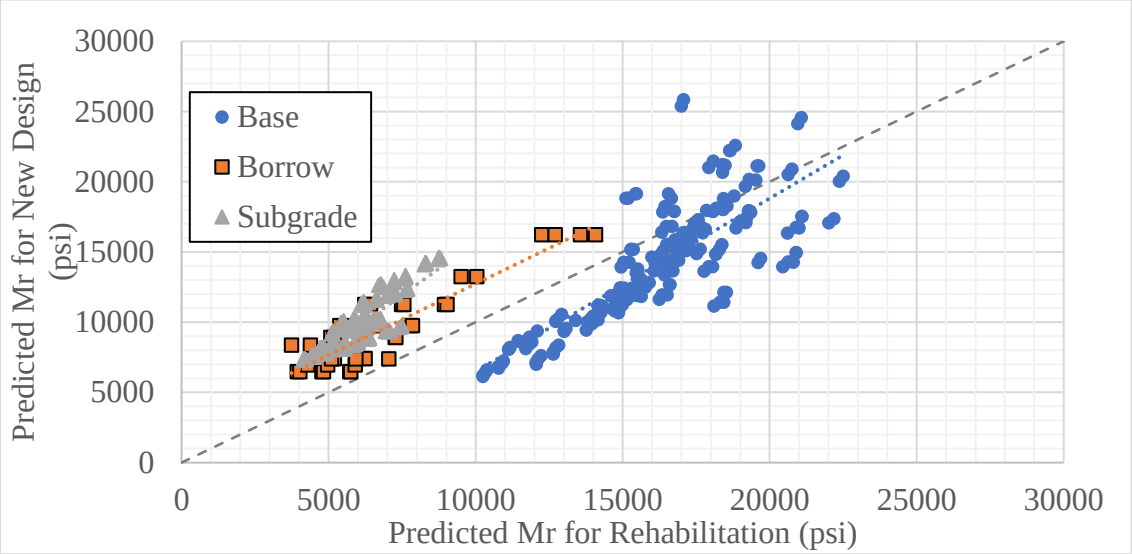

Figure 63. Comparison of New and Rehabilitation Predicted Mr (Statewide R-value Model).

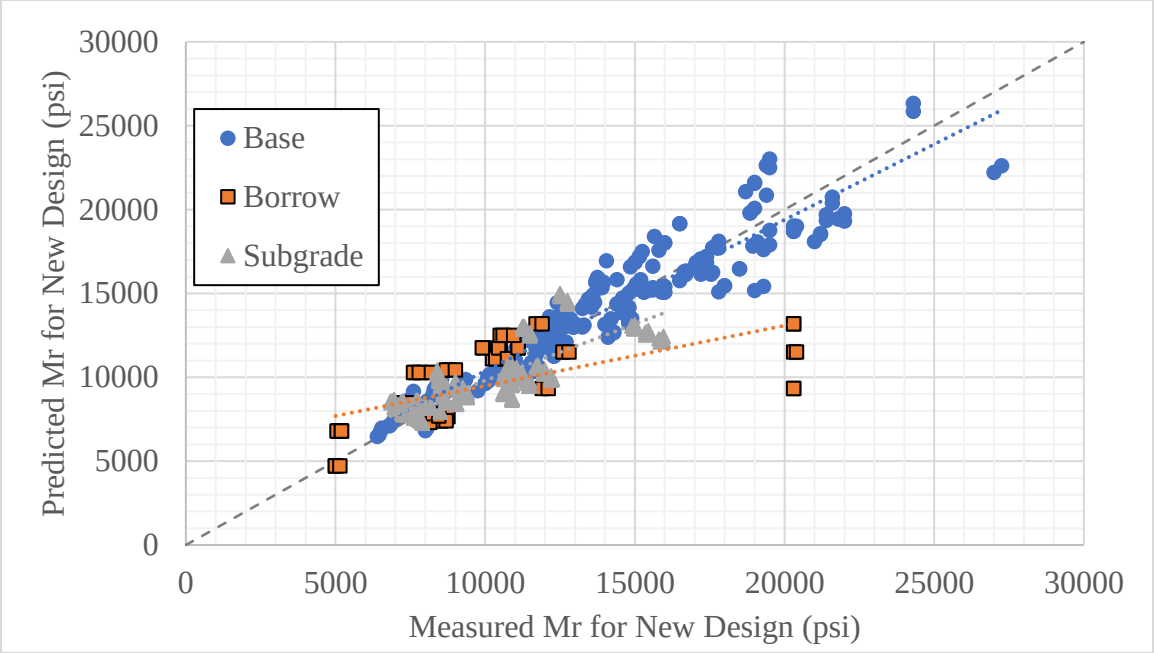

Figure 64. Variation of Measured Mr with Predicted Mr (Statewide General Model) for New Design.

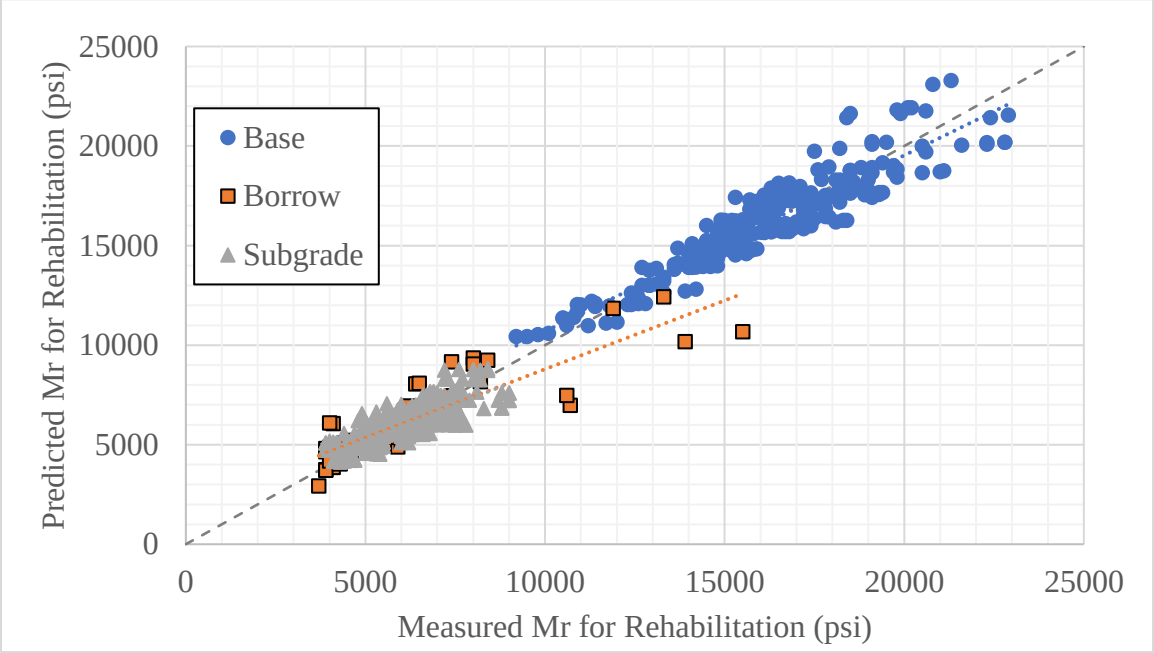

Figure 65Variation of Measured Mr with Predicted Mr (Statewide General Model) for Rehabilitation Design.

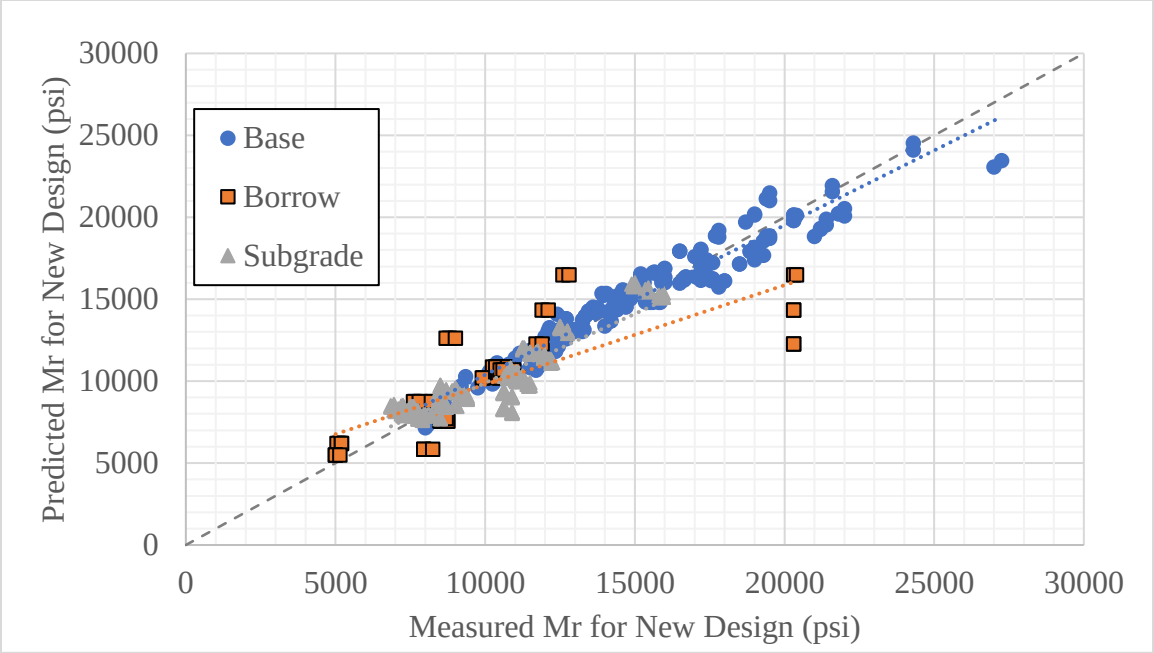

Figure 66. Variation of Measured Mr with Predicted Mr (Statewide UCS Model) for New Design.

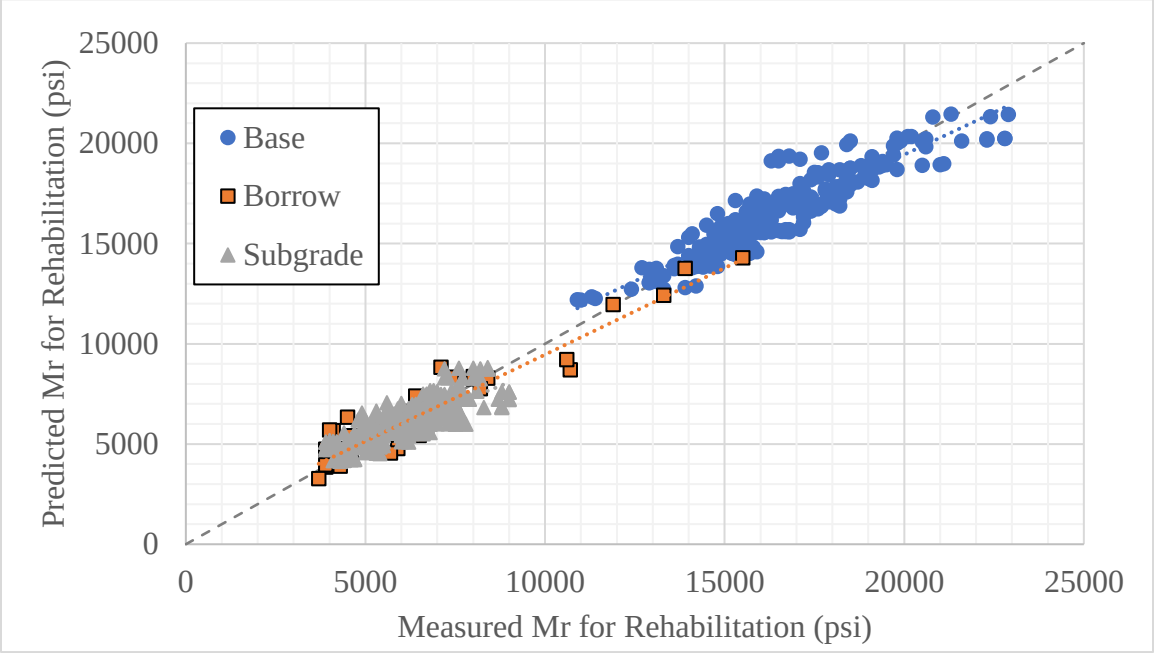

Figure 67. Variation of Measured Mr with Predicted Mr (Statewide UCS Model) for Rehabilitation Design.

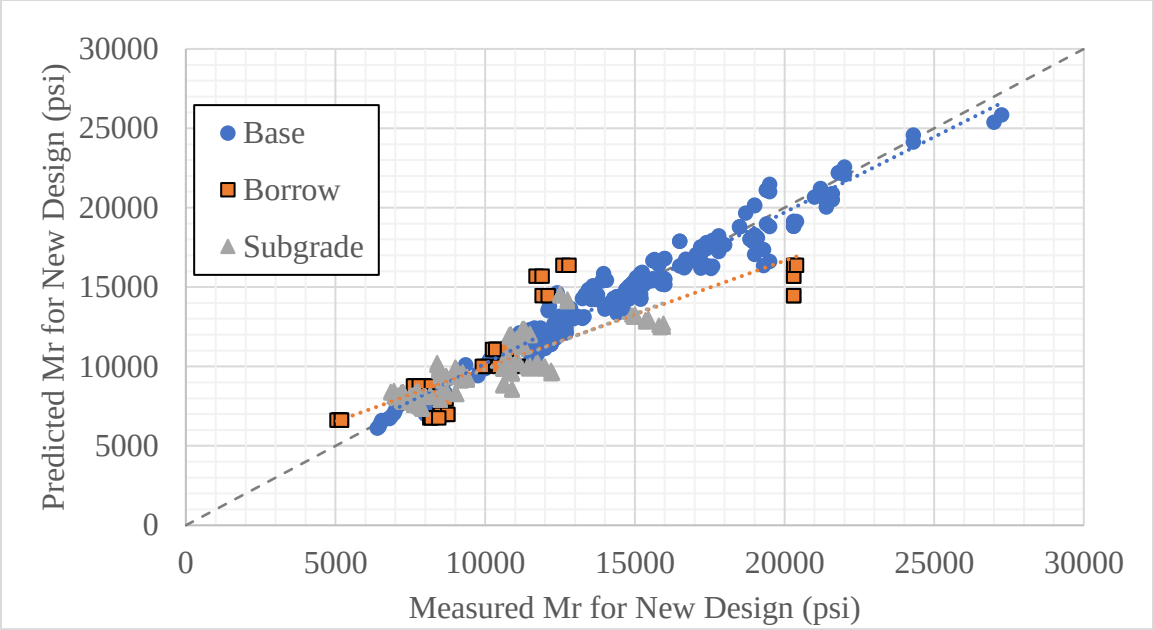

Figure 68. Variation of Measured Mr with Predicted Mr (Statewide R-value Model) for New Design.

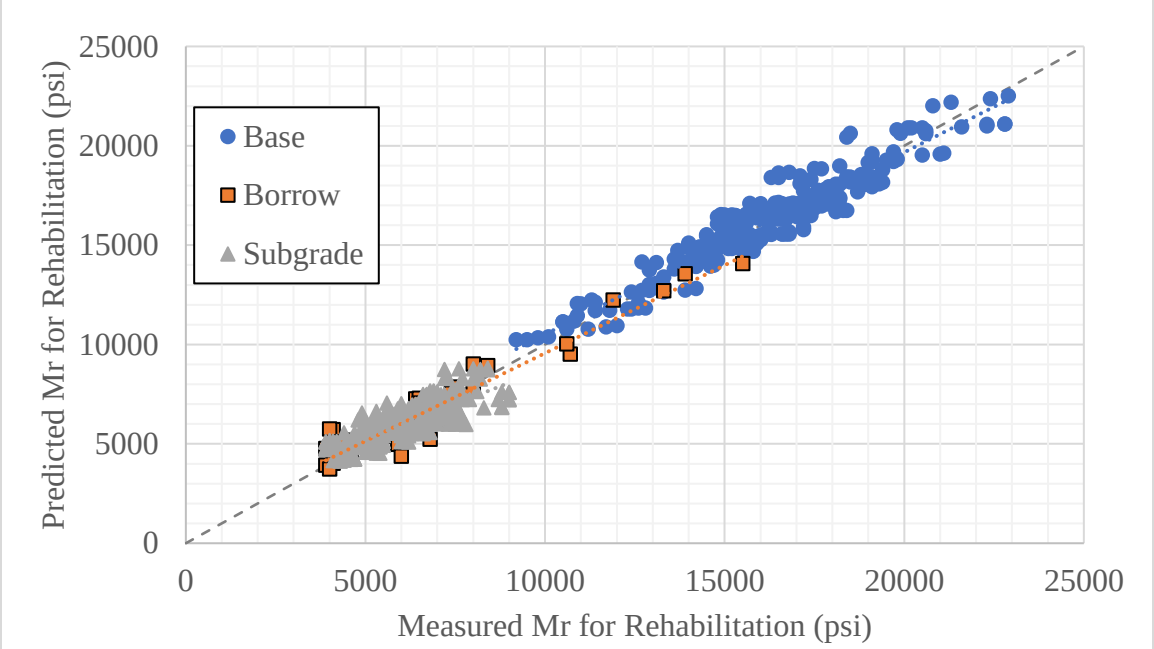

Figure 69. Variation of Measured Mr with Predicted Mr (Statewide R-value Model) for Rehabilitation Design.

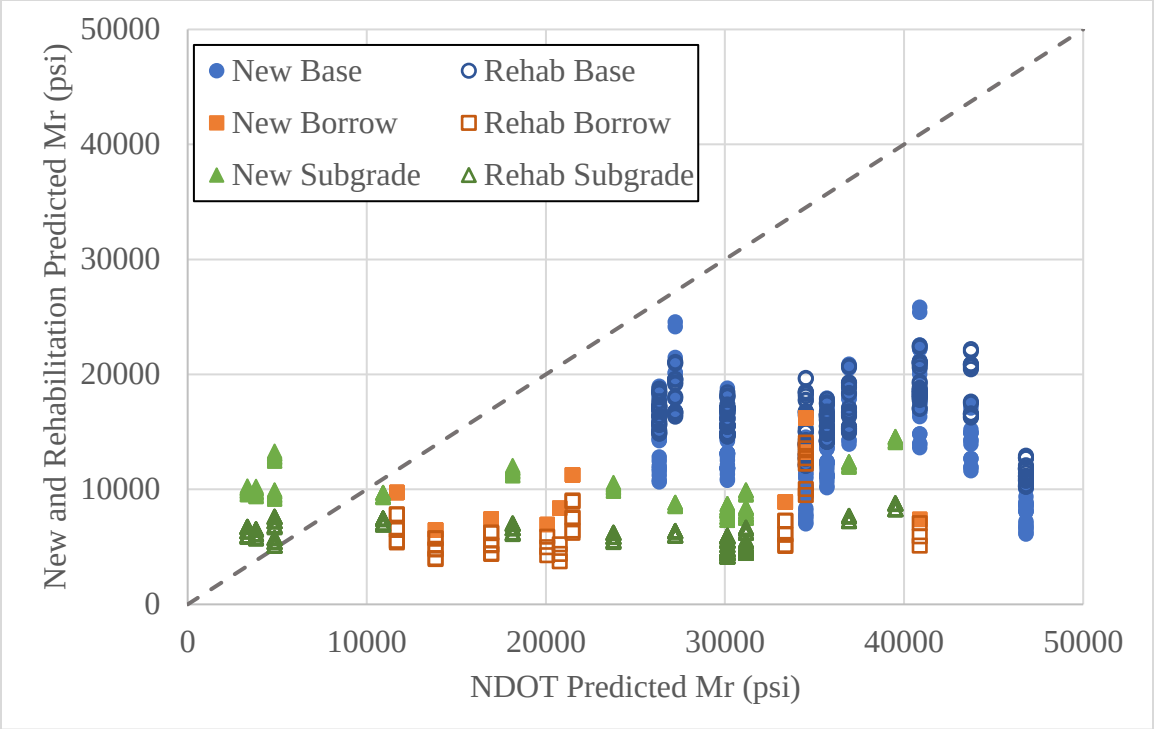

Figure 70. Comparison of NDOT Predicted Mr with New and Rehabilitation Design Predicted Mr for Nevada Materials (Statewide R-value Models).

Almost the same conclusion as District 1 project (3) can be observed from figure 63, where the Mr-R correlation equation currently used by NDOT seems to consistently overestimate the design Mr for unbound materials, except in some cases for subgrade materials where the R-value was very low.

7.3. AASHTOWare® Pavement ME Comparison

The impact of using the developed design Mr equations was assessed through the AASHTOWare® Pavement ME design software. In this comparison, the pavement structure consisted of an AC layer, a base layer, and a subgrade layer. The design was done for 25 years for a final traffic of almost 10 million ESALs. All required design inputs were obtained from the NDOT Pavement ME design manual (2) for a design in District 2, including all base parameters and performance models calibrations. Subgrade gradation and other properties were used as the default ones found in the software for an AASHTO A-7-5 classified subgrade. Knowing that in the current NDOT manual, design Mr of the base is 26000 psi regardless of the R-value, three designs were conducted for this comparison, with the only difference being in the unbound materials design Mr value as follows:

1. Using NDOT's R-value correlation equation for base and subgrade layers.
2. Using an Mr of 26000 psi for the base layer and the NDOT R-value correlation for the subgrade layer.
3. Using the developed new design R-value models for Districts 2 and 3 for the base and subgrade layers.

Table 76 shows the inputs for unbound layers, including R-value and Mr for the three designs. The resulting layer thicknesses for the three designs are presented in table 77.

Table 76. Unbound Layers R-value and Mr for the Three Designs.

Layer		Base	Subgrade
R-value		80	44
Mr (psi)	NDOT's R-value Equation	36929	10919
	Base Mr of 26000 psi	26000	10919
	Districts 2 and 3 Developed Models	10236	7705

Table 77. Pavement ME Design Results.

Mr Equation	Thickness (inch)	
	AC	Base
NDOT's R-value Equation	7.5	12
Base Mr of 26000 psi	8.0	12
Districts 2 and 3 Developed Models	9.0	12

A 12 inch thick base layer was used for the three designs for the sake of comparison. The design thickness of the AC layer decreased by 0.5 inch when using the NDOT's R-value correlation equation, compared to the design using the constant Mr value of 26000 psi. However, the AC layer's thickness increased by 1 inch when the Mr models developed in this research for new design based on the R-value were used.

Chapter 8. Conclusions and Recommendations

The objective of this research project was to develop models for predicting the design Mr values for new and rehabilitation projects for NDOT Districts 2 and 3 to be used in the design of flexible pavements using the AASHTOWare® Pavement ME software. Additional effort was done to investigate the possibility of developing statewide models for predicting the design Mr values for all Nevada materials including the results from the initial District 1 research. Outcomes of this project can also be used for the development of a more comprehensive database for the unbound materials in Nevada. The objectives were achieved by testing base, borrow, and subgrade materials sampled from NDOT Districts 2 and 3. The collected materials were tested for particle size distribution and Atterberg limits, then classified using both AAHTO and USCS soil classification systems. The specific gravity and absorption values were obtained for all materials. The modified proctor test was conducted to obtain the optimum moisture content and maximum dry density. In addition, strength parameters including the R-value, unconfined compressive strength, and resilient modulus were measured for the collected materials at their optimum moisture content. Two different methods were used to obtain the design Mr for new and rehabilitation projects. The collected materials were not enough to develop separate models for Districts 2 and 3, and hence the models developed in this study apply to both Districts.

Based on the conducted analysis in this research project, the following conclusions and recommendations can be made:

- The stress dependent behavior of the resilient modulus for base materials fits very well the Theta model.
- On the contrary to the observation found for District 1 research, the stress dependent behavior of the resilient modulus for borrow materials does not always have the best fit with the Theta model, but sometimes better fit the Uzan model. The observation on District 1 was made after analyzing few borrow materials which may not have included the various possible materials behavior.
- The stress dependent behavior of the resilient modulus for subgrade materials fits very well the Universal and Uzan model.
- In most cases, the pavement structure has a significant influence on the determination of the design Mr of unbound materials.
- The current NDOT Mr correlation with R-value overestimates the design Mr, except for some subgrade materials with very low R-value.
- Some of the developed UCS and R-value models are not recommended for use since they failed in terms of the engineering common sense. These models are the ones with negative UCS or R-value coefficients, since these properties are strength properties and are expected to positively impact the Mr.

- The design Mr values for new design for base materials in Districts 2 and 3 can be estimated from the following equations.

$$Ln(Mr_{CAB-New}) = 10.6855 - 0.027189 * H_{eq} + 0.0406 * P\#200 - 0.15704 * OMC + 0.0142 * PI \quad \text{(Eq. 80)}$$

$$Ln(Mr_{CAB-New}) = 10.5108 - 0.027179 * H_{eq} + 0.00251 * P\#3/8 + 0.03832 * P\#200 - 0.15281 * OMC \quad \text{(Eq. 81)}$$

$$Ln(Mr_{CAB-New}) = 14.45 - 0.027191 * H_{eq} - 0.05697 * P\#3/4 - 0.00945 * P\#40 + 0.12045 * P\#200 \quad \text{(Eq. 82)}$$

- The design Mr values for rehabilitation for the base materials in Districts 2 and 3 can be estimated from the following equation.

$$Ln(Mr_{CAB-Rehab}) = 12.033 - 0.012366 * H_{eq} - 0.02901 * P\#\,3/4 - 0.0071 * P\#40 + 0.08106 * P\#200 \quad \text{(Eq. 83)}$$

- The design Mr values for new design for the borrow materials in Districts 2 and 3 can be estimated from the following equations.

$$Ln(Mr_{BOR-New}) = 12.28 - 0.0647 * P\#1.5 + 0.00787 * P\#3/4 + 0.01279 * P\#200 + 0.01669 * MDD + 0.01454 * PI \quad \text{(Eq. 84)}$$

$$Ln(Mr_{BOR-New}) = 12.04 - 0.0614 * P\#1.5 + 0.00817 * P\#3/4 + 0.0161 * MDD + 0.01392 * PI + 0.00632 * UCS \quad \text{(Eq. 85)}$$

$$Ln(Mr_{BOR-New}) = 9.344 - 0.02498 * P\#3/8 + 0.01503 * \text{LL} + 0.02242 * \text{R} - \text{value} \quad \text{(Eq. 86)}$$

- The design Mr values for rehabilitation for the borrow materials in Districts 2 and 3 can be estimated from the following equations.

$$Ln(Mr_{BOR-Rehab}) = 13.15 - 0.0174 * H_{eq} - 0.0681 * P\#1.5 + 0.01836 * P\#1 + 0.01024 * MDD + 0.0192 * PI \quad \text{(Eq. 87)}$$

$$Ln(Mr_{BOR-Rehab}) = 9.607 - 0.01661 * H_{eq} - 0.02736 * OMC + 0.01648 * PI + 0.00539 * UCS \quad \text{(Eq. 88)}$$

$$Ln(Mr_{BOR-Rehab}) = 8.446 - 0.01685 * H_{eq} + 0.01696 * P\#1 - 0.01712 * P\#3/8 + 0.01042 * P\#40 + 0.02744 * PI + 0.00759 * R - value \quad \text{(Eq. 89)}$$

- The design Mr values for new design for the subgrade materials in Districts 2 and 3 can be estimated from the following equation.

$$Ln(Mr_{SG-New}) = 7.913 - 0.026875 * P\#3/8 + 0.07316 * OMC + 0.0231 * MDD \quad \text{(Eq. 90)}$$

- The design Mr values for rehabilitation for the subgrade materials in Districts 2 and 3 can be estimated from the following equation.

$$Ln(Mr_{SG-Rehab}) = 13.034 - 0.003485 * H_{eq} - 0.04932 * P\#1 + 0.005425 * P\#40 + 0.003188 * MDD \quad \text{(Eq. 91)}$$

- The design Mr values for new design for the base materials throughout Nevada can be estimated from the following equations.

$$Ln(Mr_{CAB-New}) = 12.92 - 0.02865 * H_{eq} - 0.0691 * P\#1 + 0.05993 * P\#\,3/4 - 0.01454 * P\#\,3/8 + 0.02669 * P\#40 + 0.04493 * P\#200 - 0.22338 * OMC \quad \text{(Eq. 92)}$$

$$Ln(Mr_{CAB-New}) = 6.533 - 0.028607 * H_{eq} + 0.0422 * P\#\,3/4 - 0.00912 * P\#\,3/8 + 0.01466 * P\#40 + 0.05761 * P\#200 - 0.20149 * OMC + 0.00543 * MDD \quad \text{(Eq. 93)}$$

$$Ln(Mr_{CAB-New}) = 5.788 - 0.028626 * H_{eq} + 0.03241 * P\#\,3/4 - 0.002819 * P\#4 + 0.1149 * P\#200 - 0.26949 * OMC + 0.02638 * R - value \quad \text{(Eq. 94)}$$

$$Ln(Mr_{CAB-New}) = 5.452 - 0.028753 * H_{eq} + 0.03079 * P\#\,3/4 + 0.10738 * P\#200 - 0.26878 * OMC + 0.00264 * MDD + 0.00897 * PI + 0.02701 * R - value \quad \text{(Eq. 95)}$$

- The design Mr values for rehabilitation for the base materials throughout Nevada can be estimated from the following equations.

$$Ln(Mr_{CAB-Rehab}) = 7.556 - 0.01168 * H_{eq} + 0.02689 * P\#3/4 \quad \text{(Eq. 96)}$$
$$- 0.00995 * P\#3/8 + 0.00829 * P\#40 + 0.04442 * P\#200$$
$$- 0.12585 * OMC + 0.00546 * MDD + 0.04769 * PI$$

$$Ln(Mr_{CAB-Rehab}) = 8.108 - 0.011915 * H_{eq} + 0.02287 * P\#3/4 \quad \text{(Eq. 97)}$$
$$- 0.007292 * P\#3/8 + 0.04454 * P\#200 - 0.12418 * OMC$$
$$+ 0.00392 * MDD + 0.0406 * PI$$

$$Ln(Mr_{CAB-Rehab}) = 7.604 - 0.011713 * H_{eq} + 0.02089 * P\#3/4 \quad \text{(Eq. 98)}$$
$$- 0.003264 * P\#3/8 + 0.06318 * P\#200 - 0.15673 * OMC$$
$$+ 0.022 * PI + 0.01265 * R - value$$

- The design Mr values for new design for the borrow materials throughout Nevada can be estimated from the following equations.

$$Ln(Mr_{BOR-New}) = 9.75 - 0.0528 * P\#1.5 + 0.00866 * P\#4 \quad \text{(Eq. 99)}$$
$$- 0.02357 * P\#40 + 0.0576 * P\#200 + 0.02983 * MDD$$

$$Ln(Mr_{BOR-New}) = 27.59 - 0.1943 * P\#1.5 - 0.0282 * P\#40 \quad \text{(Eq. 100)}$$
$$- 0.0603 * OMC + 0.02836 * LL - 0.0388 * PI$$
$$+ 0.0258 * R - value$$

$$Ln(Mr_{BOR-New}) = 11.646 - 0.03607 * P\#1 - 0.03453 * P\#40 \quad \text{(Eq. 101)}$$
$$+ 0.0408 * P\#200 - 0.1043 * OMC + 0.01973 * LL$$
$$- 0.0291 * PI + 0.02831 * R - value$$

- The design Mr values for rehabilitation for the borrow materials throughout Nevada can be estimated from the following equations.

$$Ln(Mr_{BOR-Rehab}) = 6.745 - 0.02379 * H_{eq} - 0.00807 * P\#3/8 \quad \text{(Eq. 102)}$$
$$+ 0.01511 * P\#4 - 0.03116 * P\#40 + 0.05823 * P\#200$$
$$+ 0.02283 * MDD$$

$$Ln(Mr_{BOR-Rehab}) = 10.805 - 0.01854 * H_{eq} - 0.02183 * P\#\,3/4 \quad \text{(Eq. 103)}$$
$$+ 0.01114 * P\#\,3/8 - 0.03433 * P\#40 + 0.07736 * P\#200$$
$$- 0.1261 * OMC + 0.01408 * R - value$$

- The design Mr values for new design for the subgrade materials throughout Nevada can be estimated from the following equations.

$$Ln(Mr_{SG-New}) = 11.976 - 0.00581 * H_{eq} - 0.03079 * P\#1 \quad \text{(Eq. 104)}$$
$$+ 0.002527 * P\#40 + 0.00309 * MDD + 0.00289 * PI$$

$$Ln(Mr_{SG-New}) = 11.81 - 0.00479 * H_{eq} - 0.0316 * P\#1 \quad \text{(Eq. 105)}$$
$$+ 0.003287 * P\#40 + 0.004016 * MDD + 0.003029 * UCS$$

- The design Mr values for rehabilitation for the subgrade materials throughout Nevada can be estimated from the following equation.

$$Ln(Mr_{SG-Rehab}) = 11.204 - 0.007215 * H_{eq} - 0.02151 * P\#1 \quad \text{(Eq. 106)}$$
$$+ 0.005381 * P\#40 - 0.02116 * OMC + 0.001836 * LL$$

These equations will be applicable for the range of data that was used to develop the models. A database of resilient modulus and soil properties for level 3 input for the AASRHOWare®Pavement ME software can be established in the future using all the results from the tests conducted on Nevada materials.

When comparing models for Nevada materials combined and separated, there was no consistent answer as to which way is better; hence, it is recommended to try both sets of equations and judge based on the results they present. Obtaining more base materials is highly recommended for the future, since the base materials collected in this study were very weak, as all of them ended up having a design Mr of less than 20000 psi.

Chapter 9. References

(1) Transportation Officials. *Mechanistic-Empirical Pavement Design Guide: A Manual of Practice*. AASHTO (2008).

(2) Hajj, E., P. Sebaaly, and P. Nabhan. "Manual for designing flexible pavements in Nevada using AASHTOWare pavement-ME design." *Nevada Department of Transportation* (2015).

(3) Sebaaly, Peter E., Jeyakaran Thavathurairaja, and Elie Hajj. Characterization of Unbound Materials (Soils/Aggregates) Mechanistic-Empirical Pavement Design Guide (MEPDG). No. P361-16-803. Nevada. Dept. of Transportation (2018).

(4) Von Quintus, H. L., Boudreau, R., and Cooley, A. *Precision and Bias of Resilient Modulus Test*. Washington D.C. (2015).

(5) ARA, and ERES Consultants. *Guide for Mechanistic-Emperical Design of New and Rehabilitated Pavement Structures - Final Report Chapter 2: Design Inputs-Material Characterizations*. National Cooperative Highway Research Program, Washington DC (2004).

(6) Puppala, Anand J. *Estimating stiffness of subgrade and unbound materials for pavement design*. Vol. 382. Transportation Research Board (2008).

(7) Yau, Amber, and Harold L. Von Quintus. *Study of LTPP laboratory resilient modulus test data and response characteristics*. No. FHWA-RD-02-051; 3032.1. Turner-Fairbank Highway Research Center (2002).

(8) Ceylan, Halil, Sunghwan Kim, Kasthurirangan Gopalakrishnan, and Omar G. Smadi. *MEPDG work plan task no. 8: Validation of pavement performance curves for the mechanistic-Empirical pavement design guide*. (2009).

(9) Mokwa, Robert L., and Michelle Akin. *Measurement and Evaluation of Subgrade Soil Parameters: Phase I–Synthesis of Literature*. No. FHWA/MT-09-006/8199. Montana. Dept. of Transportation. Research Programs (2009).

(10) Kim, S. Sonny, Steve Pahno, Stephan A. Durham, Jidong Yang, and Mi G. Chorzepa. *Prediction of Resilient Modulus From the Laboratory Testing of Sandy Soils*. No. FHWA-GA-19-1725. Georgia. Department of Transportation. Office of Performance-Based Management & Research (2019).

(11) Heukelom, W., and AsJG Klomp. "Dynamic testing as a means of controlling pavements during and after construction." In *International Conference on the Structural Design of Asphalt PavementsUniversity of Michigan, Ann Arbor*, vol. 203, no. 1. (1962).

(12) Powell, H. Jefferson. "The original understanding of original intent." *Harv. L. Rev.* 98: 885 (1984).

(13) Drumm, E. C., Y. Boateng-Poku, and T. Johnson Pierce. "Estimation of subgrade resilient modulus from standard tests." *Journal of Geotechnical Engineering* 116, no. 5: 774-789. (1990).

(14) Lee, Woojin, N. C. Bohra, A. G. Altschaeffl, and T. D. White. "Resilient modulus of cohesive soils." *Journal of Geotechnical and Geoenvironmental Engineering* 123, no. 2: 131-136. (1997).

(15) Hossain, M. Shabbir, and Wan Soo Kim. *Estimation of subgrade resilient modulus using the unconfined compression test*. No. FHWA/VCTIR 15-R12. Virginia Center for Transportation Innovation and Research (2014).

(16) Darter, Michael I., Harold Von Quintus, Biplab B. Bhattacharya, and Jagannath Mallela. Calibration and implementation of the AASHTO mechanistic-empirical pavement design guide in Arizona. No. FHWA-AZ-14-606. Arizona. Dept. of Transportation. Research Center (2014).

(17) ADOT Pavement Design Manual, Arizona Department of Transportation (2017). Available online at: https://apps.azdot.gov/files/materials-manuals/Preliminary-Engineering-Design/PavementDesignManual.pdf

(18) Yeh, S.-T., and Su, C.-K. Resilient Properties of Colorado Soils. Colorado Department of Highways, Denver, CO. (1989).

(19) Chang, N. Y., H. H. Chiang, and L. C. Jiang. RESILIENT MODULUS OF GRANULAR SOILS WITH FINES CONTENTS. FINAL REPORT. No. CDOT-DTD-R-95-9. (1995).

(20) CDOT Pavement Design Manual, Colorado Department of Transportation (2012). Available online at: https://spl.cde.state.co.us/artemis/traserials/tra18p28internet/tra18p282012internet.pdf

(21) Mallela, Jagannath, Leslie Titus-Glover, Suri Sadasivam, Biplab Bhattacharya, Michael Darter, and Harold Von Quintus. Implementation of the AASHTO mechanistic-empirical pavement design guide for Colorado. No. CDOT-2013-4. Colorado. Dept. of Transportation. Research Branch (2013).

(22) CDOT ME Pavement Design Manual, Colorado Department of Transportation (2021). Available online at: https://www.codot.gov/business/designsupport/materials-and-geotechnical/manuals/2021-m-e-pave-design-manual

(23) Idaho Transportation Department. Materials Manual, Section 500-Pavement Design. Boise, ID: Idaho Transportation Department (2011).

(24) Bayomy, Fouad, Sherif El-Badawy, and Ahmed Awed. Implementation of the MEPDG for flexible pavements in Idaho. No. FHWA-ID-12-193. Idaho Transportation Department (2012).

(25) El-Badawy, S. M., F. M. Bayomy, and S. M. Miller. “Prediction of the Subgrade Resilient Modulus for Implementation of the MEPDG in Idaho.” pp. 4762-4772 In J. Han and D. E. Alzamora, editors. Geo-Frontiers 2011: Advances in Geotechnical Engineering. Reston, VA : American Society of Civil Engineers, Geotechnical Special Publication No. 211 (2011).

(26) Kim D., and Siddiki, N. Z. “Simplification of Resilient Modulus Testing for Subgrades,” Publication No.: FHWA/IN/JTRP-2005/23, SPR-2633N, Indiana Department of Transportation, Division of Research, West Lafayette, Indiana (2006).

(27) Baladi, G. Y., T. Dawson, and C. Sessions. "Pavement subgrade MR design values for michigan’s seasonal changes, final report." Michigan Department of Transportation, Construction and Technology Division, PO Box 30049 (2009).

(28) Titus-Glover, Leslie, Chetana Rao, and Suriyanarayanan Sadasivam. Local Calibration of the Pavement ME for Missouri. No. cmr 20-007. Missouri. Department of Transportation. Construction and Materials Division (2020).

(29) Richardson, David Newton, Thomas M. Petry, Yu-Ning Louis Ge, Yuh-Puu Han, and Steven Michael Lusher. "Resilient moduli of typical Missouri soils and unbound granular base materials." (2009).

(30) Akin, Michelle, and Robert Mokwa. Measurement and Evaluation of Subgrade Soil Parameters: Phase I–Synthesis of Literature. No. FHWA/MT-09-006/8199. (2009).

(31) Hossain, Zahid, Musharraf Zaman, and Curtis Doiron. "Regression Modeling of Resilient Modulus of Unbound Aggregates." Journal of Marine Science and Technology 23, no. 3: 388-398. (2015).

(32) Darter, Michael I., Leslie Titus-Glover, and Harold L. Von Quintus. Implementation of the mechanistic-empirical pavement design guide in Utah: Validation, calibration, and development of the UDOT MEPDG user's guide. No. UT-09.11. Utah. Dept. of Transportation. Research Division (2009).

(33) UDOT Pavement Design Manual of Instruction, Utah Department of Transportation (2019). Available online at: https://www.udot.utah.gov/main_old/uconowner.gf?n=20339215312776663

(34) Jackson, Kirk David. Laboratory resilient modulus measurements of aggregate base materials in Utah. Brigham Young University (2015).

(35) Hossain, M. Shabbir. Characterization of subgrade resilient modulus for Virginia soils and its correlation with the results of other soil tests. No. VTRC 09-R4. Virginia Transportation Research Council (2008).

(36) Hossain, M. Shabbir. Characterization of Unbound for Use in the New Mechanistic-Empirical Pavement Design Procedure Pavement Materials From Virginia Sources. No. FHWA/VTRC 11-R6. (2010).

(37) Hossain, M. Shabbir, and D. Stephen Lane. Development of a catalog of resilient modulus values for aggregate base for use with the mechanistic-empirical pavement design guide (MEPDG). No. FHWA/VCTIR 15-R13. Virginia Center for Transportation Innovation and Research (2015).

(38) Muench, S. T., J. P. Mahoney, and L. M. Pierce, "WSDOT Pavement Guide" Washington State Department of Transportation, Internet Module [Online] Available http://training.ce.washington.edu/WSDOT/, (accessed April 30, 2009).

(39) Eggen, Paul, and Don Brittnacher. Determination of influences on support strength of crushed aggregate base course due to gradational, regional, and source variations. Wisconsin Highway Research Program. (2004).

(40) Titi, Hani H., Mohammed B. Elias, and Sam Helwany. Determination of typical resilient modulus values for selected soils in Wisconsin. No. WHRP 06-06. (2006).

(41) Ng, Kam Weng, Harold L. Von Quintus, Khaled Ksaibati, Daniel Hellrung, and Zachary Hutson. Characterization of material properties for mechanistic-empirical pavement design in Wyoming. No. FHWA-WY-17/01F. Wyoming. Department of Transportation (2016).

(42) Nevada Department of Transportation (NDOT), Material Test Manual (2019). Available online at: https://www.dot.nv.gov/doing-business/about-ndot/ndot-divisions/operations/materials-section/materials-test-manual

(43) American Association of State Highway and Transportation Officials (AASHTO), Standard Specifications for Transportation Materials and Methods of Sampling and Testing, Washington, D.C. (2021).

(44) Annual book of ASTM Standards, American Society for Testing and Materials, ASTM International, West Conshohocken, Pennsylvania (2021).

(45) Hicks, Russell Gary. *Factors influencing the resilient properties of granular materials*. University of California, Berkeley (1970).

(46) Witczak, M. W. The Universal Airport Pavement Design System; Report I of IV: Granular Material Characterization. Department of Civil Engineering, University of Maryland (1988).

(47) AASHTO Design Guide. Guide for Design of Pavement Structures. American Association of State Highway and Transportation Officials, p. 700. (1993).

(48) NCHRP 1-37A. "Guide for Mechanistic-Empirical Design of New and Rehabilitated Pavement Structures." Final Report for NCHRP 1-37A Project. (2004).

(49) AASHTOWare Pavement ME Design software. American Association of State Highway and Transportation Officials (AASHTO), Available online at: http://me-design.com/MEDesign/.

(50) NDOT Pavement Structural Design and Policy Manual, Nevada Department of Transportation (1996).

(51) 3D-Move Analysis software® V2.1. Reno, NV. (2013). Available online at: http://www.arc.unr.edu/Software.html#3DMove (accessed September 19, 2017).

(52) Nabizadeh, H., Hajj, E. Y., Siddharthan, R., Elfass, S., Sebaaly, P. E. "Estimation of In-Situ Shear Strength Parameters for Subgrade Layer Using Non-destructive Testing." The Roles of Accelerated Pavement Testing in Pavement Sustainability, pp. 525-538, Springer, Cham (2016).

(53) Nabizadeh, H., Hajj, E. Y., Siddharthan, R., Elfass, S., Nimeri, N. "Application of Falling Weight Deflectometer for the Estimation of in-situ Shear Strength Parameters of Subgrade layer." Bearing Capacity of Roads, Railways and Airfields, pp. 743-749, Taylor & Francis Group. (2017).

(54) M.R. Thompson, R.P. Elliot, ILLI-PAVE based response algorithms for design of conventional flexible pavements, Transp. Res. Record 1043: 50–57. (1985).

(55) W. Liu, T. Scullion, MODULUS 6.0 for Windows: User's Manual. Texas Transportation Institute, The Texas A&M University System, Federal Highway Administration, Publication: FHWA/TX-05/0-1869-2, (October 2001).

(56) Minitab, LLC, 2021. *Minitab*, Available at: https://www.minitab.com.

(57) D'Agostino, R. B. Tests for the normal distribution. Goodness-of-fit techniques, 68, 576. (1986).

(58) Fox, J., & Monette, G. Generalized collinearity diagnostics. Journal of the American Statistical Association, 87(417), 178-183. (1992).

Appendix A

Moisture-density relationship and resilient modulus laboratory test results are shown in this appendix.

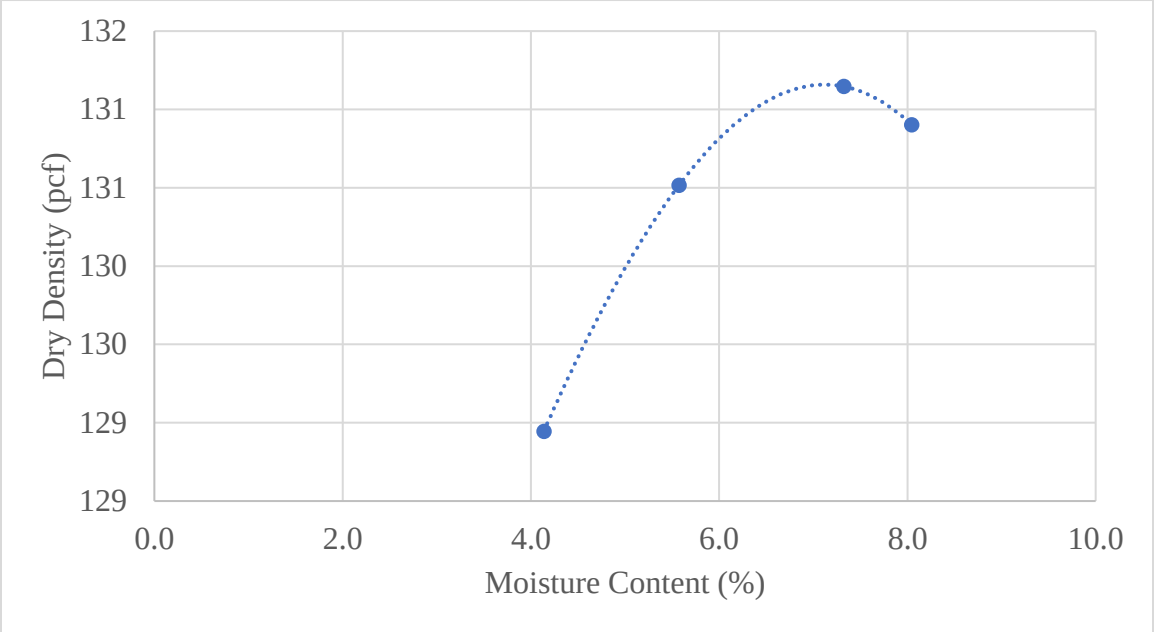

Figure A. 1 Goni Base Moisture-Density Curve.

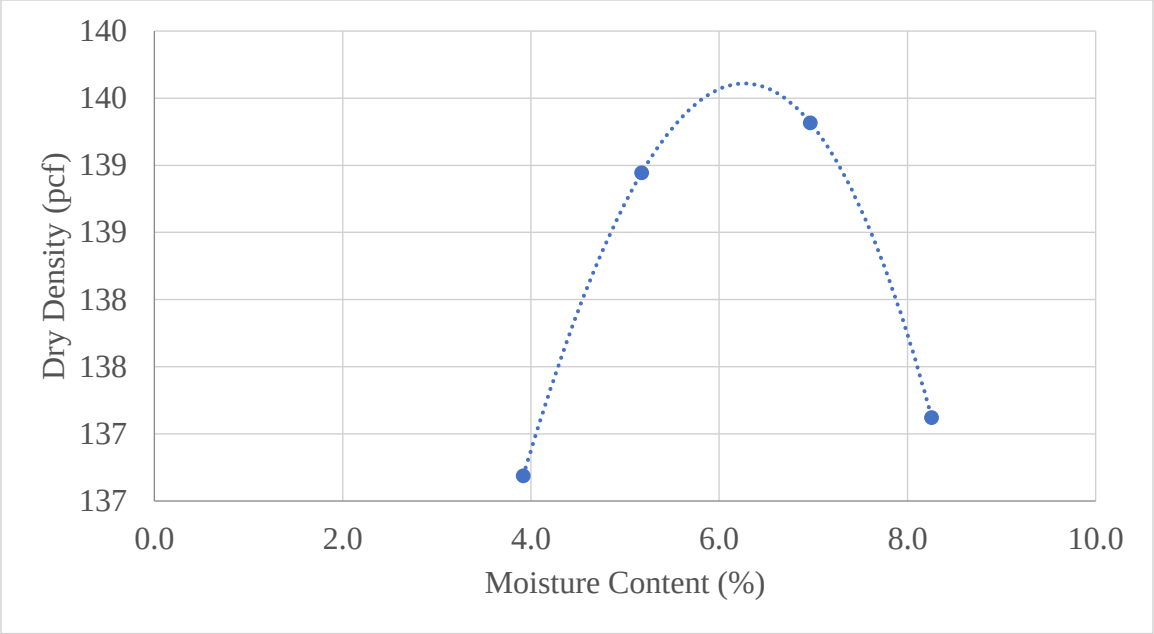

Figure A. 2 Spanish Springs Base Moisture-Density Curve.

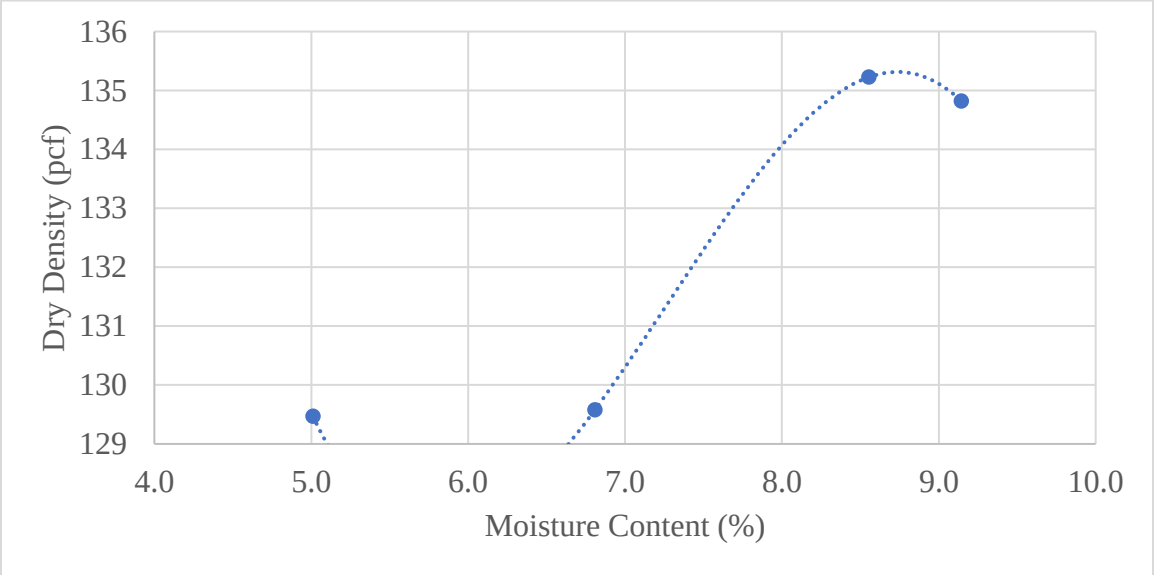

Figure A. 3 Lockwood Base Moisture-Density Curve.

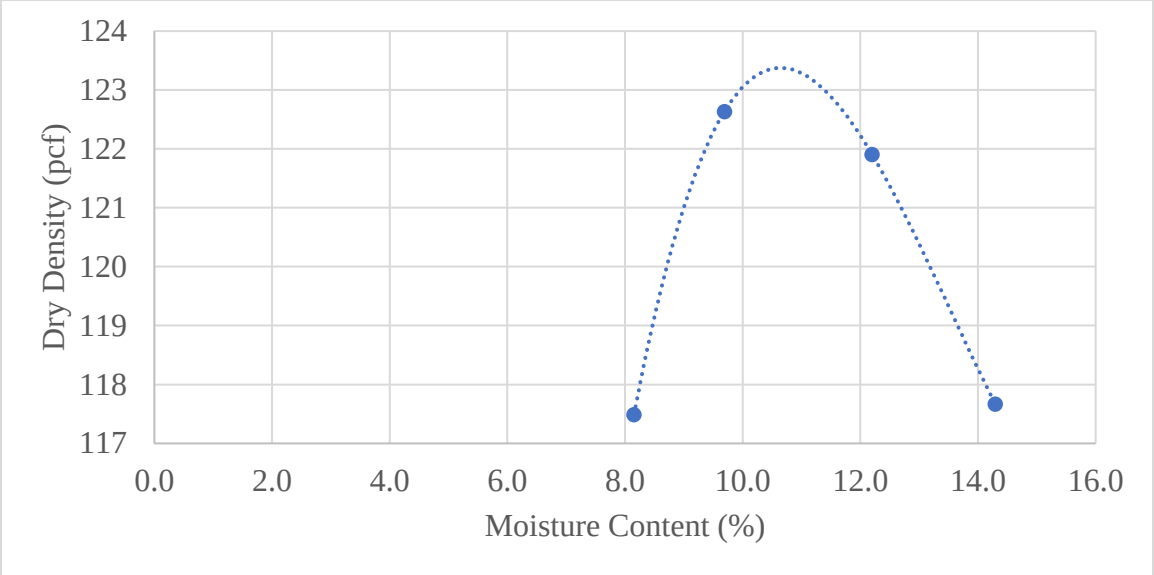

Figure A. 4 Trico Base A Moisture-Density Curve.

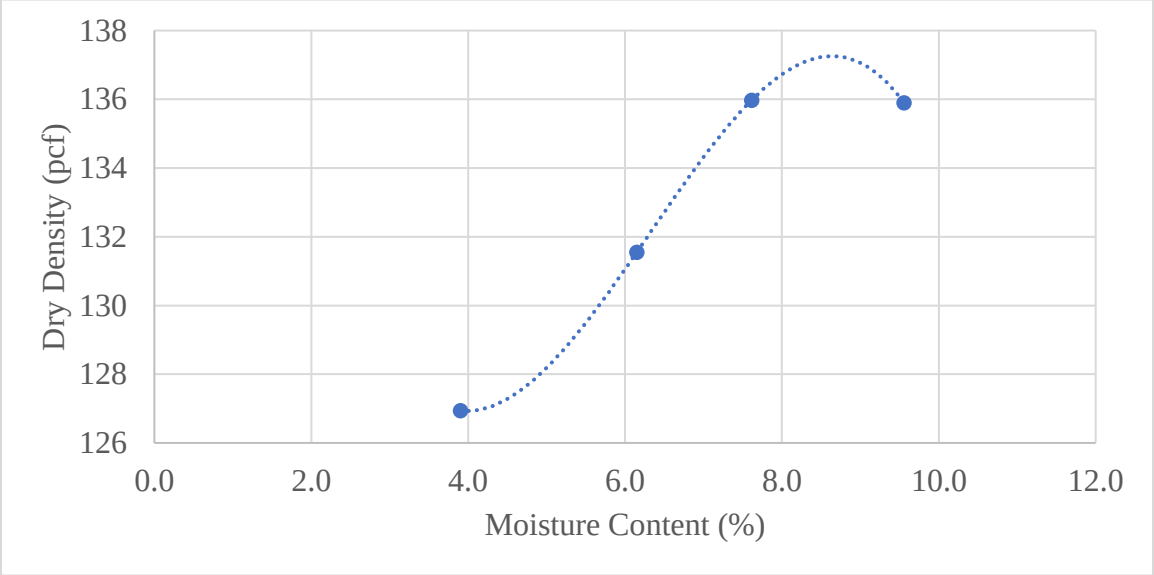

Figure A. 5 Trico Base B Moisture-Density Curve.

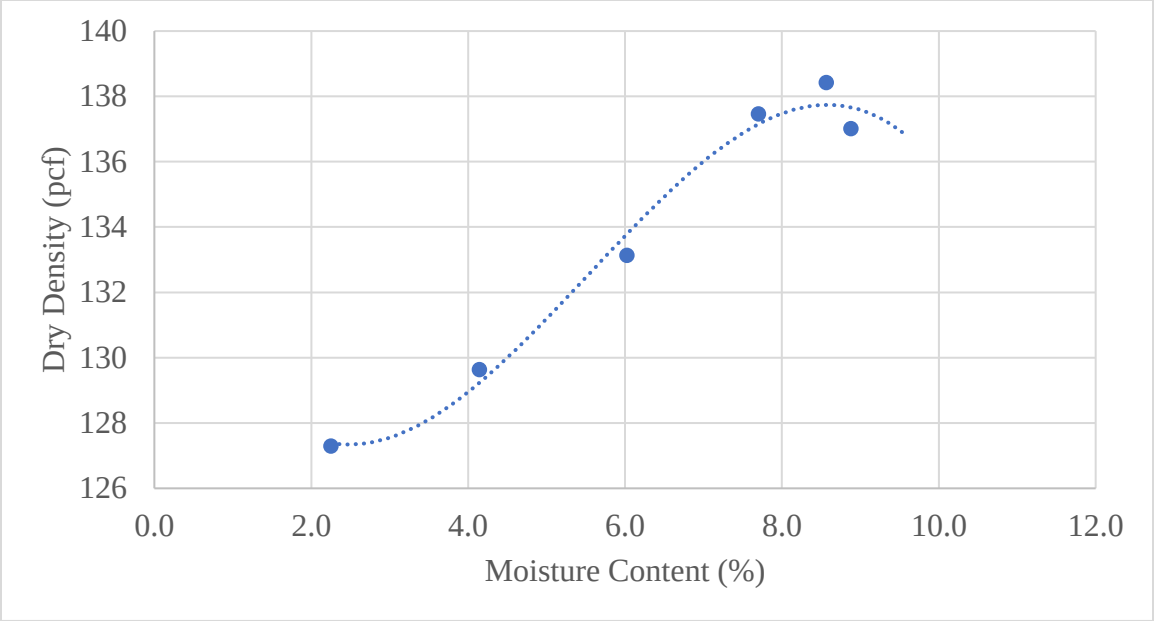

Figure A. 6 Lockwood Borrow Moisture-Density Curve.

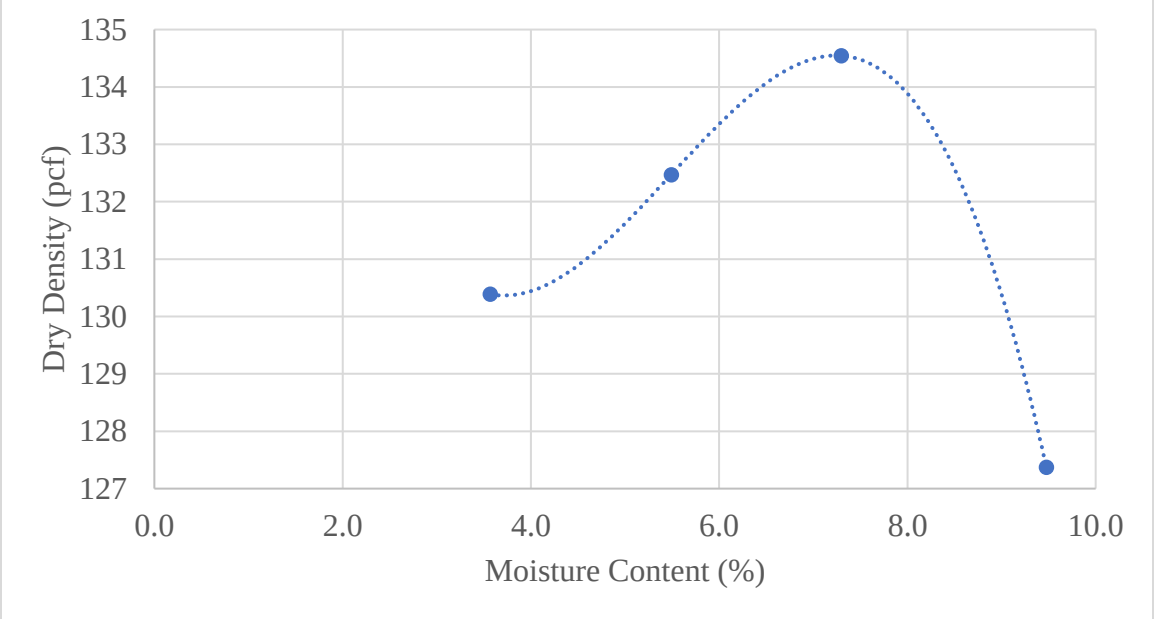

Figure A. 7 Goni Borrow Moisture-Density Curve.

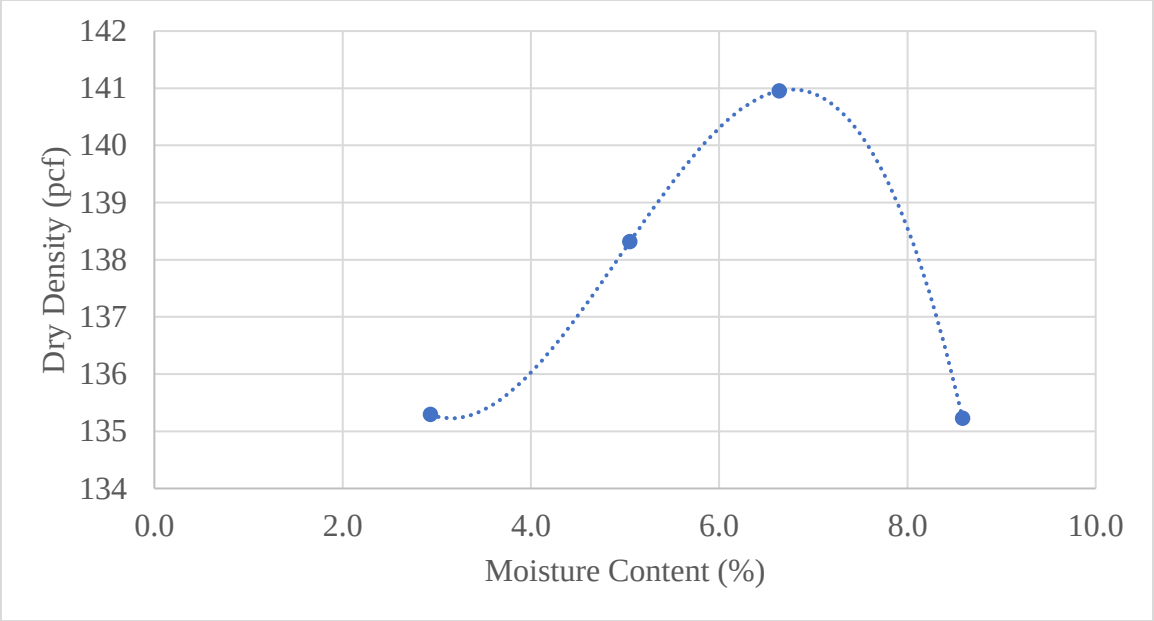

Figure A. 8 Imlay Borrow Moisture-Density Curve.

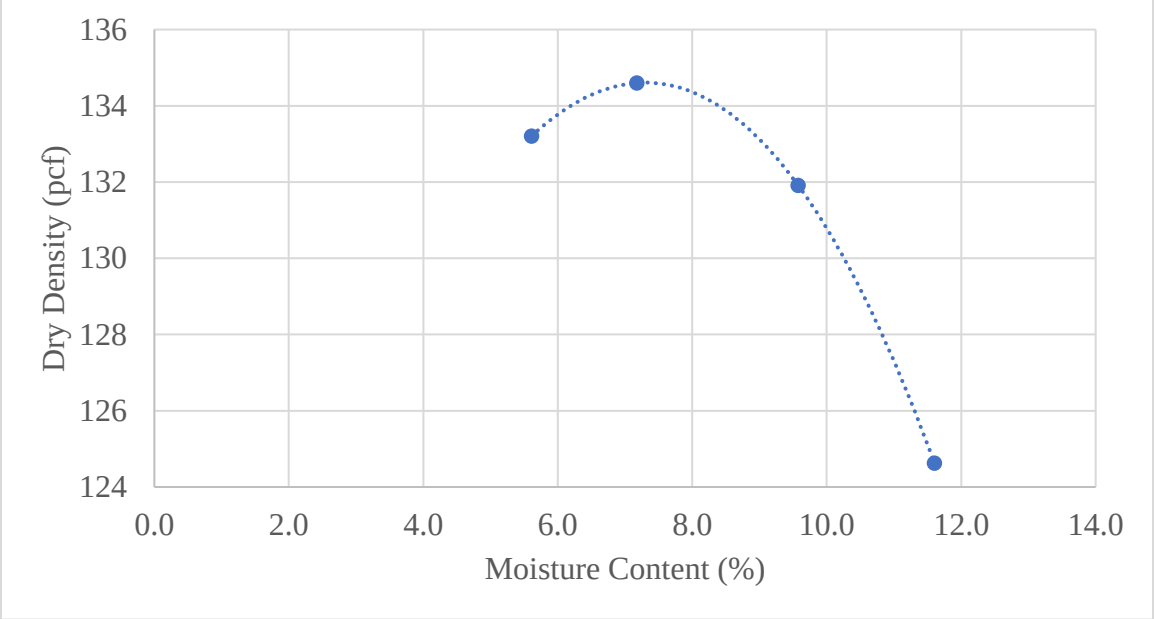

Figure A. 9 Spanish Springs Borrow Moisture-Density Curve.

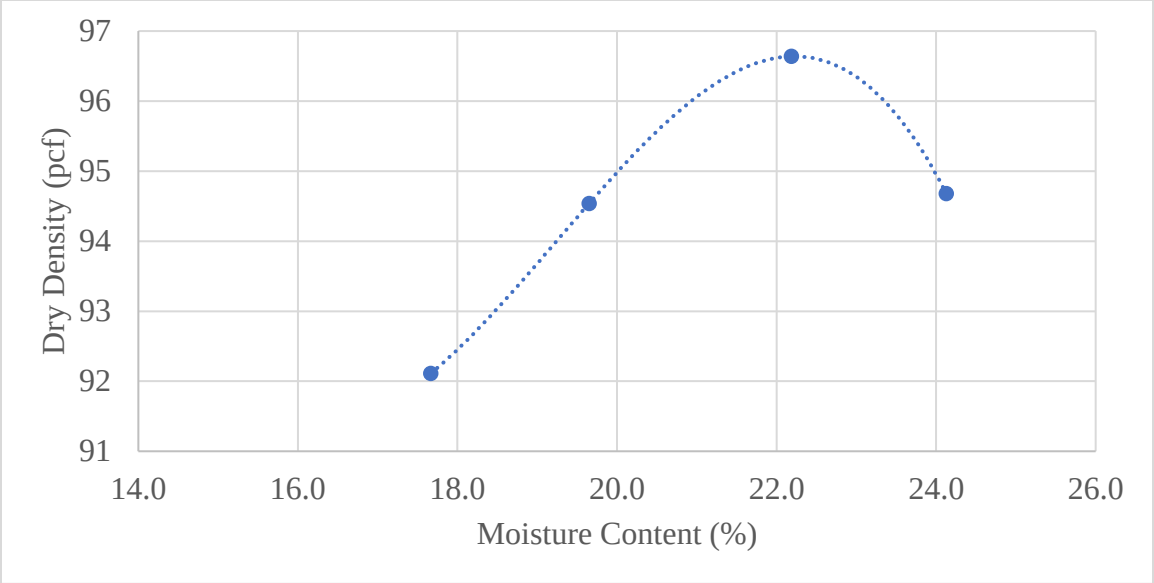

Figure A. 10 Trico Borrow Moisture-Density Curve.

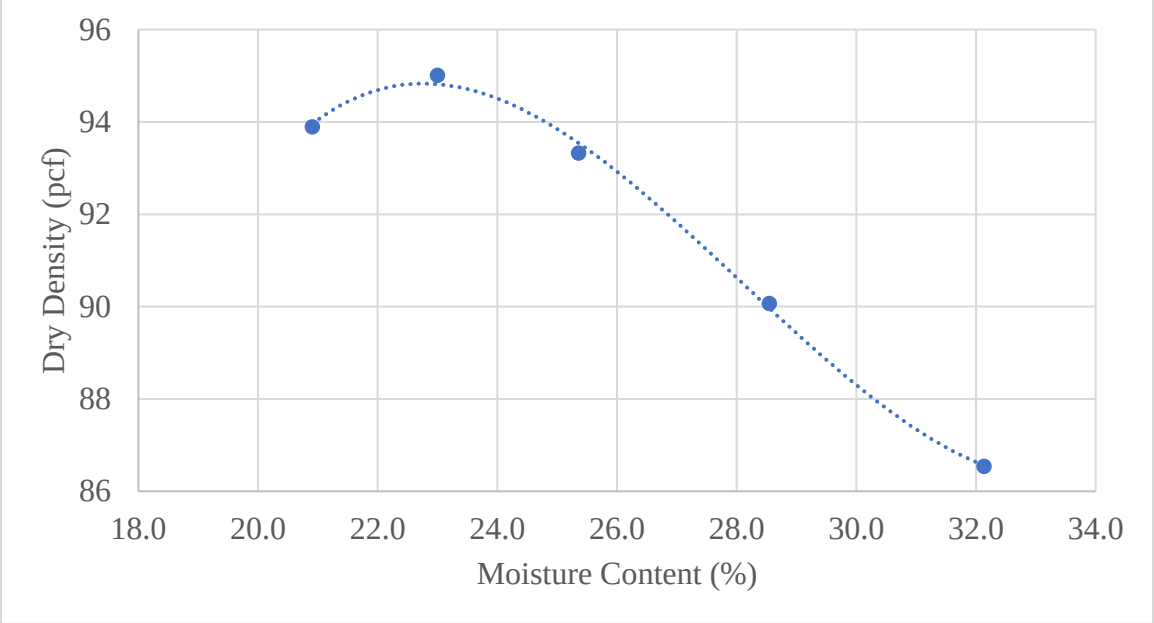

Figure A. 11 Fallon Big Dig Subgrade 2 Moisture-Density Curve.

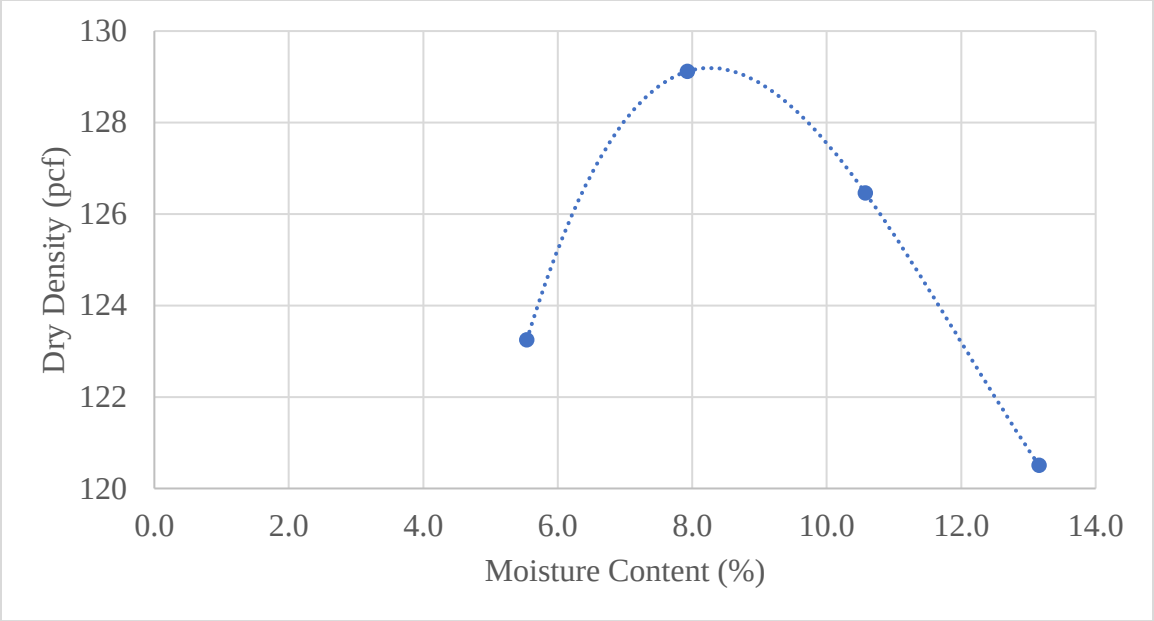

Figure A. 12 Reno Spaghetti Bowl Subgrade Moisture-Density Curve.

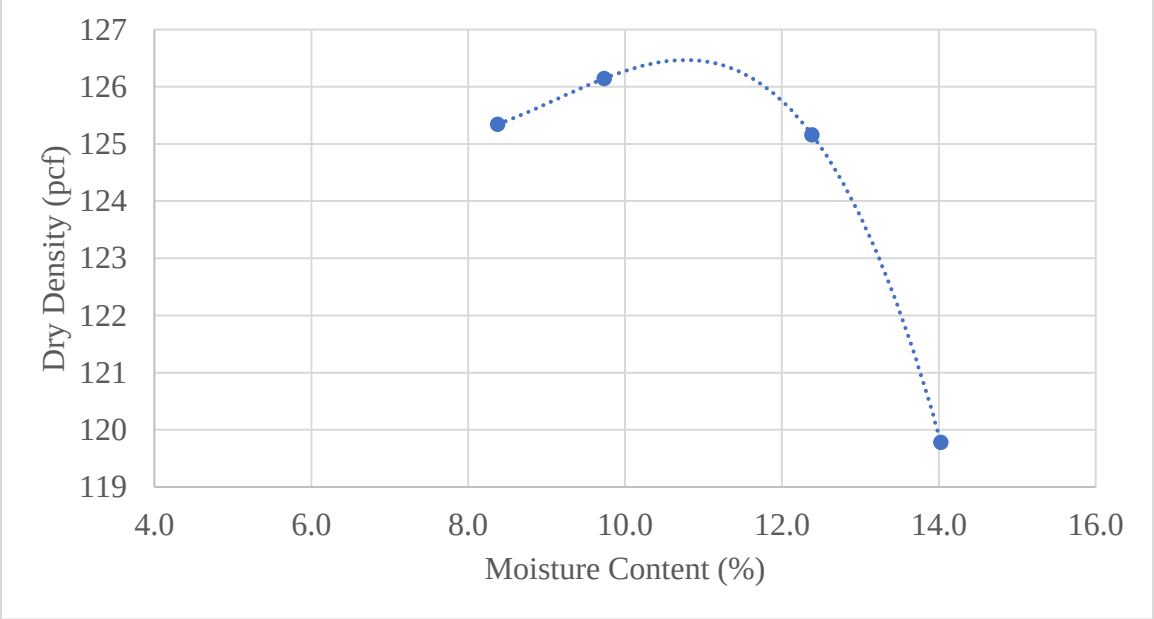

Figure A. 13 Reno Kings Row Subgrade Moisture-Density Curve.

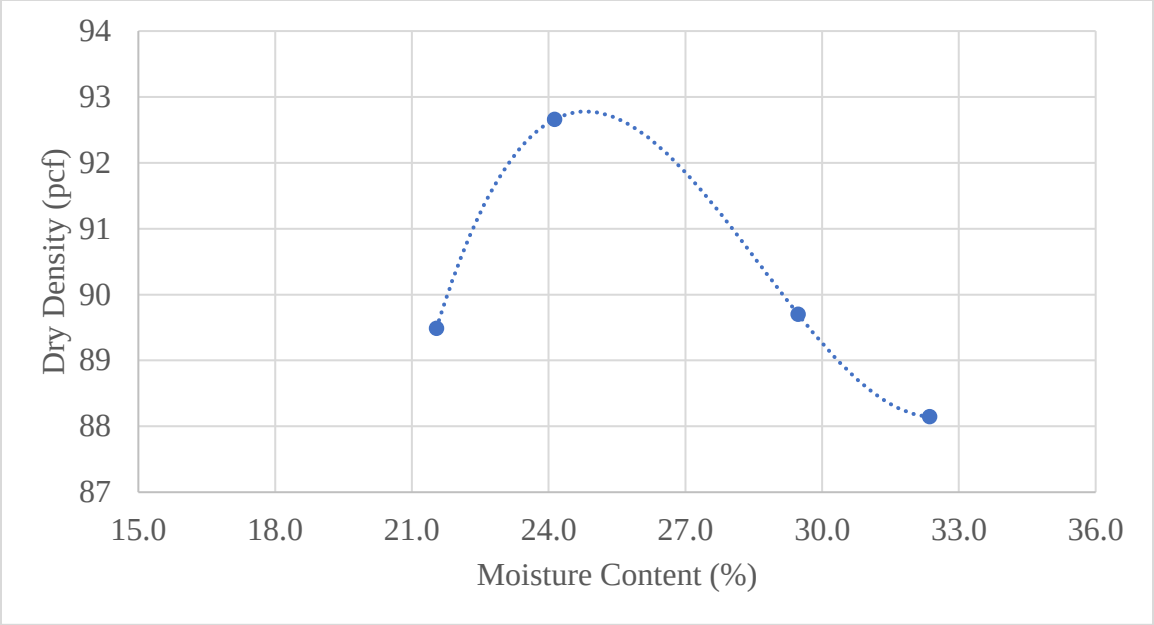

Figure A. 14 Lemmon Dr. Subgrade 1 Moisture-Density Curve.

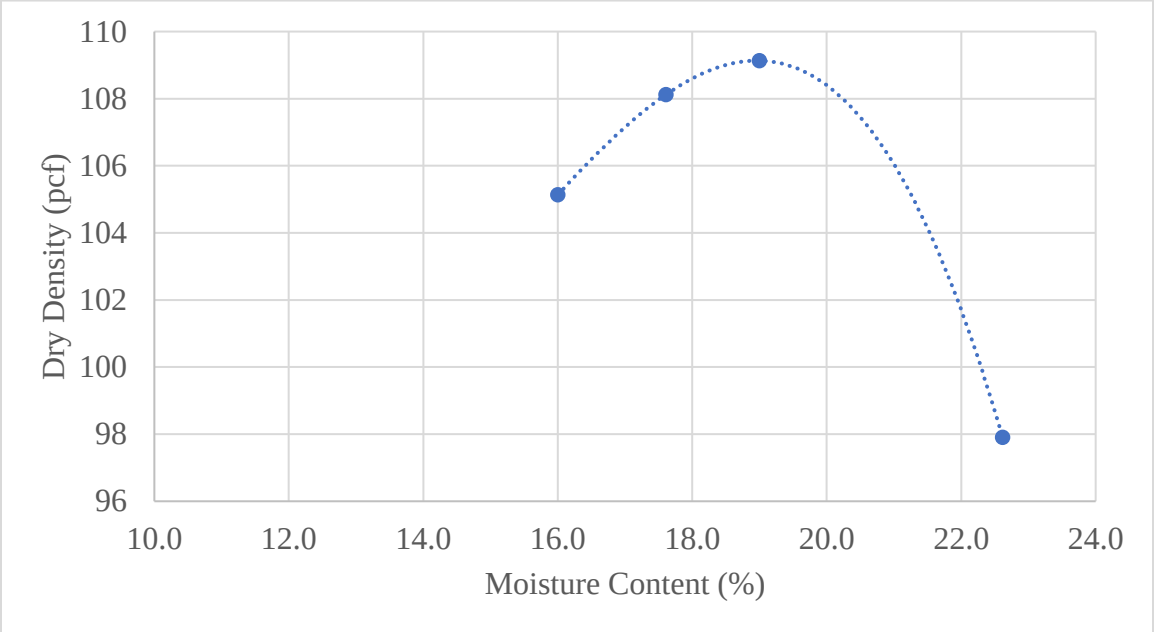

Figure A. 15 Lemmon Dr. Subgrade 2 Moisture-Density Curve.

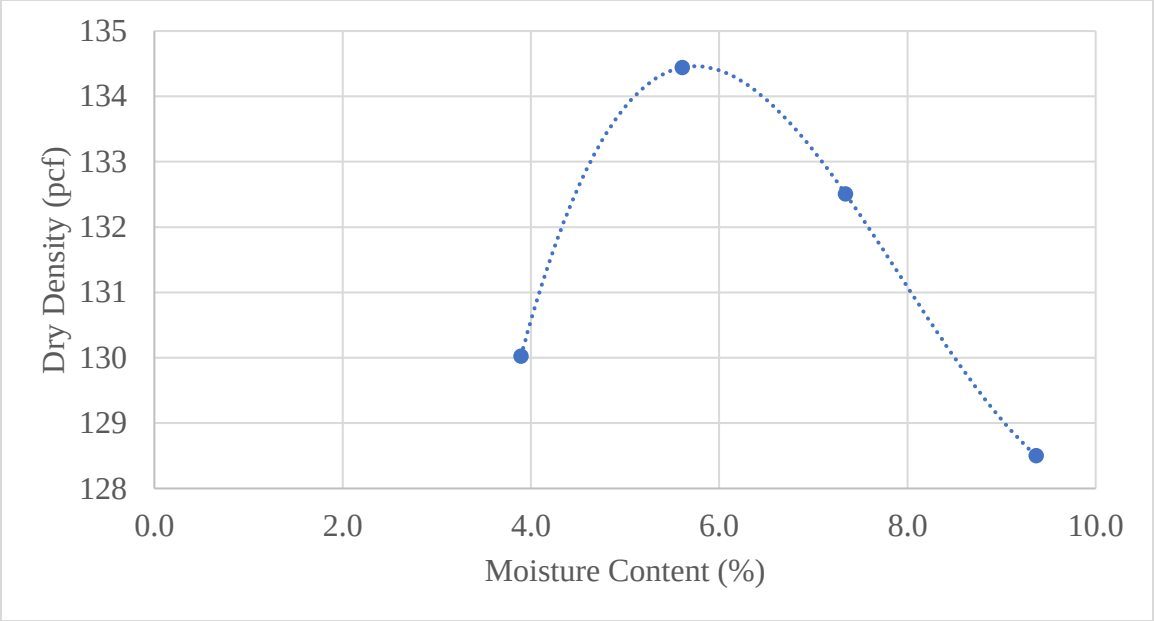

Figure A. 16 Carlin Base Moisture-Density Curve.

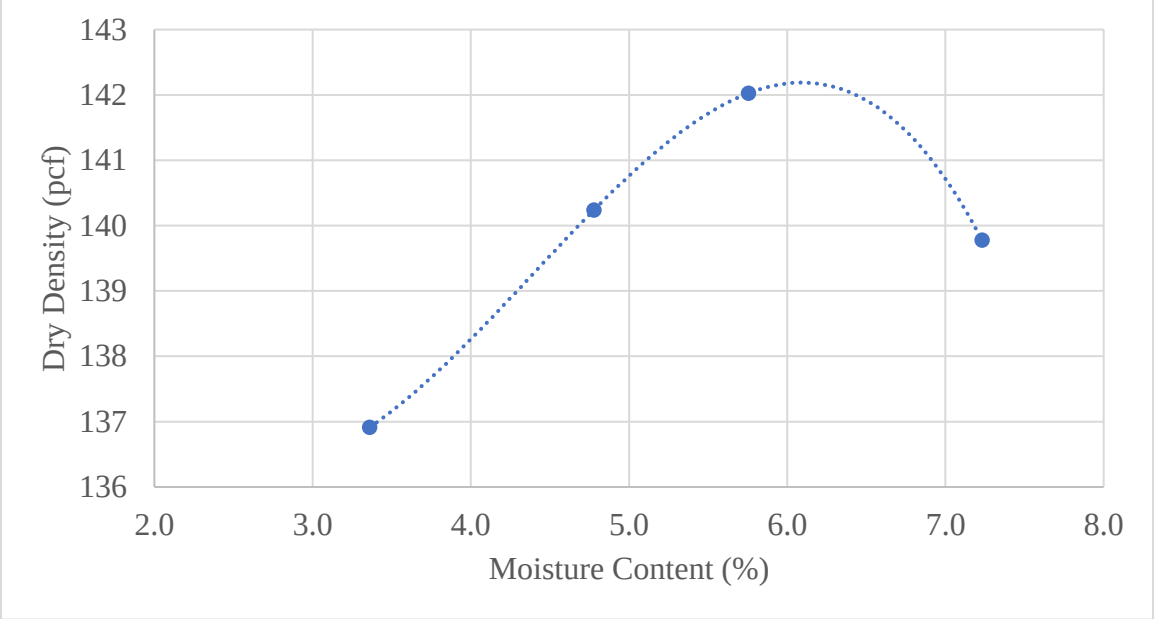

Figure A. 17 Sonoma Base Moisture-Density Curve.

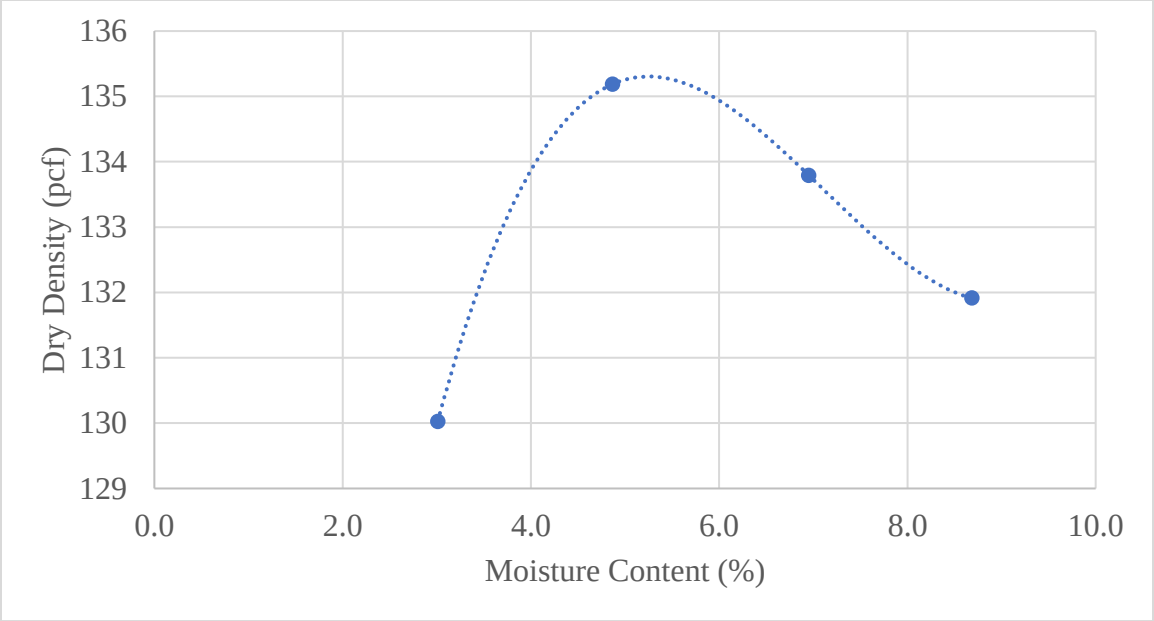

Figure A. 18 Vega Base Moisture-Density Curve.

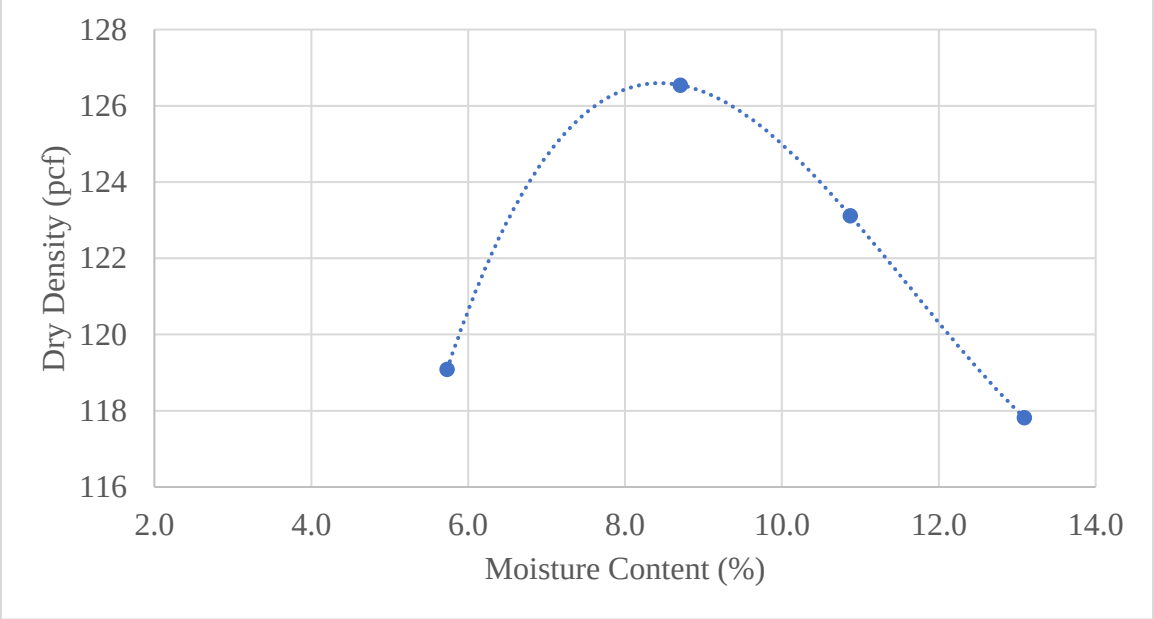

Figure A. 19 Silver State Base Moisture-Density Curve.

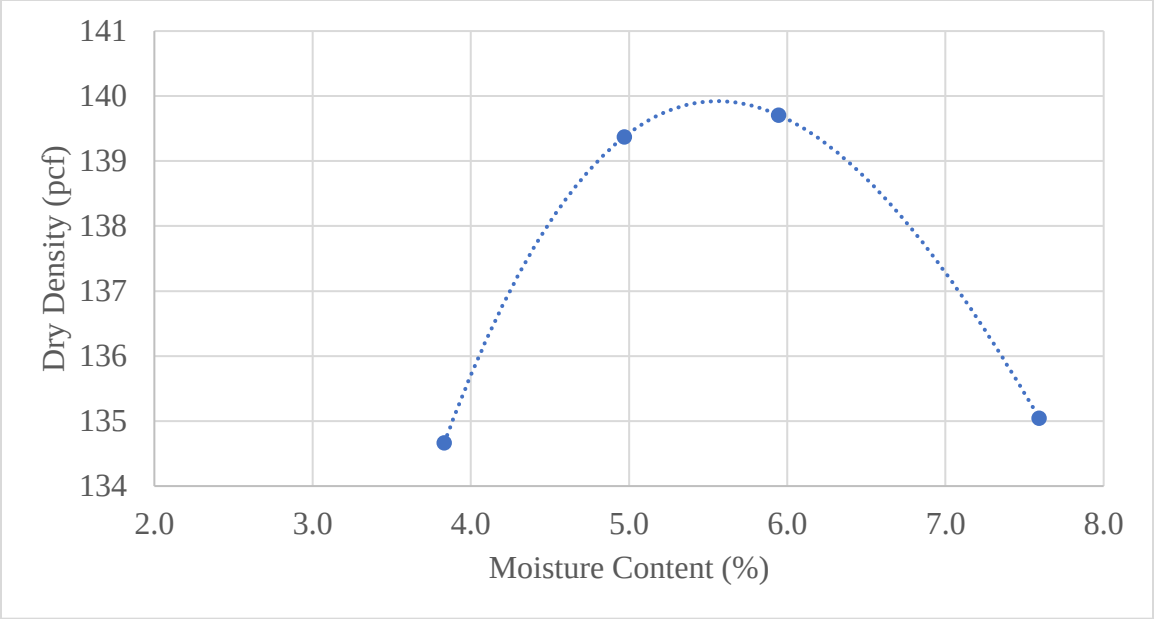

Figure A. 20 Sonoma Borrow Moisture-Density Curve.

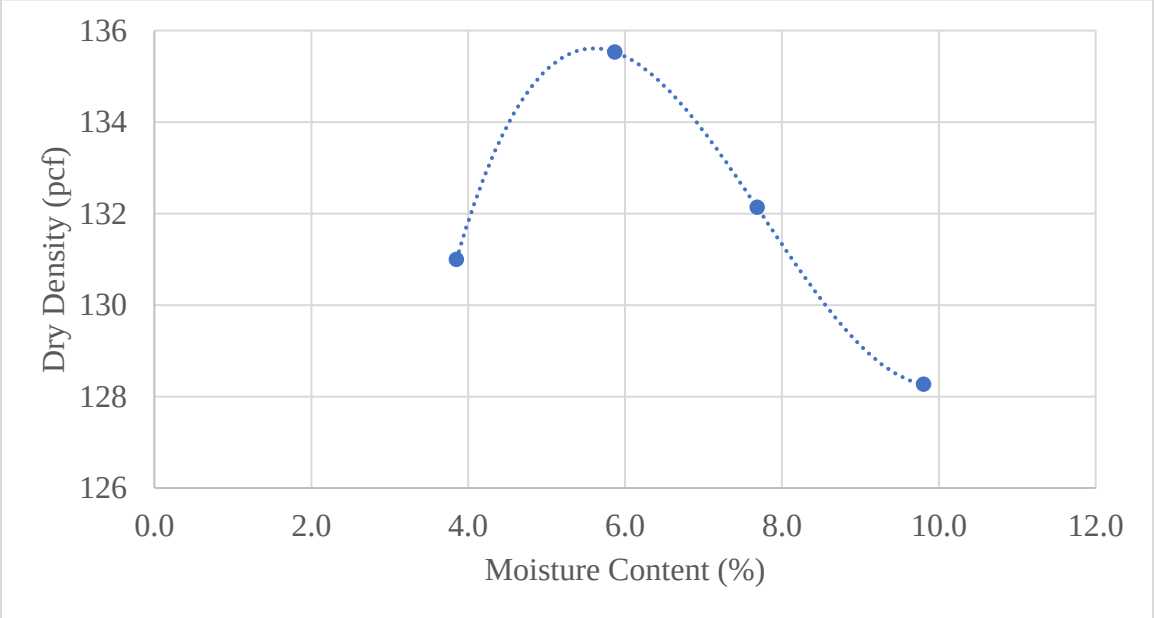

Figure A. 21 Vega Borrow Moisture-Density Curve.

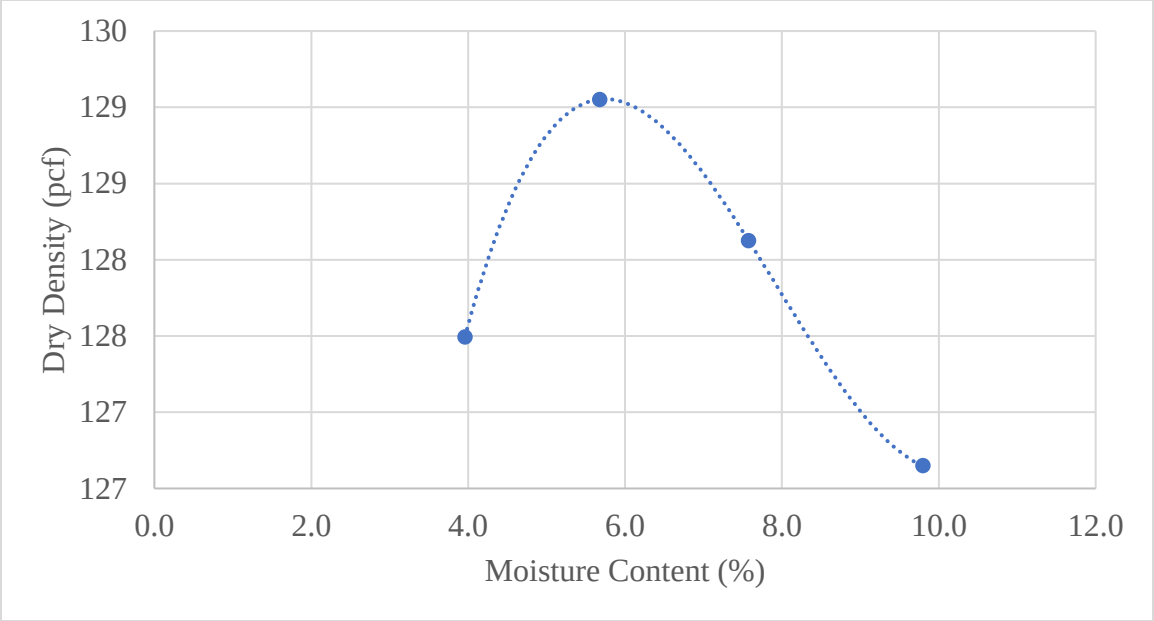

Figure A. 22 Silver State Borrow Moisture-Density Curve.

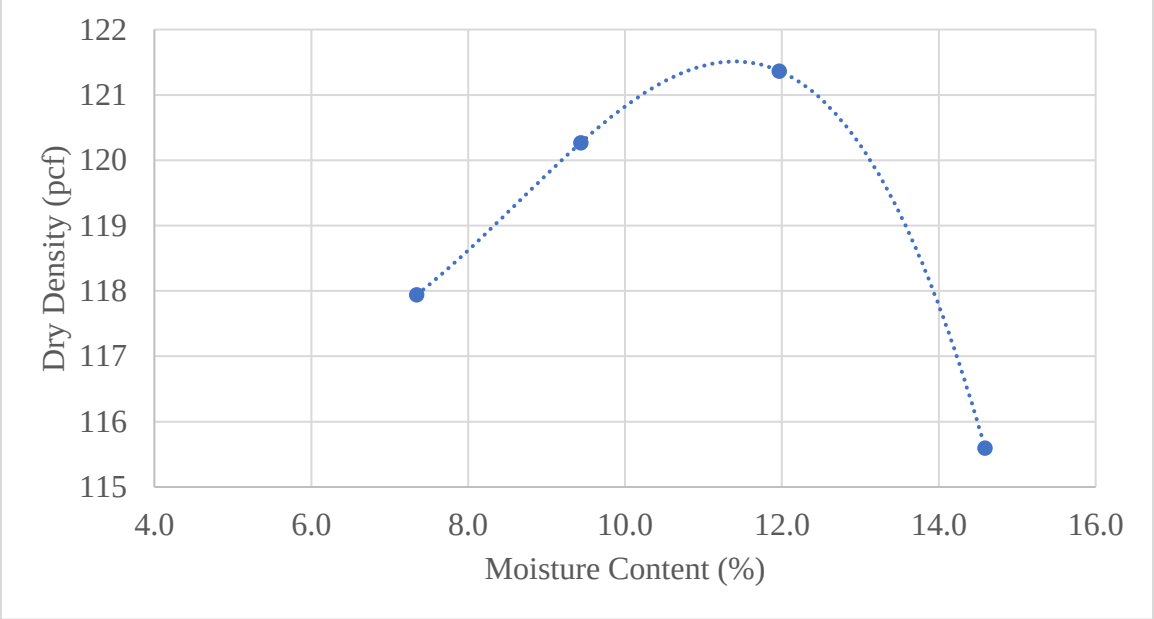

Figure A. 23 Elko Borrow 2 Moisture-Density Curve.

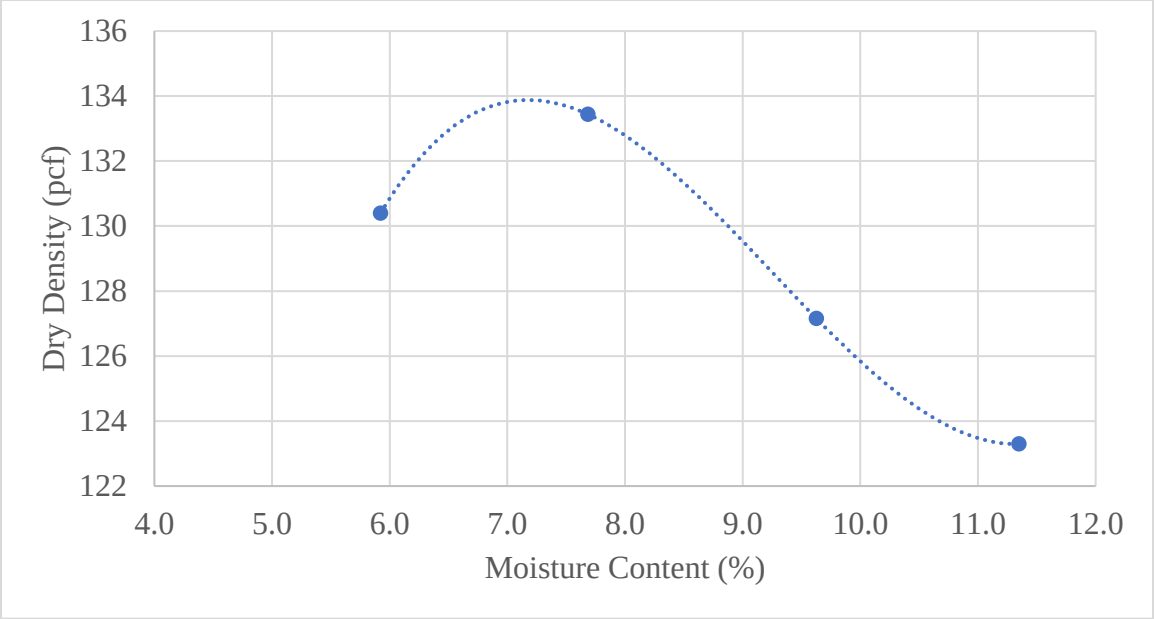

Figure A. 24 NDOT Contract #3817 Subgrade Moisture-Density Curve.

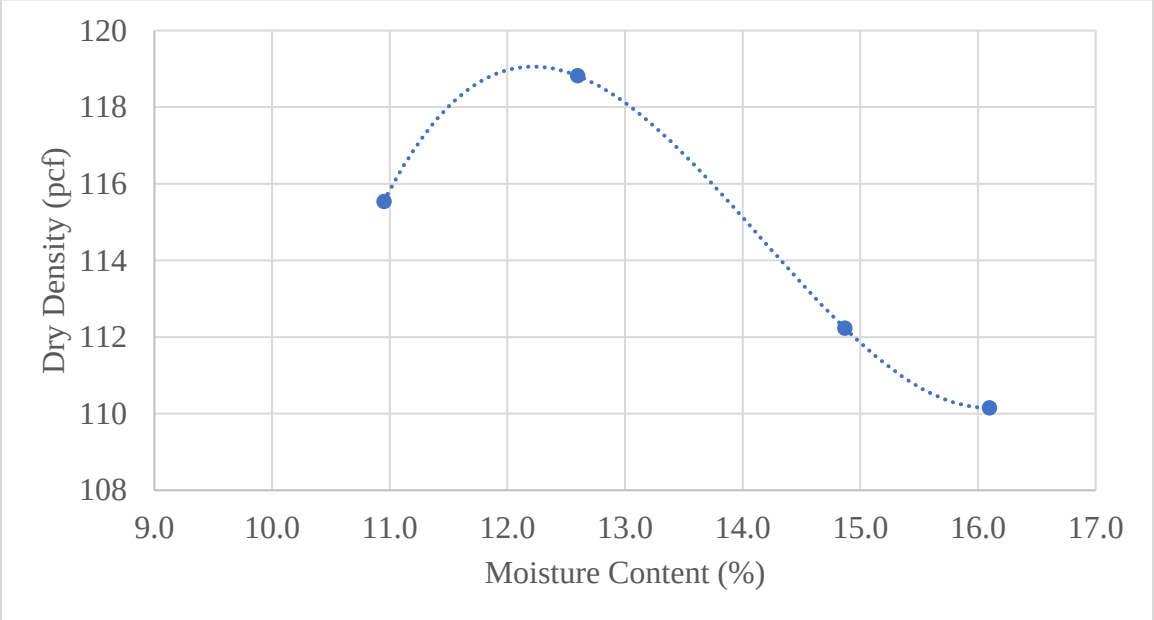

Figure A. 25 NDOT Contract #3824 Subgrade Moisture-Density Curve.

Table A. 1 Summary of Resilient Modulus Test Results for Lockwood Base.

Sequence	Cyclic Axial Stress (psi)	Contact Stress (psi)	Confine Stress (psi)	Axial Resilient Modulus (psi)	Deviator Stress, σd (psi)	Sigma 1 (psi)	Sigma 3 (psi)	Bulk Stress, θ (psi)	Octahedral Shear Stress (psi)
1	13.5	1.5	14.5	26,213	13.5	29.5	14.5	58.6	7.1
2	2.7	0.3	2.5	11,522	2.7	5.5	2.5	10.6	1.4
3	5.4	0.6	2.5	12,039	5.4	8.5	2.5	13.6	2.8
4	8.1	0.9	2.5	13,219	8.1	11.5	2.5	16.6	4.2
5	4.5	0.5	4.5	13,373	4.5	9.6	4.5	18.7	2.4
6	9.0	1.0	4.5	15,731	9.0	14.5	4.5	23.6	4.7
7	13.5	1.5	4.5	17,525	13.5	19.6	4.5	28.7	7.1
8	9.0	1.0	9.5	19,909	9.0	19.5	9.5	38.6	4.7
9	17.9	2.0	9.5	23,683	17.9	29.5	9.5	48.6	9.4
10	26.7	3.0	9.5	26,097	26.7	39.3	9.5	58.4	14.0
11	9.0	1.0	14.5	22,617	9.0	24.5	14.5	53.6	4.7
12	13.5	1.5	14.5	25,130	13.5	29.5	14.5	58.6	7.1
13	26.7	3.0	14.5	30,466	26.7	44.3	14.5	73.4	14.0
14	13.5	1.5	19.5	28,661	13.5	34.6	19.5	73.7	7.1
15	18.0	2.0	19.5	31,171	18.0	39.5	19.5	78.6	9.4
16	34.8	4.0	19.5	36,936	34.8	58.3	19.5	97.4	18.3

Table A. 2 Summary of Resilient Modulus Test Results for Imlay Base.

Sequence	Cyclic Axial Stress (psi)	Contact Stress (psi)	Confine Stress (psi)	Axial Resilient Modulus (psi)	Deviator Stress, σd (psi)	Sigma 1 (psi)	Sigma 3 (psi)	Bulk Stress, θ (psi)	Octahedral Shear Stress (psi)
1	13.5	1.5	14.6	35,495	13.5	29.6	14.6	58.8	7.1
2	2.7	0.3	2.6	15,158	2.7	5.6	2.6	10.8	1.4
3	5.4	0.6	2.6	16,001	5.4	8.6	2.6	13.8	2.8
4	8.1	0.9	2.6	17,174	8.1	11.6	2.6	16.8	4.3
5	4.6	0.5	4.6	18,020	4.6	9.6	4.6	18.8	2.4
6	9.0	1.0	4.6	20,360	9.0	14.6	4.6	23.8	4.7
7	13.5	1.5	4.6	22,113	13.5	19.6	4.6	28.8	7.1
8	9.0	1.0	9.6	26,109	9.0	19.6	9.6	38.8	4.7
9	18.0	2.0	9.6	30,068	18.0	29.6	9.6	48.8	9.4
10	26.7	3.0	9.6	32,246	26.7	39.3	9.6	58.5	14.0
11	9.0	1.0	14.6	30,017	9.0	24.6	14.6	53.8	4.7
12	13.4	1.5	14.6	31,878	13.4	29.5	14.6	58.7	7.0
13	26.7	3.0	14.6	37,627	26.7	44.3	14.6	73.5	14.0
14	13.5	1.5	19.6	36,868	13.5	34.6	19.6	73.8	7.1
15	18.0	2.0	19.6	39,624	18.0	39.6	19.6	78.8	9.4
16	34.8	4.0	19.6	45,569	34.8	58.4	19.6	97.6	18.3

Table A. 3 Summary of Resilient Modulus Test Results for Goni Base.

Sequence	Cyclic Axial Stress (psi)	Contact Stress (psi)	Confine Stress (psi)	Axial Resilient Modulus (psi)	Deviator Stress, σd (psi)	Sigma 1 (psi)	Sigma 3 (psi)	Bulk Stress, θ (psi)	Octahedral Shear Stress (psi)
1	13.5	1.5	14.4	16,767	13.5	29.5	14.4	58.4	7.1
2	2.7	0.3	2.4	6,804	2.7	5.4	2.4	10.3	1.4
3	5.4	0.6	2.4	7,161	5.4	8.4	2.4	13.3	2.8
4	8.1	0.9	2.4	7,639	8.1	11.5	2.4	16.4	4.3
5	4.5	0.5	4.4	7,994	4.5	9.5	4.4	18.4	2.4
6	9.0	1.0	4.4	8,857	9.0	14.5	4.4	23.4	4.7
7	13.5	1.5	4.4	9,580	13.5	19.4	4.4	28.3	7.1
8	9.0	1.0	9.4	11,905	9.0	19.4	9.4	38.3	4.7
9	18.0	2.0	9.4	13,447	18.0	29.4	9.4	48.3	9.4
10	26.3	3.0	9.4	14,438	26.3	38.8	9.4	57.7	13.8
11	9.0	1.0	14.4	13,577	9.0	24.4	14.4	53.3	4.7
12	13.5	1.5	14.4	14,812	13.5	29.4	14.4	58.3	7.1
13	26.7	3.0	14.4	17,762	26.7	44.1	14.4	73.0	14.0
14	13.6	1.5	19.4	18,105	13.6	34.5	19.4	73.4	7.1
15	18.0	2.0	19.4	19,451	18.0	39.4	19.4	78.3	9.4
16	34.5	4.0	19.4	22,829	34.5	57.9	19.4	96.8	18.1

Table A. 4 Summary of Resilient Modulus Test Results for Spanish Springs Base.

Sequence	Cyclic Axial Stress (psi)	Contact Stress (psi)	Confine Stress (psi)	Axial Resilient Modulus (psi)	Deviator Stress, σd (psi)	Sigma 1 (psi)	Sigma 3 (psi)	Bulk Stress, θ (psi)	Octahedral Shear Stress (psi)
1	13.5	1.5	14.5	15,761	13.5	29.5	14.5	58.5	7.1
2	2.6	0.3	2.5	9,045	2.6	5.5	2.5	10.5	1.4
3	5.4	0.6	2.5	10,608	5.4	8.5	2.5	13.5	2.8
4	8.1	0.9	2.5	12,324	8.1	11.5	2.5	16.6	4.3
5	4.5	0.5	4.5	9,227	4.5	9.5	4.5	18.5	2.4
6	9.0	1.0	4.5	12,534	9.0	14.5	4.5	23.5	4.7
7	13.5	1.5	4.5	15,034	13.5	19.5	4.5	28.6	7.1
8	9.0	1.0	9.5	11,358	9.0	19.5	9.5	38.5	4.7
9	18.0	2.0	9.5	16,790	18.0	29.5	9.5	48.6	9.4
10	26.6	3.0	9.5	19,911	26.6	39.1	9.5	58.1	13.9
11	9.0	1.0	14.5	10,625	9.0	24.6	14.5	53.6	4.7
12	13.5	1.5	14.5	13,278	13.5	29.5	14.5	58.6	7.1
13	26.8	3.0	14.5	20,592	26.8	44.3	14.5	73.4	14.1
14	13.6	1.5	19.5	14,074	13.6	34.6	19.5	73.6	7.1
15	18.0	2.0	19.5	17,004	18.0	39.5	19.5	78.6	9.4
16	34.7	4.0	19.5	24,801	34.7	58.2	19.5	97.2	18.2

Table A. 5 Summary of Resilient Modulus Test Results for Trico Base A.

Sequence	Cyclic Axial Stress (psi)	Contact Stress (psi)	Confine Stress (psi)	Axial Resilient Modulus (psi)	Deviator Stress, σd (psi)	Sigma 1 (psi)	Sigma 3 (psi)	Bulk Stress, θ (psi)	Octahedral Shear Stress (psi)
1	13.5	1.5	14.6	21,552	13.5	29.5	14.6	58.6	7.1
2	2.7	0.3	2.6	11,009	2.7	5.5	2.6	10.7	1.4
3	5.4	0.6	2.6	10,940	5.4	8.6	2.6	13.7	2.8
4	8.1	0.9	2.5	11,406	8.1	11.6	2.5	16.7	4.3
5	4.5	0.5	4.6	12,433	4.5	9.6	4.6	18.7	2.4
6	8.9	1.0	4.6	13,049	8.9	14.5	4.6	23.6	4.7
7	13.5	1.5	4.6	14,218	13.5	19.6	4.6	28.7	7.1
8	9.0	1.0	9.6	16,954	9.0	19.6	9.6	38.7	4.7
9	18.0	2.0	9.6	18,850	18.0	29.5	9.6	48.6	9.4
10	26.6	3.0	9.6	20,188	26.6	39.2	9.6	58.3	14.0
11	9.0	1.0	14.6	19,362	9.0	24.6	14.6	53.7	4.7
12	13.5	1.5	14.6	20,727	13.5	29.6	14.6	58.7	7.1
13	26.8	3.0	14.6	23,660	26.8	44.3	14.6	73.4	14.0
14	13.5	1.5	19.6	23,547	13.5	34.6	19.6	73.7	7.1
15	18.0	2.0	19.6	24,807	18.0	39.5	19.6	78.7	9.4
16	34.7	4.0	19.6	28,454	34.7	58.3	19.6	97.4	18.2

Table A. 6 Summary of Resilient Modulus Test Results for Trico Base B.

Sequence	Cyclic Axial Stress (psi)	Contact Stress (psi)	Confine Stress (psi)	Axial Resilient Modulus (psi)	Deviator Stress, σd (psi)	Sigma 1 (psi)	Sigma 3 (psi)	Bulk Stress, θ (psi)	Octahedral Shear Stress (psi)
1	13.5	1.5	14.5	18,756	13.5	29.5	14.5	58.4	7.1
2	2.7	0.3	2.5	8,545	2.7	5.5	2.5	10.4	1.4
3	5.4	0.6	2.5	8,989	5.4	8.5	2.5	13.4	2.8
4	8.1	0.9	2.5	9,990	8.1	11.5	2.5	16.4	4.2
5	4.5	0.5	4.5	9,856	4.5	9.4	4.5	18.4	2.4
6	9.0	1.0	4.5	11,574	9.0	14.4	4.5	23.4	4.7
7	13.5	1.5	4.5	13,029	13.5	19.4	4.5	28.3	7.1
8	9.0	1.0	9.5	14,923	9.0	19.5	9.5	38.4	4.7
9	18.0	2.0	9.5	17,964	18.0	29.5	9.5	48.4	9.4
10	26.7	3.0	9.5	19,896	26.7	39.1	9.5	58.0	14.0
11	9.0	1.0	14.5	16,341	9.0	24.5	14.5	53.4	4.7
12	13.5	1.5	14.5	18,454	13.5	29.5	14.5	58.4	7.1
13	26.7	3.0	14.5	22,686	26.7	44.2	14.5	73.1	14.0
14	13.5	1.5	19.5	20,412	13.5	34.5	19.5	73.4	7.1
15	18.0	2.0	19.5	22,200	18.0	39.5	19.5	78.4	9.4
16	34.8	4.0	19.5	27,130	34.8	58.2	19.5	97.1	18.3

Table A. 7 Summary of Resilient Modulus Test Results for Carlin Base.

Sequence	Cyclic Axial Stress (psi)	Contact Stress (psi)	Confine Stress (psi)	Axial Resilient Modulus (psi)	Deviator Stress, σd (psi)	Sigma 1 (psi)	Sigma 3 (psi)	Bulk Stress, θ (psi)	Octahedral Shear Stress (psi)
1	13.5	1.5	14.4	32,812	13.5	29.5	14.4	58.3	7.1
2	2.7	0.3	2.4	14,986	2.7	5.4	2.4	10.3	1.4
3	5.4	0.6	2.4	15,693	5.4	8.4	2.4	13.3	2.8
4	8.1	0.9	2.4	16,910	8.1	11.4	2.4	16.3	4.2
5	4.5	0.5	4.4	18,085	4.5	9.4	4.4	18.3	2.4
6	9.0	1.0	4.4	20,297	9.0	14.4	4.4	23.2	4.7
7	13.5	1.5	4.4	21,922	13.5	19.4	4.4	28.3	7.1
8	9.0	1.0	9.4	26,459	9.0	19.4	9.4	38.2	4.7
9	18.0	2.0	9.4	29,442	18.0	29.4	9.4	48.2	9.4
10	26.7	3.0	9.4	31,135	26.7	39.1	9.4	58.0	14.0
11	9.0	1.0	14.4	30,487	9.0	24.4	14.4	53.3	4.7
12	13.5	1.5	14.4	32,223	13.5	29.4	14.4	58.3	7.1
13	26.7	3.0	14.4	36,342	26.7	44.1	14.4	73.0	14.0
14	13.5	1.5	19.4	36,119	13.5	34.4	19.4	73.2	7.1
15	18.0	2.0	19.4	38,249	18.0	39.5	19.4	78.3	9.4
16	34.7	4.0	19.4	42,256	34.7	58.1	19.4	97.0	18.2

Table A. 8 Summary of Resilient Modulus Test Results for Sonoma Base.

Sequence	Cyclic Axial Stress (psi)	Contact Stress (psi)	Confine Stress (psi)	Axial Resilient Modulus (psi)	Deviator Stress, σd (psi)	Sigma 1 (psi)	Sigma 3 (psi)	Bulk Stress, θ (psi)	Octahedral Shear Stress (psi)
1	13.5	1.5	14.4	31,561	13.5	29.4	14.4	58.3	7.1
2	2.7	0.3	2.4	13,521	2.7	5.4	2.4	10.3	1.4
3	5.4	0.6	2.4	14,263	5.4	8.4	2.4	13.3	2.8
4	8.1	0.9	2.4	15,647	8.1	11.5	2.4	16.3	4.2
5	4.5	0.5	4.4	15,901	4.5	9.5	4.4	18.4	2.4
6	9.0	1.0	4.4	18,445	9.0	14.4	4.4	23.3	4.7
7	13.5	1.5	4.4	20,736	13.5	19.4	4.4	28.3	7.1
8	9.0	1.0	9.4	24,134	9.0	19.4	9.4	38.3	4.7
9	18.0	2.0	9.4	28,228	18.0	29.4	9.4	48.3	9.4
10	26.7	3.0	9.4	30,616	26.7	39.2	9.4	58.1	14.0
11	9.0	1.0	14.4	28,156	9.0	24.4	14.4	53.3	4.7
12	13.5	1.5	14.4	30,069	13.5	29.5	14.4	58.4	7.1
13	26.8	3.0	14.4	35,427	26.8	44.2	14.4	73.1	14.0
14	13.5	1.5	19.4	34,492	13.5	34.5	19.4	73.3	7.1
15	18.0	2.0	19.4	36,460	18.0	39.4	19.4	78.3	9.4
16	34.8	4.0	19.4	42,215	34.8	58.3	19.4	97.2	18.3

Table A. 9 Summary of Resilient Modulus Test Results for Vega Base.

Sequence	Cyclic Axial Stress (psi)	Contact Stress (psi)	Confine Stress (psi)	Axial Resilient Modulus (psi)	Deviator Stress, σd (psi)	Sigma 1 (psi)	Sigma 3 (psi)	Bulk Stress, θ (psi)	Octahedral Shear Stress (psi)
1	13.5	1.5	14.3	22,494	13.5	29.3	14.3	58.0	7.1
2	2.7	0.3	2.3	10,862	2.7	5.3	2.3	10.0	1.4
3	5.4	0.6	2.3	11,619	5.4	8.3	2.3	13.0	2.8
4	8.1	0.9	2.3	12,259	8.1	11.3	2.3	16.0	4.2
5	4.5	0.5	4.3	12,158	4.5	9.3	4.3	18.0	2.4
6	9.0	1.0	4.3	14,099	9.0	14.3	4.3	23.0	4.7
7	13.5	1.5	4.3	15,485	13.5	19.3	4.3	28.0	7.1
8	9.0	1.0	9.3	17,344	9.0	19.4	9.3	38.0	4.7
9	18.0	2.0	9.3	20,523	18.0	29.3	9.3	48.0	9.4
10	26.5	3.0	9.3	22,077	26.5	38.8	9.3	57.5	13.9
11	9.1	1.0	14.3	19,610	9.1	24.4	14.3	53.1	4.7
12	13.5	1.5	14.3	21,499	13.5	29.4	14.3	58.0	7.1
13	26.7	3.0	14.3	25,599	26.7	44.0	14.3	72.7	14.0
14	13.5	1.5	19.3	23,933	13.5	34.3	19.3	73.0	7.1
15	18.0	2.0	19.3	25,995	18.0	39.4	19.3	78.0	9.4
16	34.5	4.0	19.3	30,953	34.5	57.9	19.3	96.5	18.2

Table A. 10 Summary of Resilient Modulus Test Results for Silver State Base.

Sequence	Cyclic Axial Stress (psi)	Contact Stress (psi)	Confine Stress (psi)	Axial Resilient Modulus (psi)	Deviator Stress, σd (psi)	Sigma 1 (psi)	Sigma 3 (psi)	Bulk Stress, θ (psi)	Octahedral Shear Stress (psi)
1	13.5	1.5	14.4	21,052	13.5	29.4	14.4	58.3	7.1
2	2.7	0.3	2.4	10,391	2.7	5.4	2.4	10.2	1.4
3	5.4	0.6	2.4	10,938	5.4	8.4	2.4	13.2	2.8
4	8.1	0.9	2.4	12,252	8.1	11.4	2.4	16.3	4.2
5	4.5	0.5	4.4	11,252	4.5	9.4	4.4	18.3	2.4
6	9.0	1.0	4.4	13,518	9.0	14.4	4.4	23.2	4.7
7	13.5	1.5	4.4	15,661	13.5	19.4	4.4	28.3	7.1
8	9.0	1.0	9.4	15,661	9.0	19.4	9.4	38.3	4.7
9	18.0	2.0	9.4	19,783	18.0	29.4	9.4	48.2	9.4
10	26.6	3.0	9.4	22,148	26.6	39.0	9.4	57.8	13.9
11	9.0	1.0	14.4	18,474	9.0	24.4	14.4	53.3	4.7
12	13.5	1.5	14.4	20,145	13.5	29.4	14.4	58.2	7.0
13	26.7	3.0	14.4	24,725	26.7	44.1	14.4	72.9	14.0
14	13.5	1.5	19.4	22,334	13.5	34.4	19.4	73.3	7.1
15	18.0	2.0	19.4	24,214	18.0	39.4	19.4	78.3	9.4
16	34.6	4.0	19.4	29,482	34.6	58.0	19.4	96.9	18.2

Table A. 11 Summary of Resilient Modulus Test Results for Lockwood Borrow.

Sequence	Cyclic Axial Stress (psi)	Contact Stress (psi)	Confine Stress (psi)	Axial Resilient Modulus (psi)	Deviator Stress, σd (psi)	Sigma 1 (psi)	Sigma 3 (psi)	Bulk Stress, θ (psi)	Octahedral Shear Stress (psi)
1	13.5	1.5	14.6	28,603	13.5	29.6	14.6	58.9	7.1
2	2.7	0.3	2.6	11,011	2.7	5.6	2.6	10.9	1.4
3	5.4	0.6	2.6	12,190	5.4	8.6	2.6	13.8	2.8
4	8.1	0.9	2.6	13,520	8.1	11.6	2.6	16.9	4.2
5	4.5	0.5	4.6	12,989	4.5	9.7	4.6	18.9	2.4
6	9.0	1.0	4.6	15,396	9.0	14.6	4.6	23.9	4.7
7	13.5	1.5	4.6	17,584	13.5	19.7	4.6	28.9	7.1
8	9.0	1.0	9.6	21,351	9.0	19.6	9.6	38.9	4.7
9	18.0	2.0	9.6	25,646	18.0	29.7	9.6	48.9	9.5
10	26.6	3.0	9.6	27,933	26.6	39.3	9.6	58.5	14.0
11	9.0	1.0	14.6	25,252	9.0	24.6	14.6	53.9	4.7
12	13.5	1.5	14.6	27,576	13.5	29.6	14.6	58.9	7.1
13	26.7	3.0	14.6	32,901	26.7	44.4	14.6	73.6	14.0
14	13.5	1.5	19.6	31,841	13.5	34.7	19.6	73.9	7.1
15	18.0	2.0	19.6	34,486	18.0	39.6	19.6	78.9	9.4
16	34.8	4.0	19.6	40,467	34.8	58.4	19.6	97.7	18.3

Table A. 12 Summary of Resilient Modulus Test Results for Imlay Borrow.

Sequence	Cyclic Axial Stress (psi)	Contact Stress (psi)	Confine Stress (psi)	Axial Resilient Modulus (psi)	Deviator Stress, σd (psi)	Sigma 1 (psi)	Sigma 3 (psi)	Bulk Stress, θ (psi)	Octahedral Shear Stress (psi)
1	13.5	1.5	14.6	29,519	13.5	29.6	14.6	58.8	7.1
2	2.7	0.3	2.6	12,284	2.7	5.6	2.6	10.7	1.4
3	5.4	0.6	2.6	12,962	5.4	8.6	2.6	13.7	2.8
4	8.1	0.9	2.6	13,745	8.1	11.6	2.6	16.7	4.2
5	4.5	0.5	4.6	13,657	4.5	9.6	4.6	18.7	2.4
6	9.0	1.0	4.6	15,811	9.0	14.6	4.6	23.7	4.7
7	13.5	1.5	4.6	17,592	13.5	19.6	4.6	28.7	7.1
8	9.0	1.0	9.6	20,669	9.0	19.6	9.6	38.7	4.7
9	18.0	2.0	9.6	24,473	18.0	29.6	9.6	48.7	9.4
10	26.7	3.0	9.6	26,805	26.7	39.3	9.6	58.4	14.0
11	9.0	1.0	14.6	24,722	9.0	24.6	14.6	53.7	4.7
12	13.5	1.5	14.6	26,442	13.5	29.6	14.6	58.7	7.1
13	26.8	3.0	14.6	31,724	26.8	44.4	14.6	73.5	14.1
14	13.5	1.5	19.6	30,930	13.5	34.6	19.6	73.7	7.1
15	18.1	2.0	19.6	33,188	18.1	39.6	19.6	78.8	9.5
16	34.8	4.0	19.6	38,865	34.8	58.4	19.6	97.6	18.3

Table A. 13 Summary of Resilient Modulus Test Results for Goni Borrow.

Sequence	Cyclic Axial Stress (psi)	Contact Stress (psi)	Confine Stress (psi)	Axial Resilient Modulus (psi)	Deviator Stress, σd (psi)	Sigma 1 (psi)	Sigma 3 (psi)	Bulk Stress, θ (psi)	Octahedral Shear Stress (psi)
1	13.5	1.5	14.7	22,341	13.5	29.7	14.7	59.2	7.1
2	2.7	0.3	2.7	12,285	2.7	5.8	2.7	11.2	1.4
3	5.4	0.6	2.7	11,248	5.4	8.7	2.7	14.2	2.8
4	8.1	0.9	2.7	11,349	8.1	11.7	2.7	17.2	4.2
5	4.5	0.5	4.7	13,207	4.5	9.7	4.7	19.2	2.3
6	9.0	1.0	4.7	13,282	9.0	14.7	4.7	24.2	4.7
7	13.5	1.5	4.7	13,908	13.5	19.8	4.7	29.2	7.1
8	9.0	1.0	9.7	17,630	9.0	19.7	9.7	39.2	4.7
9	18.0	2.0	9.7	19,038	18.0	29.7	9.7	49.2	9.4
10	26.7	3.0	9.7	19,879	26.7	39.4	9.7	58.9	14.0
11	9.0	1.0	14.7	21,234	9.0	24.7	14.7	54.2	4.7
12	13.5	1.5	14.7	21,848	13.5	29.7	14.7	59.2	7.1
13	26.8	3.0	14.7	23,959	26.8	44.5	14.7	74.0	14.0
14	13.5	1.5	19.7	25,330	13.5	34.7	19.7	74.2	7.1
15	18.0	2.0	19.7	26,132	18.0	39.7	19.7	79.2	9.4
16	34.7	4.0	19.7	28,325	34.7	58.5	19.7	98.0	18.3

Table A. 14 Summary of Resilient Modulus Test Results for Spanish Springs Borrow.

Sequence	Cyclic Axial Stress (psi)	Contact Stress (psi)	Confine Stress (psi)	Axial Resilient Modulus (psi)	Deviator Stress, σd (psi)	Sigma 1 (psi)	Sigma 3 (psi)	Bulk Stress, θ (psi)	Octahedral Shear Stress (psi)
1	13.5	1.5	14.8	26,434	13.5	29.7	14.8	59.3	7.1
2	2.7	0.3	2.8	17,877	2.7	5.8	2.8	11.3	1.4
3	5.4	0.6	2.8	15,017	5.4	8.8	2.8	14.3	2.8
4	8.1	0.9	2.8	14,668	8.1	11.8	2.8	17.3	4.3
5	4.5	0.5	4.8	16,698	4.5	9.7	4.8	19.2	2.3
6	9.0	1.0	4.8	16,644	9.0	14.7	4.8	24.2	4.7
7	13.5	1.5	4.8	17,113	13.5	19.8	4.8	29.3	7.1
8	9.0	1.0	9.8	21,379	9.0	19.8	9.8	39.3	4.7
9	18.0	2.0	9.8	22,015	18.0	29.7	9.8	49.2	9.4
10	26.6	3.0	9.8	22,247	26.6	39.3	9.8	58.9	13.9
11	9.0	1.0	14.8	25,984	9.0	24.8	14.8	54.3	4.7
12	13.4	1.5	14.8	26,047	13.4	29.7	14.8	59.2	7.0
13	26.6	3.0	14.8	26,943	26.6	44.4	14.8	73.9	14.0
14	13.4	1.5	19.8	30,146	13.4	34.7	19.8	74.2	7.0
15	18.0	2.0	19.8	30,565	18.0	39.8	19.8	79.3	9.4
16	34.5	4.0	19.8	30,748	34.5	58.2	19.8	97.7	18.1

Table A. 15 Summary of Resilient Modulus Test Results for Trico Borrow.

Sequence	Cyclic Axial Stress (psi)	Contact Stress (psi)	Confine Stress (psi)	Axial Resilient Modulus (psi)	Deviator Stress, σd (psi)	Sigma 1 (psi)	Sigma 3 (psi)	Bulk Stress, θ (psi)	Octahedral Shear Stress (psi)
1	13.5	1.5	14.7	15,417	13.5	29.7	14.7	59.1	7.1
2	2.7	0.3	2.7	7,312	2.7	5.7	2.7	11.1	1.4
3	5.4	0.6	2.7	6,891	5.4	8.7	2.7	14.1	2.8
4	8.1	0.9	2.7	7,233	8.1	11.7	2.7	17.0	4.2
5	4.5	0.5	4.7	7,850	4.5	9.7	4.7	19.1	2.4
6	9.0	1.0	4.7	8,509	9.0	14.7	4.7	24.0	4.7
7	13.5	1.5	4.7	9,424	13.5	19.7	4.7	29.0	7.1
8	9.0	1.0	9.7	11,540	9.0	19.7	9.7	39.0	4.7
9	18.0	2.0	9.7	13,026	18.0	29.6	9.7	49.0	9.4
10	26.3	3.0	9.7	13,637	26.3	39.0	9.7	58.4	13.8
11	9.0	1.0	14.7	14,143	9.0	24.7	14.7	54.1	4.7
12	13.5	1.5	14.7	14,428	13.5	29.7	14.7	59.0	7.1
13	26.6	3.0	14.7	16,151	26.6	44.2	14.7	73.6	13.9
14	13.5	1.5	19.7	16,639	13.5	34.7	19.7	74.1	7.1
15	18.0	2.0	19.7	17,297	18.0	39.7	19.7	79.0	9.4
16	34.4	4.0	19.7	19,469	34.4	58.0	19.7	97.4	18.1

Table A. 16 Summary of Resilient Modulus Test Results for Sonoma Borrow.

Sequence	Cyclic Axial Stress (psi)	Contact Stress (psi)	Confine Stress (psi)	Axial Resilient Modulus (psi)	Deviator Stress, σd (psi)	Sigma 1 (psi)	Sigma 3 (psi)	Bulk Stress, θ (psi)	Octahedral Shear Stress (psi)
1	13.5	1.5	14.6	29,601	13.5	29.6	14.6	58.7	7.1
2	2.7	0.3	2.6	14,686	2.7	5.6	2.6	10.7	1.4
3	5.4	0.6	2.6	14,716	5.4	8.6	2.6	13.7	2.8
4	8.1	0.9	2.6	15,737	8.1	11.6	2.6	16.7	4.3
5	4.5	0.5	4.6	16,531	4.5	9.6	4.6	18.7	2.4
6	9.0	1.0	4.6	18,259	9.0	14.6	4.6	23.7	4.7
7	13.5	1.5	4.6	20,360	13.5	19.6	4.6	28.7	7.1
8	9.0	1.0	9.6	23,583	9.0	19.6	9.6	38.7	4.7
9	18.0	2.0	9.6	27,027	18.0	29.5	9.6	48.7	9.4
10	26.8	3.0	9.6	29,132	26.8	39.3	9.6	58.4	14.0
11	9.0	1.0	14.6	28,057	9.0	24.6	14.6	53.7	4.7
12	13.6	1.5	14.6	29,812	13.6	29.6	14.6	58.7	7.1
13	26.7	3.0	14.6	33,586	26.7	44.3	14.6	73.4	14.0
14	13.5	1.5	19.6	34,012	13.5	34.5	19.6	73.6	7.0
15	18.0	2.0	19.6	35,390	18.0	39.5	19.6	78.6	9.4
16	34.8	4.0	19.6	40,694	34.8	58.4	19.6	97.5	18.3

Table A. 17 Summary of Resilient Modulus Test Results for Vega Borrow.

Sequence	Cyclic Axial Stress (psi)	Contact Stress (psi)	Confine Stress (psi)	Axial Resilient Modulus (psi)	Deviator Stress, σd (psi)	Sigma 1 (psi)	Sigma 3 (psi)	Bulk Stress, θ (psi)	Octahedral Shear Stress (psi)
1	13.5	1.5	14.4	29,155	13.5	29.4	14.4	58.2	7.1
2	2.7	0.3	2.4	14,050	2.7	5.4	2.4	10.1	1.4
3	5.4	0.6	2.4	14,556	5.4	8.4	2.4	13.2	2.8
4	8.1	0.9	2.4	15,385	8.1	11.4	2.4	16.2	4.3
5	4.5	0.5	4.4	16,383	4.5	9.4	4.4	18.2	2.4
6	9.0	1.0	4.4	18,220	9.0	14.4	4.4	23.2	4.7
7	13.5	1.5	4.4	19,613	13.5	19.4	4.4	28.2	7.1
8	9.0	1.0	9.4	23,319	9.0	19.4	9.4	38.1	4.7
9	18.0	2.0	9.4	26,427	18.0	29.4	9.4	48.1	9.4
10	26.6	3.0	9.4	27,299	26.6	39.0	9.4	57.8	14.0
11	9.0	1.0	14.4	26,337	9.0	24.4	14.4	53.2	4.7
12	13.5	1.5	14.4	28,367	13.5	29.4	14.4	58.1	7.1
13	26.7	3.0	14.4	32,477	26.7	44.1	14.4	72.9	14.0
14	13.5	1.5	19.4	31,715	13.5	34.4	19.4	73.2	7.1
15	18.0	2.0	19.4	33,904	18.0	39.4	19.4	78.2	9.4
16	34.6	4.0	19.4	38,014	34.6	58.0	19.4	96.8	18.2

Table A. 18 Summary of Resilient Modulus Test Results for Silver State Borrow.

Sequence	Cyclic Axial Stress (psi)	Contact Stress (psi)	Confine Stress (psi)	Axial Resilient Modulus (psi)	Deviator Stress, σd (psi)	Sigma 1 (psi)	Sigma 3 (psi)	Bulk Stress, θ (psi)	Octahedral Shear Stress (psi)
1	13.5	1.5	14.7	22,616	13.5	29.7	14.7	59.0	7.1
2	2.7	0.3	2.7	10,249	2.7	5.6	2.7	11.0	1.4
3	5.4	0.6	2.7	10,520	5.4	8.7	2.7	14.0	2.8
4	7.2	0.8	2.7	10,479	7.2	10.7	2.7	16.0	3.8
5	4.5	0.5	4.7	12,240	4.5	9.7	4.7	19.0	2.4
6	9.0	1.0	4.7	13,219	9.0	14.7	4.7	24.0	4.7
7	12.5	1.5	4.7	13,568	12.5	18.6	4.7	28.0	6.6
8	9.0	1.0	9.7	17,906	9.0	19.6	9.7	39.0	4.7
9	18.0	2.0	9.7	19,550	18.0	29.7	9.7	49.0	9.4
10	26.4	3.0	9.7	19,873	26.4	39.1	9.7	58.5	13.9
11	9.0	1.0	14.7	20,391	9.0	24.7	14.7	54.0	4.7
12	13.5	1.5	14.7	21,660	13.5	29.7	14.7	59.0	7.1
13	26.6	3.0	14.7	24,427	26.6	44.3	14.7	73.6	14.0
14	13.5	1.5	19.7	24,650	13.5	34.7	19.7	74.0	7.1
15	18.0	2.0	19.7	26,110	18.0	39.7	19.7	79.0	9.4
16	34.5	4.0	19.7	29,440	34.5	58.2	19.7	97.5	18.2

Table A. 19 Summary of Resilient Modulus Test Results for Elko Borrow 1.

Sequence	Cyclic Axial Stress (psi)	Contact Stress (psi)	Confine Stress (psi)	Axial Resilient Modulus (psi)	Deviator Stress, σd (psi)	Sigma 1 (psi)	Sigma 3 (psi)	Bulk Stress, θ (psi)	Octahedral Shear Stress (psi)
1	13.5	1.5	14.4	21,785	13.5	29.4	14.4	58.2	7.1
2	2.7	0.3	2.4	11,037	2.7	5.4	2.4	10.3	1.4
3	5.4	0.6	2.4	10,883	5.4	8.4	2.4	13.3	2.8
4	8.1	0.9	2.4	11,511	8.1	11.4	2.4	16.3	4.3
5	4.5	0.5	4.4	12,029	4.5	9.4	4.4	18.3	2.4
6	9.0	1.0	4.4	13,371	9.0	14.4	4.4	23.3	4.7
7	13.5	1.5	4.4	14,381	13.5	19.4	4.4	28.2	7.1
8	9.0	1.0	9.4	16,780	9.0	19.4	9.4	38.2	4.7
9	17.9	2.0	9.4	18,990	17.9	29.4	9.4	48.2	9.4
10	26.5	3.0	9.4	19,466	26.5	38.9	9.4	57.7	13.9
11	9.0	1.0	14.4	19,602	9.0	24.4	14.4	53.2	4.7
12	13.5	1.5	14.4	20,456	13.5	29.4	14.4	58.3	7.1
13	26.6	3.0	14.4	23,335	26.6	44.0	14.4	72.9	14.0
14	13.5	1.5	19.4	23,214	13.5	34.4	19.4	73.3	7.1
15	18.0	2.0	19.4	24,458	18.0	39.4	19.4	78.2	9.4
16	34.4	4.0	19.4	27,428	34.4	57.8	19.4	96.6	18.1

Table A. 20 Summary of Resilient Modulus Test Results for Elko Borrow 2.

Sequence	Cyclic Axial Stress (psi)	Contact Stress (psi)	Confine Stress (psi)	Axial Resilient Modulus (psi)	Deviator Stress, σd (psi)	Sigma 1 (psi)	Sigma 3 (psi)	Bulk Stress, θ (psi)	Octahedral Shear Stress (psi)
1	13.5	1.5	14.4	24,839	13.5	29.4	14.4	58.3	7.1
2	2.7	0.3	2.4	15,657	2.7	5.4	2.4	10.3	1.4
3	5.4	0.6	2.4	14,849	5.4	8.4	2.4	13.3	2.8
4	8.1	0.9	2.4	14,700	8.1	11.4	2.4	16.3	4.3
5	4.5	0.5	4.4	16,714	4.5	9.4	4.4	18.3	2.4
6	9.0	1.0	4.4	16,573	9.0	14.4	4.4	23.3	4.7
7	13.5	1.5	4.4	16,773	13.5	19.4	4.4	28.2	7.1
8	9.0	1.0	9.4	20,809	9.0	19.4	9.4	38.3	4.7
9	18.0	2.0	9.4	20,907	18.0	29.4	9.4	48.2	9.4
10	26.4	3.0	9.4	20,610	26.4	38.8	9.4	57.6	13.9
11	9.0	1.0	14.4	24,794	9.0	24.4	14.4	53.3	4.7
12	13.5	1.5	14.4	24,270	13.5	29.4	14.4	58.3	7.1
13	26.5	3.0	14.4	24,177	26.5	43.9	14.4	72.8	13.9
14	13.5	1.5	19.4	27,198	13.5	34.4	19.4	73.3	7.1
15	18.0	2.0	19.4	27,419	18.0	39.4	19.4	78.2	9.4
16	34.2	4.0	19.4	27,469	34.2	57.6	19.4	96.5	18.0

Table A. 21 Summary of Resilient Modulus Test Results for Fallon Big Dig Subgrade 1.

Sequence	Cyclic Axial Stress (psi)	Contact Stress (psi)	Confine Stress (psi)	Axial Resilient Modulus (psi)	Deviator Stress, σd (psi)	Sigma 1 (psi)	Sigma 3 (psi)	Bulk Stress, θ (psi)	Octahedral Shear Stress (psi)
1	3.7	0.4	5.4	9,527	3.7	9.5	5.4	20.2	1.9
2	1.8	0.2	5.4	9,485	1.8	7.4	5.4	18.2	1.0
3	3.6	0.4	5.4	9,530	3.6	9.4	5.4	20.2	1.9
4	5.4	0.6	5.4	9,455	5.4	11.4	5.4	22.2	2.8
5	7.2	0.8	4.4	9,203	7.2	12.4	4.4	21.2	3.8
6	9.0	1.0	5.4	10,072	9.0	15.4	5.4	26.2	4.7
7	1.8	0.2	3.4	9,102	1.8	5.4	3.4	12.2	0.9
8	3.6	0.4	3.4	8,209	3.6	7.4	3.4	14.2	1.9
9	5.4	0.6	3.4	8,187	5.4	9.4	3.4	16.2	2.8
10	7.2	0.8	3.4	8,779	7.2	11.4	3.4	18.2	3.8
11	9.0	1.0	3.4	9,316	9.0	13.4	3.4	20.2	4.7
12	1.8	0.2	1.4	7,478	1.8	3.4	1.4	6.2	0.9
13	3.6	0.4	1.4	6,973	3.6	5.4	1.4	8.2	1.9
14	5.4	0.6	1.4	7,298	5.4	7.4	1.4	10.2	2.8
15	7.2	0.8	1.4	8,040	7.2	9.4	1.4	12.2	3.8
16	9.0	1.0	1.4	8,663	9.0	11.4	1.4	14.2	4.7

Table A. 22 Summary of Resilient Modulus Test Results for Fallon Big Dig Subgrade 2.

Sequence	Cyclic Axial Stress (psi)	Contact Stress (psi)	Confine Stress (psi)	Axial Resilient Modulus (psi)	Deviator Stress, σd (psi)	Sigma 1 (psi)	Sigma 3 (psi)	Bulk Stress, θ (psi)	Octahedral Shear Stress (psi)
1	3.6	0.4	5.8	9,131	3.6	9.8	5.8	21.4	1.9
2	1.8	0.2	5.8	8,627	1.8	7.8	5.8	19.5	0.9
3	3.6	0.4	5.8	9,436	3.6	9.8	5.8	21.5	1.9
4	5.4	0.6	5.8	9,195	5.4	11.8	5.8	23.5	2.8
5	7.2	0.8	4.8	8,794	7.2	12.8	4.8	22.5	3.8
6	9.0	1.0	5.8	9,098	9.0	15.8	5.8	27.5	4.7
7	1.8	0.2	3.8	9,366	1.8	5.8	3.8	13.4	0.9
8	3.6	0.4	3.8	9,041	3.6	7.8	3.8	15.5	1.9
9	5.4	0.6	3.8	8,948	5.4	9.8	3.8	17.5	2.8
10	7.2	0.8	3.8	8,901	7.2	11.8	3.8	19.5	3.8
11	9.0	1.0	3.8	8,903	9.0	13.8	3.8	21.5	4.7
12	1.8	0.2	1.8	8,706	1.8	3.8	1.8	7.5	0.9
13	3.6	0.4	1.8	8,438	3.6	5.8	1.8	9.5	1.9
14	5.4	0.6	1.8	8,378	5.4	7.8	1.8	11.5	2.8
15	7.2	0.8	1.8	8,387	7.2	9.8	1.8	13.5	3.8
16	9.0	1.0	1.8	8,423	9.0	11.8	1.8	15.4	4.7

Table A. 23 Summary of Resilient Modulus Test Results for Reno Spaghetti Bowl Subgrade.

Sequence	Cyclic Axial Stress (psi)	Contact Stress (psi)	Confine Stress (psi)	Axial Resilient Modulus (psi)	Deviator Stress, σd (psi)	Sigma 1 (psi)	Sigma 3 (psi)	Bulk Stress, θ (psi)	Octahedral Shear Stress (psi)
1	3.6	0.4	5.4	13,410	3.6	9.4	5.4	20.3	1.9
2	1.8	0.2	5.4	13,509	1.8	7.4	5.4	18.3	0.9
3	3.6	0.4	5.4	13,472	3.6	9.4	5.4	20.3	1.9
4	5.4	0.6	5.4	13,388	5.4	11.4	5.4	22.3	2.8
5	7.2	0.8	4.4	12,933	7.2	12.4	4.4	21.2	3.8
6	9.0	1.0	5.4	13,883	9.0	15.4	5.4	26.3	4.7
7	1.8	0.2	3.4	13,111	1.8	5.4	3.4	12.3	0.9
8	3.6	0.4	3.4	12,157	3.6	7.4	3.4	14.3	1.9
9	5.4	0.6	3.4	12,005	5.4	9.4	3.4	16.2	2.8
10	7.3	0.8	3.4	12,487	7.3	11.5	3.4	18.3	3.8
11	9.0	1.0	3.4	13,002	9.0	13.4	3.4	20.2	4.7
12	1.8	0.2	1.4	10,974	1.8	3.4	1.4	6.3	0.9
13	3.6	0.4	1.4	10,516	3.6	5.4	1.4	8.2	1.9
14	5.4	0.6	1.4	10,736	5.4	7.4	1.4	10.2	2.8
15	7.2	0.8	1.4	11,283	7.2	9.4	1.4	12.2	3.8
16	9.0	1.0	1.4	11,921	9.0	11.4	1.4	14.3	4.7

Table A. 24 Summary of Resilient Modulus Test Results for Reno Kings Row Subgrade.

Sequence	Cyclic Axial Stress (psi)	Contact Stress (psi)	Confine Stress (psi)	Axial Resilient Modulus (psi)	Deviator Stress, σd (psi)	Sigma 1 (psi)	Sigma 3 (psi)	Bulk Stress, θ (psi)	Octahedral Shear Stress (psi)
1	3.6	0.4	5.7	21,294	3.6	9.7	5.7	21.1	1.9
2	1.8	0.2	5.7	22,265	1.8	7.7	5.7	19.1	0.9
3	3.6	0.4	5.7	21,501	3.6	9.7	5.7	21.1	1.9
4	5.4	0.6	5.7	20,591	5.4	11.7	5.7	23.1	2.8
5	7.2	0.8	4.7	18,838	7.2	12.7	4.7	22.0	3.8
6	9.0	1.0	5.7	19,442	9.0	15.7	5.7	27.1	4.7
7	1.8	0.2	3.7	20,141	1.8	5.7	3.7	13.1	0.9
8	3.6	0.4	3.7	18,674	3.6	7.7	3.7	15.0	1.9
9	5.4	0.6	3.7	17,938	5.4	9.7	3.7	17.0	2.8
10	7.2	0.8	3.7	17,718	7.2	11.7	3.7	19.1	3.8
11	9.0	1.0	3.7	17,846	9.0	13.7	3.7	21.0	4.7
12	1.8	0.2	1.7	17,150	1.8	3.7	1.7	7.0	0.9
13	3.6	0.4	1.7	15,073	3.6	5.7	1.7	9.1	1.9
14	5.5	0.6	1.7	14,985	5.5	7.7	1.7	11.1	2.8
15	7.1	0.8	1.7	15,055	7.1	9.6	1.7	13.0	3.7
16	9.0	1.0	1.7	15,228	9.0	11.7	1.7	15.1	4.7

Table A. 25 Summary of Resilient Modulus Test Results for Lemmon Dr. Subgrade 1.

Sequence	Cyclic Axial Stress (psi)	Contact Stress (psi)	Confine Stress (psi)	Axial Resilient Modulus (psi)	Deviator Stress, σd (psi)	Sigma 1 (psi)	Sigma 3 (psi)	Bulk Stress, θ (psi)	Octahedral Shear Stress (psi)
1	3.6	0.4	5.5	10,835	3.6	9.5	5.5	20.5	1.9
2	1.8	0.2	5.5	11,491	1.8	7.5	5.5	18.6	0.9
3	3.6	0.4	5.5	10,826	3.6	9.5	5.5	20.6	1.9
4	5.4	0.6	5.5	10,193	5.4	11.5	5.5	22.5	2.8
5	7.2	0.8	4.5	9,552	7.2	12.5	4.5	21.5	3.8
6	9.0	1.0	5.5	9,701	9.0	15.5	5.5	26.6	4.7
7	1.8	0.2	3.5	11,161	1.8	5.6	3.5	12.6	1.0
8	3.6	0.4	3.5	10,193	3.6	7.5	3.5	14.6	1.9
9	5.4	0.6	3.5	9,482	5.4	9.5	3.5	16.6	2.8
10	7.2	0.8	3.5	9,264	7.2	11.5	3.5	18.6	3.8
11	9.0	1.0	3.5	9,167	9.0	13.5	3.5	20.6	4.7
12	1.8	0.2	1.5	9,975	1.8	3.5	1.5	6.6	1.0
13	3.6	0.4	1.5	8,948	3.6	5.5	1.5	8.6	1.9
14	5.4	0.6	1.5	8,490	5.4	7.5	1.5	10.6	2.8
15	7.2	0.8	1.5	8,379	7.2	9.5	1.5	12.6	3.8
16	9.0	1.0	1.5	8,286	9.0	11.5	1.5	14.6	4.7

Table A. 26 Summary of Resilient Modulus Test Results for Lemmon Dr. Subgrade 2.

Sequence	Cyclic Axial Stress (psi)	Contact Stress (psi)	Confine Stress (psi)	Axial Resilient Modulus (psi)	Deviator Stress, σd (psi)	Sigma 1 (psi)	Sigma 3 (psi)	Bulk Stress, θ (psi)	Octahedral Shear Stress (psi)
1	3.6	0.4	5.5	13,816	3.6	9.6	5.5	20.6	1.9
2	1.8	0.2	5.5	14,848	1.8	7.5	5.5	18.6	0.9
3	3.6	0.4	5.5	14,160	3.6	9.6	5.5	20.7	1.9
4	5.4	0.6	5.5	13,512	5.4	11.5	5.5	22.6	2.8
5	7.2	0.8	4.5	12,704	7.2	12.6	4.5	21.7	3.8
6	9.0	1.0	5.5	12,912	9.0	15.5	5.5	26.6	4.7
7	1.7	0.2	3.5	14,614	1.7	5.5	3.5	12.6	0.9
8	3.6	0.4	3.5	13,546	3.6	7.5	3.5	14.6	1.9
9	5.4	0.6	3.5	13,238	5.4	9.6	3.5	16.7	2.8
10	7.2	0.8	3.5	12,827	7.2	11.6	3.5	18.7	3.8
11	9.0	1.0	3.5	12,403	9.0	13.5	3.5	20.6	4.7
12	1.8	0.2	1.5	12,414	1.8	3.6	1.5	6.7	1.0
13	3.6	0.4	1.5	11,812	3.6	5.6	1.5	8.6	1.9
14	5.4	0.6	1.5	11,744	5.4	7.5	1.5	10.6	2.8
15	7.2	0.8	1.5	11,467	7.2	9.5	1.5	12.6	3.8
16	9.0	1.0	1.5	11,272	9.0	11.5	1.5	14.6	4.7

Table A. 27 Summary of Resilient Modulus Test Results for NDOT Contract #3817 Subgrade.

Sequence	Cyclic Axial Stress (psi)	Contact Stress (psi)	Confine Stress (psi)	Axial Resilient Modulus (psi)	Deviator Stress, σd (psi)	Sigma 1 (psi)	Sigma 3 (psi)	Bulk Stress, θ (psi)	Octahedral Shear Stress (psi)
1	3.5	0.5	5.5	10,923	3.5	9.5	5.5	20.4	1.9
2	1.8	0.2	5.5	9,694	1.8	7.5	5.5	18.5	0.9
3	3.6	0.4	5.5	10,891	3.6	9.5	5.5	20.4	1.9
4	5.4	0.6	5.5	11,358	5.4	11.5	5.5	22.5	2.8
5	7.2	0.8	4.5	10,833	7.2	12.5	4.5	21.5	3.8
6	9.0	1.0	5.5	12,145	9.0	15.5	5.5	26.5	4.7
7	1.8	0.2	3.5	8,514	1.8	5.5	3.5	12.5	1.0
8	3.6	0.4	3.5	8,584	3.6	7.5	3.5	14.5	1.9
9	5.4	0.6	3.5	9,175	5.4	9.5	3.5	16.5	2.8
10	7.2	0.8	3.5	9,942	7.2	11.5	3.5	18.5	3.8
11	9.0	1.0	3.5	10,440	9.0	13.5	3.5	20.4	4.7
12	1.8	0.2	1.5	6,274	1.8	3.5	1.5	6.5	0.9
13	3.6	0.4	1.5	6,899	3.6	5.5	1.5	8.4	1.9
14	5.4	0.6	1.5	7,769	5.4	7.5	1.5	10.5	2.8
15	7.2	0.8	1.5	8,324	7.2	9.5	1.5	12.4	3.8
16	9.0	1.0	1.5	8,753	9.0	11.5	1.5	14.4	4.7

Table A. 28 Summary of Resilient Modulus Test Results for NDOT Contract #3824 Subgrade.

Sequence	Cyclic Axial Stress (psi)	Contact Stress (psi)	Confine Stress (psi)	Axial Resilient Modulus (psi)	Deviator Stress, σd (psi)	Sigma 1 (psi)	Sigma 3 (psi)	Bulk Stress, θ (psi)	Octahedral Shear Stress (psi)
1	3.6	0.4	5.4	15,312	3.6	9.4	5.4	20.2	1.9
2	1.8	0.2	5.4	16,601	1.8	7.4	5.4	18.2	0.9
3	3.6	0.4	5.4	15,542	3.6	9.4	5.4	20.2	1.9
4	5.4	0.6	5.4	14,710	5.4	11.4	5.4	22.2	2.8
5	7.2	0.8	4.4	13,526	7.2	12.4	4.4	21.2	3.8
6	9.0	1.0	5.4	14,381	9.0	15.4	5.4	26.2	4.7
7	1.8	0.2	3.4	14,979	1.8	5.4	3.4	12.2	0.9
8	3.6	0.4	3.4	12,814	3.6	7.4	3.4	14.2	1.9
9	5.4	0.6	3.4	12,374	5.4	9.4	3.4	16.2	2.8
10	7.2	0.8	3.4	12,604	7.2	11.4	3.4	18.2	3.8
11	9.0	1.0	3.4	12,975	9.0	13.4	3.4	20.2	4.7
12	1.8	0.2	1.4	11,876	1.8	3.4	1.4	6.2	0.9
13	3.6	0.4	1.4	10,225	3.6	5.4	1.4	8.2	1.9
14	5.4	0.6	1.4	10,253	5.4	7.4	1.4	10.1	2.8
15	7.2	0.8	1.4	10,814	7.2	9.4	1.4	12.2	3.8
16	9.0	1.0	1.4	11,361	9.0	11.4	1.4	14.1	4.7